TECHNISCHE UNIVERSITÄT DRESDEN

FACULTY OF ENVIRONMENTAL SCIENCES

Using hydrological models and digital soil mapping for the assessment and management of catchments: A case study of the Nyangores and Ruiru catchments in Kenya (East Africa)

DISSERTATION

submitted for the award of the degree

Doctor rerum naturalium (Dr. rer.nat.)

by

Ann Wahu Kamamia

MSc Hydro Science and Engineering

Supervisors: Prof. Dr. Karl-Heinz Feger, TU Dresden
Prof. Dr. Stefan Julich, Eberswalde University for Sustainable Development
Dr. Hosea Mwangi, JKUAT, Kenya
Dr. Joseph Sang, JKUAT, Kenya

Reviewers: Prof. Dr. Karl-Heinz Feger, TU Dresden
Prof. Dr. Martin Volk, UFZ Leipzig
Prof. Dr. Lutz Breuer, Justus-Liebig University Gießen

Defended on 28th April, 2023

"To waste, to destroy our natural resources, to skin and exhaust the land instead of using it so as to increase its usefulness, will result in undermining in the days of our children the very prosperity which we ought by right to hand down to them amplified and developed."

Theodore Roosevelt

DECLARATION OF CONFORMITY

I confirm that this copy is identical with the original dissertation entitled:

"Using hydrological models and digital soil mapping for the assessment and management of catchments: A case study of the Nyangores and Ruiru catchments in Kenya (East Africa)."

Dresden, _____

_____

DECLARATION OF INDEPENDENT WORK AND CONSENT

According to Technische Universität Dresden

1. I hereby assure that I have produced the present work without inadmissible help from third parties and without aids other than those stated; ideas taken directly or indirectly from external sources are identified as such.
2. When selecting and evaluating material and also when producing the manuscript, I have not received help from anyone.
3. No further persons were involved in the intellectual production of the present work. In particular, I have not received help from a commercial doctoral advisor. No third parties have received monetary benefits from me, either directly or indirectly for work related to the content of the presented dissertation.
4. The work has not previously been presented in the same or similar format to another examination body in Germany or abroad, nor has it-unless it is a cumulative dissertation been published.
5. If this concerns a cumulative dissertation in accordance with section 10 para. 2, I assure compliance with the conditions laid down herein.
6. I confirm that I acknowledge the doctoral regulations of the faculty of Environmental Sciences of the Technische Universität Dresden.

Dresden, _____

_____

Ann Wahu Kamamia

LIST OF PAPERS

The cumulative thesis on developing agroforestry scenarios and the use of digitally mapped soils builds on four chapters, three of which have already been published in peer-reviewed journals in the field of soil science and catchment management. The format of the Papers follows the requirements of the respective journals.

A detailed description of each concept is included within the individual papers provided in Part 2. Paper I and III are open access journals and hence the authors retain copyright. Paper IV is reprinted with permission from Environmental Earth Sciences journal. Paper II is ready for submission in a peer-reviewed journal

1. Kamamia, A. W., Mwangi, H. M., Feger, K.-H., & Julich, S. (2019). Assessing the impact of a multimetric calibration procedure on modelling performance in a headwater catchment in Mau Forest, Kenya. Journal of Hydrology: Regional Studies, 21, 80–91. https://doi.org/10.1016/j.ejrh.2018.12.005

2. Kamamia, A.W., Strauch, M. , Mwangi, H.M.; Feger, K.H., Julich, S. (2022): Modelling crop production, river low flow, and sediment load trade-offs under agroforestry land-use scenarios in Nyangores catchment, Kenya. Journal of Frontiers in Forests and Global Change. https://doi.org/10.3389/ffgc.2022.1046371

3. Kamamia, A. W., Vogel, C., Mwangi, H. M., Feger, K.-H., Sang, J., & Julich, S. (2021). Mapping soil aggregate stability using digital soil mapping: A case study of Ruiru reservoir catchment, Kenya. Geoderma Regional, 24, e00355. https://doi.org/10.1016/j.geodrs.2020.e00355

4. Kamamia, A.W., Vogel, C.; Mwangi, H.M.; Feger, K.H.; Sang, J.; Julich, S. (2022) Using Soil Erosion as an Indicator for Integrated Water Resources Management: A Case Study of Ruiru Drinking Water Reservoir, Kenya. Environmental Earth Sciences, 81 (21), 502. https://doi.org/10.1007/s12665-022-10617-0

ACKNOWLEDGEMENTS

I would like to thank the Graduate Academy-Technical University, Dresden for providing me with financial assistance through the “Promotion of Early-Career Female Scientists” scholarship program and the Institute of Soil Science and Site Ecology for providing me with a comfortable office in which I was able to work with minimum distractions.

Additionally, I would like to individually thank my supervisors. First, Dr. Stefan Julich and Prof Karl-Heinz Feger, my main supervisors in Germany, for their continuous support. Thank you for introducing me to soil science, assisting me during the different scholarship application processes, thoroughly reviewing my draft manuscripts and for always having your doors open for questions and discussions. In the same breath, I would like to thank my second set of supervisors in Kenya, Dr. Hosea Mwangi and Dr. Joseph Sang. Thank you for assisting me during my various research stays in Kenya including the intense fieldwork, and for quick and valuable feedback and mentorship. It will indeed be an honour to continue working with all of you. Special thanks go to Dr. Cordula Vogel who tirelessly assisted me in developing important research concepts and commenting on my manuscripts.

My deep appreciation goes to my dear friends; - Franz, Kendi, Yana, Mario, Stephan, Eva, Benjamin for your constructive honest criticism that made me better. Nobody has been more supportive to me than my loving family- My Father-Edward, my mother- Lydiah, my dear sisters- Lucy and Eva and my brothers- Andrew and Lawrence. Words cannot express the gratitude I feel for your constant support, advice and encouragement throughout this period. I could not have made it without all of you. Last but not least, I would like to thank God for thus far He has brought me.

THESIS AT A GLANCE

PART A: SYNTHESIS

The synthesis overviews and fuses the major concepts, methods and ideas from the four individual papers with existing knowledge within the scientific subject of catchment management. In particular, it points out where the different concepts overlap and diverge which influences the nature and impact of the findings.

PART B: PAPERS

Paper I

Aim: To calibrate the Soil and Water Assessment Tool using the segmented flow duration curve (FDC) and compare it with the hydrograph.

Evaluation method: Pareto optimization, multiple statistical analysis

Conclusion: The multi-metric FDC improved the calibration of low and very low segments and has a potential for use by watershed resource managers working in low-flow environments.

Paper II

Aim: To use the SWAT model together with a generic land-use optimization tool to identify and quantify functional trade-off between environmental sustainability and food production in Nyangores catchment.

Evaluation method: land-use optimization based on Mean annual minimum low flow indicator, sediment yield and maize and soybean harvest yield

Conclusion: Land-use optimization tools can be used to solve complex land allocation problems based on different objectives.

Paper III

Aim: To assess the potential of digital Soil Mapping (DSM) of soil aggregate stability as a proxy for soil erosion mapping in data scarce tropical areas.

Evaluation method: conditioned latin hypercube sampling, fast-wetting aggregate stability test, digital soil mapping

Conclusion: With limited soil samples, use of computing power, improved prediction techniques such as machine learning and freely available covariates/environmental variables, DSM can effectively be applied to predict soil properties for a catchment with little to no existing soil data.

Paper IV

Aim: To determine if spatio-temporal assessment of erosion be an effective tool in influencing the allocation of timely soil erosion mitigation measures.

Evaluation method: Land-use classification using Landsat image, revised universal soil loss empirical model

Conclusion: Yearly erosion risk maps misrepresent the true dimensions of soil loss with averages disguising areas of low and high potential. With monthly erosion risk maps, landscape-scale measures including timely allocation of scarce erosion mitigation and protection measures as well as time-dependent planting and harvesting techniques for agriculture, can be purposely incorporated.

SUMMARY

Human activities on land have a direct and cumulative impact on water and other natural resources within a catchment. This land-use change can have hydrological consequences on the local and regional scales. Sound catchment assessment is not only critical to understanding processes and functions but also important in identifying priority management areas. The overarching goal of this doctoral thesis was to design a methodological framework for catchment assessment (dependent upon data availability) and propose practical catchment management strategies for sustainable water resources management. The Nyangores and Ruiru reservoir catchments located in Kenya, East Africa were used as case studies. A properly calibrated Soil and Water Assessment Tool (SWAT) hydrologic model coupled with a generic land-use optimization tool (Constrained Multi-Objective Optimization of Land-use Allocation-CoMOLA) was applied to identify and quantify functional trade-offs between environmental sustainability and food production in the 'data-available' Nyangores catchment. This was determined using a four-dimension objective function defined as (i) minimizing sediment load, (ii) maximizing stream low flow and (iii and iv) maximizing the crop yields of maize and soybeans, respectively. Additionally, three different optimization scenarios, represented as i.) agroforestry (Scenario 1), ii.) agroforestry + conservation agriculture (Scenario 2) and iii.) conservation agriculture (Scenario 3), were compared. For the data-scarce Ruiru reservoir catchment, alternative methods using digital soil mapping of soil erosion proxies (aggregate stability using Mean Weight Diameter) and spatial-temporal soil loss analysis using empirical models (the Revised Universal Soil Loss Equation-RUSLE) were used. The lack of adequate data necessitated a data-collection phase which implemented the conditional Latin Hypercube Sampling. This sampling technique reduced the need for intensive soil sampling while still capturing spatial variability. The results revealed that for the Nyangores catchment, adoption of both agroforestry and conservation agriculture (Scenario 2) led to the smallest trade-off amongst the different objectives i.e. a 3.6% change in forests combined with 35% change in conservation agriculture resulted in the largest reduction in sediment loads (−78%), increased low flow (+14%) and only slightly decreased crop yields (−3.8% for both maize and soybeans). Therefore, the advanced use of hydrologic models with optimization tools allows for the simultaneous assessment of different outputs/objectives

and is ideal for areas with adequate data to properly calibrate the model. For the Ruiru reservoir catchment, digital soil mapping (DSM) of aggregate stability revealed that susceptibility to erosion exists for cropland (food crops), tea and roadsides, which are mainly located in the eastern part of the catchment, as well as deforested areas on the western side. This validated that with limited soil samples and the use of computing power, machine learning and freely available covariates, DSM can effectively be applied in data-scarce areas. Moreover, uncertainty in the predictions can be incorporated using prediction intervals. The spatial-temporal analysis exhibited that bare land (which has the lowest areal proportion) was the largest contributor to erosion. Two peak soil loss periods corresponding to the two rainy periods of March–May and October–December were identified. Thus, yearly soil erosion risk maps misrepresent the true dimensions of soil loss with averages disguising areas of low and high potential. Also, a small portion of the catchment can be responsible for a large proportion of the total erosion. For both catchments, agroforestry (combining both the use of trees and conservation farming) is the most feasible catchment management strategy (CMS) for solving the major water quantity and quality problems. Finally, the key to thriving catchments aiming at both sustainability and resilience requires urgent collaborative action by all stakeholders. The necessary stakeholders in both Nyangores and Ruiru reservoir catchments must be involved in catchment assessment in order to identify the catchment problems, mitigation strategies/roles and responsibilities while keeping in mind that some risks need to be shared and negotiated, but so will the benefits.

Key words: Land-use, catchment assessment, data-scarce, digital soil mapping, pareto, calibration, hydrologic models, machine learning algorithms, sampling, empirical models, aggregate stability

TABLE OF CONTENTS

List of Figures

List of Tables

ABBREVIATIONS

CLHS	Conditioned Latin Hypercube Sampling
GA	Genetic Algorithm
GIS	Geographic Information Systems
GVI	Green Vegetation Index
DEM	Digital Elevation Model
DSM	Digital Soil Mapping
FDC	Flow Duration Curve
GloSEM	Global Soil Erosion Model
HRU	Hydrologic Response Unit
KGE	kling-gupta efficiency
MODIS	Moderate Resolution Imaging Spectroradiometer
MWD	Mean Weight Diameter
NDVI	Normalized Difference Vegetative Difference
NSAG	Non-Dominated Sorting Genetic Algorithm
NSE	Nash-Sutcliffe efficiency
OLI	Operational Land Imager
PBIAS	Probability of bias
REG_SL	Regional Soil Loss
RMSE	root-mean square error
RSR	RMSE observations standard deviation ratio
RUSLE	Revised Universal Soil Loss Equation
SAGA	System for Automated Geoscientific Analyses
SOC	Soil Organic Carbon
SWAT	Soil Water Assessment Tool
TNSP	Three North Shelterbelt Project
TWI	Topographic Wetness Index
WRMA	Water Resource Management Authority
WRUA	Rural Water Resource Association
WOCAT	World Overview of Conservation Approaches and Technology

PART A: SYNTHESIS

1. INTRODUCTION

1.1 Catchment management

This section lays the foundation for the research topic by presenting a background of the major concepts and ideas that are addressed in detail within the individual papers.

A catchment is defined as the smallest drainage unit from which the runoff drains to a common outlet. This term has been used interchangeably with others such as drainage area, watershed and basin. The term 'watershed' is the standard term in the USA (Shukla, 2011). The term 'catchment' is the standard used in Europe, Australia and certain Asian countries and as such will be adopted in all subsequent chapters. Every stream, tributary or river has an associated catchment, and small catchments aggregate to become larger catchments (Vergara, 1991). The size of catchments varies and is a feature that determines the complexity of its management. Catchments form part of the ecosystem and provide a multitude of ecosystem services. An ecosystem is a dynamic complex of plant, animal and microbial communities and the non-living environment interacting as a functional unit. Ecosystem services are the benefits people obtain from ecosystems. They include provisional services such as food, water and timber; regulating services such as climate, flood, disease and water regulation; and cultural services that provide recreation and aesthetics and supporting services such as nutrient cycling and soil formation (Millenium Ecosystem Assessment , 2005).

Natural and anthropogenic factors can have a direct and cumulative negative impact on the capacity of catchments to provide ecosystem services, a process referred to as land degradation (Lal, 1993; Perry et al., 2000). The main processes of land degradation are physical, chemical and biological degradation. Physical degradation causes a decrease in soil structure and includes compaction, crusting, erosion, desertification and anaerobiosis (Lal, 1997). The major chemical degradation processes include soil acidification, leaching, salinization and loss of fertility. Biological processes include those leading to a decline in biodiversity and total and/or biomass carbon (Lal, 1997). Today, soil erosion – a process in which soil particles are detached from within a cohesive soil matrix and subsequently moved downslope by different transport agents (Kinnell, 2010) – is the main form of land

degradation. This is driven by land-use changes and unsustainable land practices. Soil erosion has resulted in local, regional and hydrological consequences. For example, unsustainable land practices have led to structure degradation in the top soil, which holds the bulk of the organic matter required for plant growth. On-site effects include soil acidification, biological degradation and a decline in soil structure and fertility (Kamamia et al., 2019). Off-site effects include siltation and sedimentation of water bodies and irrigation channels, which affect marine and freshwater ecosystems. Human-induced global warming has further exacerbated the degradation processes by altering seasonal and annual flood cycles, prolonging droughts, changing the distribution of rainfall and raising the temperature (Ferrier & Jenkins, 2009). About 65% of Sub-Saharan Africa is regarded as degraded (Vlek et al., 2010). This is the main factor underlying the low crop productivity and deterioration of water resources. Land degradation in catchments has caused or increased poverty among the vulnerable (the poor, women and indigenous communities), who comprise the majority of the population and who depend on these catchments for food and income (Millennium Ecosystem Assessment, 2005). Rapid population growth in this region continues to increase pressure on the existing and already deteriorated catchment resources to a point where options regulating the use of these resources at sustainable levels become irrelevant. This creates a downward spiral of further land degradation and increased vulnerability of the people to the negative consequences. Degradative processes have critical limits beyond which the various effects are irreversible, and ecosystem services cannot be restored (Hooper et al., 2007; Lal, 1997). The costs incurred in attempts to restore these services have also been regarded as higher than the cost of preventing degradation (Millennium Ecosystem Assessment, 2005).

Therefore, there is a need for proper management of the use of catchment resources, with their many conflicting uses, and mitigation of their deterioration – a process referred to as catchment management. This is defined as the integrated utilization, regulation and care of water and land resources in a catchment with the aim of meeting pre-defined development goals (SCSA, 1982). Catchment management in the broader sense means maintaining the equilibrium between elements of the natural ecosystem or vegetation, land or water on the one hand and human activities on the other hand (Dubey, 2018). Catchment management must encompass the core elements of environmental, economic and social sustainability. Sustainability can occur only when the needs of people and the

capacity of the natural resource base to meet those needs are balanced over time (Mwangi et al., 2016 a, b). This is a complex process which must be approached in a holistic and participatory manner. The multiple resources within a catchment, including forests, pastures, agricultural land, surface water and groundwater, are all linked through the hydrological cycle. Therefore, any form of management must be undertaken along hydrological boundaries, which may at times conflict with administrative boundaries (SCSA, 1982). Sound catchment management plans must also involve all relevant stakeholders (individuals and institutions) who shape the catchment landscape due to their activities. Conventional catchment management focused on the use of hydrological engineering to solve the various technical problems related to water management. However, experience has shown that the success of program implementation depends on the effective participation of all relevant stakeholders in the planning, implementation, maintenance and monitoring of the different initiatives (Mwangi et al., 2016a,b). Catchment management comprises diverse activities addressing proper land use, prevention of land degradation, maintenance and improvement of soil fertility, conservation and proper use of water, erosion control, flood protection, sediment reduction and increasing the productivity of all land uses (Khan et al., 2017; Mwangi et al., 2016a). Due to the dynamic nature of catchment hydrology, stakeholders and availability of resource catchment management plans differ.

An assessment of the status of catchment resources is a pre-requisite of meeting the challenges of catchment management. This step has different dimensions, including the natural and human sciences and stakeholder involvement (Jakeman & Letcher, 2003). Under the natural science dimension, we are able to understand the nature of the processes occurring in the catchment, such as physical pathways for the movement of water/nutrients and pollutants, water balances and deposition areas. Under the human science dimension, assessments aid in identifying current and future catchment pressures and demands, as well as the social/political situation in the catchment (Ferrier & Jenkins, 2009; Jakeman & Letcher, 2003). Stakeholders are imperative for identifying the priority processes and problems, determining the spatial and temporal scale of the catchment assessment and ultimately developing management plans. At times catchment assessments may fail due to a lack of focus on real problems or a lack of understanding of the real problem. Here the insights obtained from the failed analysis can be used to

conceptualize a clearer problem(s).

1.2 Tools to support catchment assessment and management

Integrated hydrological models are fundamental tools for the integrative and iterative assessment and management of catchments (Jakeman & Letcher, 2003). They provide a way of exploring and explaining the different matter fluxes on the hydrologic cycle components and determining the direction and magnitude of change in relation to different management strategies. They serve as tools that can be adopted by stakeholders to produce the information needed to develop catchment management interventions (Jakeman & Letcher, 2003). Application of models requires the integration of site-specific knowledge, regional calibration, environmental scenarios and social problems at different levels of complexity (Duffy & Yu, 2018). Different models exist and are grouped on the basis of model input, parameters and the extent of physical principles applied in the model. With regards to the complexity and availability of input data, models are broadly classified as empirical, conceptual and physically based (Singh, 2018). Empirical models are the least data intense, do not simulate physical processes and are based on a cause-and-effect relationships (Devia et al., 2015). Conceptual models describe the different components of the hydrologic cycle using semi-empirical equations. Physical-based models such as the Soil and Water Assessment Tool (SWAT) (Arnold et al., 1998) are more data intense and represent hydrological processes and the inter-link between these processes in a more complex manner. Model parameters are assessed not only through field studies but also through calibration, suggesting that large data sets of hydrological and meteorological records are required. A large number of parameters are introduced into physically based models, which may lead to the problem of over-parameterization, denoting that a large number of parameters may not necessarily translate to better model performance or better representation of the hydrologic processes (Shukla, 2011; Singh, 2018). Over the years, catchment models have been used to advance the scientific understanding of processes, parameters and uncertainty. This is due to increased computing power; better optimization techniques; advancement in numerical mathematics; increased spatial and temporal modelling scales; the development of tools for data acquisition, storage, retrieval and dissemination and the development of instruments for measuring the different hydrologic variables (Singh, 2018).

Recently, the use of physically based hydrologic models has been complemented with land-

use optimization tools to determine the right balance/trade off amongst the different catchment ecosystem services (Kaim et al., 2018). This is because in reality, catchments have multifunctional uses and are shared by different stakeholders who may have multiple and contradicting aims and interests which they seek to promote and defend. Land-use optimization tools explore a large number of land-use management configurations for the optimization amongst various objectives (Chapagain et al., 2021; Lautenbach et al., 2013). Possible non-dominated solutions are solved by either maximizing or minimizing the different objectives. This is done using algorithms such as the genetic algorithm (GA) (Mitchell, 1996), which forms its basis from biological evolution. GAs such as the non-dominated sorting algorithm (NSAG-II) start with an initial population and use concepts such as selection, mating and mutations to create the next set of populations and ultimately determine the solutions (Kaim et al., 2018). Parameters to be optimized are encoded in a genome, and the individuals in a population are then evaluated on the basis of objective functions. The fitness of the simulation within a generation determines whether or not it will be selected for the next generation (i.e. solutions with higher rankings survive and are selected to reproduce). Mating within a generation is performed by crossover operators, which randomly combine the genomes of two individuals. Moreover, the genome of the offspring can be randomly changed (mutation) (Lautenbach et al., 2013). An implicit elitism strategy ensures that the best solutions ever found in the search history are retained in the population throughout the optimization process (Wang et al., 2019). Land-use optimization tools using the NSAG-II have been used to solve complex land allocation problems based on different objectives. Lautenbach et al. (2013) analysed the biophysical trade-off between bioenergy and crop production using a hydrological model coupled with NSAG-II. Rodriguez et al. (2011) as well as Panagopoulos et al. (2012) applied SWAT and NSAG-II in the selection and placement of best management practices, which minimized pollution in a cost-effective way. Still, the fundamental problem limiting the use of hydrologic models and consequently of land-use optimization tools is the availability of data, of which soil and soil properties are important inputs.

Soil surveys and in-situ soil erosion studies are expensive and time consuming to fulfil the large demand for soil information for environmental modelling and monitoring (Lagacherie, 2008). Besides, new areas of interest have emerged related to soil science, such as soil pollution mapping, land quality mapping, biochemical cycling and erosion risk

mapping, which were not traditionally investigated. The scarcity of soil spatial data has stimulated the development of digital soil mapping (DSM) (Lagacherie, 2008). DSM is defined as the creation and population of spatial soil information systems by numerical models inferring the spatial and temporal variations of soil types and properties from observations and knowledge from related environmental variables (Lagacherie, 2008). DSM has been applied to overcome the limitations of traditional soil surveys that employ polygon data, which undergo generalization within spatial as well as parameter domains due to scalability (A-Xing et al., 2007). Using high-resolution data representing soil-forming covariates, point data and a suit of interpolation techniques, estimates of soil property/function/threats, spatial maps can be derived. DSM has been successfully applied in data-scarce areas to yield satisfactory predictions of different soil properties and vulnerabilities (Kamamia et al., 2021). At times, the soil properties of interest may be difficult to measure, resulting in the use of proxies. By definition, 'proxies' are measurable variables that are used in place of variables that are difficult to measure (Lea et al., 2014). A correlation between the proxy and the variable of interest must be established. Proxies have been used in different fields, such as i) medicine to collect data on patients (Tachikawa et al., 2019) and when testing the potency of new drugs (Emmerich & Deutz, 2018); ii.) econometrics for forecasting purposes (Mitruţ & Bratu, 2014); iii.) Logistics to optimize delivery costs (Geiger & Sevaux, 2011); iv.) palaeoceanography to reconstruct past ocean states (Tachikawa et al., 2019) and soil science to assess organic matter turnover, susceptibility to erosion, soil biochemical activities and soil hydrological processes (Delelegn et al., 2017). The challenges faced in determining soil erosion have resulted in the use of other soil properties ('proxies') that are strongly related to soil erosion (Bissonnais, 2016). Soil aggregate stability was recommended as a proxy for erosion susceptibility (Bissonnais, 2016). The continuous regional spatial mapping of such proxies through DSM can facilitate the application of appropriate conservation and management strategies. Within DSM, the use of machine learning algorithms (data mining tools used for predictive purposes) has also gained popularity only within the past two decades. Conventionally, spatial soil prediction was embedded within the geostatistical framework, which was unable to adequately equate non-linear relationships and capture gradual changes in soil variation and was computationally more demanding for large datasets (Wadoux et al., 2020). By contrast, machine learning algorithms can represent non-linear/non-parametric relationships (which are predominant in nature) and can easily

handle large datasets (Singh et al., 2016; Wadoux et al., 2020). Depending on the algorithm and data available, two main techniques can be applied: 'supervised' or 'unsupervised'. Supervised learning requires an external dataset (training dataset) from which the different input-output patterns/relationships are 'learnt' and an inferred function produced. The algorithm is then deployed for prediction purposes. In unsupervised learning, the algorithm produces an inferred function to reveal a concealed structure from a set of data (Ray, 2019). Different machine learning algorithms exist, such as regression algorithms, instance-based algorithms, Decision Tree Algorithms, Bayesian algorithms, clustering algorithms etc. (Ray, 2019; Singh et al., 2016). Regression algorithms, such as Ordinary Least Squares, Linear Regression and Logistic Regression, are approaches of supervised learning used to model continuous variables and undertake predictions. Decision Tree Algorithms, such as Classification and Regression Trees, and cubist models are also supervised machine learning approaches that continuously split data based on features (Malone et al., 2017). Each node represents a feature in an instance, and each branch corresponds to a value that the node assumes (Maglogiannis, 2007). Each terminal node contains linear regression models, which are then used for prediction. The tree is reduced to a set of rules which elicit the paths from the top to the bottom of the tree (Maglogiannis, 2007; Malone et al., 2017). While decision trees can handle different data types, they can be unstable and are prone to sampling errors. Bayesian algorithms, such Bayesian Networks, require an expert who builds the graphical model and probability tables exhibiting the probability relationship amongst a set of variables. A training data set is then used to learn both the structure of the model and the parameters in the probability tables. A sample data set is then predicted based on this probability distribution. This algorithm cannot handle high-dimension datasets as they are spatially and temporally infeasible (Singh et al., 2016). Instance-based algorithms, such as k-Nearest neighbour, use a database with data points grouped into several classes. The algorithm then classifies the sample data according to the different classes based on the principle that instances within a dataset will generally exist in close proximity to other instances that have similar properties (Maglogiannis, 2007). This algorithm is non-parametric and is suited for multi-modal classification. However, large training sets lower its computational power. Clustering algorithms, such as k-means and hierarchical clustering, are a form of unsupervised classification that solves for clustering problems and is applied when variables are large. This algorithm is sensitive to outliers, initial points and local optima (Singh et al., 2016).

Finally, the use of simple models to measure catchment processes such as soil erosion and transport of resulting suspended material still remains prevalent in many data-scarce areas where it is impossible to obtain the substantial data required to match the physically based models. The advances above have rendered the models more accurate in their applicability. For example, the revised universal soil loss equation (Renard et al., 2017) (RUSLE), an extension of the Universal Soil Loss Equation (Wischmeier & Smith, 1978), is an empirically based model that was conventionally applied to quantify long-term average soil loss. This soil loss depends on erosion risk factors, which include rainfall erosivity (R-factor), soil erodibility (K-factor), slope steepness and length (LS-factor), cover management (C-factor) and support practices (P-factor). Previous studies dealt with soil loss as a static process and calculated this on an annual basis. Recent application of RUSLE have been complemented by the application of GIS, remote sensing technologies and DSM (Angulo-Martínez et al., 2009; Gaubi et al., 2017) to develop high-resolution spatio-temporal estimates of soil loss. The different erosion risk factors have been adjusted to match this. Schmidt et al. (2018) applied the RUSLE equation on Swiss grassland in a sub-annual way by varying the R-factor and the C-factor, which they identified as the main triggers of soil erosion. The R-factor highly correlates with rainfall amount and intensity (Schmidt et al., 2016). Hence, it is expected that there will be inter-annual and seasonal variation of this factor wherefrom dynamic soil erosion risks can be identified. The C-factor approximates the effect of plants as well as soil cover, biomass and disturbing activities on erosion. Seasonal dynamics and growth curve highly influence erosion and should be adjusted to reflect this. The results of this analysis revealed that the mean monthly soil loss by water was 48 times higher in summer as compared to winter, suggesting that catchment management efforts should be accelerated during the summer and should focus on the specific erosion hotpots. The K-factor, expressing the susceptibility of a soil to be detached and transported by rainfall and runoff (Renard et al., 2017), was initially obtained through long-term soil erosion studies or the use of soil property data (Wischmeier & Smith, 1958). Nowadays, this factor has been be mapped through interpolation methods (Addis & Klik, 2015; Avalos et al., 2018) and machine learning algorithms such as the cubist method (Panagos et al., 2014). Higher quality satellite images and GIS techniques have improved the P-factor which includes erosion control measures such as contour cropping, terracing, grass strips and all other enhancements that reduce slope length (Renard et al., 2017) and the LS-factor, which accounts for the effects of slope steepness and length on erosion (Alexandridis et al., 2015).

1.3 Catchment management strategies (CMSs)

Soil and water conservation practices (SWC), also referred to as Best Management Practices (BMP) or catchment management strategies (CMS), are the primary steps of catchment management whose purpose is to enhance agricultural productivity and offer protection. Specifically, they decrease runoff rates, improve soil fertility, retard soil erosion and increase soil-moisture availability and groundwater recharge (WOCAT, 2017). Conservation practices can be divided into in-situ and ex-situ practices. Ex-situ watershed management practices reduce peak discharge in order to reclaim gully formation and harvest a substantial amount of runoff, which increases groundwater recharge and irrigation potential in catchments. In situ management practices are those made within agricultural fields and can include structural, agronomic and vegetative measures. Structural measures involve design and construction with stone, concrete, earth and wood. They are often constructed long term and lead to a change in slope. Although extremely effective in reducing sediment loss, they are expensive to install and maintain (Liniger et al., 2002). They include contour bunding/graded bunding, check dams and gully control structures, land levelling/land smoothening, bench terracing, farm ponds, percolation ponds, waterways and diversion drains (WOCAT, 2017). Agronomic measures are associated with annual crops and are repeated routinely with each season. They are also un-zoned and independent of slope (WOCAT, 2017). They focus on managing the soil to minimize soil erosion and improving fertility, thus promoting better vegetative growth. These measures include contour farming, intercropping, strip cropping, conservation/minimum/no-tillage systems and mulching. Vegetative measures perform the same role as agronomic measures but are often zoned, longer in duration and often lead to a change in slope. They include grass strips, hedge rows and agroforestry systems (Kumawat et al., 2020). For small-scale agricultural production, as is commonly practiced in Kenya, both agronomic and vegetative measures are regarded as feasible catchment management options. This is because they do not require substantial effort and costs to adopt. They also allow farmers to adjust the designs based on the local context. These measures have been found to be effective in reducing land degradation, especially when combined. Mwangi et al. (2015) evaluated the impact of different conservation practices on water and sediment yield in the Sasumua catchment. They reported that

implementation of a 10-m filter strip reduced sediment inflow to the river by 35%, and contour farming reduced sediment flow by 24%. When the two methods were combined, there was a reduction of 41%. Similarly, Gathagu et al. (2018) reported a 63% reduction when combining a 3-m filter strip with contour farming in the Thika-Chania catchment, Kenya. Nevertheless, many small-scale farmers may not adopt CMS for various reasons, such as agricultural losses as most CMSs occupy space and lack of short-term benefits in the form of increased and assured income.

Agroforestry vegetative measures in particular have been the focus of many catchment management programs as they are highly effective in the restoration of deforested areas. Agroforestry is the interaction of agriculture and trees, including the agricultural use of trees (World Agroforestry, 2021). This comprises growing trees on farms and the wider landscape scale (e.g. agri-Silviculture, alley cropping, silvi-pasture) and tree-crop production (agri-horticulture). The contribution of trees to resilience-carbon sequestration, nitrogen fixation and as a source of income has been ranked higher and more long term than that of other catchment management strategies (Speranza, 2010). Forests play a dominant role in partitioning precipitation due to three distinctive features: i.) The foliage above ground that form a number of layers composing the total thickness of the protective canopy; ii.) The accumulation of dead and decaying plant remains on the ground surface constituting the forest floor that protect the soil from raindrop impact while filtering out the finer pores that may clog the larger pores and iii.) The forest soils that are formed below together with the living and dead roots and subsurface stems that permeate the soils (Reynolds et al., 1988). The consequences of deforestation on the hydrology of the catchment have been covered by numerous studies. While the effects are difficult to assess in quantitative terms, there is a general consensus that they predominantly include: impaired water quality, degraded aquatic and terrestrial habitats, loss of biodiversity, contamination of underground aquifers and increased risks of flooding and erosion damage (Calder, 1993; Mwangi et al., 2016c; Zhang, 2020; Zhang et al., 2014; Zhang & Schwärzel, 2017), most of which last for many years. The impact of forests is most marked in areas experiencing very high rainfall where tree interception mitigates flooding by offsetting a large proportion of the storm-producing rainfall and by allowing the build-up of soil moisture deficits during small rainfall events. Thus, the benefits accrued by trees are undeniable. Initiatives such as the New York Declaration on Forests endorsed by over 200

governments are working to promote the establishment of trees globally (Forest Declaration, 2021). The Three North Shelterbelt Project (TNSP) and the Grain for Green reforestation Program in China are the world's largest reforestation programs that sought to restore the degraded Loess plateau covering an area of 640,000 km^2 (Zhang & Schwärzel, 2017). Although this program was successful in reducing the sediment by almost 80%, the average discharge in the basin in 2007 was about 30% of what it was in the 1960s (Zhang & Schwärzel, 2017). This change was linked to the unplanned rapid afforestation that had occurred in the catchment (Zhang et al., 2014). In particular, the authors attributed the reduction in baseflow to the tree stands. Thus, proper catchment assessment to determine the proportion of the catchment that can virtually be converted to tree cover and other conservation measures and the ramifications of this change on ecosystem services is a necessary and crucial step to ensure the sustainability of catchments.

1.4 Concept and research objectives

The overarching goal of this doctoral thesis was to design a methodological framework for catchment assessment and propose practical catchment management strategies for sustainable water resources management with the help of digital soil mapping, modelling and the application of land-use optimization tools. This framework is applied within the Nyangores and Ruiru catchments in Kenya (East Africa), which face different challenges in data availability and threats to natural resources. These two study areas were selected on the basis of data availability, the nature of problems within the catchment and location.

The research objectives were:

a.) To calibrate a hydrological model (Soil and Water Assessment Tool - SWAT) for scenario analysis for the Nyangores catchment.

b.) To use the SWAT model together with a generic land-use optimization tool (CoMOLA) to identify and quantify the functional trade-off between environmental sustainability and food production in the Nyangores catchment.

c.) To assess the potential of Digital Soil Mapping (DSM) of soil aggregate stability as a proxy for soil erosion mapping in Ruiru catchment.

d.) To determine if spatio-temporal erosion assessment is an effective tool for influencing the allocation of timely soil erosion mitigation measures in the Ruiru catchment.

To achieve the above-stated objectives, the following research questions were addressed:

1. Can the calibration of multi-metric indices on the flow duration curve improve the performance of the SWAT model?

2. Can the SWAT model coupled with CoMOLA adequately identify and quantify different agroforestry land-use combinations, providing a trade-off between environmental sustainability and food production in the Nyangores catchment?

3. Is digital mapping of aggregate stability a potential method for easily and quickly mapping soil erosion 'hotspots', particularly for areas with data scarcity?

4. Can the spatio-temporal application of the revised universal soil loss equation (RUSLE) determine the impact of rainy periods on soil loss and the contribution of the different land-use classes to sediment yield in the Ruiru catchment?

These research objectives and questions were tackled comprehensively in the individual papers, and this synthesis will attempt to connect the broad methodology and ideas presented in Figure 1.

The research articles included in this thesis are:

Paper I: Kamamia, A.W., Mwangi, H.M.,Feger, K.H., Julich, S. (2019). Assessing the impact of a multimetric calibration procedure on modelling performance in a headwater catchment in Mau Forest, Kenya. Journal of Hydrology: Regional Studies, 21, 80–91. https://doi.org/10.1016/j.ejrh.2018.12.005

Paper II: Kamamia, A.W., Strauch, M., Mwangi, H.M., Feger, K.H., Sang, J. Julich, S. (2022). Modelling crop production, river low flow, and sediment load trade-offs under agroforestry land-use scenarios in Nyangores catchment, Kenya. Journal of Frontiers in Forests and Global Change. https://doi.org/10.3389/ffgc.2022.1046371

Paper III: Kamamia, A.W., Vogel, C., Mwangi, H.M., Feger, K.H., Sang, J., Julich, S. (2021): Mapping soil aggregate stability using digital soil mapping: A case study of Ruiru reservoir catchment, Kenya. Geoderma Regional 24, e00355.
https://doi.org/10.1016/j.geodrs.2020.e00355

Paper IV: Kamamia, A.W., Vogel, C., Mwangi, H.M., Feger, K.H., Sang, J., Julich, S. (2022): Using Soil Erosion as an Indicator for Integrated Water Resources Management: A Case Study of Ruiru Drinking Water Reservoir, Kenya. Environmental Earth Sciences, 81 (21), 502.
https:// doi.org/10.1007/s12665-022-10617-0

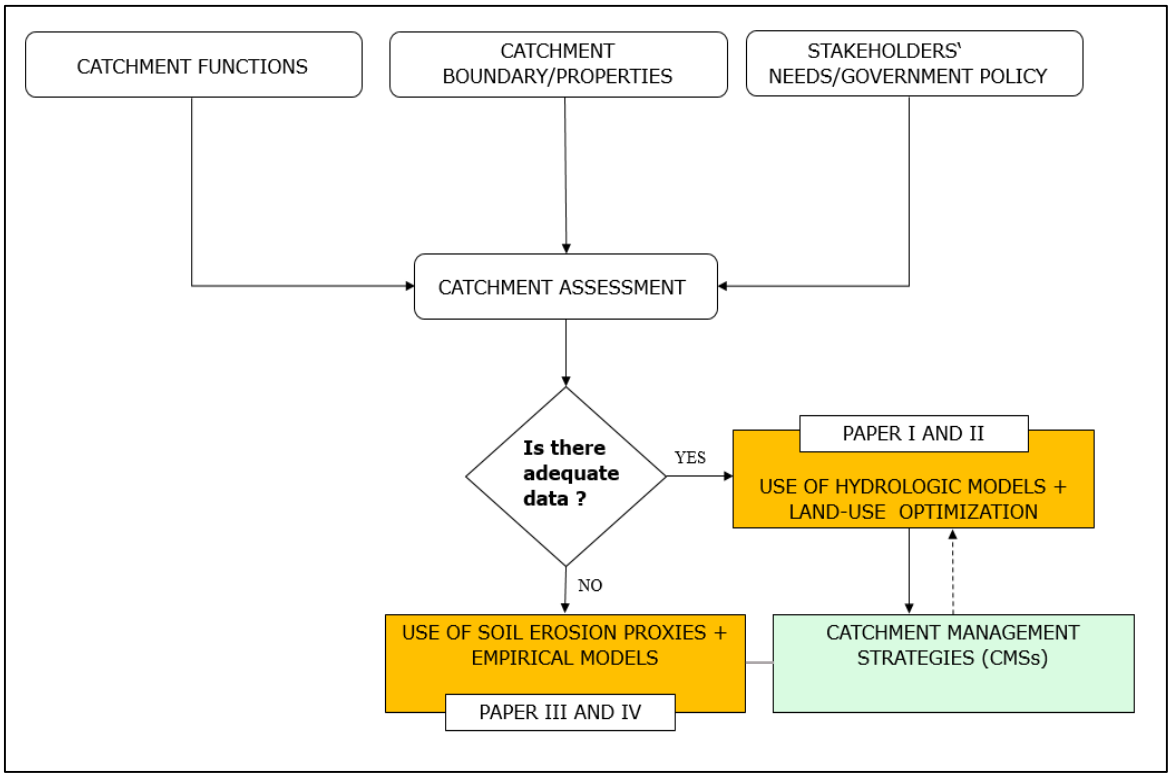

Figure 1: Conceptual framework of the doctoral research

Papers I and II, addressing research questions 1 and 2, present an ideal catchment assessment situation. Using a properly calibrated physical-based model coupled with the CoMOLA land-use optimization tool, the most optimum agroforestry arrangements based on mean annual minimum stream low-flow indicator, sediment load, and crop yield of maize and soybeans were determined. This methodology proved an ideal tool for providing a trade-off between environmental sustainability and food production in order to achieve a certain ecological status.

Paper III addressed research question 3 and confirmed that with limited soil samples, the use of computing power, improved prediction techniques such as machine learning and freely available covariates/environmental variables, DSM can be applied effectively to predict erosion susceptibility for a catchment with little to no existing soil data. The empirical RUSLE model was used for a spatio-temporal analysis of erosion dynamics (Paper IV, research question 4) and concluded that yearly erosion risk maps misrepresent the true dimensions of soil loss with averages disguising areas of low and high potential. At times, a small portion of the catchment is responsible for a large proportion of the total erosion. The use of spatio-temporal analysis is ideal for identifying 'where' and 'when' erosion control using different catchment management strategies should be focused.

2. MATERIAL AND METHODS

This section will first provide a short description of the two study areas and will reflect upon their unique challenges. Next, the different methodologies implemented within the individual Papers guided by Figure 1 will be summarized. In this sub-section the intersecting concepts and differences between the different Papers will be provided in grey boxes.

2.1. STUDY AREA

2.1.1. NYANGORES CATCHMENT

The Nyangores catchment (presented in Paper I and II) is part of the greater Mara River basin which is shared between Kenya and Tanzania and covers a total area of 694 km^2. The main river in the catchment is the Nyangores river. The altitude ranges from 2970 m at the Mau escarpment to 1905 m at Bomet rain gauging station. The mean annual rainfall ranges between 1000 mm and 1750 mm (Mati et al., 2008). Rainfall peaks twice a year: March–May (long rainy season) and September–November (short rainy season). Andosols are the dominant soils. The Nyangores catchment holds the largest proportion of montane forests within the Mara basin, and the rest is covered by small-scale agriculture. The Nyangores catchment presents a somewhat complex situation due to its location as a headwater within a major transboundary catchment. This means that there are numerous stakeholders located both within and outside the catchment who depend on it for survival. A study by the Rural Water Resource Association (WRUA) identified water scarcity and water pollution as the major water problems faced in the catchment (WRMA, 2011). They linked this to deforestation, planting of eucalyptus trees on riparian land and riverbank encroachment. The impacts of deforestation on water resources are already being felt within the larger Mara basin. For instance, the wildlife dwelling within the Masai Mara (Kenya) and Serengeti (Tanzania) preserves located in the middle of the Mara catchment at times lack water during dry periods (Mwangi et al., 2016a). The various lodges located within this area also draw large quantities of water for their daily operations. At times, this leads to conflicts with the small- and medium-scale pastoral herdsmen who have to scramble for the little that is left despite it being heavily polluted. On the Tanzanian side (lowest part of the larger mara basin), sediment deposition in the existing wetlands has more than doubled over the last 30 years (WRMA, 2011). This situation has been further aggravated by extreme water events such as protracted droughts and floods in the

catchment. Moreover, the high population within the Nyangores catchment, projected to increase at 3%–4% per annum, continues to mount pressure on the existence of the remaining forests (Kamamia et al., 2019). To reconcile the land-use conflict, a favourable trade-off amongst ecosystem services must be established.

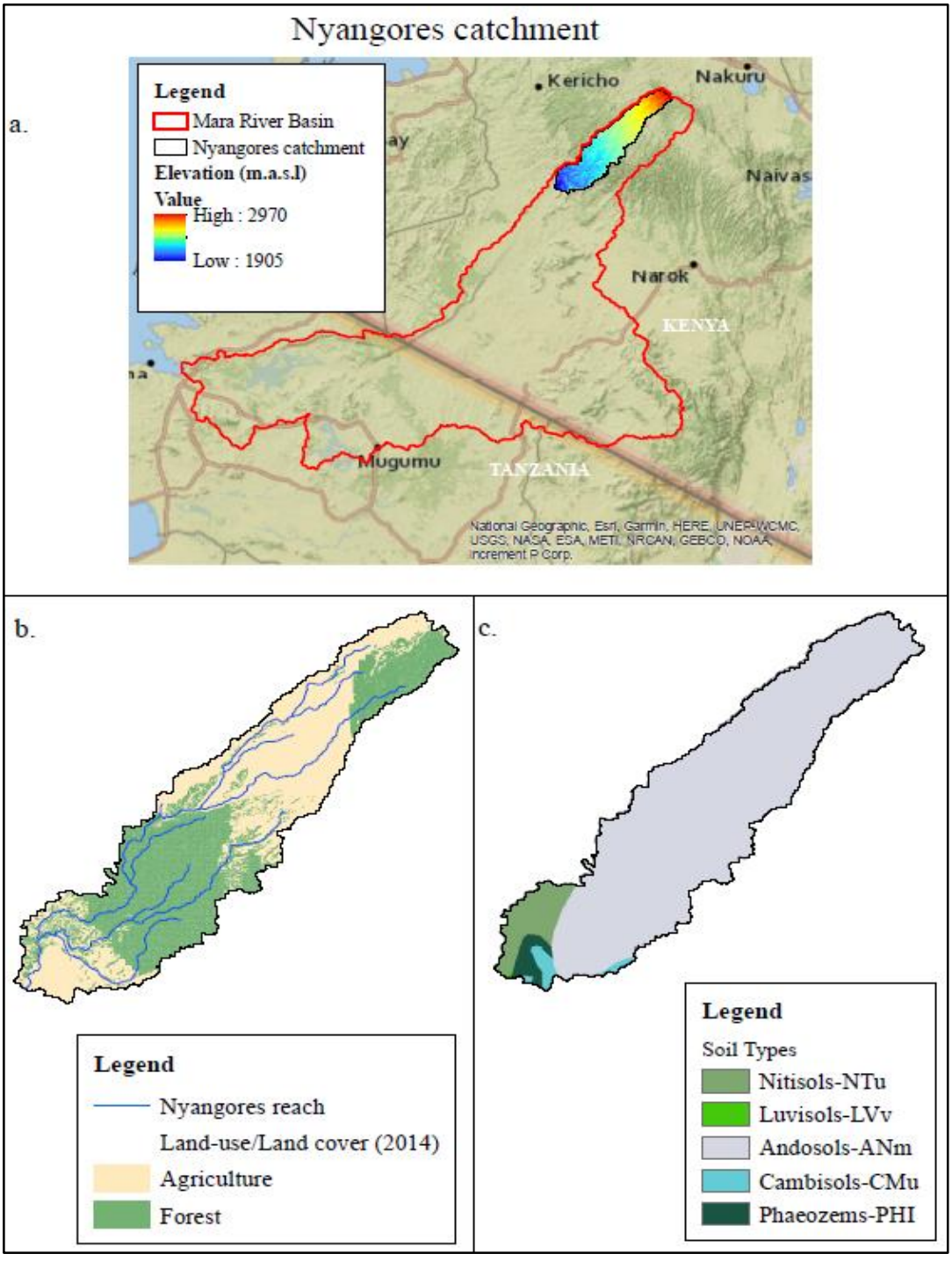

Figure 2: The Nyangores catchment. a.) Location b.) Land-use/Land cover and c.) Soil Types.

2.1.2. RUIRU RESERVOIR CATCHMENT

The Ruiru reservoir catchment (Presented in Papers III and IV) is located near Githunguri in Kiambu County, Kenya. The catchment covers an area of 51 km^2 from the Uplands area close to the Rift Valley escarpments to the Ruiru Reservoir at the catchment's outlet. The major source of water feeding this catchment is the Ruiru river. An average annual rainfall of 1300–1500 mm is received in the catchment. The long rains are experienced between March and May, while the short rains are experienced between October and December. Temperatures range between 13.0 and 24.9 °C. Temperatures are highest from January to March and lowest in July and August (Nyakundi et al., 2017). Nitisols are the dominating soils in the catchment, and a small portion of Andosols can be found in the upper part of the catchment (Fig. 3a). These soils are influenced by pyroclastic and igneous volcanic parent material. The region belongs to the tea-dairy zone and subsistence farming is characterised by low-input low-output production (Kamamia et al., 2021). Currently, the Ruiru reservoir, located within the Ruiru catchment, is one of the four main sources of water for Nairobi, the capital of Kenya.

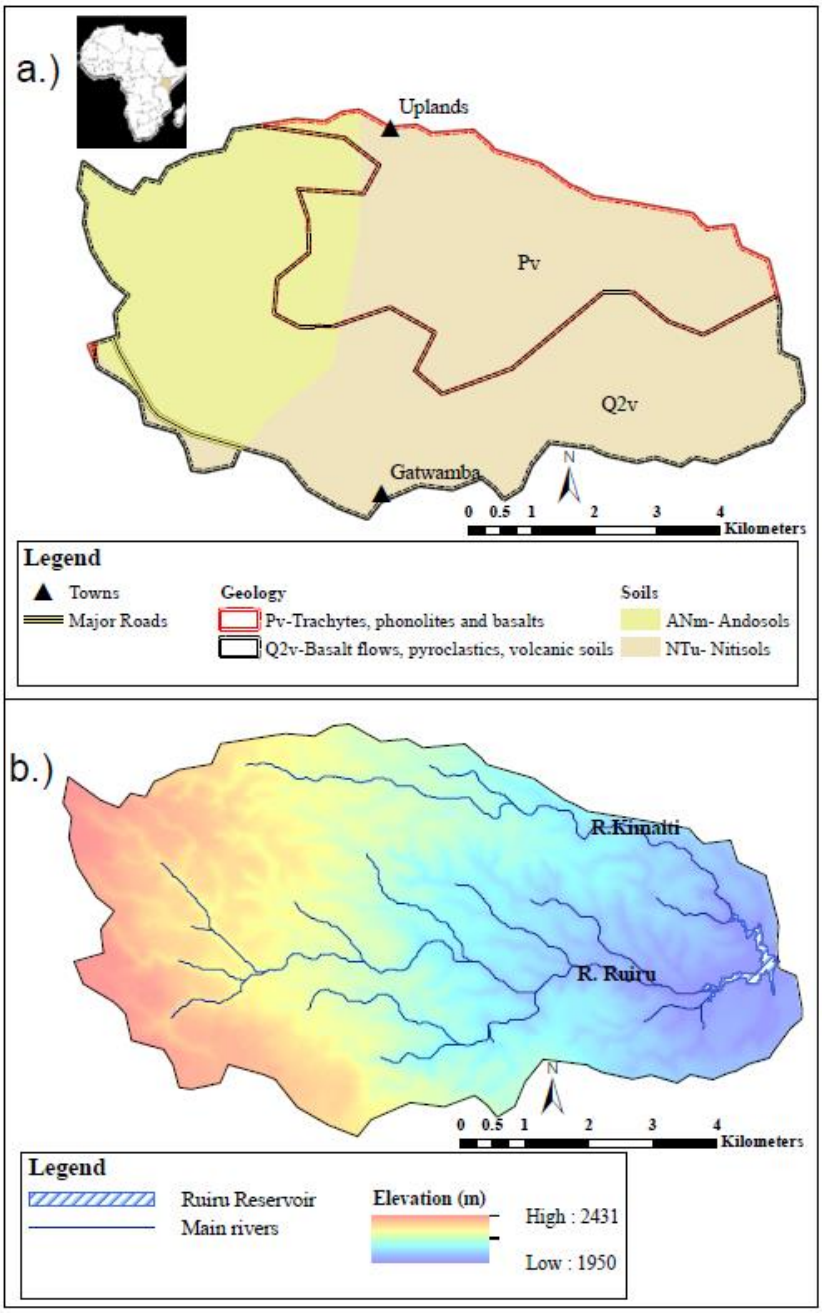

Figure 3: The Ruiru catchment. a.) Location, geology and soil types b.) Elevation and main rivers.

The management of this reservoir has changed hands from its commissioning in 1949 during the colonial time and is now under the Nairobi Water and Sewerage Company (Sang et al., 2017). A bathymetric survey by Maloi et al. (2016) reported a 14% reduction in the reservoir's capacity due to siltation in the catchment. Further reservoir sedimentation studies revealed successions of basin-wide light-coloured layers reflecting Fe-rich soil material. This indicates that sedimentation does not occur steadily over time but in pulses, for instance at the onset of rainfall events. Research extending to the catchment of this

drinking water reservoir seeks to bridge the source-to-sink connection by: i.) Identifying the potential erosion hotspots and ii.) Assessing their spatio-temporal distribution.

2.2. Using the SWAT conceptual model and land-use optimization

Paper I and II focuses on Nyangores catchment (summary provided in Table 1) with considerable amount of climate, land-use, soil and discharge data. This was deemed adequate for the use of SWAT.

Table 1: Summary of materials and methods used for Papers I and II

Study area:	**Nyangores catchment**
Materials/software:	
Raster/vector data: DEM, Land-use and soil map Climate data: Observed data on relative humidity, wind speed, maximum temperature, minimum temperature and solar radiation Literature data on yield and sediment output Software: ArcGIS (ArcMap 10.3), CoMOLA land-use optimizer	
Main Methods:	
Pareto calibration based on FDC, multi-objective optimization of land-use configurations	

A multimetric calibration method (5-FDC) (Kamamia et al., 2019) focusing more on low flows on the flow duration curve is the subject of Paper I. Using Latin Hypercube Sampling importance sampling, 6000 independent parameter sets were generated and runoff simulated. The observed data (discharge, runoff ratio, proportion of precipitation translated to evapotranspiration) was then compared to that simulated using pareto ensembles from both the multimetric flow duration curve and the hydrograph. The parameter distribution of the pareto ensembles for each procedure was plotted. This distribution was linked to the performance of the model with regards to water balance components.

Paper II involved coupling the SWAT model with a land-use optimization tool CoMOLA (Strauch et al., 2019) in the selection of different land-use configuration scenarios at the HRU level, the smallest spatial unit comprising unique land-use, soil conditions and relief (i.e. slope). A four-dimension objective function i.e. maximize mean annual minimum stream low-flow indicator, minimize sediment load, maximize maize yield and soybean yield was integrated into the SWAT-CoMOLA. This was then employed to assess three different catchment management strategies (CMSs), which included i.) adoption of agroforestry only, Scenario 1, ii.) adoption of agroforestry + contour farming + vegetative grass filter strips, Scenario 2 and iii.) adoption of contour farming + vegetative grass filter strips, Scenario 3. For all scenarios, CoMOLA was run separately using an initial population of 100 and for 500 generations. Lastly, in order to compare the different scenarios with each other and the baseline, a mid-range of the pareto solutions was determined. This is based on the distance of the pareto-optimal solutions to the 'ideal point' described as the best set of solutions to each independent objective (Strauch et al., 2019).

BOX 1: Method comparison of Paper I and Paper II

Apart from using the same hydrological model, both studies recognize the concept of equifinality that acknowledges that there is no single optimal solution; rather, a set of pareto solutions exist that give comparable output. In order to account for this, a multicriteria approach simultaneously optimizing and trading off several user-selected performance criteria was used to generate pareto calibration parameter sets (Paper I). Likewise, the land-use optimization tool (Paper II) was used for multi-objective optimization of the different land-use allocation options to develop pareto land-use allocation patterns using the CoMOLA genetic algorithm.

Paper II is an extension of Paper I and highlighted the strength of the combined use of SWAT+ CoMOLA to effectively identify and quantify functional trade-off between environmental sustainability and food production in Nyangores catchment.

2.3. Using soil erosion proxies and empirical models

Papers III and IV focused on the methodology (summarized on Table 2) applicable in data-scarce areas and for the Ruiru catchment only.

Table 2: Summary of materials and methods used for Papers III and IV.

Study area:	**Ruiru reservoir catchment**
Materials/software:	
Covariate terrain data: slope, aspect, plan curvature, profile curvature, aspect, relief elevation, TWI, Hillshading, soil map, geology map, land use map Covariate spectral data: Landsat 8 OLI Band 4 and Band 5 (wet and dry season), NDVI, GVI Software: ArcGIS (ArcMap 10.3), SAGA-GIS, R statistical software, QGIS Main laboratory equipment: Vario TOC Cube Elementar equipment (Elementar Analysensysteme GmbH, Langenselbold, Germany), Sedimat 4-12 equipment (Umwelt-Geräte-Technik (UGT) GmbH, Müncheberg, Germany), EijkelKamp wet sieving apparatus (Eijkelkamp Soil & Water, Giesbeek, Netherlands), sieves	
Main Methods:	
Fieldwork: determining sampling distribution using CLHS, georeferencing and soil sampling Laboratory Experiments: Gravimetric determination of water content, wet sieving and sedimentation method, dry combustion method, fast wetting method of aggregate stability Analysis: statistical analysis, DSM, Landsat classification, RUSLE factors aggregation	

The absence of data necessitated a data-collection phase. The Latin Hypercube Sampling method (Paper III) effectively reduced the intensity of this process and produced an unbiased sampling scheme. Soil sampling in the Ruiru catchment was undertaken between January and March 2019. A total of 90 samples from the top 0–30 cm soil were

collected for analysis purposes. Core ring samples were additionally collected for bulk density determination. The samples collected from the topsoil were sieved (<2 mm) and air dried. Aliquots of the soil samples were transported back to Germany for texture analysis (combined sieve and pipette method), pH, organic carbon (Corg) and aggregate stability (fast wetting method) tests. Covariate data collected for digital soil mapping included a digital elevation model from which different derivatives (aspect elevation, hillshading, plan curvature, slope, topographic wetness index) were extracted and spectral data. Aggregate stability, measured using the Mean Weight Diameter index (MWD), was used as a soil erosion proxy. Paper III provides a detailed description of the aggregate stability fast wetting test (Bissonnais, 1996) undertaken on the soil samples to measure this property. The cubist method with regression kriging was thereafter applied to create a continuous map of the MWD. Reiteratively, this method was applied to determine the soil erosivity factor (K-factor) in Paper IV. This is one of the erosion risk factors included in the revised universal soil loss equation (RUSLE) (Renard et al., 2017). In Paper IV, monthly soil erosion risk maps were developed by multiplying the K-factor with the monthly rainfall erosivity factor (R-factor), slope steepness and length factor (LS-factor), monthly cover management factor (C-factor) and support practices factor (P-factor), using Eq.1

$$A_{monthly} = \mathrm{R}_{month} * K * L * S * C_{month} * P \quad \text{(Eq.1)}$$

Where:

$A_{month}\ is\ the\ monthly\ soil\ loss\ in\ t\ ha^{-1}month^{-1}$

$R\ is\ the\ rainfall\ erosivity\ (MJ\ mm\ ha^{-1}\mathrm{h}\ year)$

$K\ is\ the\ soil\ erodibility\ factor\ (t\ ha^{-1}R\ unit^{-1})$

$LS\ is\ the\ topographic\ factor\ (dimensionless)$

$C\ is\ the\ cropping\ management\ factor\ (dimensionless)$

$P\ is\ the\ practice\ support\ factor\ (dimensionless)$

As a final step, the monthly estimates were compared with the Global soil erosion model (GloSEM) (Panagos et al., 2016).

BOX 2: Method comparison of Paper III and Paper IV

Papers III and IV used soil data analysed from a field survey. Furthermore, they implemented DSM using the cubist method machine learning algorithm with regression kriging. Both analyses resulted in static spatial maps which informed the catchment management strategies (CMSs) suggested.

While Paper III focuses mainly on the implementation of DSM for mapping the aggregate stability proxy, Paper IV implements this only for the calculation of the erodibility factor following Schwertmann (1987), which was thereafter integrated into
the soil loss equation to yield the total soil loss given in tons/hectare/month.

3. RESULTS AND DISCUSSION

Based on the underlying research questions, this chapter synthesizes both published and unpublished major findings of this research. The results and discussion are presented in terms of modelling/mapping extent and aim to answer each individual research question while still encompassing the broader objective.

The results from the modelling studies presented in Papers I and II and Papers III and IV demonstrate the differences in the model structure complexities and the diversity of the results. In Papers I and II, the SWAT model was first calibrated on the flow duration curve. Thereafter, the calibrated model was complemented with a land-use optimization tool to create possible land-use allocation combinations guided by objectives providing a trade-off between environmental sustainability and food production. Within Paper III, using readily available data (DEM and derivatives from satellite images) as covariates and measured point data, a predictive spatial map for the aggregate stability was developed. In Paper IV, the Revised Universal Soil Loss Equation (RUSLE) complemented with the cubist-kriging interpolation method for the erodibility factor (K-factor) was employed to develop monthly soil erosion risk maps for the Ruiru catchment.

3.1. Assessing multi-metric calibration performance using the SWAT model

RQ1: Can calibration on multi-metric flow duration curve improve the performance of the SWAT model?

Within Paper I, discharge data for the period 1972–1978 was used for calibration and validation purposes. The selection of this period was based on the quality and continuity of the data. The results demonstrate that the limitations faced by conventional calibration can be overcome by **i.)** using a flow duration curve (FDC), which relies on discharge magnitudes rather than time series; **ii.)** undertaking a multi-metric calibration on the FDC; **iii.)** aggregating multiple statistical methods to assess the quality of the calibration runs and **iv)** selecting a pareto parameter set rather than a single set.

The first step in using a hydrologic model involves calibration using observed data. Calibration is an effort to better parameterize a model to a given set of local conditions. It involves adjusting parameter values (describing physical, chemical and biological processes) within their respective plausible ranges and comparing the model predictions with observed data (Arnold et al., 2012). Most often, discharge is used for calibration

purposes. This conventional form of calibration is based on the hydrograph presented as a discharge time series. This means that it is impossible to adopt where there is a temporal mismatch between input and output data (Westerberg et al., 2011). As an alternative, the flow duration curve (FDC), which relies on discharge magnitudes rather than time series, is applicable for data-scarce areas where temporal coverage is poor (Pfannerstill et al., 2017). Splitting the FDC into five segments depicting the very low, low, mid, high and very high discharge magnitudes (5-FDC) produced a set of calibration runs that adequately depicted the response of the catchment to the different watershed functions. When the 5-FDC was compared with the normal calibration based on the hydrograph (normal calibration procedure-NCP), the 5-FDC improved the calibration of low and very low segments, whereas the NCP performed better where the peak flows were concerned. The low and very low flows are related to the interaction of base flow with riparian evapotranspiration during extended dry periods, and the high and very high flows signal the response of the catchment to high-intensity precipitation events (Kamamia et al., 2019; Yilmaz et al., 2010). It follows that the choice of a calibration method should be influenced by the purpose of modelling.

Multiple statistical methods, such as the root-mean square error (RMSE), Nash-Sutcliffe efficiency (NSE) and the Kling-Gupta efficiency (KGE), can then be used to assess the quality of the predictions and obtain a final parameter set. There exists no single statistical model that adequately covers all the phases of the hydrograph. Using a single statistic can lead to undue emphasis on matching one aspect of the hydrograph at the expense of another (Moriasi et al., 2007). Aggregating them offers an option for exploiting the strengths of the different statistical measures (Wadoux et al., 2020). The Pareto optimization technique implemented during the calibration process allowed for the identification of parameter sets (Pareto ensembles) that realized an optimal trade-off point amongst multiple objective functions selected. During calibration, different parameter sets may produce similar outputs, especially where different statistical measures are employed, thus the need for a multi-objective calibration approach. For the Nyangores catchment, improved calibration on the 5-FDC for low flows is potentially useful for watershed resource managers working in low-flow environments. With better representation of low flows, they can establish effective limits to ensure that there is no over-allocation of water.

3.2. Land-use optimization using SWAT-CoMOLA for the Nyangores catchment

RQ 2: Can the SWAT model coupled with CoMOLA adequately identify and quantify different agroforestry land-use combinations, thus providing a trade-off between environmental sustainability and food production in the Nyangores catchment?

The SWAT-CoMOLA application yielded different agroforestry land-use combinations that were dependent on environmental sustainability (mean annual minimum stream low-flow indicator and sediment yield objectives) and food production (maize yield and soybean yield objectives). A general outlook of the three scenarios [Scenario 1—forests only, Scenario 2—forests + conservation agriculture, Scenario 3—conservation agriculture only] displayed that environmental sustainability favoured the planting of more trees and conservation agriculture, whereas food production favoured mostly conventional agriculture. When the mid-range solutions of the scenarios were compared, a +8% change from agriculture to forest for Scenario 1 resulted in a decrease in sediment load (−66%). This change was accompanied by a 5.2%, 12.8% and 11.4% decrease in the mean annual minimum stream low-flow indicator and crop yield of maize and soybean, respectively. Within Scenario 2, a 3.6% conversion to forest paired with a 35% conversion to conservation agriculture resulted in a decrease in sediment load (−78%). This also resulted in smaller decrease in crop yield (maize and soybean production decreased by 3.8% and 3.4%, respectively) and a positive increase in the MAM low-flow indicator (14%). Similarly, Scenario 3 recorded a comparable crop yield reduction (~−3%), a lower increase in mean annual minimum low-flow indicator output (+5%) and sediment load (−41%). Therefore, Scenario 2 proved to be the most superior.

The outputs and the mid-range spatial maps of Scenario 1 and Scenario 2 exhibited the importance of trees in reducing sedimentation, especially in the upper part of the catchment. The reduction of soil erosion in the Nyangores catchment is significant as the majority of people consume water directly from the stream without any form of treatment (Mwangi et al. 2016a). Trees possess a dense upper storey, under storey litter and extensive tree roots, which altogether reduce the erosive power of raindrops, improve soil aggregation and increase the resistance of soils to erosion. This allows the trees to moderate peak runoff, thereby reducing sedimentation in the rivers (Veldkamp et al., 2020). This could explain why the land-use optimization tool allocated trees to areas with the highest elevation, which experience the highest precipitation in the catchment

(regardless of slope). The results of Scenarios 2 and 3 shed light on the impact of conservation agriculture (defined by contour farming and use of a filter grass strip of 5 m) on increasing the mean annual minimum stream low flow. The ridges and troughs created by contouring act as barriers to water flow, thereby allowing it more time to infiltrate, which reduces surface runoff and soil erosion (Mwangi et al., 2015). Likewise, vegetative grass strips slow down run-off and trap sediments. As they do not possess as extensive rooting systems as trees, they enhance the recharge of aquifers, ensuring that the water is released to the streams as base flow during extended dry periods. For the Nyangores catchment, combining both the use of trees and conservation farming is the most feasible option for solving the major water quantity and quality problems while ensuring agricultural sustainability.

Land-use optimization tools such as CoMOLA allow for the incorporation of stakeholders. This can be done before or after the optimization process. When incorporated before, stakeholders are imperative not only for identifying the main problems in the catchment but also for defining the multi-objectives and designing feasible solutions that the communities would be willing to adopt. However, including the stakeholders before the optimization process may constrain the search space for feasible solutions (Strauch et. al, 2019). This is solved by involving them in the selection of the preferred solution once the Pareto optimal solutions are reached (Lee & Lautenbach, 2016). The spatial visualization results indicate that this is a classic example of an upstream/downstream kind of trade-off. Since the upstream forest establishment and management are oriented towards the welfare of the downstream community, the upstream farmers can be paid by the downstream stakeholders for foregoing their previous agricultural practices. Finally, well-designed regulatory measures prohibiting deforestation must be enforced in the Nyangores catchment to ensure its sustainability.

3.3. Digital soil mapping of soil aggregate stability

RQ 3: Is digital mapping of aggregate stability a potential method for easily and quickly mapping soil erosion 'hotspots', particularly for areas with data scarcity?

A major challenge which is faced in the application of DSM in data-scarce areas such as the Ruiru catchment is: what is the optimal sample size for DSM? Within Paper III, an improved sampling technique – conditioned Latin Hypercube Sampling (CLHS) involving sampling on the covariate rather than the geographic space – was applied (Kamamia et al., 2021). The different sampling sizes were compared against the environmental covariates. This is an important step to determine if the sampling distribution adequately covers the environmental covariate feature space. Tools such as density plots, box plots and chi-square can be used to assess this distribution (Brungard & Boettinger, 2010). A favourable sampling size should provide enough samples for use in predictive models used in DSM. Predictive models exploit the relationship between soil properties, sampling and soil-forming factors to make predictions. Most of the soil-forming factors come in the form of digitally available data, such as the digital elevation model, remote sensing images, geological survey maps etc. With recent advancement in remote sensing techniques and the emergence of regional and global soil databases, products that better delineate the soil forming factors/covariates can be obtained. For example, MODIS and Sentinel-2A data provide high-resolution surface spatiotemporal data, even in areas that are inaccessible (Lagacherie, 2008). Furthermore, the use of machine-learning algorithms for prediction allow for the learning of data without explicit instructions, can uncover patterns/structure in very large datasets and create digital soil maps with their associated accuracies. At the same time, it must be stressed that the application of DSM is only as good as: i.) The observed point properties data influenced by the sampling density; ii.) the ability of the covariates to explain the variability of the target variable iii.) and the spatial resolution of the data on environmental variables. The results of Paper III demonstrate that the combined use of CLHS and DSM reduced the need for intensive soil sampling and was able to capture aggregate stability variability. This methodology can be adopted in many other data-scarce areas such as Kenya where data is constrained by low government investment, few soil scientists and the long periods required to complete soil surveys.

The results from digital soil mapping of aggregate stability presented in Paper III reveal that susceptibility to erosion is imminent under cropland, some tea plantations, roadsides and

deforested areas in the western part of the catchment. The low aggregate stability observed on the roadsides revealed an often-overlooked soil erosion contributor, especially in the rural tropics laden with earthen feeder roads (Kamamia et al., 2021). Proper grading of these roads and stabilization of the roadsides mostly using vegetation (i.e. grass) could offer a more practical solution for the catchment studied. The results of variable aggregate stability for land uses under different management practices also illustrate that land management influences the intensity of soil erosion and can serve to either mitigate or amplify soil loss in the Ruiru catchment. For example, some well-managed tea plantations recorded aggregate stability similar to that under undisturbed natural forests (Kamamia et al., 2021). By contrast, some plantations revealed inherently low aggregate stability, close to that of bare land. The map of predicted aggregate stability for the study area was effective in identifying potentially degraded areas for which catchment management strategies (CMS) should be developed and suggested that options that increase soil organic matter (SOM) should be carefully integrated, focusing first on the most critical areas to ensure a maximum impact on the reduction of sedimentation.

3.4. Spatio-temporal analysis using the revised universal soil loss equation (RUSLE)

RQ 4: Can spatio-temporal analysis with the revised universal soil loss equation (RUSLE) determine the impact of rainy periods on soil loss and the contribution of the different land-use classes to sediment yield in the Ruiru catchment?

In Paper IV, the RUSLE was applied to determine the intra-annual soil loss variability and was adjusted to local conditions. In particular, the R-factor and C-factor were adjusted for every month to account for the natural temporal variability of precipitation and plant growth (cf. Schmidt et al., 2019). The K-factor, LS-factor and P-factor either show multi-annual variability or are static and were therefore not included in the temporal analysis. This resulted in maps of monthly erosion risk.

The RUSLE is an empirically based erosion model originally developed to estimate the annual average soil erosion (tons per ha per year) and was developed for smaller catchments (Benavidez et al., 2018). Improvements and modifications of the RUSLE have made it applicable to larger spatial scales, including coarser resolution representation at the global scale, thus making it ideal for application in data-scarce areas. Furthermore, its

easy applicability and availability of numerous studies for comparison purposes explains why its use remains attractive despite many uncertainties (Alewell et al., 2019). The uncertainties observed by the RUSLE are due to the lack of long-term soil loss data with which to compare the results and the lack of data for calibration purposes. However, it is a good first step to determine the soil loss as estimates rather than absolute values (Benavidez et al., 2018). Hammad et al. (2004) compared observed soil loss data to i.) RUSLE on an annual basis based on global datasets and ii.) RUSLE with adjusted sub-factors. They reported that the initial application of the RUSLE over-estimated the soil loss by a factor of 3 while the adjusted RUSLE based on soil moisture, land cover and support practices reduced the model error by 14%.

The spatio-temporal analysis of soil loss laid bare the dynamic distribution with higher soil loss occurring during the long rains and lower soil loss occurring during the short rains. Thus, time-specific land management practices such as mulching before the onset of the rains for areas under cropland and tea and agroforestry were suggested as a solution for areas recording high soil losses. At the same time, the soil erosion studies revealed permanent erosion hotspots such as deforested areas where more long-term solutions should be sought. Most of these areas in the Ruiru catchment are either bare or under tea plantation. Veldkamp et al. (2020) reported that deforestation for tree cash crops such as tea plantations reduces the SOM content below 50 cm more than does deforestation for cropland. Worse still, the results also confirmed that soil loss is higher in deforested areas left bare than areas under any other land use left bare. The highest soil loss was from bare land under deforested land and not that around homesteads, roadsides or even fallow agricultural land. This may have been influenced by a combination of many factors such as location (most of the forests are located in areas with high elevation without steep slopes), climate and notably the drastic change in inputs of litter or organic residues that occurs during clear-cut deforestation. Lastly, although reforestation has been proposed as a solution to previously deforested areas, the results also reveal that reversing the effects of deforestation may take time, and the soil properties under reforested trees (especially in the sub-soil) may still differ from those under undisturbed natural forested soils (cf. Veldkamp et al., 2020). Therefore, in addition to improved land management practices, effective policies to curb deforestation must be enforced in the Ruiru catchment to ensure its sustainability.

4. CRITICAL ASSESSMENT OF THE METHODS USED

4.1. Assessing the suitability of data for modelling and overcoming data challenges

There is an urgent need to better manage catchments in order to ensure their sustainability. One response to this demand is through the acquisition of scientifically backed information. Tools and methods such as models and digital soil mapping can be used to bridge this information gap. One argument for the use of distributed physically based hydrologic models such as SWAT is that they are more realistic and can be used for a broad range of topics, such as assessing the impact of land-use change, climate, management of water, sediment, agricultural and chemical yields for catchment management (Neitsch et al., 2011; Shukla, 2011). Nevertheless, such models require high input of data such as rainfall, temperature, topography, vegetation and hydrogeology in addition physical parameters describing the various chemical, biological and physical processes. Acquisition and preparation of a suitable dataset is an important and very demanding step. Variable data exists in terms of temporal intervals: hourly, daily, monthly etc. and in terms of spatial extent: global data, field data and regional data (Bonell & Bruijnzeel, 2005). After the acquisition of available data, the main question posed is: How then does one check the quality of this data to ensure that it is suitable for the modelling one wishes to undertake? This is a complex process as no common and structured process exists (Van Loon & Refsgaard, 2005). Different experts apply different approaches to accessing the suitability of data, often because it is difficult to provide quantitative estimates of the level of certainty/uncertainty (Benke, 2007). Here, it is better not to attempt to provide a step-by-step procedure for assessing data quality but rather to provide different facets of the term ‘suitable’ that should be considered. First, the integrity of the data must be assessed mostly through the metadata. Information on sources of data, instrument type, measuring technique, sampling technique, any pre-analysis done etc., provided with the dataset, should be checked against the minimum standards required to match the model complexity and purpose. Where the source of data is unknown, units are inconsistent, transcription errors are present, the data collection method is not approved or data tampering is suspected, then this data should be eliminated from the dataset. Second, the dataset characteristics should be assessed. Aspects such as length, scales, missing values and data frequency should match the modelling purpose. For example, for climate-change analysis, a minimum of 50 years of recorded meteorological data is

suggested (Bonell & Bruijnzeel, 2005). For hydrological analysis, an ideal dataset should include average, wet and dry years to ensure that all relevant hydrological processes are activated. Any missing values and gaps should be examined and decisions on whether or not to fill missing values made. Where frequencies and scales differ, decisions of whether or not to aggregate/summarize/harmonize data to ensure consistency should be made. The modeller must also be able to obtain adequate information, especially for the most influential parameters, from the data available. For all missing information, the use of surrogate data, i.e. data that is used in place of unavailable data ostensibly required by the model should be considered. This may include data obtained from published literature. Finally, the data required for calibration and validation must be selected carefully. Data used for calibration purposes directly influences the results of the modelling exercise. Assuming that the catchment problems have been properly identified, it is presumed that the performance of the model simulation for both calibration and validation is a strong indicator of the adequacy of the dataset used. Thus, the calibration process itself should be as robust as possible to adequately assess model performance. Ideal calibration should i.) use multiple statistical measures to assess the quality of outputs, ii.) consider more than one constituent of the hydrologic cycle and iii.) assess the uncertainty of the model inputs that translates to the model responses (Gupta et al., 1998; Kamamia et al., 2019; Moriasi et al., 2007; Westerberg et al., 2011). Model evaluation guidelines such as that provided by Moriasi et al. (2007) categorize model performance (depending on the calibration and statistics) as 'very good', 'good', 'fair' or 'satisfactory'. Good model performance means that the model closely matches the behaviour of the real system it represents (Gupta et al., 1998). Moriasi et al. (2007) proposed that stricter performance ratings be followed where the model use will lead to serious consequences, such as change in policies and water regulation.

However, models are only abstract representations of the reality, and as such they naturally have distinct limitations. It is important that the modellers understand the model structure and parameterization to employ it in the required context to overcome these limitations. Moreover, they should properly communicate the implications of these limitations for the modelling results, as they are important in informing decisions (Bremer et al., 2020). Most hydrologic models were developed for the biophysical conditions of the temperate zone and may not adequately represent similar processes occurring differently in the tropics. For example, the plant growth component of the SWAT is based on temperature climate which

is characterized with day-length driven dormancy and seasonal shedding (Neitsch et al., 2011), which do not occur in the tropics. Thus, it is not able to simulate perennial vegetation dynamics in the tropics. Within Paper I, several adjustments to the plant growth component were made to ensure the continuous growth of both trees and perennials.

When faced with insufficient data for physically based models, the modeller may opt for simpler empirical models. Empirical models, also referred to as black box models, explain the relation between input and output of the data relationship (Devia et al., 2015). Despite being less data intense than physically based models (see chapter 1) good quality input data is critical for reducing uncertainty during their application. At the regional scale, input data may not exist, resulting in the use of global data to extract the required input parameters. Although global datasets are now readily available and highly evolved, making them useful in these models, they are not subservient to observed/real measured data. Good quality data for regional assessment refers not only to the accuracy of the input data but also to the spatial and temporal resolution of it. These characteristics are difficult to achieve for coarse global products (Wohl et al., 2012). Most of the global data is prepared from extrapolation methods, with most observed/measured data coming from the developed countries. For instance, the rainfall erosivity data that serves as an input in the global soil Erosion Map (GloSEM) was prepared using data from 3,625 precipitation stations, with Europe contributing 48% (Borrelli et al., 2017). Africa contributed only 5% to the database, meaning that there is higher uncertainty in soil loss estimates of Africa and observed data is necessary to correct for this (Wohl et al., 2012). Consequently, global data includes a lot of generalization in which relevant information is lost. This was verified by the analysis of Paper IV, where regional monthly erosion soil maps developed using the empirically based revised universal soil loss equation (RUSLE) displayed small-scale spatial soil heterogeneity, which exposed various erosion hotspots that were not captured by the global soil erosion map (GloSEM). This implies that with good quality data, empirical models are adequate and important in analysing trends and exposing critical source areas and sinks.

In many regions in Africa, and at the regional scale, obtaining the data required to drive hydrologic models or even simple empirical models still remains a challenge. This research has established that this challenge can be overcome by exploiting improved sampling and predictive methods and outputs from advanced remote-sensing techniques. Improved

sampling methods, such as conditioned Latin Hypercube Sampling (cLHS), reduce the need for intensive soil sampling while still capturing spatial variability (Kamamia et al., 2021). Improved prediction tools, such as data-mining tools, have highly evolved and are designed to explore large amounts of data and different parameters. Satellite-based technologies, such as Landsat TM Enhanced Thematic Mapper (ETM+), Moderate Resolution Imaging Spectoradiometer (MODIS), Advanced Speceborne Thermal Emission and Reflection Radiometer (ASTER), now provide readily and freely available digital images wherefrom environmental indicators such as land-use/land cover can be obtained with high precision (Lagacherie, 2008; Mora-Vallejo et al., 2008). New sensors, such as laser, radar and hyperspectral imagers, now provide more absolute and spatially dense measurements of variables only measurable from the ground (Bonell & Bruijnzeel, 2005). This information provides a cost-effective mechanism for extrapolation of point-based measurements using techniques such as digital soil mapping (DSM). Furthermore, DSM allows for easy inclusion of the estimation of the quality of predictions through uncertainty analysis, which increases their acceptability. Uncertainty analysis is often neglected in the evaluation of complex systems but is inherent in models owing to the inherent uncertainties of the processes they represent. Uncertainties in the results stem from uncertainties in data input, calibration data, imperfect model structure and the parameters estimated (Solomatine & Shrestha, 2009). Thus, it is important for decision makers to know the confidence level of the predictions, as catchment-management decisions are based on these results. The analysis in Paper III validated that with limited soil samples, the use of computing power, machine learning and freely available covariates/environmental variables, DSM can be applied effectively to predict aggregate stability for a catchment with little observed data. The prediction interval was attached to this prediction, thus acknowledging the uncertainty in the predictions.

4.2. Selecting catchment management strategies based on catchment assessment

Outputs from basic application of hydrologic modelling for catchment management comprise information on runoff, soil erosion, sedimentation, streamflow, flood forecasting, drought assessment and water quality and quantity. These outputs (in isolation) are similar to those produced using the methods prescribed for data-scarce areas. Although methods for data-scarce catchment assessment are able to maintain a thorough representation of the main environmental and anthropogenic factors, they reduce a very complex system into a simple one for one objective/process (Borrelli et al., 2017). Accordingly, catchment management strategies (CMS) must be directed towards solving a single objective. For example, digital soil mapping was undertaken on aggregate stability to site erosion hotspots (paper III). Likewise, the revised universal soil loss equation (Paper IV) was applied for erosion prediction. Time-dependent CMS, such as timely tilling of land, and more permanent CMS, such as road embankments and terraces, were recommended for dynamic and permanent erosion hotspots (Papers III and IV). The effectiveness of such CMSs can only be assessed by adjusting the inputs to reflect the changes and reanalysing for the same objective. Yet, it is known that most CMS improve multiple ecosystem services concurrently (Kamamia et al., 2021), e.g. terraces not only control erosion but also have an effect on runoff reduction, soil water storage, transport and discharge and nutrient enhancement (Kosmowski, 2018), all of which cannot be simultaneously simulated and quantified using simple catchment assessment methods.

Advanced use of hydrologic models allows for different outputs/objectives to be assessed simultaneously. Catchment management problems are usually diverse and inter-related (Mwangi et al., 2016a, b). Hydrologic models adequately depict the various catchment components and processes (including their interconnectivity) within the hydrologic cycle. They are also able to integrate across spatial and temporal scales. This ensures better understanding of the major catchment problems. Different CMSs can be simulated using models, either in isolation or combined. The implications of the CMSs on the various ecosystem services and at different scales can be assessed iteratively (Bremer et al., 2020). Hydrologic models have been supplemented with multi-objective optimization tools that manipulate simulations of different CMSs to automatically produce non-dominated solutions which can then be deliberated upon by the relevant stakeholders (Paper II).

5. CONCLUSION AND RECOMMENDATIONS

This research was motivated by a transition towards developing knowledge- to- concrete actions. It serves as a harbinger of how to solve unprecedented catchment problems in areas with or/and without data and provides readily implementable solutions adapted to their own complex local conditions and circumstances. It provides a conceptual scientific structure for catchment management, which in the past had mostly been guided by comparative evaluations based on intuition, past experience and political assessments alone.

As recommendations, further studies in the Nyangores catchment should include assessment of the impact of adopting additional vegetative, agronomic, management and structural measures (not covered). For example, it would be worthwhile to assess the effect of no till/minimum tillage/conservation tillage, the use of terraces and contour bunds (either in isolation or combined) on water resources. Cost-benefit analysis implementing CMSs should be incorporated to include both on-/off-site and long-/short-term benefits. This evaluation offers a traceable procedure for translating impacts into economic terms that are easily understood by stakeholders. Future research should also extend the use of CoMOLA to the larger Mara basin. Studies such as Dick et al. (2014) and Lee and Lautenbach (2016) have reported that some functions such as those leading to water regulation may be diminished at smaller scales, and there is a need to consider interactions across multiple scales. For the Ruiru catchment, further studies should be undertaken to test hypotheses such as the impact and intensity of the onset of the rainfall on soil loss in the catchment and the role of landscape factors in controlling soil loss.

The accuracy of model outputs, especially for regional catchment assessments rely heavily on the availability of quality data. Therefore, given the insufficient data in both Nyangores and Ruiru catchments, more effort should be put into setting up data acquisition infrastructure such as river gauging stations, climate stations, sediment samplers and yield records where they do not exist. Soil data acquisition through integrative field campaigns is especially important not only in the study areas but also in many catchments throughout Kenya that remain largely unexplored. Such field campaigns would aid in improving our understanding of the tropical soil-water-atmosphere nexus and in designing better catchment management plans. It has been reported that climate change compounded with anthropogenic activities has resulted in greater spatial-temporal variability in different

aspects of hydrology: fluxes of energy and water within vegetation, as well as land surface and subsurface, in ways that are unknown and would be exposed with stringent monitoring (Wohl et al., 2012).

Finally, the key to thriving catchments aiming at both sustainability and resilience requires urgent collaborative action by all stakeholders. Gone are the days where responses to land degradation were solved in a purely technical way. Social acceptability of catchment management strategies by stakeholders such as farmers dictate the success of their implementation. For both the Ruiru reservoir and the Nyangores catchment, public education of the issues surrounding land degradation must be communicated. The necessary stakeholders must then be involved in catchment assessment in order to identify the catchment problems, mitigation strategies/roles and responsibilities while keeping in mind that some risks need to be shared and negotiated, but so will the benefits.

6. REFERENCES

Addis, H. K., & Klik, A. (2015). Predicting the spatial distribution of soil erodibility factor using USLE nomograph in an agricultural watershed, Ethiopia. *International Soil and Water Conservation Research*, *3*(4), 282–290. https://doi.org/10.1016/j.iswcr.2015.11.002

Alewell, C., Borrelli, P., Meusburger, K., & Panagos, P. (2019). Using the USLE: Chances, challenges and limitations of soil erosion modelling. *International Soil and Water Conservation Research*, *7*(3), 203–225. https://doi.org/10.1016/j.iswcr.2019.05.004

Alexandridis, T. K., Sotiropoulou, A. M., Bilas, G., Karapetsas, N., & Silleos, N. G. (2015). The Effects of Seasonality in Estimating the C-Factor of Soil Erosion Studies. *Land Degradation & Development*, *26*(6), 596–603. https://doi.org/10.1002/ldr.2223

Angulo-Martínez, M., López-Vicente, M., Vicente-Serrano, S. M., & Beguería, S. (2009). Mapping rainfall erosivity at a regional scale: A comparison of interpolation methods in the Ebro Basin (NE Spain). *Hydrology and Earth System Sciences*, *13*(10), 1907–1920. https://doi.org/10.5194/hess-13-1907-2009

Arnold, J. G., Moriasi, D. N., Gassman, P. W., Abbaspour, K., White, M. J., Srinivasan, R., Santhi, C., Harmel, R. D., van Griensven, A., Van Liew, M. W., Kannan, N., & Jha, M. K. (2012). SWAT: Model Use, Calibration, and Validation. *Transactions of the ASABE*, *55*(4), 1491–1508. https://doi.org/10.13031/2013.42256

Arnold, J. G., Srinivasan, R., Muttiah, R. S., & Williams, J. R. (1998). Large Area Hydrologic Modeling and Assessment Part I: Model Development1. *JAWRA Journal of the American Water Resources Association*, *34*(1), 73–89. https://doi.org/10.1111/j.1752-1688.1998.tb05961.x

Avalos, F. A. P., Silva, M. L. N., Batista, P. V. G., Pontes, L. M., & Oliveira, M. S. de. (2018). Digital soil erodibility mapping by soilscape trending and kriging. *Land Degradation & Development*, *29*(9), 3021–3028. https://doi.org/10.1002/ldr.3057

A-Xing, Z., Burt, J. E., Moore, A. C., & Smith, M. P. (2007, January). *SoLIM: A New Technology for Soil Mapping Using GIS, Expert Knowledge & Fuzzy Logic Overview Prepared by*. ResearchGate. https://www.researchgate.net/publication/237540442_SoLIM_A_New_Technology_For_Soil_Mapping_Using_GIS_Expert_Knowledge_Fuzzy_Logic_Overview_Prepared_by

Benavidez, R., Jackson, B., Maxwell, D., & Norton, K. (2018). A review of the (Revised) Universal Soil Loss Equation ((R)USLE): With a view to increasing its global applicability and improving soil loss estimates. *Hydrology and Earth System Sciences*, *22*(11), 6059–6086. https://doi.org/10.5194/hess-22-6059-2018

Benke, K. author. (2007). *Uncertainty modelling and risk analysis in hydrology and spatial systems*. Dept. of Primary Industries.

Bissonnais, Y. L. (2016). Aggregate stability and assessment of soil crustability and erodibility: I. Theory and methodology. *European Journal of Soil Science*, *67*(1), 11–21. https://doi.org/10.1111/ejss.4_12311

Bissonnais, Y. (1996). Aggregate stability and assessment of soil crustability and erodibility: II. Theory and methodology. *European Journal of Soil Science*, *47*(4), 425–437. https://doi.org/10.1111/j.1365-2389.1996.tb01843.x

Bonell, M., & Bruijnzeel, L. A. (Eds.). (2005). *Forests, Water and People in the Humid Tropics: Past, Present and Future Hydrological Research for Integrated Land and Water Management*.

Cambridge University Press. https://doi.org/10.1017/CBO9780511535666

Borrelli, P., Robinson, D. A., Fleischer, L. R., Lugato, E., Ballabio, C., Alewell, C., Meusburger, K., Modugno, S., Schütt, B., Ferro, V., Bagarello, V., Oost, K. V., Montanarella, L., & Panagos, P. (2017). An assessment of the global impact of 21st century land use change on soil erosion. *Nature Communications*, *8*(1), 2013. https://doi.org/10.1038/s41467-017-02142-7

Bremer, L. L., Hamel, P., Ponette-González, A. G., Pompeu, P. V., Saad, S. I., & Brauman, K. A. (2020). Who Are We Measuring and Modeling for? Supporting Multilevel Decision-Making in Watershed Management. *Water Resources Research*, *56*(1), e2019WR026011. https://doi.org/10.1029/2019WR026011

Brungard, C. W., & Boettinger, J. L. (2010). Conditioned Latin Hypercube Sampling: Optimal Sample Size for Digital Soil Mapping of Arid Rangelands in Utah, USA. In J. L. Boettinger, D. W. Howell, A. C. Moore, A. E. Hartemink, & S. Kienast-Brown (Eds.), *Digital Soil Mapping: Bridging Research, Environmental Application, and Operation* (pp. 67–75). Springer Netherlands. https://doi.org/10.1007/978-90-481-8863-5_6

Calder, I. R. (1993). Hydrologic Effects of Land-use change. In *Handbook of Hydrology*. McGraw-Hill. https://www.mheducation.co.uk/handbook-of-hydrology-9780070397323-emea

Chapagain, A., Shimabuku, M., Morrison, J., Brill, G., Matthews, J. H., Davis, K., Ruckstuhl, S., & Strong, C. (2021). *Water Resilience Assessment Framework*. Alliance for Global Water Adaptation, CEO Water Mandate, International Water Management Institute, Pacific Institute, and World Resources Institute. https://ceowatermandate.org/wp-content/uploads/2021/08/CEOWater_WRAF_r5_web.pdf

Delelegn, Y. T., Purahong, W., Blazevic, A., Yitaferu, B., Wubet, T., Göransson, H., & Godbold, D. L. (2017). Changes in land use alter soil quality and aggregate stability in the highlands of northern Ethiopia. *Scientific Reports*, *7*(1), 13602. https://doi.org/10.1038/s41598-017-14128-y

Devia, G. K., Ganasri, B. P., & Dwarakish, G. S. (2015). A Review on Hydrological Models. *Aquatic Procedia*, *4*, 1001–1007. https://doi.org/10.1016/j.aqpro.2015.02.126

Dick, J., Maes, J., Smith, R. I., Paracchini, M. L., & Zulian, G. (2014). Cross-scale analysis of ecosystem services identified and assessed at local and European level. *Ecological Indicators*, *38*, 20–30. https://doi.org/10.1016/j.ecolind.2013.10.023

Dubey, S. (2018). A Review of Approach Pattern of Watershed Management in Agroforestry, Climate Change, Social Aspects and Livelihoods. *International Journal of Science and Research (IJSR)*, *7*(10), 169–175.

Duffy, C. J., & Yu, X. (2018). *Hillslope and Watershed Hydrology*. MDPI. https://www.mdpi.com/books/pdfview/book/717

Emmerich, M. T. M., & Deutz, A. H. (2018). A tutorial on multiobjective optimization: Fundamentals and evolutionary methods. *Natural Computing*, *17*(3), 585–609. https://doi.org/10.1007/s11047-018-9685-y

Ferrier, R. C., & Jenkins, A. (2009). *Handbook of Catchment Management*. John Wiley & Sons.

Forest Declaration. (2021, August 13). *Forest Declaration*. https://forestdeclaration.org/

Gathagu, J. N., Mourad, K. A., & Sang, J. (2018). Effectiveness of Contour Farming and Filter Strips on Ecosystem Services. *Water*, *10*(10), 1312. https://doi.org/10.3390/w10101312

Gaubi, I., Chaabani, A., Ben Mammou, A., & Hamza, M. H. (2017). A GIS-based soil erosion prediction using the Revised Universal Soil Loss Equation (RUSLE) (Lebna watershed, Cap Bon, Tunisia). *Natural Hazards*, *86*(1), 219–239. https://doi.org/10.1007/s11069-016-2684-3

Geiger, M. J., & Sevaux, M. (2011). The Biobjective Inventory Routing Problem – Problem Solution and Decision Support. In J. Pahl, T. Reiners, & S. Voß (Eds.), *Network Optimization* (pp. 365–378). Springer. https://doi.org/10.1007/978-3-642-21527-8_41

Gupta, H. V., Sorooshian, S., & Yapo, P. O. (1998). Toward improved calibration of hydrologic models: Multiple and noncommensurable measures of information. *Water Resources Research*, *34*(4), 751–763. https://doi.org/10.1029/97WR03495

Hammad, A. A., Lundekvam, H., & Børresen, T. (2004). Adaptation of RUSLE in the Eastern Part of the Mediterranean Region. *Environmental Management*, *34*(6), 829–841. https://doi.org/10.1007/s00267-003-0296-7

Hooper, B. P., Sabatier, P. A., Focht, W., Lubell, M., Trachtenberg, Z., Vedlitz, A., & Matlock, M. (2007). Swimming Upstream. Collaborative Approaches to Watershed Management. *Knowledge, Technology & Policy*, *20*(3), 215–217. https://doi.org/10.1007/s12130-007-9023-7

Jakeman, A. J., & Letcher, R. A. (2003). Integrated assessment and modelling: Features, principles and examples for catchment management. *Environmental Modelling and Software*, *6*(18), 491–501. https://doi.org/10.1016/S1364-8152(03)00024-0

Kaim, A., Cord, A. F., & Volk, M. (2018). A review of multi-criteria optimization techniques for agricultural land use allocation. *Environmental Modelling & Software*, *105*, 79–93. https://doi.org/10.1016/j.envsoft.2018.03.031

Kamamia, A. W., Mwangi, H. M., Feger, K.-H., & Julich, S. (2019). Assessing the impact of a multimetric calibration procedure on modelling performance in a headwater catchment in Mau Forest, Kenya. *Journal of Hydrology: Regional Studies*, *21*, 80–91. https://doi.org/10.1016/j.ejrh.2018.12.005

Kamamia, A. W., Vogel, C., Mwangi, H. M., Feger, K.-H., Sang, J., & Julich, S. (2021). Mapping soil aggregate stability using digital soil mapping: A case study of Ruiru reservoir catchment, Kenya. *Geoderma Regional*, *24*, e00355. https://doi.org/10.1016/j.geodrs.2020.e00355

Khan, H. F., Yang, Y. C. E., Xie, H., & Ringler, C. (2017). A coupled modeling framework for sustainable watershed management in transboundary river basins. *Hydrology and Earth System Sciences*, *21*(12), 6275–6288. https://doi.org/10.5194/hess-21-6275-2017

Kinnell, P. I. A. (2010). Event soil loss, runoff and the Universal Soil Loss Equation family of models: A review. *Journal of Hydrology*, *385*(1), 384–397. https://doi.org/10.1016/j.jhydrol.2010.01.024

Kosmowski, F. (2018). Soil water management practices (terraces) helped to mitigate the 2015 drought in Ethiopia. *Agricultural Water Management*, *204*, 11–16. https://doi.org/10.1016/j.agwat.2018.02.025

Kumawat, A., Yadav, D., Samadharmam, K., & Rashmi, I. (2020). Soil and Water Conservation Measures for Agricultural Sustainability. In *Soil Moisture Importance*. IntechOpen. https://doi.org/10.5772/intechopen.92895

Lagacherie, P. (2008). Digital Soil Mapping: A State of the Art. In A. E. Hartemink, A. McBratney, & M. de L. Mendonça-Santos (Eds.), *Digital Soil Mapping with Limited Data* (pp. 3–14). Springer Netherlands. https://doi.org/10.1007/978-1-4020-8592-5_1

Lal, R. (1993). Tillage effects on soil degradation, soil resilience, soil quality, and sustainability. *Soil and Tillage Research*, *27*(1), 1–8. https://doi.org/10.1016/0167-1987(93)90059-X

Lal, R. (1997). Degradation and resilience of soils. *Philosophical Transactions of the Royal Society B: Biological Sciences*, *352*(1356), 997–1010. https://doi.org/10.1098/rstb.1997.0078

Lautenbach, S., Volk, M., Strauch, M., Whittaker, G., & Seppelt, R. (2013). Optimization-based trade-off analysis of biodiesel crop production for managing an agricultural catchment. *Environmental Modelling & Software*, *48*, 98–112. https://doi.org/10.1016/j.envsoft.2013.06.006

Lea, D., Bull, V., Duncan, R., & Webb, S. S. (2014). *Oxford Learner's Dictionary of Academic English*. Oxford University Press.

Lee, H., & Lautenbach, S. (2016). A quantitative review of relationships between ecosystem services. *Ecological Indicators*, *66*, 340–351. https://doi.org/10.1016/j.ecolind.2016.02.004

Liniger, H. P., Cahill, D., Critchley, W., van Lynden, G. W. J., & Schwilch, G. (2002). Categorization of SWC Technologies and Approaches. *Yumpu.Com*. 12th ISCO Conference, Beijing.

Maglogiannis, I. G. (2007). *Emerging Artificial Intelligence Applications in Computer Engineering: Real Word AI Systems with Applications in EHealth, HCI, Information Retrieval and Pervasive Technologies*. IOS Press.

Maloi, S. K., Sang, J. K., Raude, J. M., Mutwiwa, U. N., Mati, B. M., & Maina, C. W. (2016). Assessment of Sedimentation Status of Ruiru Reservoir, Central Kenya. *American Journal of Water Resources*, *4*(4), 77–82. https://doi.org/10.12691/ajwr-4-4-1

Malone, B. P., Minasny, B., & McBratney, A. B. (2017). *Using R for Digital Soil Mapping*. Springer International Publishing. https://doi.org/10.1007/978-3-319-44327-0

Mati, B. M., Mutie, S., Gadain, H., Home, P., & Mtalo, F. (2008). Impacts of land-use/cover changes on the hydrology of the transboundary Mara River, Kenya/Tanzania. *Lakes & Reservoirs: Science, Policy and Management for Sustainable Use*, *13*(2), 169–177. https://doi.org/10.1111/j.1440-1770.2008.00367.x

Millennium Ecosystem Assessment (MEA). (2005). Island Press.

Mitchell, M. (1996). *An Introduction to Genetic Algorithms*. A Bradford Book.

Mitruț, C., & Bratu, M. S. (2014). A Procedure for Selecting the Best Proxy Variable Used in Predicting the Consumer Prices Index in Romania. *Procedia Economics and Finance*, *10*, 178–184. https://doi.org/10.1016/S2212-5671(14)00291-3

Mora-Vallejo, A., Claessens, L., Stoorvogel, J., & Heuvelink, G. B. M. (2008). Small scale digital soil mapping in Southeastern Kenya. *Catena*, *76*(1), 44–53. https://doi.org/10.1016/j.catena.2008.09.008

Moriasi, D. N., Arnold, J. G., Van Liew, M. W., Bingner, R. L., Harmel, R. D., & Veith, T. L. (2007). Model Evaluation Guidelines for Systematic Quantification of Accuracy in Watershed Simulations. *Transactions of the ASABE*, *50*(3), 885–900. https://doi.org/10.13031/2013.23153

Mwangi, H. M., Julich, S., & Feger, K.-H. (2016a). Introduction to Watershed Management. In L. Pancel & M. Köhl (Eds.), *Tropical Forestry Handbook* (pp. 1869–1896). Springer Berlin Heidelberg. https://doi.org/10.1007/978-3-642-54601-3_153

Mwangi, H. M., Julich, S., Patil, S. D., McDonald, M. A., & Feger, K.-H. (2016b). Modelling the impact of agroforestry on hydrology of Mara River Basin in East Africa. *Hydrological Processes*, *30*(18), 3139–3155. https://doi.org/10.1002/hyp.10852

Mwangi, H. M., Julich, S., Patil, S. D., McDonald, M. A., & Feger, K.-H. (2016c). Relative contribution of land use change and climate variability on discharge of upper Mara River, Kenya. *Journal of Hydrology: Regional Studies*, *5*, 244–260. https://doi.org/10.1016/j.ejrh.2015.12.059

Mwangi, J. K., Shisanya, C. A., Gathenya, J. M., Namirembe, S., & Moriasi, D. N. (2015). A modeling approach to evaluate the impact of conservation practices on water and sediment yield in Sasumua Watershed, Kenya. *Journal of Soil and Water Conservation*, *70*(2), 75–90. https://doi.org/10.2489/jswc.70.2.75

Neitsch, S. L., Arnold, J. G., Kiniry, J. R., & Williams, J. R. (2011). *Soil and Water Assessment Tool Theoretical Documentation Version 2009* (Technical Report No. 406; Texas Water Resources Institute Technical Report). Texas Water Resources Institute. https://swat.tamu.edu/media/99192/swat2009-theory.pdf

Nyakundi, R., Mwangi, J., Makokha, M., & Obiero, C. (2017). Analysis of Rainfall Trends and Periodicity in Ruiru Location, Kenya. *International Journal of Scientific and Research Publications*, *7*(3), 28–39.

Panagopoulos, Y., Makropoulos, C., & Mimikou, M. (2012). Decision support for diffuse pollution management. *Environmental Modelling & Software*, *30*, 57–70. https://doi.org/10.1016/j.envsoft.2011.11.006

Panagos, P., Borrelli, P., Spinoni, J., Ballabio, C., Meusburger, K., Begueria, S., Klik, A., Michaelides, S., Petan, S., Hrabalikova, M., Olsen, P., Aalto, J., Lakatos, M., Rymszewicz, A., Dumitrescu, A., Percec Tadic, M., Diodato, N., Kostalova, J., Rousseva, S., … Alewell, C. (2016). Monthly Rainfall Erosivity: Conversion Factors for Different Time Resolutions and Regional Assessments. *Water*, *8*(119), Article 119. https://ec.europa.eu/jrc/en/publication/monthly-rainfall-erosivity-conversion-factors-different-time-resolutions-and-regional-assessments

Panagos, P., Meusburger, K., Ballabio, C., Borrelli, P., & Alewell, C. (2014). Soil erodibility in Europe: A high-resolution dataset based on LUCAS. *Science of The Total Environment*, *479–480*, 189–200. https://doi.org/10.1016/j.scitotenv.2014.02.010

Perry, C. H., Miller, R. C., Kaster, A. R., & Brooks, K. N. (2000). *Watershed management implications of agroforestry expansion on Minnesota's farmlands*. https://www.nrs.fs.fed.us/pubs/42060

Pfannerstill, M., Bieger, K., Guse, B., Bosch, D. D., Fohrer, N., & Arnold, J. G. (2017). How to Constrain Multi-Objective Calibrations of the SWAT Model Using Water Balance Components. *JAWRA Journal of the American Water Resources Association*, *53*(3), 532–546. https://doi.org/10.1111/1752-1688.12524

Ray, S. (2019). A Quick Review of Machine Learning Algorithms. *2019 International Conference on Machine Learning, Big Data, Cloud and Parallel Computing (COMITCon)*, 35–39. https://doi.org/10.1109/COMITCon.2019.8862451

Renard, K. G., Laflen, J. M., Foster, G. R., McCool, D. K., Laflen, J. M., Foster, G. R., & McCool, D. K. (2017, October 19). *The Revised Universal Soil Loss Equation*. Soil Erosion Research Methods; Routledge. https://doi.org/10.1201/9780203739358-5

Reynolds, E. R. C., Thompson, F. B., & University, U. N. (1988). *Forests, climate, and hydrology:*

United Nations University. https://digitallibrary.un.org/record/196372

Rodriguez, H. G., Popp, J., Maringanti, C., & Chaubey, I. (2011). Selection and placement of best management practices used to reduce water quality degradation in Lincoln Lake watershed. *Water Resources Research*, *47*(1). https://doi.org/10.1029/2009WR008549

Sang, J., Raude, J., Mati, B., Mutwiwa, U., & Ochieng, F. (2017). Dual Echo Sounder Bathymetric Survey for Enhanced Management of Ruiru Reservoir, Kenya. *Journal of Sustainable Research in Engineering*, *3*(4), 113-118.

Schmidt, S., Alewell, C., & Meusburger, K. (2018). Mapping spatio-temporal dynamics of the cover and management factor (C-factor) for grasslands in Switzerland. *Remote Sensing of Environment*, *211*, 89–104. https://doi.org/10.1016/j.rse.2018.04.008

Schmidt, S., Alewell, C., & Meusburger, K. (2019). Monthly RUSLE soil erosion risk of Swiss grasslands. *Journal of Maps*, *15*(2), 247–256. https://doi.org/10.1080/17445647.2019.1585980

Schmidt, S., Alewell, C., Panagos, P., & Meusburger, K. (2016). *Seasonal Dynamics of Rainfall Erosivity in Switzerland* [Preprint]. Ecohydrology/Modelling approaches. https://doi.org/10.5194/hess-2016-208

SCSA. (1982). Resource conservation glossary. Ankeny, Iowa. USA.

Shukla, M. (2011). *Soil Hydrology, Land Use and Agriculture- Measurement and Modelling*.

Schwertmann, U., Vogl, W., & Kainz, M. (1987). Bodenerosion durch Wasser: Vorhersage des Abtrags und Bewertung von Gegenmaßnahmen. Ulmer, Stuttgart

Singh, A., Thakur, N., & Sharma, A. (2016). A review of supervised machine learning algorithms. *2016 3rd International Conference on Computing for Sustainable Global Development (INDIACom)*, 1310–1315.

Singh, V. P. (2018). Hydrologic modeling: Progress and future directions. *Geoscience Letters*, *5*(1), 15. https://doi.org/10.1186/s40562-018-0113-z

Solomatine, D. P., & Shrestha, D. L. (2009). *A novel method to estimate model uncertainty using machine learning techniques*. https://doi.org/10.1029/2008WR006839

Speranza, C. I. (2010). *Resilient adaptation to climate change in African agriculture*. Deutsches Institut für Entwicklungspolitik. https://www.die-gdi.de/uploads/media/Studies_54.pdf

Strauch, M., Cord, A. F., Pätzold, C., Lautenbach, S., Kaim, A., Schweitzer, C., Seppelt, R., & Volk, M. (2019). Constraints in multi-objective optimization of land use allocation – Repair or penalize? *Environmental Modelling & Software*, *118*, 241–251. https://doi.org/10.1016/j.envsoft.2019.05.003

Tachikawa, K., R, A., L., V., & C., J. (2019). Trace element and isotope proxies in paleoceanography: Starting a new synergic effort around marine geochemical proxies. *Past Global Changes Magazine*, *27*(1). https://doi.org/10.22498/pages.27.1.35

Van Loon, E., & Refsgaard, J. C. (2005). *Guidelines for assessing data uncertainty in river basin management studies*. Geological Survey of Denmark and Greenland.

Veldkamp, E., Schmidt, M., Powers, J. S., & Corre, M. D. (2020). Deforestation and reforestation impacts on soils in the tropics. *Nature Reviews Earth & Environment*, *1*(11), 590–605.

https://doi.org/10.1038/s43017-020-0091-5

Vergara, N. T. (1991). CHAPTER 9. The Potential Role of Agroforestry in Watershed Management. In *Watershed Resources Management* (pp. 119–130). ISEAS Publishing. https://www.degruyter.com/document/doi/10.1355/9789814345880-013/pdf

Vlek, P. L. G., Le, Q. B., & Tamene, L. (2010). Asessment of land degradation, its possible causes and threat to food security in Sub-Saharan Africa. In *Food security and soil quality*. CRC Press.

Wadoux, A. M. J.-C., Minasny, B., & McBratney, A. B. (2020). Machine learning for digital soil mapping: Applications, challenges and suggested solutions. *Earth-Science Reviews*, *210*, 103359. https://doi.org/10.1016/j.earscirev.2020.103359

Wang, Q., Wang, L., Huang, W., Wang, Z., Liu, S., & Savić, D. A. (2019). Parameterization of NSGA-II for the Optimal Design of Water Distribution Systems. *Water*, *11*(5), 971. https://doi.org/10.3390/w11050971

Westerberg, I. K., Guerrero, J.-L., Younger, P. M., Beven, K. J., Seibert, J., Halldin, S., Freer, J. E., & Xu, C.-Y. (2011). Calibration of hydrological models using flow-duration curves. *Hydrology and Earth System Sciences*, *15*(7), 2205–2227. https://doi.org/10.5194/hess-15-2205-2011

Wischmeier, W. H., & Smith, D. D. (1958). Rainfall energy and its relationship to soil loss. *Eos, Transactions American Geophysical Union*, *39*(2), 285–291. https://doi.org/10.1029/TR039i002p00285

Wischmeier, W. H., & Smith, D. D. (1978). *Predicting Rainfall Erosion Losses: A Guide to Conservation Planning*. Department of Agriculture, Science and Education Administration.

WOCAT (2017). Where the Land is Greener: Case studies and analysis of soil and water conservation initiatives worldwide. Wageningen: CTA.

Wohl, E., Barros, A., Brunsell, N., Chappell, N. A., Coe, M., Giambelluca, T., Goldsmith, S., Harmon, R., Hendrickx, J. M. H., Juvik, J., McDonnell, J., & Ogden, F. (2012). The hydrology of the humid tropics. *Nature Climate Change*, *2*(9), 655–662. https://doi.org/10.1038/nclimate1556

World Agroforestry. (2021). *What is Agroforestry?* World Agroforestry | Transforming Lives and Landscapes with Trees. https://www.worldagroforestry.org/about/agroforestry

WRMA. (2011). *Nyangores river sub-catchment management plan*. http://dpanther.fiu.edu/sobek/FIMA000012/00001

Yilmaz, K. K., Vrugt, J. A., Gupta, H. V., & Sorooshian, S. (2010). Model calibration in watershed hydrology. In *Advances in Data-Based Approaches for Hydrologic Modeling and Forecasting* (pp. 53–105). WORLD SCIENTIFIC. https://doi.org/10.1142/9789814307987_0003

Zhang, L. (2020). *Planting trees must be done with care – it can create more problems than it addresses*. The Conversation. http://theconversation.com/planting-trees-must-be-donewithcare-it-can-create-more-problems-than-it-addresses-128259

Zhang, L., Podlasly, C., Ren, Y., Feger, K.-H., Wang, Y., & Schwärzel, K. (2014). Separating the effects of changes in land management and climatic conditions on long-term streamflow trends analyzed for a small catchment in the Loess Plateau region, NW China. *Hydrological Processes*, *28*(3), 1284–1293. https://doi.org/10.1002/hyp.9663

Zhang, L., & Schwärzel, K. (2017). China's Land Resources Dilemma: Problems, Outcomes, and Options for Sustainable Land Restoration. *Sustainability*, *9*(12), 2362. https://doi.org/10.3390/su9122362

PART B: PAPERS

PAPER I

Journal of Hydrology: Regional Studies 21 (2019) 80–91

Contents lists available at ScienceDirect

Journal of Hydrology: Regional Studies

journal homepage: www.elsevier.com/locate/ejrh

Assessing the impact of a multimetric calibration procedure on modelling performance in a headwater catchment in Mau Forest, Kenya

Ann W. Kamamia[a,*], Hosea M. Mwangi[b], Karl-Heinz Feger[a], Stefan Julich[a]

[a] Institute of Soil Science and Site Ecology, Technische Universität Dresden, Pienner Str. 19, 01737 Tharandt, Germany
[b] Soil, Water and Environmental Engineering Department, Jomo Kenyatta University of Agriculture and Technology (JKUAT), Nairobi, Kenya

ARTICLE INFO

Keywords:
5 segmented Flow Duration Curve (5FDC)
Normal Calibration Procedure(NCP)
Parameter identifiability
Pareto set
Pareto analysis
Water balance
Multimetric calibration
Latin hypercube sampling
Performance metrics
Uncertainty
Prediction
Hydrologic model
Simulation
Equifinality
Base flows
Variability
Optimum
Stepwise intersection
Ensemble
Water partitioning

ABSTRACT

Study region: Nyangores catchment, Mara catchment, Kenya.
Study focus: Hydrologic models are widely used tools in watershed management to assist in decision making by representing catchment functions under alternative scenarios. This study focused on the evaluation of the 5 segment Flow Duration Curve based calibration procedure (5FDC) for the period 1975–1978 using the Soil Water Assessment Tool (SWAT). The Normal Calibration Procedure (NCP) based on the hydrograph was compared to the 5FDC. Two separate ensembles each containing 10 Pareto calibration runs were obtained individually from each method and evaluated based on their goodness-of-fit. A final Combined Procedure (CP), which was an intersection of 5FDC and NCP was executed. With this supplementary analysis, the parameter distribution and water component balance were analyzed and compared.
New hydrological insights for the region: The comparison of 5FDC and NCP shows that the 5FDC provides a better representation of the low and mid-level section of the flow duration curve as compared to the NCP, which greatly overestimates these flows. This method also closely matches the observed runoff ratios. This indicates that the 5FDC calibration may be well suited for water resource applications focused on low flows. The CP combines the advantages of both procedures by improving parameter identifiability, leading to better representation of high and low flows.

1. Introduction

Globally water demand is increasing due to factors such as population growth, increasing agricultural and industrial production. To meet this ever rising water demand, improvement in water resources management is required. Planning is a fundamental aspect of sustainable water resources management. Hydrological models are essential tools widely used in planning of water resources. Hydrologic models are able to efficiently integrate, study and evaluate different components of watershed's complex, dynamic and spatially variable hydrological processes (Niehoff et al., 2002; Bormann et al., 2007; Hulsman et al., 2009; Wagner et al., 2016). Therefore, by using reliable and accurate data, hydrological models can be used to assess present and future changes in water

* Corresponding author. Permanent Address : Institut für Bodenkunde und Standortslehre /Institute of Soil Science and Site Ecology, Technische Universität Dresden, Pienner Str. 19, 01737 Tharandt, Germany.
E-mail address: ann.kamamia@mailbox.tu-dresden.de (A.W. Kamamia).

https://doi.org/10.1016/j.ejrh.2018.12.005
Received 18 May 2018; Received in revised form 18 December 2018; Accepted 19 December 2018
Available online 27 December 2018

demands leading to informed management decisions on competing water uses. Other common applications of hydrological models in water resources management is prediction of impact (e.g. quantity, quality, timing) of land use and climate change on watershed hydrology.

A wide range of hydrological models exists. The models vary depending on how they represent the underlying hydrological processes. They also vary depending on how the hydrological components (e.g. model parameters) and processes are represented in time and space (Devi et al., 2015). Thus, the choice of hydrological model depends on the intended purpose (based on the output of the model) and the model structure including the level of detail of the model inputs, processes and the outputs. Whatever the type of hydrological model chosen, the reliability of the model in simulating accurate (or observed) outputs (e.g. runoff or sediment yield) needs to be examined (Kirchner, 2006; Wagener and Wheater, 2006; Westerberg et al., 2011). This is usually done by calibrating the model based on the desired model output(s).

Models are calibrated by adjusting parameters to improve model fit based on objective functions, which are used to evaluate the modelling efficiency (Gupta et al., 1998; Wagener and Wheater, 2006; Pfannerstill et al., 2017). Model calibration can be done manually or automatically by use of optimization algorithms such as Shuffled Complex Evaluation method (Duan et al., 1994), General Likelihood Uncertainty Estimation (GLUE) (Beven and Binley, 1992) and Bayesian recursive parameter estimation encompassing Sequential Uncertainty Fitting Algorithm (SUFI-2) (Thiemann et al., 2001). All these differ in their underlying assumptions, residual errors, possible iterations and types of uncertainties accounted for and represented explicitly (Samadi et al., 2017).

Normally, the accuracy of calibration of hydrological models is evaluated by statistically assessing the fit of simulated and observed hydrographs (Hrachowitz et al., 2013; Wambura et al., 2018). One advantage of this method (herein after referred as Normal Calibration Procedure NCP) is preservation of timing information (e.g. timing of runoff). However, although hydrographs represent an integrated measure reflecting all the complexity of flow processes occurring in the catchment, it is difficult to infer the nature of these processes directly (Beven, 1993). Where times for discharge and model input data do not overlap, calibration using this method may not be suitable (Westerberg et al., 2011).

An alternative to hydrograph calibration can involve use of Flow Duration Curve (FDC) (Westerberg et al., 2011). FDC is a cumulative frequency curve, which shows the percent of time specified discharges were equaled or exceeded (Vogel and Fennessey, 1994). The shape of the FDC is highly influenced by the climatological and geophysical characteristics of the catchment (Yokoo and Sivaplan, 2011), and calibration of the FDC involves matching discharge magnitudes. The method therefore inherently takes into account the influence of catchment characteristics during the calibration.

However, a major limitation of this method is that, unlike the NCP, the timing information is lost. Sawicz et al. (2011) found that splitting the FDC into individual segments in the calibration procedure led to an overall better representation of catchment characteristics. A study conducted by Pfannerstill et al. (2014) split the Flow Duration Curve into five segments (5FDC) representing: very high, high, mid, low, and very low flow segments. In this study, calibration on these segments within a multi-metric evaluation framework calibrated SWAT model adequately for both the high and low flows. Low flows are often of special interest to water resource managers who may need to consider minimum flows in order to avoid over-allocation of water (Dudgeon et al., 2006).

In this study, the main objective was to calibrate the Soil and Water Assessment Tool (SWAT; Arnold et al., 2012a) using the 5FDC procedure and compare it with the NCP. Additionally, a hybrid of NCP and 5FDC methods i.e. Combined Procedure (CP) was assessed. CP involved intersecting a final set of calibration runs from both the 5FDC and NCP. Specifically, this study aims to compare the differences in selection of optimum parameter ensembles for both the 5FDC and NCP approaches, in terms of efficiency criteria, parameter distribution, and water balance components in addition to assessing the CP method.

2. Material and methods

2.1. Study area

The Nyangores catchment, spanning an area of about 694 km^2, is located in the upper part of the Mara River basin (Fig. 1). Elevation ranges from 1900 m.a.s.l. to 2970 m.a.s.l. on the Mau escapements (Mwangi et al., 2016a). The mean annual temperature is approximately 25 °C. Bimodal seasonal rainfall, ranging between 1000 mm to 1750 mm, is linked to the annual oscillation of the Inter-tropical Convergence Zone (ITCZ) (Fürst et al., 2015). River Nyangores originates from the Kiringet area in the Mau Forest and joins with River Amala to form the Mara River. The population of this catchment, according to the census held in 2009 was 300,000 (Fürst et al., 2015) and an annual increase of 3% is projected (KNBS, 2010).

There was a 40% deforestation rate between 1972 and 1995 (Juston et al., 2014). This land-use shift brought about by increased permanent settlements and agriculture has continued to increase steadily to date (Juston et al., 2014; Mwangi et al., 2018). This has significantly affected the hydrological regime in the catchment (Mwangi et al., 2016a). Mango et al. (2011) reported that the conversion of forests to agricultural land has and will continue to decrease dry season flows. At the same time, an increased peak of high flows (7%), observed between 1973 and 2000, is expected to rise in the future (Mati et al., 2008; Mango et al., 2011).

2.2. Soil and Water Assessment Tool (SWAT)

SWAT (Arnold et al., 2012a) is a mesoscale and semi-distributed watershed model, developed by the Agricultural Research Service (ARS) of the United States Department of Agriculture (USDA) (Bekele and Nicklow, 2012). SWAT operates on a daily time step, and can predict the effects of alternative management decisions on water, sediment, and chemical yields (Winchell et al., 2013). The major model components include: weather, soil dynamics, hydrology, plant growth, nutrient availability, land management, and

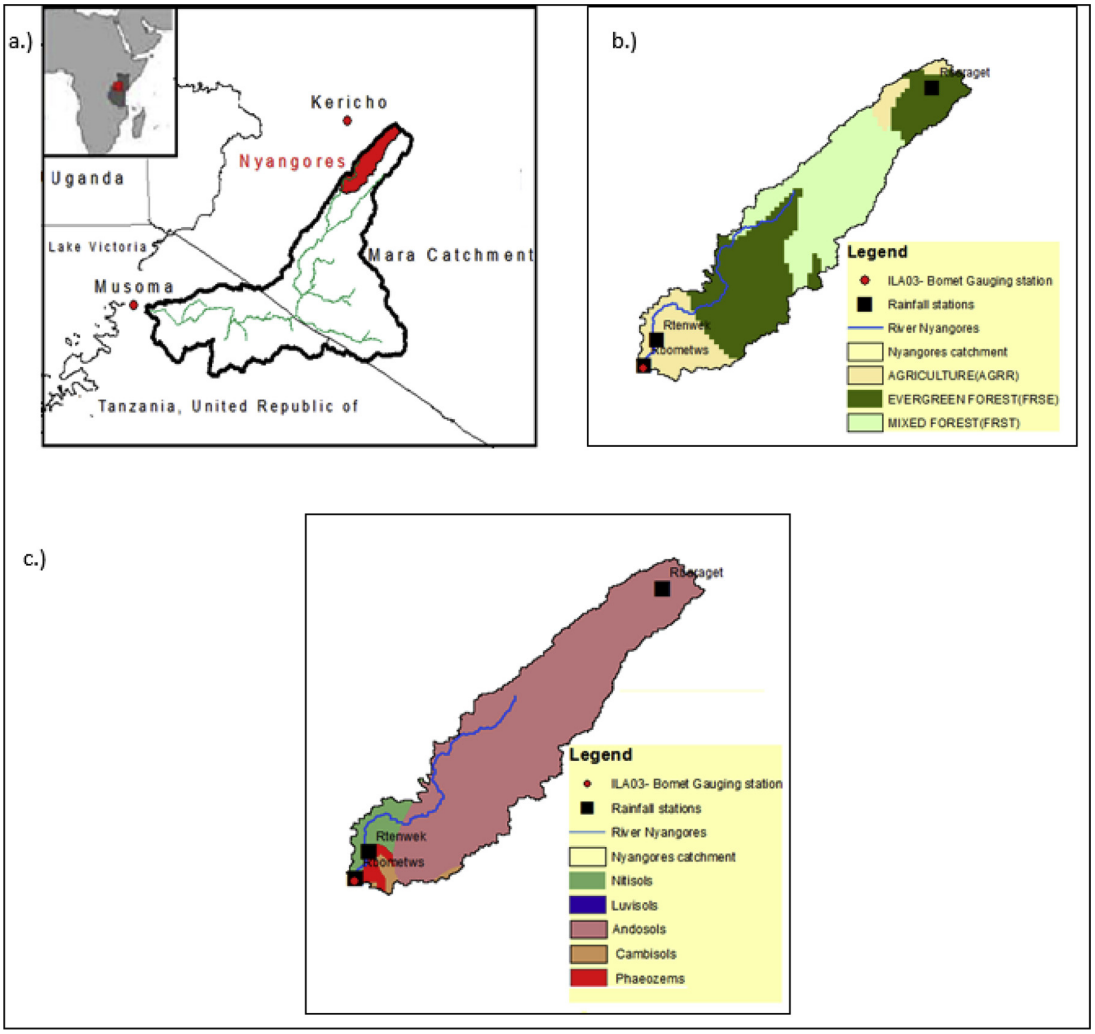

Fig. 1. Nyangores catchment. a.) Location b.) Land use c.) Soil.

pathogens. All processes are driven by the hydrologic cycle. A digital elevation model (DEM) forms the basis from which the watershed is delineated. Using the individual reaches, the basin is divided into sub-basins. Within sub-basins Hydrologic Response Units (HRU) are formed by a unique combination of land use, slope, and soil characteristics (Arnold et al., 2012a). At the HRU-Level, all processes of the hydrologic cycle are simulated. The daily volume of water yield is then estimated by solving the water budget for each HRU. A full description of the SWAT model is provided by Neitsch et al. (2005).

2.3. Catchment delineation input data

2.3.1. Hydro-meteorological data

The climatic data was obtained from the Kenya Meteorological Department (KMD) for Kisii, Kericho, and Narok stations. The data included daily data of relative humidity, wind speed, maximum and minimum temperature, and solar radiation. Daily rainfall data from twenty different individual rain gauge stations located both within and outside Nyangores catchment were used for analysis. Only three of the twenty stations are located within the Nyangores catchment, these are Baraget, Tenwek and Bomet West. The rest were included as they were located close to the centroid of the catchment. Short gaps within each data set were filled using the arithmetic mean method with the neighboring station following Mwangi et al. (2016b).

Streamflow data for the station near Bomet town (1LA03) was obtained from Water Resource Authority (WRA). This is the only gauging station with recorded data within the catchment.

2.3.2. Spatial data

The main spatial input datasets used in SWAT include the Digital Elevation Model (DEM), landuse/land cover data and soil data. The Shuttle Radar Topography Mission (SRTM) 90-m DEM was used to obtain topographic information and derive the flow pathways during watershed delineation. A land-use map of 1983 (Government of Kenya-GoK, 1983) was used for model setup, as this time period was the best match for the study. A soil vector map with a scale of 1:1 million representing the soils of the study region was obtained from the Kenya Soil Survey and Soil Terrain Database (SOTER) of the International Soil Reference and Information Centre (ISCRIC) (Batjes, 2002)

2.4. Model setup and calibration

Model setup was conducted using ArcSWAT version 2012.10.2.18. Some adjustment to the plant growth module were done according to Mwangi et al., (2016b). The adjustments were made to address the SWAT model's inability to adequately simulate perennial vegetation dynamics in the tropics (Strauch and Volk, 2013; Mwangi et al., 2016b; Alemayehu et al., 2017a, b). Trees and perennial crops in SWAT are modelled based on temperate climate, which is characterized with day-length driven dormancy and seasonal shedding and sprouting of leaves (Neitsch et al., 2005). The adjustments made included (1) increasing the minimum Leaf Area Index (LAI) from the default 0.75 to 3 for perennials, (2) reducing the Potential Heat Units (PHU) fraction from 0.15 to 0.001 and (3) using the "Kill" operation to restart the growth cycle of trees and perennial crops. The changes in the LAI are intended to ensure that continuous evapotranspiration occurs throughout the growing period of the trees and perennials (*cf.* Mwangi et al., 2016b). The adjustment in PHU ensure there is no delay in growth at the beginning of growth cycles. Plant growth in SWAT is modelled using PHU and enough heat units must be accumulated for growth to occur/start. As part of the parameterization exercise, and considering that the CN2 parameter value is adjusted daily as a function of plant evapotranspiration (Neitsch et al., 2005), the initial values for the present land uses, (FRSE (Evergreen Forest)-35, FRST (Mixed Forest)-35 and Agriculture (AGRR)-75) were modified in the database.

The model was calibrated using daily streamflow data for the station number 1LA03 near Bomet town. The data used for calibration was for the period 1972 -1978. The first three years were used as warm-up period. The selection of this period was based on quality of the data. The period had more continuous data than any other period. As indicated by Hulsman et al. (2017) there exists a long-term discharge time series between 1955 – 2015. However, the temporal coverage is poor, this is especially so for recent years. The same has also been acknowledged by other modelling studies in the watershed where authors used similar period of data for calibration e.g. Dessu and Melesse (2012) (1978–1982) and Mwangi et al., 2016b (1974–1982).

Automated Latin-Hypercube-Sampling (LHS) was performed using the FME package in R (Soetaert and Petzolt, 2010), which was used to obtain 6000 parameter sets. The model parameters selected for calibration and the range used to sample the parameter values are presented in Table 1.

2.5. Statistical and graphical model performance evaluation

Statistical performance measures quantify the ability of a model to simulate measured data (Legates and McCabe, 1999). According to studies by Guse et al. (2017) on the connective strength between model parameters and performance criteria using regression trees, a minimum of three statistical performance measures is required to represent the different parts of the hydrologic system. However, this is also dependent on the process complexity in the catchment. The different performance measures give different results based on the selected periods of observation and the types of performance measure applied (Beven, 1993). In this study, three statistical measures of performance were used (NSE, PBIAS and RSR). NSE is an ideal dimensionless objective function in

Table 1
Short description of the parameters selected for calibration and the initial value ranges.

PARAMETER NAME	DESCRIPTION	RANGES
SURLAG (surface runoff lag coefficient)	Controls the fraction of water allowed to enter the reach on any one day. As it decreases, more water is held in storage.	0-4
SOL_AWC (Soil Available Water Capacity)	Available water capacity for each soil layer. SOL_AWC = FC-PWP	−0.20-0.20
ESCO	Soil Evaporation compensation factor. As value decrease the model extracts more water from the lower levels	0 -1
CH_N2	Manning's value for the main channel	0.01-0.3
CH_K2	Effective Hydraulic Conductivity for the main channel	0-10
ALPHA_BF2	Base Flow Alpha Factor 0.1-0.3- Land responds slowly to recharge 0.9-1- Land responds fast to recharge	0.6-0.99
GW_DELAY(days)	Estimated Ground Water delay time	0-31
GW_REVAP	Groundwater re-evaporation from the shallow groundwater to the surface. As value reaches 0, water movement to upper layer is restricted	0.02-0.15
GWQMN	Threshold shallow depth required for return flow to occur. Groundwater occurs when this valued is exceeded.	150-2000
RCHRG_DP	Deep aquifer Percolation Fraction (0-1)	0.02-0.25

evaluating model performances for difference in output responses (Moriasi et al., 2015). Krause et al. (2005) concluded that its main disadvantage is its lack of sensitivity to low flow over and under-prediction. Percent Bias (PBIAS) is an error index that measures the average tendency of the simulated constituent values to be larger or smaller than the measured data. A positive value indicates the under-prediction of a model while a value of zero indicates a perfect fit of data (Moriasi et al., 2007). This may at times be deceiving as this value may be achieved where the model overpredicts as much as it underpredicts (Moriasi et al., 2015). The RMSE-observations standard deviation ratio (RSR) (Singh et al., 2004) is another error index that standardizes the Root Mean Square Error (RMSE). Its main advantage over the RMSE is its scaling factor that enables the reported values to apply to various constituents. It is also less focused on high flows. Graphical performance measures involve direct or derived visual comparison of simulated and measured data (Moriasi et al., 2015). They are usually used to complement statistical performance measures to capture distinct aspects of the model such as identifying differences in peak shapes and timings (Moriasi et al., 2015; Biondi et al., 2012). The statistical software R was used in analysis of the statistical performance measures (R Core Team, 2013). Parameter set selection was done based on the statistical metrics described above assessed using the R packages HydroGoF and HydroTSM (Zambrano-Bigiarini, 2014). Both the hydrograph and the Flow Duration Curve (FDC) graphical performance measures were used to complement this analysis.

2.6. Application of the 5FDC and NCP calibration procedure

Calibration of the FDCs and hydrographs was undertaken for the years between 1975 and 1978. This step involved the construction of FDCs using the HyroGOF package. Each FDC was split into five segments (hereafter referred to as 5FDC) according to Pfannerstill et al. (2014). This constituted the very high flows (0–5%, Q5), high flows (5–20%, Q20), medium flows (20–80%, Qmid), low flows (80–95%, Q80) and the very low flows (95–100%, Q95). The upper end of the medium flows segment applied by Pfannerstill et al. (2014) was extended from 70 to 80% to match the flow guidelines stipulated by the Water Resource Authority (WRA). This metric represents the abstraction limit (GOK, 2012). The discharge between Q50 and Q80 is referred to as available flow (GOK, 2012).

The NSE, segmented RSR, and PBIAS were used to assess the performance of the calibration runs. The RSR for each of the five segments was separately estimated and ranked for all of the 6000 model simulations arising from the 6000 parameter sets sampled by LHS. These were represented as RSR_Q5, RSR_Q20, RSR_Qmid, RSR_Q80 and RSR_Q95 (Haas et al., 2016). The best 2000 runs were then extracted from each segment and a minimum threshold determined. The optimal value of RSR is zero. These best runs were plotted with NSE against PBIAS. All simulations having an NSE value lower than zero were considered non-behavioral and were excluded from further analysis. Thereafter, these selections were intersected with each other, two at a time, starting from the very low to the very high flows to obtain a final best set of calibration runs appearing within the 2000 calibrations from each individual segment. As a final step, an overall ranking obtained from the sum of the rank of each calibration run under each performance metrics was determined as a plausibility check for the intersection undertaken. This first involved ranking the performance metrics using the minimum threshold (Lower RSR threshold value means better performance). Each calibration run under each performance metrics was then separately ranked. These ranks were then summed up and a final ranking undertaken. It was expected that the final set of calibration runs obtained through the 5FDC would hold a high ranking and would prove the intersection method as being capable of selecting an optimum set of calibration runs.

Analysis of the hydrograph-based NCP involved selection of 2000 best simulation runs from the initial 6000 based on the lowest residual RSR.

2.7. Determination of Pareto ensembles and the CP procedure

Pareto optimization technique allows for the identification of parameter sets (Pareto ensembles) that represent an optimal trade-off point between multiple objective functions or criteria used. Here every parameter set is ranked using two or more criteria represented by maximizing or minimizing objective functions/ performance criteria. The obtained set of solutions are said to be located within the defined feasible parameter space ($\theta \varepsilon \Theta$) see Equation 1. Within this space, it is impossible to improve one criterion without making the other worse. These parameter sets are referred to as a Pareto front and represent the trade-off between the criteria used. Calibration of semi-distributed hydrologic models with many parameters describing catchment behavior is often faced with parameter equifinality leading to multiple “behavioral” sets, which adequately simulate the observed flows. Acknowledging equifinality involves simultaneously optimizing and trading off the performance of several user-selected criteria to measure the different aspects of the model performance (Beven, 1993; Yilmaz et al., 2010). The more independent the contradictory selected criteria are (e.g. high and low flow prediction or hydrologic matter and fluxes), the greater is the potential for Pareto optimization to find meaningful trade-off points in the model behavior. In order to determine the model runs that adequately represented the different phases of the FDC and the hydrograph, a Pareto package (rpref- Rooks, (2016)) was applied in the R environment. An ensemble of 10 model runs minimizing PBIAS and maximizing the NSE was selected from the best calibration runs obtained from the stepwise intersection under the 5FDC. Under the NCP, the Pareto ensemble was obtained from the 2000 best simulations. The performance of the two Pareto ensembles was consequently analyzed based on parameter and water balance distribution.

Equation 1: Pareto equation.

$$Min\ or\ Max\ Fm(\theta) = \{F1(\theta),\ F2(\theta),\ F3(\theta).....Fn(\theta)\}\ \theta \varepsilon \Theta$$

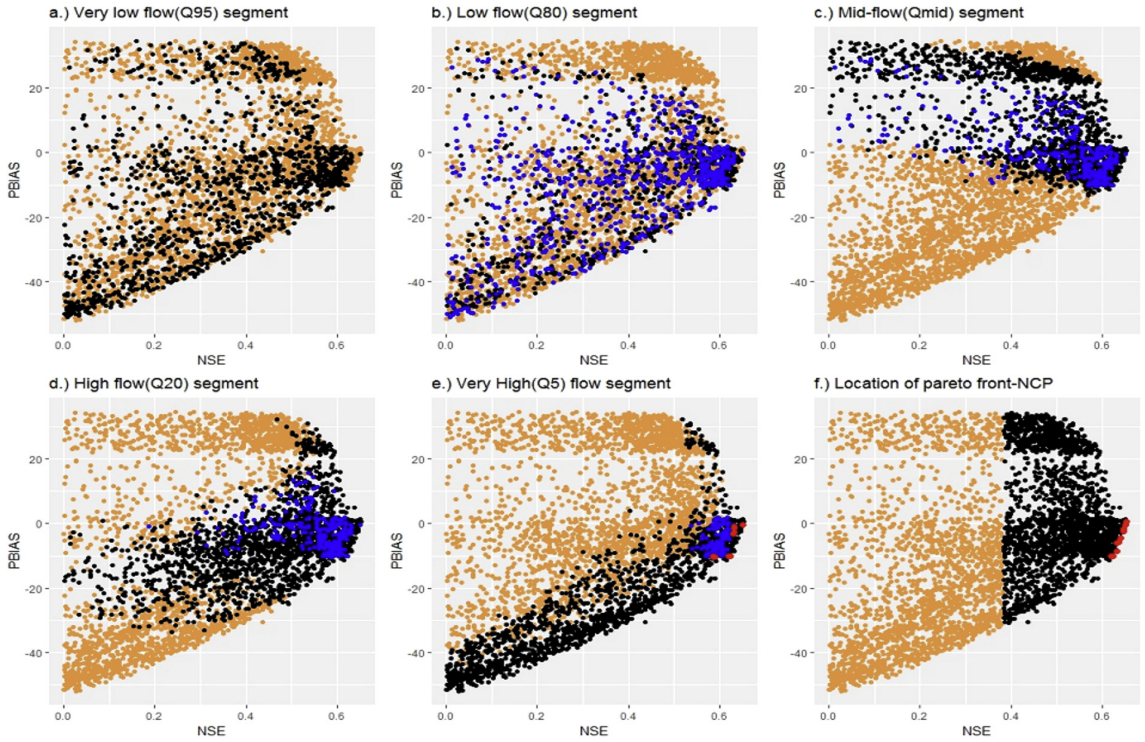

Fig. 2. Summary of performance metrics and selection of 2000 best calibration runs. Brown color scatter plots represent the initial 6000 calibration runs; black color scatter plots represent the best 2000 calibration runs as determined by threshold in each segment, the blue color scatter plots represent the result of the sequential intersection in each segment and the red scatter plots represent the location of the Pareto front. Sections a–e represent the results of the stepwise intersection in the 5FDC while section f represents the selection made by implementing the NCP (For interpretation of the references to colour in this figure legend, the reader is referred to the web version of this article).

Where;

θ *represents a vector with n parameters*

Θ *represents feasible parameter space*

$F1(\theta)$, $F2(\theta)$, $F3(\theta)$.....$Fn(\theta)$ *represent performance measures* (*PBIAS*, *NSE*, *RMSE*) *used to*

determine the distance between measured and simulated data

The main aim of the Combined Procedure (CP) was to create a hybrid that would merge the characteristics/qualities of both the NCP and 5FDC. It was hypothesized that the CP would reveal superior parameter sets that overcame any limitations exhibited by either the NCP or 5FDC in representation of both the high and low flows. The 5FDC and NCP ensembles were intersected to extract those runs that were common in both ensembles. These runs were separately analyzed and this performance was compared to that of the NCP and 5FDC.

3. Results

NSE and PBIAS relationship of the calibration runs obtained from analysis on the 5FDC and NCP procedures are summarized in Fig. 2. The very low and the very high quartiles were not very selective in the selection of calibration runs. This resulted in runs that highly overestimated (low negative PBIAS value) and underestimated (large positive PBIAS value) the observed discharge. Using the threshold (RSR presented in brackets) to assess the ranking of the metrics, the mid-segment (0.46) which performed best followed sequentially by low (0.82), high (1.70), very low (2.52), and very high (6.82) segments. The initial intersection of very low and low segments had the largest impact on the calibration runs in which they were reduced to 668. A further intersection with the mid-segment also greatly reduced these runs to 315. The impact of the high flow section slightly reduced the simulation runs to 238. The last intersection resulted in 113 runs. Determination of the Pareto ensemble led to a variable range of model runs that represented not necessarily the best parameters in each performance measure but rather, the most-optimum simulations in each segment.

2000 simulation runs from NCP were selected based on a low RSR. This highly selective procedure resulted in higher NSE values

Table 2
Summary of performance measures of Pareto ensemble obtained from 5FDC.

RUN	NSE	PBIAS	RSRQ95	RSRQ80	RSRMID	RSRQ20	RSRQ5	JOINT RANKING
471	0.65	−0.4	1.88	0.32	0.21	0.68	4.26	2
4136	0.63	−0.8	2.31	0.24	0.20	0.70	4.68	10
2754	0.63	−1.4	1.86	0.19	0.21	0.68	4.65	4
911	0.63	−2.7	1.97	0.26	0.24	0.69	4.71	9
1650	0.63	−3.3	1.19	0.47	0.25	0.72	4.89	6
1254	0.62	−10.1	1.82	0.30	0.38	1.08	3.15	41
2382	0.62	−10.2	1.51	0.37	0.39	1.00	3.53	27
4135	0.59	−10.3	2.36	0.44	0.37	0.99	3.00	86
855	0.59	−10.4	1.34	0.54	0.39	0.97	3.87	72
968	0.59	−10.1	1.25	0.51	0.41	0.93	4.53	71

but a wide range of PBIAS values. A plot of PBIAS-NSE of the calibration runs under the NCP is displayed in Fig. 2-f. The NSE range for the 2000 runs was 0.65 - 0.38 while that of PBIAS was -30.7 – 34.4.

3.1. Comparing 5FDC and NCP calibration

In order to compare the two, the Pareto ensembles under the NCP were reanalyzed using the 5FDC procedure. Tables 2 and 3 illustrate the values obtained from 5FDC and NCP respectively.

NSE values of about 0.50 are judged satisfactory for hydrologic evaluation based on a monthly time step (Moriasi et al., 2007). The two calibration procedures performed comparatively well given that, daily time step was applied during analysis. However, the 5FDC procedure gave a wider NSE range (± 0.06) as compared to that of the NCP (± 0.03). This is not surprising for NCP as the NSE is focused on high flows. A look into PBIAS results shows that all the selected simulations were within the satisfactory range. A distinct difference was noted in the low flow section of the segmented RSR values. 5FDC was superior as it resulted in much lower values (see RSRQ95). Both methods failed to preserve the peak flows with the 5FDC performing worse (see hydrograph in Fig. 3). Three calibration runs (no. 471, no. 1254 and no.2382) appeared in both the NCP and the 5FDC ensembles. These were taken to represent the calibration runs for the Combined Procedure (CP). The FDC of the 5FDC and NCP Pareto ensembles (Fig. 4) also shows that the 5FDC procedure tended to underestimate the mid lower segment (Q60-Q80) and the lower segment (Q95) less than the NCP. NCP highly overestimated the low flows. The CP produced a concession between the two methods by reducing the overestimation of the low flows by the NCP and of the peak flows by the 5FDC.

3.2. Parameter selection and water balance components

Violin boxplots presented in Fig. 5 act as a fusion between box plot and density trace. They not only show the quartile distribution and outlier values (box and whisker plot) but also illustrate the data probability density at the different values. While comparing the NCP and 5FDC, variable distribution patterns were observed for parameters with some such as the threshold water level in shallow aquifer for return flow (GWQMN), the revaporation/return flow coefficient (GW_REVAP) and SURLAG depicting opposing probability distributions. Both methods reveal the high level of uncertainty associated with groundwater contribution/base flow analysis. Three parameters exhibited striking differences in the coverage of the parameter space. This included: channel hydraulic conductivity (CH_K2), Manning's channel value (CH_N2) and the aquifer percolation coefficient (RCHG_DP). The CH_K2 is a measure of the rate of loss from the channel into the groundwater. Channels with low CH_K2 have higher transmission losses, which are assumed to enter bank storage (Neitsch et al., 2005). Channels receiving groundwater contribution have low values (Gitau and Chaubey, 2010). CH_N2 controls the flow velocity of water in the channel. Higher values reduce the velocity of water. The RCHRG_DP controls how much water is lost into the deep aquifer and considered lost from the system (Neitsch et al., 2005). The CP method had a profound impact in

Table 3
Summary of performance measures of Pareto ensemble obtained using NCP.

RUN	NSE	PBIAS	RSRQ95	RSRQ80	RSRMID	RSRQ20	RSRQ5	JOINT RANKING
1573	0.65	0.6	7.9	1.27	0.21	0.63	4.23	634
471	0.65	−0.4	1.88	0.32	0.21	0.68	4.26	2
229	0.65	−1.7	7.69	1.13	0.24	0.73	3.44	553
5665	0.65	−2.5	6.28	0.80	0.24	0.74	3.51	353
1277	0.64	−4.4	8.18	1.29	0.28	0.86	2.46	682
354	0.64	−5.9	3.88	0.43	0.30	0.83	3.79	115
2450	0.63	−6.1	4.07	0.42	0.30	0.84	3.34	105
2159	0.63	−8.5	6.03	0.73	0.37	0.92	3.16	453
1254	0.62	−10.1	1.82	0.30	0.38	1.08	3.15	41
2382	0.62	−10.2	1.51	0.38	0.39	1.00	3.53	27

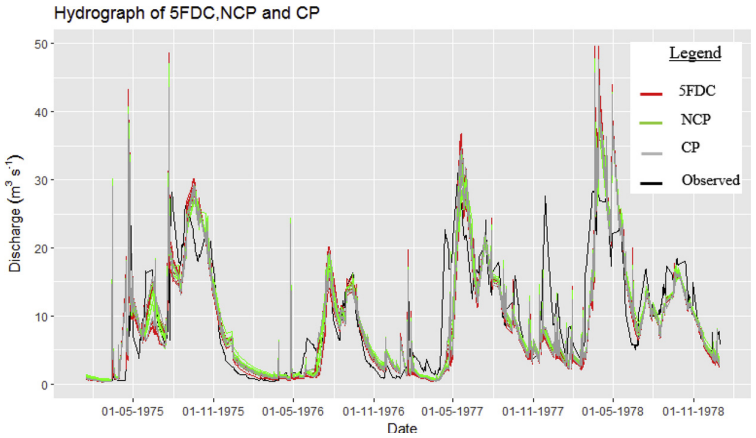

Fig. 3. Hydrograph of Pareto ensembles and observed flow.

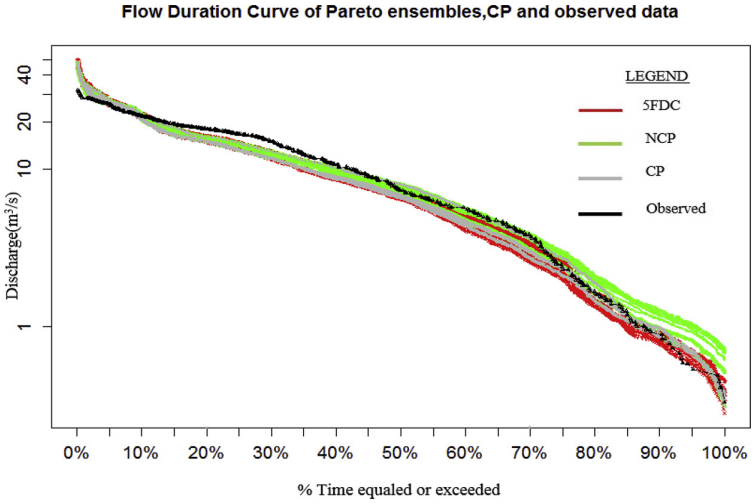

Fig. 4. FDC of Pareto ensembles, CP and observed flow.

increasing the identifiability of all parameters by reducing the uncertainty in the distribution.

Fig. 6 illustrates an average of water balance components of 5FDC, NCP, CP. The average annual rainfall for the years calibrated was 1549 mm. The standard deviation of the runs within each parameter ensemble is represented in brackets.

The highest variation within the ensembles was noted in the groundwater components. The high uncertainty observed within the parameter distribution of groundwater parameters resulted in a wider range of these water balance components. This was higher under the 5FDC. The execution of the NCP procedure resulted in higher deep aquifer recharge and total water yield. A larger proportion of the percolated water was lost into the deep aquifer and no longer contributed to the hydrologic cycle. As observable from Fig. 5, this has been restricted to the upper ranges of the parameter space. The 5FDC method on the other hand, allowed more water to infiltrate through the soil and percolate into the aquifers. Most of this water was released as groundwater flow, lateral flow and as return flow from shallow aquifers to the rooting zone of the plants. The model then impelled the evaporation of this water. CP, which proved the most superior in terms of parameter identifiability and uncertainty, produced the high amounts of shallow aquifer storage. The reduced uncertainty in parameter estimated translated to reduced variability in water balance components. This method combined the characteristics of the 5FDC and NCP.

In order to determine which of the calibration procedures closely simulated observed values, the runoff ratio and proportion of precipitation translated to evapotranspiration were calculated (see values in brackets next to procedures-Table 4). Although both methods closely simulated the observed values, the 5FDC produced better results. The CP produced values that were between the 5FDC and NCP. No procedures matched the value obtained in the third year. This may be due to the uncertainty in streamflow data as a result of the use of manual river gauges or from the use of rating equations to convert gauge heights into high flows (Juston et al., 2014).

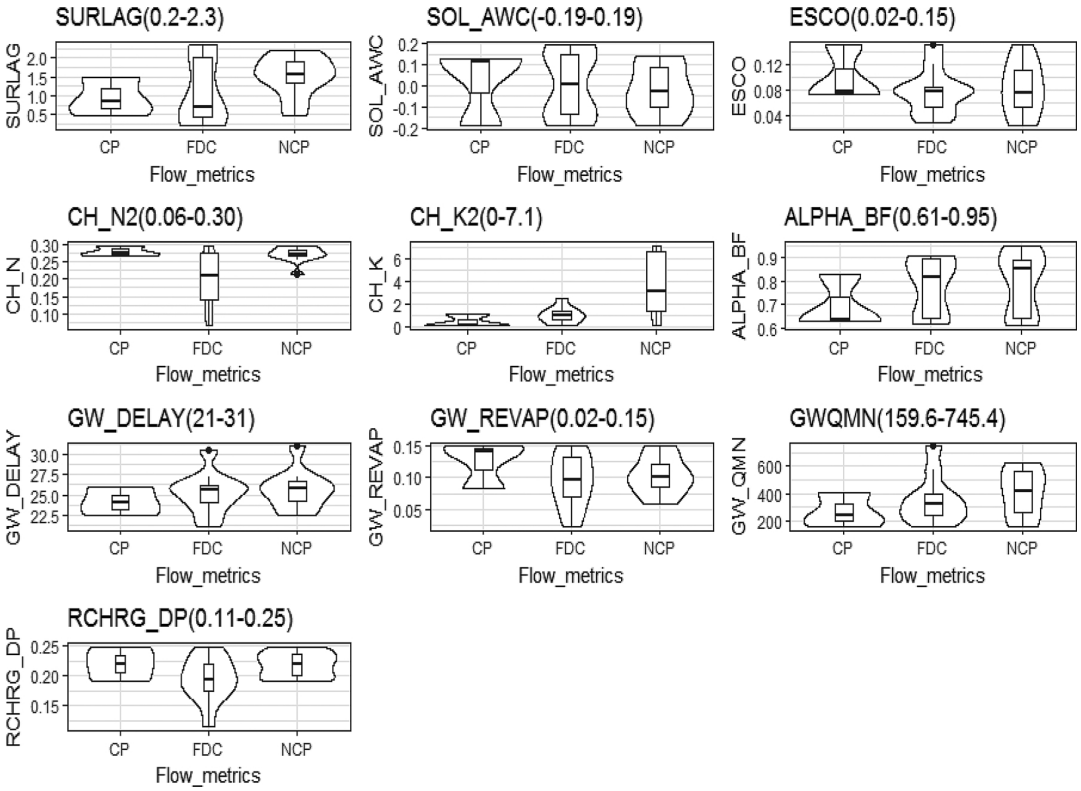

Fig. 5. Violin plots showing the quartile distribution and densities of parameters selected for calibration. Calibration range is represented in brackets.

4. Discussion

The LHS attempts to sample the response surface according to the likelihood density, and as such, areas with high likelihood are sampled more frequently (Beven, 1993). This makes this sampling method very efficient in reducing the non-behavioral parameter values by ensuring that there is no violation of practical or theoretical boundaries for each specific input parameter (Arnold et al., 2012b).

The multi-metric based system resulted from combining the segments based on their objective function performance (Van Werkhoven et al., 2009; Pfannerstill et al., 2014). The stepwise intersection of the 5FDC ensured that a satisfactory set of parameter was obtained, as the best performing simulations were selected from each segment. The high and very high flows signal the response of the catchment to high intensity precipitation events, while the mid-range focuses on moderate precipitation events. The low flow segment is related to the interaction of base flow with riparian evapotranspiration during extended dry periods (Yilmaz et al., 2010; Guse et al., 2016). The splitting of the 5FDC resulted in calibration runs that adequately represented the response of the catchment to the different watershed functions. Each performance metric had its own unique distribution pattern and rejected some poorly performing calibration runs. This is further evidenced by the performance of the Pareto runs selected under the 5FDC in the plausibility check.

The determination of a Pareto ensemble from the final set supports the equifinality theory, in that it refutes the existence of a single “best” parameter set and recognizes that numerous parameter sets may provide equivalent representations (Beven, 1993). For this reason, ensembles of 10 parameter sets were obtained for parameter analysis and water balance component evaluation for both NCP and 5FDC. The CP approach narrowed this to an ensemble of 3 parameter sets.

Parameter identification is a complex non-linear problem and numerous possible solutions might be obtained by different optimization algorithms (Nandakumar and Mein, 1997). As deduced from this study, the selection of sensitive parameters does not mean that the parameter is also identifiable. Linking the parameter performance to the FDC/hydrograph of simulated plots reveals that the NCP method better represents the mid-upper and high flows. Here, performance was based on lumped global performance measures that were likely influenced by these flows. Given the high level of uncertainty in the groundwater parameters, simulations using observed flows are more reliable. And as such, the 5FDC tends to produce better results as compared to the NCP. The water balance is the driving force behind all processes in hydrologic models (Arnold et al., 2012a). All procedures show that evapotranspiration takes the highest proportion of precipitation, and is thus an important component in this catchment. Dessu and Melesse

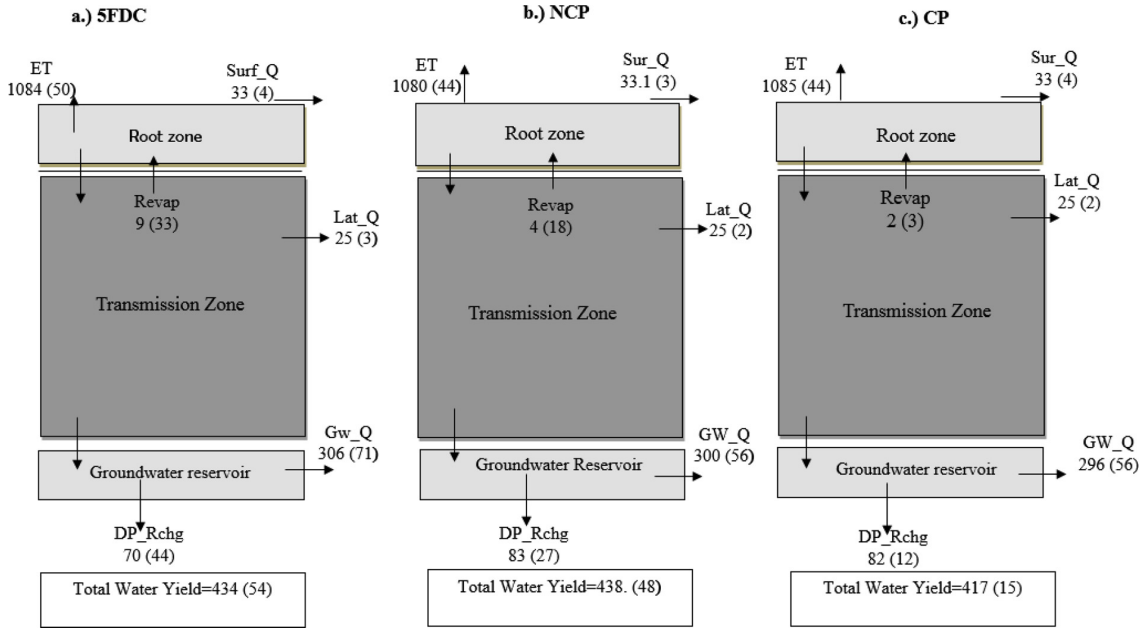

Fig. 6. Schematic view of the water balance component values for Precipitation (Prec), Evapotranspiration (ET) surface runoff (Sur_Q), Lateral flow (Lat_Q), Groundwater flow (GW_Q), Deep Aquifer recharge (DP_Rchg) and Return flow from shallow aquifer (Revap). Standard deviation of runs within each ensemble is represented in brackets. The size of the boxes is not proportional to the quantities they represent.

Table 4
Run-off ratio of ensembles for Nyangores catchment for the period.1975–1978.

YEAR	OBSERVED	5FDC (69.9%)			NCP(69.7%)			CP(70.0%)		
		min	max	Mean	min	Max	Mean	Min	Max	Mean
1975	0.29	0.28	0.32	0.31	0.3	0.34	0.32	0.30	0.34	0.31
1976	0.17	0.16	0.2	0.18	0.18	0.22	0.2	0.17	0.21	0.19
1977	0.32	0.23	0.27	0.26	0.25	0.28	0.26	0.24	0.28	0.25
1978	0.34	0.33	0.35	0.34	0.33	0.35	0.34	0.33	0.35	0.33

Average proportion of precipitation represented by evapotranspiration for all procedures˜ 70%.

(2012) reported that on a basis of a 10-year average annual water budget in Nyangores (1978–1982 and 1988–1992), evapotranspiration accounted for 70% of losses of annual rainfall input, which is similar to the results found in this study. The Nyangores catchment is located in the upper part of the larger Mara catchment and is home to one of the largest “water towers” in Kenya, the Mau Forest. Due to their leaf sizes, thickness and aerodynamic roughness, trees typically provide a large surface area for canopy interception of precipitation, and consequently evapotranspiration. Their deep and extensive roots additionally aid in extracting more water from the groundwater allowing for further evapotranspiration (Neitsch et al., 2005). The main benefit of integrating this type of analysis which incorporates both hard (discharge) and soft data (individual process data) into calibration is to ensure that parameter sets selected using both procedures simulate realistic water balance components.

While comparing the 5FDC and NCP, simulations using the Pareto ensembles revealed that under the 5FDC a large proportion of water is stored in the rooting zone or is released as base flow. This can also be linked to the higher CH_K2 values obtained under this method. This leads to an increase in bank storage, which may move to the adjacent unsaturated zone for use by plants or released as base flow (Neitsch et al., 2005). A modelling study conducted by Birundu and Mutua (2017) in the Nyangores catchment using the HBV model concluded that a major proportion of precipitation received in Nyangores catchment is stored and later released as baseflow. Some of this water could have been transpired by plants contributing to higher evapotranspiration values simulated. The lower CH_N2 values also resulted in faster response of this catchment to peak rainfall leading to overestimated high flows. This can be viewed in Fig. 3 and Fig. 4. Additionally, the 5FDC procedure exhibited runoff ratios closer to the observed values for most years. The wider range in groundwater components observed within the 5FDC Pareto ensemble can be explained by the fact that this procedure selected calibration runs that attempted to match all the phases of the hydrograph leading to a high tradeoff between the high and low flows. By contrast, the NCP was quite selective in focusing on the flows favored by the objective functions selected for analysis. The higher loss of water to deep aquifer under the NCP can be attributed to the high RCHRG_DP values. This reduces the amount of

water released as baseflow or "revaporated "into the unsaturated zone (Neitsch et al., 2005). Higher SURLAG and low SOL_AWC values also indicated that less water was retained in the soil (Neitsch et al., 2005). This could explain why this procedure performed better under the high flows. However, water resource managers are mostly concerned with ensuring availability of water to the water uses during water shortages of different levels of severity. With better representation of low flows, they can establish effective limits that ensure that there is no overallocation of water. In theory, FDCs are well suited for representing the hydrological response of the catchment. They are also easier to use and interpret even for users with limited hydrological background (Vogel and Fennessey, 1994). By reshaping the data on the basis of flow frequency, the timing component of streamflow is removed. This means they cannot be applied for purposes such as flood frequency estimation. Under the hybrid procedure (CP), both the high and low flows were adequately represented. The parameter identifiability additionally improved. This increases confidence in the simulations obtained and does not limit their applicability. CP can thus be effectively applied for scenario creation and prediction purposes.

5. Conclusion

In this study, a mesoscale hydrologic model was applied for calibration purposes to the Nyangores catchment, Kenya. The calibration period selected was from 1975 to 1978. Using LHS importance sampling, 6000 independent parameter sets were generated and runoff simulated. The observed data (discharge, runoff-ratio, proportion of precipitation translated to evapotranspiration) was then compared to that simulated using Pareto ensembles from the 5FDC, NCP and CP. Parameter distribution of the Pareto ensembles for each procedure was plotted. This distribution was linked to the performance of the model with regards to water balance components.

This study follows the approach of Pfannerstill et al. (2014) and Yilmaz et al. (2010), which developed a multi-metric framework to implement the results of an optimum parameter set that adequately represented all the phases of the hydrograph. The use of the 5FDC improved the calibration of low and very low flows. This improvement has potential for use by watershed resource managers working in low-flow environments. NCP, however, performed better than 5FDC where peak flows were considered. We additionally recognized the equifinality theory by selecting Pareto ensembles within which no single best parameter set is selected. The parameter analysis revealed differences in parameters relating to catchment properties, surface and groundwater flow between the two procedures. This corresponded with the differences in how the model partitioned the water balance components. With these differences, the intersection of the 5FDC and NCP created a hybrid (CP). This procedure merged the strengths exhibited by both the 5FDC and NCP leading to reduced parameter uncertainty. However, there is need for further studies to be undertaken to understand especially the partitioning of the water balance components. Finally, the study demonstrated that the selection of the calibration procedure should be dependent upon the purpose of the modelling exercise. The 5FDC, however, produced simulations closer to the observed values especially for the low flow volumes. This was also the case for the runoff-ratios. The 5FDC method can thus better predict low flows and long-term base flows and hence is more suitable for long-term water management.

Acknowledgements

We would like to acknowledge Water Resources Authority (WRA) and Kenya Meteorological Department (KMD) for availing climate data used in the study. Additionally, we would like to thank Daniel Robert Hawtree for proofreading an earlier version of this manuscript. This research did not receive any specific grant from funding agencies in the public, commercial, or not-for-profit sectors. We acknowledge support by the Open Access Publication Funds of the SLUB/TU Dresden.

References

Alemayehu, T., Griensven, Av., Woldegiorgis, B.T., Bauwens, W., 2017a. An improved SWAT vegetation growth module and its evaluation for four tropical ecosystems. Hydrol. Earth Syst. Sci. 21, 4449–4467. https://doi.org/10.5194/hess-21-4449-2017.

Alemayehu, T., Griensven, Av., Senay, G.B., Bauwens, W., 2017b. Evapotranspiration mapping in a heterogeneous landscape using remote sensing and global weather datasets: application to the Mara Basin, East Africa. Remote Sens. (Basel) 9, 390. https://doi.org/10.3390/rs9040390.

Arnold, J.G., Kiniry, J.R., Srinivasan, R., Williams, J.R., Haney, E.B., Neitsch, S.L., 2012a. SWAT Input/Output - Version 2012. Texas Water Resource Institute, Texas.

Arnold, J.G., Moriasi, D.N., Gassman, P.W., Abbaspour, K.C., White, M.J., Srinivasan, R., Jha, M.K., 2012b. SWAT: model use, calibration, and validation. Am. Soc. Agric. Biol. Eng. 55, 1491–1508.

Batjes, N.H., 2002. Soil Parameter Estimates for the Soil Types of the World for Use in Global and Regional Modelling (Version 2.1; July 2002). ISRIC Report 2002/02c.

Bekele, E.G., Nicklow, J.W., 2012. Multi-Objective Optimal Control Model for Watershed Management UsinG SWAT and NSGA-II. American Society of Civil Engineers 1https://doi.org/10.1061/40927(243)171.

Beven, K., 1993. Prophecy, reality and uncertainty in distributed hydrological modelling. Adv. Water Resour. 16, 41–51. https://doi.org/10.1016/0309-1708(93)90028-E.

Beven, K., Binley, A., 1992. The future of distributed models:model calibration and uncertainty prediction. Hydrol. Process. 6, 279–298. https://doi.org/10.1002/hyp.3360060305.

Biondi, D., Freni, G., Iacobellis, G., Montanari, A., 2012. Validation of hydrological models: conceptual basis, methodological approaches and a proposal for a code of practice. Phys. Chem. Earth 42-44, 70–76. https://doi.org/10.1016/j.pce.2011.07.037.

Birundu, A.M., Mutua, B.M., 2017. Analyzing the Mara river Basin Behaviour through Rainfall-Runoff modelling. Sci. Res. 8, 1118–1132. https://doi.org/10.4236/ijg.2017.89064.

Bormann, H., Breuer, L., Graff, T., Huisman, J.A., 2007. Analysing the effects of soil properties changes associated with landuse changes on the simulated water balance: a comparison of three hydrological catchment models for scenario analysis. Ecol. Modell. 209, 29–40. https://doi.org/10.1016/j.ecolmodel.2007.07.004.

Dessu, S.B., Melesse, A.M., 2012. Modelling the rainfall-runoff process of the Mara river basin using the soil Water Assessment Tool. Hydrol. Process. 26, 4038–4049. https://doi.org/10.1002/hyp.9205.

Devi, G.K., Ganasri, B.P., Dwarakish, G.S., 2015. A review of hydrologic models. Aquat. Procedia 4, 1001–1007. https://doi.org/10.1016/j.aqpro.2015.02.126.

Duan, Q., Sorooshian, S., Gupta, V.K., 1994. Optimal use of the SCE-UA global optimization method for calibrating watershed models. J. Hydrol. (Amst) 158, 265–284. https://doi.org/10.1016/0022-1694(94)90057-4.

Dudgeon, D., Arthington, A.H., Gessner, M.O., Kwabata, Z.-I., Knowler, D.J., Leveque, C., Stiassny, M.L., 2006. Freshwater biodiversity: importance, threats, status and conservation challenges. Web of Science 81, 163–182. https://doi.org/10.1017/S1464793105006950.
Fürst, J., Olang, L.O., Herrnegger, M., Wimmer, D., Omonge, P., Kipkoech, E., 2015. MaMa-Hydro Exploring Water Resources Planning and Management options in the Nyangores Headwater Catchment of the Vulnerable Maasai Mara River Basin in Kenya. Universität für Bodenkultur Wien, Austria.
Gitau, M.W., Chaubey, I., 2010. Regionalization of SWAT model parameters for use in ungauged watersheds. Water 2, 849–871. https://doi.org/10.3390/w2040849.
Government Of Kenya, 2012. Water Act 2002- Revised. Government of Kenya, Nairobi.
Government of Kenya-GoK, 1983. Land Use Map of Kenya. Produced by Survey of Kenya (500/3/83), Kenya Rangeland Ecological Monitoring Unit. Ministry of Environment and Natural Resources, Nairobi.
Gupta, H.V., Sorooshian, S., Yapo, P.O., 1998. Toward improved calibration of hydrologic models: multiple and noncommensurable measures of information. Water Resour. Res. 34, 751–763. https://doi.org/10.1029/97WR03495.
Guse, B., Pfannerstill, M., Gafurov, A., Kiesel, J., Lehr, C., Fohrer, N., 2017. Identifying the connective strength between model parameters and performance criteria. Hydrol. Earth Syst. Sci. 21, 5663–5679. https://doi.org/10.5194/hess-21-5663-2017.
Haas, M.B., Guse, B., Pfannerstill, M., 2016. A joint multi-metric calibration of a river discharge and nitrate loads with different performance measures. J. Hydrol. (Amst) 536, 534–545. https://doi.org/10.1016/j.jhydrol.2016.03.001.
Hrachowitz, M., Savenije, H., Blöschl, G., McDonnell, J., Sivapalan, M., Pomeroy, J., Troch, P., 2013. A decade of prediction in Ungauged Basin. Hydrol. Sci. J. Des Sci. Hydrol. 58, 1198–1255. https://doi.org/10.1080/02626667.2013.803183.
Hulsman, J., Breuer, L., Bormann, H., Bronstert, A., Croke, B., Frede, H., Willems, P., 2009. Assessing the impact of land use change on hydrology be ensemble modelling (LUCHEM) III: scenario analysis. ScienceDirect 32, 159–170. https://doi.org/10.1016/j.advwatres.2008.06.009.
Hulsman, P., Bogaard, T.A., Savenje, H.H., 2017. Modeling the Mara river Basin with data uncertainty using water levels for calibration. Hydrol. Earth Syst. Sci. 22, 5081–5095. https://doi.org/10.5194/hess-2017-661.
Juston, J., Jansson, P.E., Gustafsson, D., 2014. Rating Curve uncertainty and change detection in discharge time series: case study with 44-year historic data from the Nyangores River, Kenya. Hydrol. Process. 28, 2509–2532. https://doi.org/10.1002/hyp.9786.
Kirchner, J.W., 2006. Getting the right answers for the right reasons: Linking measurements, analyses, and models to advance the science of hydrology. Water Resour. Res. 42. https://doi.org/10.1029/2005WR004362.
Krause, P., Boyle, D.P., Bäse, F., 2005. Comparison of different efficiency criteria for hydrological model assessment. Adv. Geosci. 5, 89–97.
Legates, D.R., McCabe, G.J., 1999. Evaluating the use of "goodness-of-fit" measures in hydrologic and hydroclimatic model evaluation. Water Resour. Res. 35, 233–241. https://doi.org/10.1029/1998WR900018.
Mango, L.M., Melesse, A.M., McClain, M.E., Gann, D., Setegn, S., 2011. Land use and climate change impacts on the hydrology of the upper Mara River Basin, Kenya. Hydrol. Earth Syst. Sci. Discuss. 15, 2245–2258. https://doi.org/10.5194/hess-15-2245-2011.
Mati, B.M., Mutie, S., Gadain, H., Home, P., 2008. Impacts of Land-use/ cover changes on the hydrology of the transboundary Mara river, Kenya/Tanzania. Lakes Reserv. 13, 169–177. https://doi.org/10.1111/j.1440-1770.2008.00367.x.
Moriasi, D.N., Arnold, J.G., Van Liew, M.W., Harmel, D.R., 2007. Model evaluation guidelines for systematic quantification of accuracy in watershed simulations. Soil Water Division of ASABE 50, 885–900 doi:10.1.1.532.2506&rep=rep1&type=pdf.
Moriasi, D.N., Gitau, M.W., Pai, N., Daggupati, P., 2015. Hydrologic and water quality models: performance measures and evaluation criteria. Am. Soc. Agric. Biol. Eng. 58, 1763–1785. https://doi.org/10.13031/trans.58.10715.
Mwangi, H.M., Julich, S., Patil, S.D., McDonald, M.A., Feger, K.H., 2016a. Relative contribution of land use change and climate variability on discharge of upper Mara River, Kenya. J. Hydrol. Reg. Stud. 5, 244–260.
Mwangi, H.M., Julich, S., Sopan, P.D., McDonald, M.A., Feger, K.H., 2016b. Modelling the impact of agroforestry on the hydrology of Mara river Basin in East Africa. Hydrol. Process. 30, 3139–3155. https://doi.org/10.1002/hyp.10852.
Mwangi, H.M., Lariu, P., Julich, S., Patil, S., McDonald, M., Feger, K.H., 2018. Characterizing the intensity and dynamics of land use change in Mara river Basin, East Africa. Forests 9, 8.
Nandakumar, N., Mein, R.G., 1997. Uncertainty in Rainfall-Runoff model simulations and the implications for predicting the hydrologic effects of land-use change. J. Hydrol. (Amst) 192, 211–232.
Neitsch, S.L., Arnold, J.G., Kiniry, J.R., Williams, J.R., 2005. Soil and Water Assessment Tool Theoretical Documentation. Agriculture Research Service, Texas.
Niehoff, D., Fritsch, U., Bronstert, A., 2002. Land-use impacts on storm-runoff generation: scenario land-use change and simulation of hydrological response in a meso-scale catchment in SW-Germany. J. Hydrol. (Amst) 267, 80–93.
Pfannerstill, M., Guse, B., Fohrer, N., 2014. Smart low flow signature metrics for an improved overall performance evaluation of hydrologic models. J. Hydrol. (Amst) 510, 447–458. https://doi.org/10.1016/j.jhydrol.2013.12.044.
Pfannerstill, M., Bieger, K., Guse, B., Bosch, D.D., Arnold, J.G., 2017. How to constrain multi-objective calibrations of the SWAT modelling using water balance components. J. Am. Water Resour. Assoc. 53, 532–546. https://doi.org/10.1111/1752-1688.12524.
R Core Team, 2013. R: a Language and Environment for Statistical Computing. R Foundation for Statistical Computing, Vienna.
Rooks, P., 2016. Computing pareto frontiers and database preferences with the rPref package. R J. 8, 393–404.
Samadi, S., Tufford, D.L., Carbone, G.J., 2017. Assessing parameter uncertainty of a semi-distributed hydrology modelling for a shallow aquifer dominated en-vironmanetal system. J. Am. Water Resour. Assoc. 53, 1368–1382.
Sawicz, K., Wagener, T., Sivapalan, M., Troch, P.A., Carrillo, G., 2011. Catchment classification: empirical analysis of hydrologic similarity based on catchment function in the eastern USA. Hydrol. Earth Syst. Sci. 15, 2895–2911. https://doi.org/10.5194/hess-15-2895-2011.
Singh, J.H., Knapp, V., Demissie, M., 2004. Hydrologic Modelling of the Iroquois River Watershed Usinf HSPF and SWAT. Illinois State Geological Survey, Illnois.
Soetaert, K., Petzolt, T., 2010. Inverse modelling,Sensitivity and monte carlo analysis in r using package FME. J. Stat. Softw. https://doi.org/10.18637/jss.v033.i03.
Strauch, M., Volk, M., 2013. SWAT plant growth modification for improved modeling of perennial vegetation in the tropics. Ecol. Modell. 269, 98–112. https://doi.org/10.1016/j.ecolmodel.2013.08.013.
Thiemann, M., Trosset, M., Gupta, H., Sorooshian, S., 2001. Bayesian recursive parameter estimation for hydrologic models. Water Resour. Res. 37, 2521–2535. https://doi.org/10.1029/2000WR900405.
Van Werkhoven, K., Wagener, T., Reed, P., Tang, Y., 2009. Sensitivity-guided reduction of parametric dimensionality for multi-objective calibration of watershed models. Adv. Water Resour. 32, 1154–1169. https://doi.org/10.1016/j.advwatres.2009.03.002.
Vogel, R.M., Fennessey, N.M., 1994. Flow- duration curves. I: new interpretation and confidence intervals. J. Water Resour. Plan. Manag. 120, 485–504.
Wagener, T., Wheater, H.S., 2006. Parameter estimation and regionalization for continuous rainfall-runoff models including uncertainty. J. Hydrol. 320, 132–154.
Wagner, P.D., Bhallamudi, M.S., Narasimhan, B., Kantakumar, L.N., Sudheer, K., Kumar, S., Fiener, P., 2016. Dynamic integration of landuse changes in a hydrology assessment of a rapidly Indian catchment. ScienceDirect 539, 153–164. https://doi.org/10.1016/j.scitotenv.2015.08.148.
Wambura, F.J., Dietrich, O., Gunnar, L., 2018. Improving a distributed hydrological model using evapotranspiration-related boundary condition as additional con-straints in a data-scarce river basin. Hydrol. Process. 32, 759–775. https://doi.org/10.1002/hyp.11453.
Westerberg, I.K., Guerrero, J.L., Younger, P.M., Beven, K.J., Seibert, J., Halldin, S., Xu, C.Y., 2011. Calibration of hydrologic models using flow duration curves. Hydrol. Earth Syst. Sci. 15, 2205–2227. https://doi.org/10.5194/hess-15-2205-2011.
Winchell, M., Srinivasan, R., Di Luzio, M., Arnold, J., 2013. ArcSWAT interface for SWAT 2012, user's Guide. Blackland Research and Extension Center. Texas Agrilife Research, Texas.
Yilmaz, K.K., Vrugt, J.A., Gupta, H.V., Sorooshian, S., 2010. Model Calibration in Watershed Hydrology: Advances in Data-based Approaches for Hydrologic Modelling and Forecasting. World Scientific Publishing Company, Arizona. https://doi.org/10.1142/9789814307987_0003.
Yokoo, Y., Sivaplan, M., 2011. Towards reconstructiom of the flow duration curve: development of a conceptual framework with a physical basis. Hydrol. Earth Syst. Sci. 15, 2805–2819. https://doi.org/10.5194/hess-15-2805-2011.
Zambrano-Bigiarini, M., 2014. Package HdroGOF. https://cran.r-project.org/web/packages/hydroGOF/hydroGOF.pdf.

TYPE Original Research
PUBLISHED 05 December 2022
DOI 10.3389/ffgc.2022.1046371

frontiers | Frontiers in Forests and Global Change

OPEN ACCESS

EDITED BY
Mehebub Sahana,
Manchester University, United States

REVIEWED BY
Mohamed Kefi,
Centre de Recherches et des Technologies des Eaux, Tunisia
Mohammad Arif,
Central University of Jharkhand, India
Anil Kumar Singh,
Academy of Scientific and Innovative Research (AcSIR), India

*CORRESPONDENCE
Ann W. Kamamia
ann.kamamia@mailbox.tu-dresden.de

SPECIALTY SECTION
This article was submitted to Tropical Forests, a section of the journal Frontiers in Forests and Global Change

RECEIVED 16 September 2022
ACCEPTED 15 November 2022
PUBLISHED 05 December 2022

CITATION
Kamamia AW, Strauch M, Mwangi HM, Feger K-H, Sang J and Julich S (2022) Modelling crop production, river low flow, and sediment load trade-offs under agroforestry land-use scenarios in Nyangores catchment, Kenya. *Front. For. Glob. Change* 5:1046371. doi: 10.3389/ffgc.2022.1046371

Modelling crop production, river low flow, and sediment load trade-offs under agroforestry land-use scenarios in Nyangores catchment, Kenya

Ann W. Kamamia[1]*, Michael Strauch[2], Hosea M. Mwangi[3], Karl-Heinz Feger[1], Joseph Sang[3] and Stefan Julich[4]

[1]Institute of Soil Science and Site Ecology, Technische Universität Dresden, Dresden, Germany, [2]Department of Computational Landscape Ecology, Helmholtz Centre for Environmental Research GmbH-UFZ, Leipzig, Germany, [3]Department of Soil, Water, and Environmental Engineering, Jomo Kenyatta University of Agriculture and Technology, Nairobi, Kenya, [4]Faculty of Landscape Management and Nature Conservation, Eberswalde University for Sustainable Development, Eberswalde, Germany

The largest impact of land-use change on catchment hydrology can be linked to deforestation. This change, driven by exponential population growth, intensified food and industrial production, has resulted in alterations in river flow regimes such as high peaks, reduced base flows, and silt deposition. To reverse this trend more extensive management practices are becoming increasingly important, but can also lead to severe losses in agricultural production. Land-use optimization tools can help catchment managers to explore numerous land-use configurations for the evaluation of trade-offs amongst various uses. In this study, the Soil and water assessment tool (SWAT) model was coupled with a genetic algorithm to identify land-use/management configurations with minimal trade-offs between environmental objectives (reduced sediment load, increased stream low flow) and the crop yields of maize and soybean in Nyangores catchment (Kenya). During the land-use optimization, areas under conventional agriculture could either remain as they are or change to agroforestry or conservation agriculture (CA), where the latter was represented by introducing contour farming and vegetative filter strips. From the sets of the resulting Pareto-optimal solutions we selected mid-range solutions, representing a fair compromise among all objectives, for further analysis. We found that a combined measure implementation strategy (agroforestry on certain sites and conservation agriculture on other sites within the catchment) proved to be superior over single measure implementation strategies. On the catchment scale, a 3.6% change to forests combined with a 35% change to CA resulted in highly reduced sediment loads (−78%), increased low flow (+14%) and only slightly decreased crop yields (<4%). There was a tendency of the genetic algorithm to implement more extensive management practices in the upper part of the catchment while leaving conventional agriculture in the lower

part. Our study shows that a spatially targeted implementation strategy for different conservation management practices can remarkably improve environmental sustainability with only marginal trade-offs in crop production at the catchment-level. Incentive policies such as payments for ecosystem services (PES), considering upstream and downstream stakeholders, could offer a practical way to effect these changes.

KEYWORDS

sustainability, multi-objectives, ecosystem services, agroforestry, sediment load, CoMOLA, Pareto optimization, land-use configurations

Introduction

The largest impact of land-use change on catchment hydrology can be linked to deforestation. This change, driven by exponential population growth, intensified food and industrial production (Foley et al., 2005; Kamamia et al., 2022), has resulted in alterations in the river flow regime such as high peaks, reduced base flows, and silt deposition in water bodies and reservoirs (Bajocco et al., 2012; Borrelli et al., 2017; Kamamia et al., 2021). Furthermore, climate change has accelerated land degradation by intensifying extreme events such as droughts and floods whose ramifications have been especially felt in the developing countries (Borrelli et al., 2017). Mounting evidence suggests an exacerbation of this situation by 2050 with more pronounced changes at the sub-regional/catchment scale (Boretti and Rosa, 2019). In Kenya, deforestation has greatly impacted the five major water towers (Mount Kenya, Mau Forest, Aberdare Forest, Mount Elgon, and Cherangani) which supply about 75% of the total freshwater and which support important ecosystems that are vital for the country's sustainable production. Deforestation in Mount Kenya, Aberdare Forest, Mount Elgon, and Cherangani water towers has led to a decline in rainfall amounts (e.g., less cloud water interception) accompanied by shifting rainfall patterns thereby reducing their productivity (Mwangi et al., 2020). Additionally, climate change impacts associated with weather variability such as high temperatures have increased forest fires incidents, further threatening the existing forests (Schmitz and Kihara, 2021). Mulinge et al. (2016) reported a 32% decrease in forest cover for the Mau forest water tower (in which the Nyangores catchment is located) between 2001 and 2009. They attributed this to population expansion which stimulated: (i) an extension of cropland (with unsustainable agricultural practices) into forested areas, (ii) an encroachment of marginal lands and forests by pastoralist communities, and (iii) an increased demand for fuel wood and timber (Cohen et al., 2006; Mulinge et al., 2016; Kogo et al., 2020).

In this regard, catchment management is necessary in order to protect the natural ecosystem as well as to achieve a sustainable use of agricultural land in degraded areas. Soil and water conservation practices also referred to as catchment management strategies (CMSs) are the primary steps of catchment management whose purpose is to enhance agricultural productivity and protect catchments. Specifically, they aim at decreasing runoff rates, improving soil fertility, retarding soil erosion, and thus increasing soil-moisture availability and groundwater recharge (WOCAT, 2007). Agroforestry has in particular been the focus of many catchment management programs in the developing world (many countries in Africa, Asia, and Latin America whose economies are agriculture-driven) (World Agroforestry, 2021). Agroforestry has been considered a key pathway to restoring degraded ecosystems and achieving food security globally. Within these systems, reforestation efforts have been scaled up to combat the alarming rates of deforestation and forest degradation. The contribution of trees to carbon sequestration, nitrogen fixation and provision of a source of income has been ranked higher and is perceived more sustainable than other CMSs (Speranza, 2010). However, in order to reap the numerous benefits offered by trees, it is imperative to determine at the catchment scale where and what proportion of land can reasonably be converted. Since trees consume more water than other vegetation (Mwangi et al., 2016a; Kirschke et al., 2018) an improper allocation could magnify an already existing water scarcity situation. Moreover, CMSs threaten the productive capacity of catchments as their implementation may lead to losses in agricultural production. Thus, there is need for a comprehensive and systematic understanding of the possible adverse effects of agroforestry and its combination with other CMSs on the different ecosystem services. Tools such as hydrologic models have been used to conceptualize the impacts of the climatic and anthropogenic changes on the different sub-processes within the hydrologic cycle (Legesse et al., 2003). For instance, Asres and Awulachew (2010), Strauch and Volk (2013), and Memarian et al. (2014) used the soil water assessment tool (SWAT) hydrologic model in different tropical countries to assess the impact of land-use/land cover change on water discharge and sediment load. Mango et al. (2011) investigated the impact of complete deforestation and climate change on the catchment water balance in the

Nyangores catchment-Kenya, using the SWAT model. Mwangi et al. (2016a) extended this study to assess the effect of implementing different agroforestry scenarios on the various water balance components. In the two latter studies, only a few pre-selected options were evaluated to characterize possible futures. Cao et al. (2011) and Seppelt et al. (2013) argue that classical approaches of scenario analysis result in the exclusion of more optimal solutions not considered during the scenario selection/formulation step. Also, using certain model outputs in isolation, focusing on only one target service, can prompt the enhancement of one ecosystem service while masking the deterioration of other essential ecosystem services.

Therefore, the use of such models for developing spatially-explicit catchment management plans has been supplemented with land-use optimization tools (Lautenbach et al., 2013; Verhagen et al., 2018; Strauch et al., 2019; Kaim et al., 2021). In reality, catchments have multifunctional uses, shared by different stakeholders who may have contradicting aims and interests (objectives) which they seek to defend (Kaim et al., 2020). Land-use optimization tools offer a solution by exploring a large number of land-use management configurations for the simultaneous optimization of various objectives (Lautenbach et al., 2013; Chapagain et al., 2021). Land-use optimization tools differ in the number of objectives, scale applied and the timing of inclusion of stakeholders and decision makers (Strauch et al., 2019). Multi-objective optimization problems can be solved using either scalarization or Pareto-based methods. Scalarizing methods combine multiple objective functions into one single scalar function, e.g., using a weighted sum. Pareto-based methods present the different trade-offs as a Pareto frontier which is a set of optimal solutions to the respective multi-objective optimization problem (Kaim et al., 2018). Within a Pareto frontier, no objective can be further improved without compromising the other objectives. Possible solutions are identified either by maximizing or minimizing the different objectives using genetic algorithms (GAs) (Deb et al., 2002). Genetic algorithms start with an initial population and use concepts such as selection, mating, and mutations to create the next set of solutions (Kaim et al., 2018). Parameters to be optimized are encoded in a genome and the individuals in a population are then evaluated based on objective functions. GAs are highly explorative and gradient free which means that they can deal with complex, non-linear and discontinuous problems (Mitchell, 1996; Kaim et al., 2018). However, these algorithms are unconstrained by nature and have to be modified to reflect real world scenarios. In terms of land-use allocation, this could include setting rules constricting the conversion of one land-use to another and/or setting the minimum and maximum area that can possibly be converted (Strauch et al., 2019). Land-use optimization tools using the non-sorting Genetic Algorithm-II (NSGA-II) have proven to solve complex land allocation problems based on the optimization of different user specified objectives. Wicki et al. (2021) applied a land-use optimization tool to aid in planning green and dense cities based on a trade-off between urban ecosystem services and compactness. Kaim et al. (2020) coupled SWAT and a bird species distribution model with NSGA-II in order to optimize land management strategies for biodiversity, water quality and quantity, and agricultural production. On the resulting set of Pareto-optimal solutions, they applied stakeholder preferences to identify "best-compromise" solutions. Rodriguez et al. (2011) as well as Panagopoulos et al. (2012) applied SWAT and NSGA-II in the selection and placement of best management practices which minimized pollution in a cost effective way. Also, Lautenbach et al. (2013) coupled SWAT with NSGA-II. They analyzed the biophysical trade-off between bioenergy crop production and stream water quality and quantity.

The Nyangores sub-catchment management plan (WRUA, 2011) created by the Mara River Water Users Association indicated that this catchment faces severe water quality and quantity problems. In order to address this situation, they proposed reforestation using indigenous trees in addition to the adoption of water and soil conservation measures. However, this report lacks information on exactly how and where within the catchment these measures should be targeted. This poses a potential challenge for all stakeholders in the area. Against this background, the main objective of this study is to determine functional trade-offs between environmental sustainability and food production in the Nyangores catchment, Kenya. To achieve this purpose, we coupled SWAT with NSGA-II to explore different land-use combinations representing the best-possible trade-off (or Pareto) solutions in a four-dimensional objective space defined by (i) minimizing sediment load, (ii) maximizing stream low flow, and (iii, iv) maximizing the crop yields of maize and soybeans, respectively. To the best of our knowledge, no previous study has considered the consequences of implementing the proposed CMSs for different, partly conflicting, dimensions of sustainability in the Nyangores catchment. This study therefore aims to provide practical solutions for solving the major problems experienced in the catchment. Moreover, although agroforestry is well promoted as a way of restoring trees in many other developing countries, its impact on several ecosystem services is not well researched (Muthee et al., 2022). The methodology adopted here can be customized for these regions. It also allows for an easy inclusion of stakeholders who can then be involved in developing targeted policy interventions which balance environmental goals and the social needs of the existing population.

Materials and methods

Nyangores catchment

The Nyangores catchment (**Figure 1A**) covers a total area of 694 km^2 and is part of the greater Mara River basin

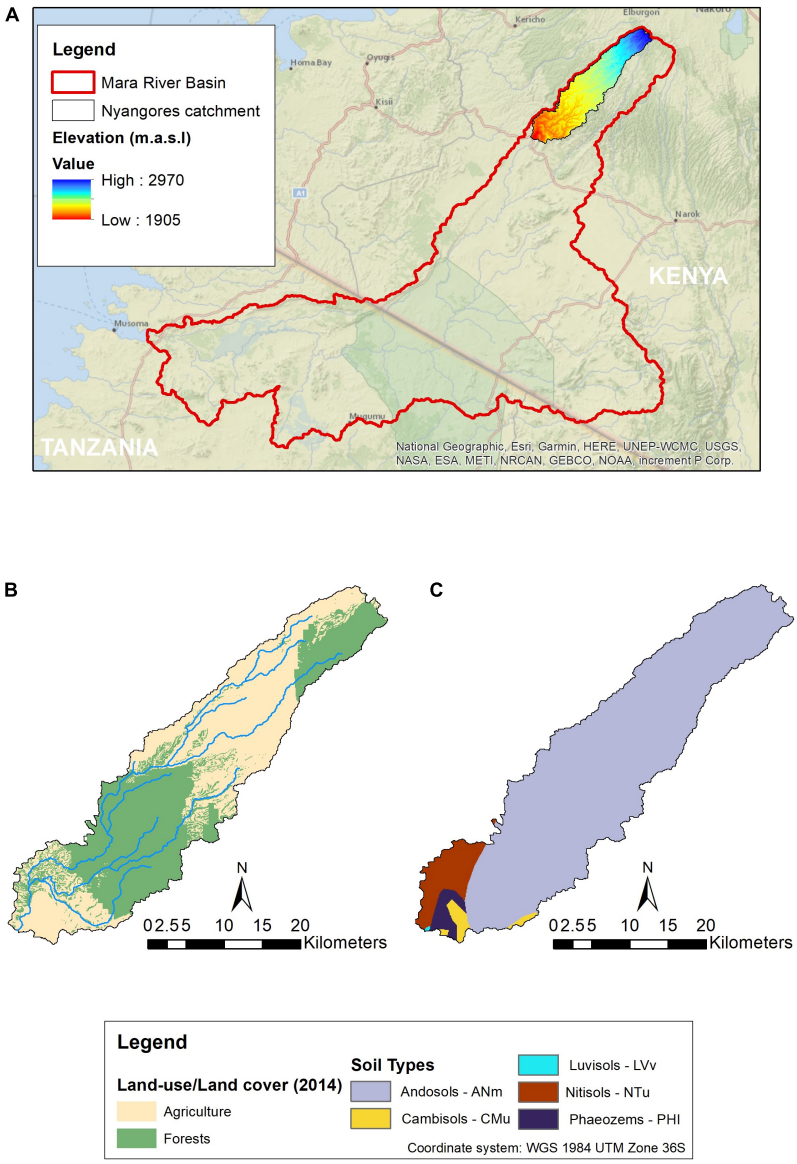

FIGURE 1
Nyangores catchment **(A)** location and elevation, **(B)** land-use/land cover, and **(C)** soil types.

which is shared between Kenya (65%) and Tanzania (35%). The altitude ranges from 2,970 m at the Mau escarpment to 1,905 m at Bomet stream gauging station. The mean annual rainfall ranges between 1,000 and 1,750 mm (Mati et al., 2008). Rainfall peaks twice a year: March–May (long rainy season) and September-November (short rainy season). The main river in the catchment is the Nyangores River (**Figure 1B**). Andosols, characterized by favorable aggregate structure and high porosity, are the dominant soils in the catchment (**Figure 1C**). The Nyangores catchment holds the largest proportion of Montane forests within the Mara basin and the remaining area is covered by small-scale agriculture. The main crops grown in the catchment include: maize, beans, soybeans, sorghum, potatoes, and oilseeds. In areas with high rainfall uncertainty the farmers practice intercropping (Omonge et al., 2020). Otherwise, maize is primarily grown within the first long rainy season (April/May) and harvested in September while the other crops take advantage of the short rains and are harvested in February, thus completing a crop rotation schedule. A major land-use shift from forest to agriculture has significantly affected the hydrological regime (water quality and quantity) in the catchment (Mwangi et al., 2016a). This has raised concern as the middle part of the Mara River basin hosts a major wildlife-reserve ecosystem, that heavily relies on the water resources (Mati et al., 2008; Mwangi et al., 2016a). Omonge et al. (2020) predicted an increase in water scarcity in the area driven

by population expansion (+4% per annum) and intensified agriculture. Thus, there is urgent need for the development and implementation of CMSs to combat the water crisis in the catchment while still ensuring continued and sustained food production.

Datasets

A 30-m digital elevation model (DEM) and Landsat-8 operational land imager (OLI) were downloaded from the Earth Explorer hosted by the United States Geological Survey (EarthExplorer-USGS, 2019). A soil map (scale 1: 250,000) and soil database were obtained from the Soil and Terrain (SOTER) database of the International Soil Reference and Information Centre (ISCRIC) (Batjes, 2008). A land-use map (1983) coinciding with the period selected for calibration and validation was sourced from the Survey of Kenya (SOK). Furthermore, daily rainfall data for 20 stations located in and within the vicinity of the Nyangores catchment, and climate data (relative humidity, wind speed, maximum and minimum temperature, and solar radiation) from Narok, Kericho, and Kisii weather stations were obtained from the Kenya Meteorological Department (KMD). Discharge data for the only existing stream gauging station-LA03-Bomet was obtained for calibration purposes. The presence of data gaps limited the calibration period to the 4 year period from 1975 to 1978.

Due to lack of observed sediment load data, a time series was determined by relating discharge at the catchment outlet and sediment concentration (SC) using Eq 1 (Kiragu, 2009), which was specifically developed for the study area, and Eq 2 (Bartram et al., 1996).

$$SC = 19.77 + 22.42 * Log\ Q \quad (1)$$

where:
SC is the sediment concentration $\left(\frac{mg}{l}\right)$.
Q is the discharge in m^3/s. and

$$SL = Q * SC * 0.0864 \quad (2)$$

where SL is the suspended sediment load in tonnes/day.

Supplementary Appendix I provides a summary of the datasets used for the analysis.

Soil water assessment tool base scenario set-up

The SWAT model is a continuous time, semi-distributed process based river basin model (Arnold et al., 2012). Soil water assessment tool operates on a daily time step and was developed to determine the impact of land use and management on water, sediment, agricultural, and chemical yields. In SWAT, the catchments are divided into sub-catchments which are further divided into hydrologic response units (HRUs) which consist of homogeneous land use, management, soil, and slope. These units are represented as a percentage of the total catchment area. The main components include: weather, hydrology, soil properties, plant growth, nutrition, pesticides, bacteria, pathogens, and land management. A detailed description is provided by the theoretical documentation (Neitsch et al., 2011).

The model setup and calibration for discharge was done following Kamamia et al. (2019) using the ArcSWAT version 2012.10.2.18. The DEM-30 m was loaded into the ArcGIS environment (ArcMap version 10.2) and used as a base for watershed delineation. All other inputs (land use map, soil map) were prepared and entered into the model. The slope was divided into four classes: 0–10, 10–20, 20–30, and above 30%. Potential evaporation was calculated using the Priestly and Taylor method (1972) which is based on radiation. The following adjustments were made to adequately simulate growth of perennial vegetation dynamics in the tropics (c.f., Mwangi et al., 2016a; Kamamia et al., 2019). (i) Lowering the Potential Heat Units (PHU) from 0.15 to 0.001, (ii) Increasing the minimum leaf area index (LAI) from 0.75 to 3 to ensure continuous evapotranspiration of trees and perennials (iii) Using the "kill" operation to restart the growth cycle of trees and perennial crops. The curve number (CN2) parameter was also adjusted depending on plant evapotranspiration. Using the set of most sensitive parameters presented in **Supplementary Appendix II**, calibration for discharge and sediment were undertaken simultaneously. R^2 and Nash-Sutcliffe efficiency (NSE) were used as statistical indices to assess the ability of the model to match the data observed. The R^2 estimates how well the model variance prediction represents those of the observed values. These values range from 0 (no correlation) to 1 (perfect correlation) (Moriasi et al., 2007). The NSE measures how well the simulated output matches the observed along a 1:1 regression line. NSE values $\leq$0 indicate that the observed data mean is more accurate than the simulated output (Moriasi et al., 2007). For simulating sediment loads, performance values of 0.55 and 0.62 were achieved for NSE and R^2, respectively.

Maize and soybean were selected for the modeling exercise to represent the crops to be grown during the long and short rains, respectively. Using a 2014 land-use map, the agricultural HRUs were adjusted to reflect the actual cropping seasons indicated in section "Nyangores catchment". According to literature, annual maize yield in Nyangores catchment is between 2,500 and 4,000 kg/ha (Ngome et al., 2013) while that of soybean is averaged at 1,000–2,500 kg/ha (FAO, 2011). This is considerably lower than the potential of 6,000 kg/ha for maize and 30% higher for soybeans. During planting, inorganic fertilizer diammonium phosphate (18%N, 20%P) is applied at the average rate of 135 kg/ha which is also well below the recommended 250 kg/ha (Munialo et al., 2020). Despite a

slight improvement in output over the last two decades, the low application of both organic and inorganic fertilizers, poor soil management and climate and pest related hazards have contributed to what would be still regarded as low yield output (Munialo et al., 2020). The hand-hoeing method was selected to represent tillage in the SWAT agricultural management files. Planting and harvesting dates for Maize and Soybean were set to 1st April and 31st August and 1st October and 15th February, respectively. The biomass outputs of both crops were checked against the values obtained in literature (see section "Nyangores catchment") and the PHUs adjusted accordingly. Moreover, the management files were adjusted to represent the land use of 2014. Mwangi et al. (2016b) estimated that climate variability only contributed 2.5% to the changes in streamflow in the catchment between 1980 and 2014 while the rest was linked to land-use change. Thus, it was necessary to adjust this to capture the drastic land-use change. The already calibrated model was run one last time to reflect the aforementioned adjustments and obtain the final base scenario model.

Set-up of catchment management strategies scenarios and use of land-use optimization tool

The main CMSs can be classified as structural, agronomic, and vegetative measures (Liniger et al., 2002). Structural measures (such as terraces and contour banks) lead to a change in slope. They are mainly permanent and often require high inputs of labor and capital for installation (Liniger et al., 2002; Mwangi, 2011). Agronomic measures, usually associated with annual crops are applied regularly in each season and include contour cropping/mixed/cover cropping and mulching (Mati et al., 2008; Mwangi, 2011; Gathagu et al., 2018). Vegetative measures use perennial grasses and trees over a long time. For small-scale farming, vegetative and agronomic measures are prescribed as they are easier to adopt, cost less and still lead to an improvement of the catchment (Liniger et al., 2002; Mwangi, 2011). These CMSs can be used in isolation or combination with other measures. Mwangi et al. (2015) evaluated the impact of different conservation practices on water and sediment yield in the Sasumua catchment in Kenya. When implemented in isolation, a 10 m filter strip and contour farming reduced sediment inflow to the river by 35 and 24%, respectively. When combined, a 41% sediment reduction was recorded. Reforestation practices in which woody perennials are deliberately grown in deforested areas have been used to restore degraded areas (Mwangi, 2011; Mwangi et al., 2015). Trees within this system provide both productive and protective functions. Among the productive functions, the five "Fs" (fuel wood, food, fodder/feed, fiber, and fertilizer) (Atangana et al., 2014) are principal. The protective functions include shade, reduction in wind speed, erosion control, carbon sequestration, and climate change adaptation (Atangana et al., 2014; Nair et al., 2021).

Therefore, agroforestry and agronomic scenarios were implemented at the HRU level and slope-wise for the agricultural land use only. In ArcSWAT version 2012.10.2.18, agroforestry was simulated as woodlots. Contour farming and vegetative filter strips were selected to represent agronomic vegetative measures. Contour farming is a form of agriculture where farming activities are done across the slope rather than up and down the slope (Liniger et al., 2002). The rows of crops planted across the slope block water flow allowing it more time to infiltrate which reduces surface run-off and erosion. In order to represent contour farming, the CN2 value of all agricultural HRUs in the SWAT model were reduced by three units according to Mwangi et al. (2015). Furthermore, the Universal Soil Loss Equation (USLE_P) parameter was adjusted according to Neitsch et al. (2011) depending on the slope of the HRU. In order to represent the vegetative filter strips such as Napier grass, the width of edge-of-field filter strip parameter (FILTERW) was set at 5 m according to Mwangi (2011) who reported that the combined use of contour farming and a 5 m vegetative filter strip produced the largest reduction in sediment load (∼73%). Three different scenarios were represented by three different model setups. These were the adoption of: (i) agroforestry only – Scenario 1, (ii) agroforestry + contour farming + vegetative filter strips (CA) – Scenario 2, and (iii) CA only– Scenario 3.

Objective functions and constrained multi-objective optimization algorithm

In this study, four different objective functions were selected to be optimized with the genetic algorithm NSGA-II. The functions describe catchment-scale environmental and economic values that can be directly derived from SWAT model outputs:

i) Minimize average sediment load (Sed_ld) in tons/year at the gauging station (**minimize-$\int_1$**).
ii) Maximize discharge under low flow conditions measured using the mean annual minimum (MAM) stream low-flow indicator in L/s (**minimize-$\int_2$**).
iii) Maximize catchment-wide total harvested maize yield (Mai_yld) in kilotons/year (**minimize-$\int_3$**).
iv) Maximize catchment-wide total harvested soybean yield (Soy_yld) in kilotons/year (**minimize-$\int_4$**).

Soil water assessment tool was coupled with NSGA-II using CoMOLA, a generic Python environment for Constrained Multi-objective Optimization of Land use Allocation (Strauch et al., 2019). This software is available at: https://github.com/

michstrauch/CoMOLA. The tool has been applied for a wide range of spatially explicit models in multiple case studies (Verhagen et al., 2018; Bartkowski et al., 2020; Kaim et al., 2020; Schwarz et al., 2020; Witing et al., 2022). CoMOLA supports user-defined models or objective functions and allows for basic land use constraints, such as (i) transition rules defining which type of land use can be converted into another and (ii) minimum and maximum area proportions of each land use type within the study area. In this study, land use was optimized for a set of 98 HRUs, which are currently used for conventional agriculture. The HRUs could either remain as conventional agriculture, change to forest (in scenario 1) or change to forest or CA (in scenario 2) or change to CA (in scenario 3). By optimizing agricultural HRUs only, all existing forests remained at the same location.

Figure 2 displays a schematic view of the CoMOLA workflow, which is inspired by biological evolution: The group of 98 HRUs with its base scenario setup (conventional agriculture) is defined as the starting individual. Based on the starting individual and the pre-defined transition rules, CoMOLA starts an evolutionary process by creating a set of different HRU configurations. Each HRU configuration is called an individual and is represented by a genome, i.e., a string of integers (n = 98) encoding the land cover and management of each HRU. All individuals of one generation form a population which changes over generations due to selection and variation (i.e., combination and mutation): Using the objective functions described above, each individual is assigned fitness values representing the achieved values for the four objectives, which are derived from running SWAT. Based on their fitness values, the algorithm applies a Pareto ranking for all individuals. Best performing individuals are archived and selected for mating to generate a new (offspring) population. In mating, each offspring individual is generated by a random combination (crossover) of two genomes. The likelihood of mating increases for individuals with a higher Pareto rank. Additional random mutations increase the diversity of genomes to consider a wide range of different HRU configurations. Mating and mutation can result in constraint-violating (so-called "infeasible") offspring individuals. Genomes of infeasible individuals are modified using a repair operation described in Strauch et al. (2019). The entire procedure, from fitness value calculation to offspring generation and genome repairing, is repeated for a pre-defined number of generations.

The genetic algorithm was run with a population size (PS) of 100 for a total 500 generations (M_Gen). We chose a crossover rate (CR) of 0.9 and a mutation rate (MR) of 0.01. The recommended ranges for PS and CR are (40–100) and (0.80–0.98), respectively. The MR should be set to 1/no. of genes (i.e., HRUs) within the genome of an individual (Strauch et al., 2019; Wang et al., 2019). PS defines the number of individuals (i.e., HRU configurations or SWAT model runs) per generation. M_Gen determines the number of generations over which the NSGA-II will evolve. A larger number M_Gen ensures a better convergence while a smaller number of PS may propagate premature convergence. CR drives the optimization search while the MR prevents the population from being confined in the local optima.

Lastly, in order to compare the different scenarios, the mid-range Pareto solution for each case was determined following Strauch et al. (2019). This is the numerically "best" compromise solution (i.e., the solution that is closest to the mean of each objective).

Results and discussion

Optimization within Scenario 1 considered a change from conventional agriculture to forest. The shape of the Pareto front (**Figure 3**) depicted a clear trade-off between the objectives crop yield and sediment load reduction. The higher the share of forests, the higher was the reduction in sediment load, but this came at the cost of less achievable crop yield. As it was only possible to change cropland to forest and not vice versa, all solutions had lower crop yields and a higher sediment load reduction compared to the *status quo*, which is represented by conventional agriculture in all cropland HRUs. With reference to the *status quo*, and at the mid-range position, Sed_ld decreased by 66%. This was accompanied by a decrease in the MAM of 5.2%. Furthermore, Mai_yld and Soy_yld production decreased by 12.8 and 11.4% respectively.

Likewise, **Figure 4** illustrated a negative relationship between crop yield and Sed_ld for Scenario 2. At the mid-range position, Sed_ld decreased significantly by 78% while the MAM increased by 14%. Mai_yld and Soy_yld production decreased by 3.8 and 3.4%, respectively. Scenario 3 (**Figure 5**) showed a comparable loss in crop production. This also resulted in a significantly lower reduction in sediment yield reduction (−41%) and a smaller increase in the MAM (+5%). A similar trend was observed by Kennedy et al. (2016) for a catchment in Brazil. They reported a trade-off between agricultural productivity and both water quality and biodiversity using a greedy heuristic algorithm, which - unlike the genetic algorithm - progressively builds toward a global optimum solution by focusing on local optimum solutions at each stage. Similarly, Femeena et al. (2018) reported a trade-off between food and biofuel production and nutrient pollution (represented as Nitrate and Total Phosphorous). Lee and Lautenbach (2016) assessed the relationships existing among the different ecosystem services and concluded that the relationship between regulating (e.g., sediment load) and most provisioning ecosystem (maize and soybean yield) services is dominated by trade-offs, where the increase of one service happens at the expense of the other.

Forests (as in Scenario 1) had a high impact in reducing sediment loads but also resulted in decreased MAM, Mai_yld

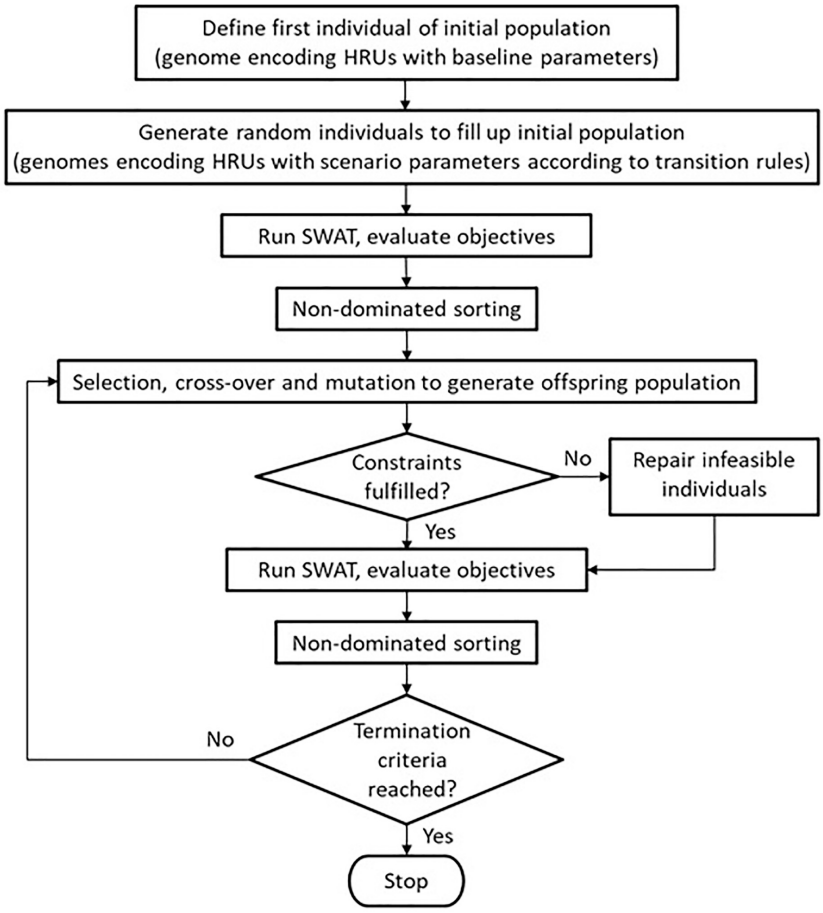

FIGURE 2
Flow chart of the CoMOLA optimization process for SWAT applications.

and Soy_yld (see **Table 1**). The combined use of trees and CA (Scenario 2), in contrast, not only reduced the sediment load, but also increased the MAM for a large number of solutions (all yellowish dots in **Figure 4**). Additionally, it led to a lower reduction in crop yield as compared to implementing each conservation measure individually, making it the most superior Scenario. In principle, forests are characterized by three primary elements that account for the distinctive movement and action of water. First, the foliage above ground forms a number of layers that compose the total thickness of the canopy. Second, the accumulation of dead and decaying plant remains on the ground surface constitute the forest floors (Reynolds et al., 1988). Both the canopy and litter intercept precipitation and modify the raindrop size and velocity. This reduces the impact of rain drop on soil surface resulting in reduced soil erosion. Last, the extensive and deeper root networks permeate the soil and are able to extract water from the soils and groundwater storages. During the dry season, the tree roots extend deeper than those of most vegetation and extract water from the groundwater storages, making it unavailable in the streams (Reynolds et al., 1988; Mwangi et al., 2016b). Nevertheless, the benefits of forests far outweigh the negative consequences. Mango et al. (2011) modeled the impact of a complete deforestation of the Nyangores catchment and conversion to agriculture. This resulted in a 31% increase in overland flow, 2% increase in evapotranspiration, >9% decrease in groundwater discharge and a 3% decrease in total water yield.

Contour farming (in Scenarios 2 and 3) halts surface runoff and in that increases water infiltration into the soil layers. The ridges and troughs created by contouring act as barriers to water flow, allowing it more time to infiltrate into the shallow aquifers. An increment of water in the shallow aquifer implies that this water can gradually be released during the dry season (Gathagu et al., 2018). Vegetative filter strips may allow some of the surface runoff with sediments to pass. The width of the filter strip determines the trapping efficiency. Generally, the wider the grass strip, the higher the trapping efficiency. Studies such as Gathagu et al. (2018) concluded that increasing the vegetative grass filter strip beyond 30 m increased the amount of sediment trapped by insignificant percentages while others such

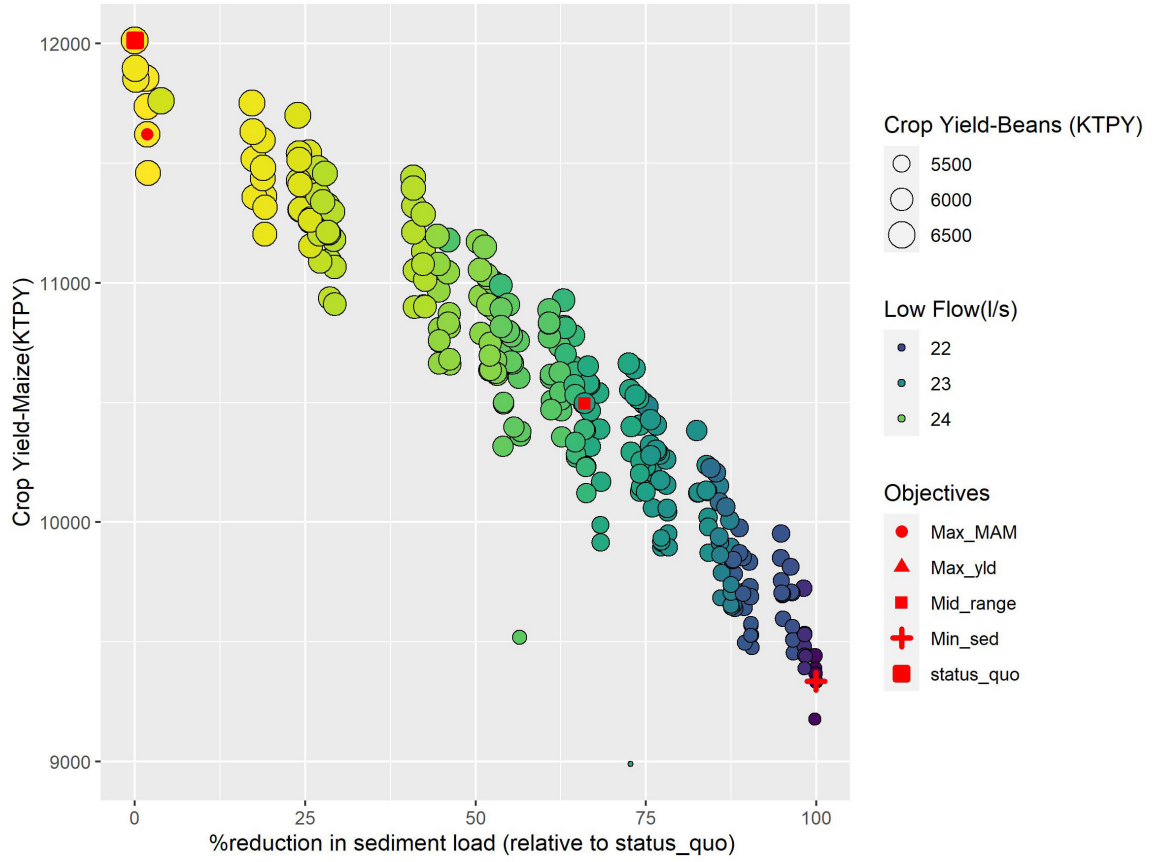

FIGURE 3
Performance of the pareto solutions of scenario 1 for MAM, sediment load and crop yield objective functions.

as Mwangi et al. (2015) recorded the highest sediment reduction within the first 3 m of filter strip width. Accordingly, the most optimum filter strip should be one that ensures the highest sediment reduction at the smallest width. The implementation of both contour farming and a 3-m filter strip had the highest impact on increasing the MAM stream low flow indicator. Unlike trees, these measures do not possess extensive roots systems which can tap into these aquifers during extended dry periods. This ensures that the water is released to the streams as base flow. In the Nyangores catchment, the small-scale farmers (who are the majority) practice hand-hoeing. Important parameters of soil loss such as the surface roughness obtained from the tillage depth are lower with hand-hoeing method as compared to mechanized tillage. Therefore, the actual soil loss in the catchment may be lower than that simulated in the study. Regardless, some studies have reported similar magnitudes using the SWAT model. For instance, Gathagu et al. (2018) concluded that the implementation of contour farming and filter strips reduced sediments by 63% in the Thika-Chania catchment in Kenya. Mwangi (2011) reported a 73% sediment load reduction for combining contour farming with a 5 m grass strip.

Most of the small-scale farming in Nyangores catchment is rain-fed and its potential remains extremely low as a result of the unsustainable farming practices and the effects of climate change (see section "Soil water assessment tool base scenario set-up"). The reduction in yield in all scenarios is a consequence of the reduction in cultivated land taken up by implementing the CMSs. But, it is expected that over time the positive effects of implementing the CMSs will result in increased crop yield. A review of the impacts of well-maintained soil and water conservation practices on crop yield by Adimassu et al. (2017) concluded that there exists a positive relationship between the age of CMSs and crop yield (although not linear). Meaning that under these conditions, the longer the time a CMS has been established, the higher the crop yield. Jat et al. (2014) reported a prominent improvement in yield after 2–3 years in a CA system when compared to a conventional tillage (CT) system of a 7 year rice-wheat system. Tanto and Laekemariam (2019) reported that adopting terracing and grass bunds CMS for 5 years increased wheat yield by 72.8% for a catchment in Southern Ethiopia. This is because, most of the CMS such as those implemented in the study are effective in: (i) reducing soil loss/increasing soil depth, (ii) reducing nutrient loss (iii), increasing moisture

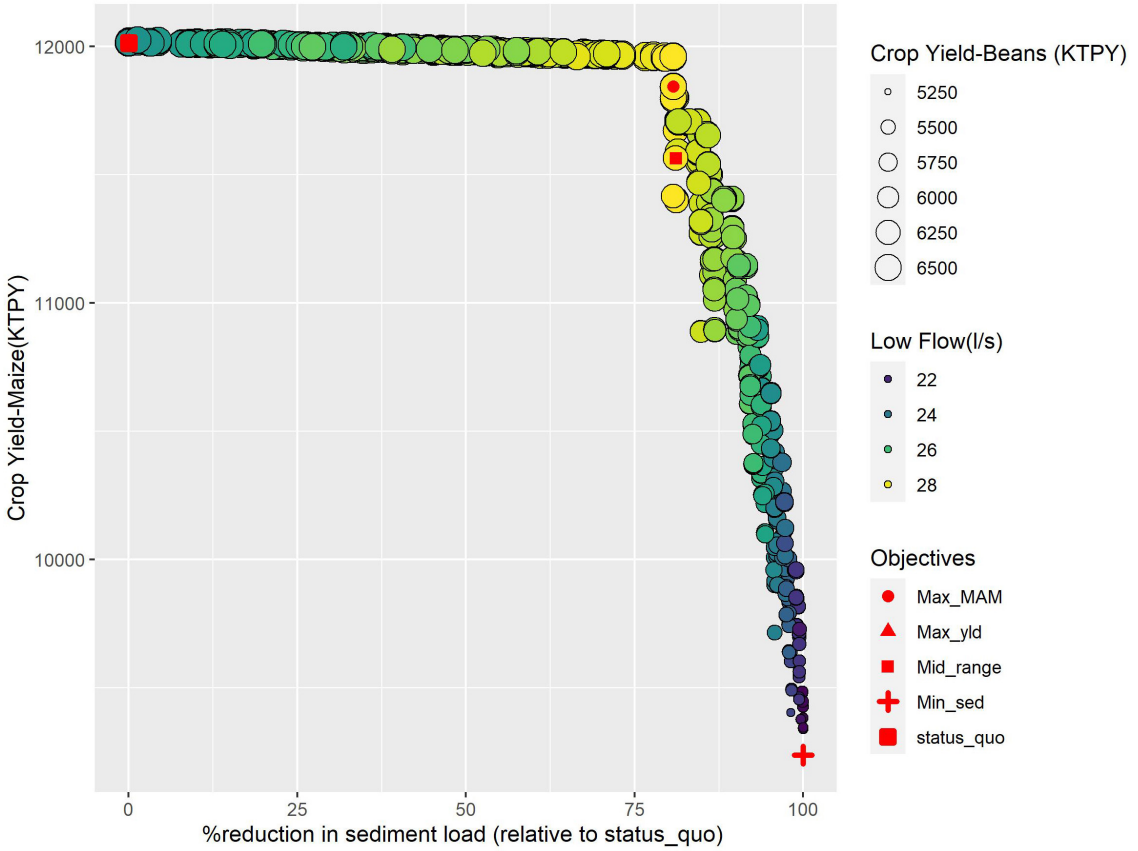

FIGURE 4
Performance of the pareto solutions of scenario 2 for MAM, sediment load and crop yield objective functions.

retention, and (iv) increasing baseflow. In view of this, the trade-off between sediment load, baseflow and crop yield need not be a major deterrent for the adoption of Scenario 2; which is the most feasible option for solving the major water quantity and quality problems while ensuring agricultural sustainability.

The mid-range output for Scenarios 1 and 2 clearly exhibits CoMOLAs tendency to allocate the different Land Use/Land Cover (LULC) in the headwater of the catchment. For Scenario 1 mid-range solution, all the HRUs that changed to forests (+8%) were located in the upper part of the catchment (see **Figure 6**). The upper part of the catchment has the highest elevation but not necessarily the highest slopes. Konrad (1996) reported a strong positive relationship between precipitation and elevation in mountainous regions. With orographic features enhancing precipitation, higher erosion rates are expected in the upper part of the catchment. Although Andosols (the dominant soils) are considered well aggregated, their resistance to water erosion decreases significantly when high rainfall intensities are exposed on bare/poorly maintained agricultural land. Khamsouk et al. (2002) concluded that Andosols have a high susceptibility to compaction which occurs when put under agriculture. High rainfall intensities are able to take off chunks of aggregated topsoil as a whole leading to high erosion rates. This can be confirmed by the map of sediment load (**Supplementary Figure 1**) which presented these areas as having the highest sediment load in the base Scenario.

Within Scenario 2, the change to CA (~35%) dominated over that of forests (3.6%). This can be attributed to its effect on improving MAM while not greatly reducing the yields of maize and soybean, all of which carry equal weight in the optimization process due to Pareto ranking. With most of the upper part of the catchment already allocated to forests, the mid-range solution also displayed the tendency of CoMOLA to locate CA on the extreme ends of the mid-section of the catchment bordering the forests and in areas possessing high slopes. The latter trend was also observed within Scenario 3 where the change to CA was ~42%. Most of the areas having high slopes in the mid-section are already under forests but there were a few still under conventional agriculture that were selected in this mid-range output. Most of the mid-section can be classified as having a slope range of between 10 and 20%, thus experiencing mostly sheet and rill erosion (Khamsouk et al., 2002). All cropland with slopes <10% (majorly the lower part) was not considered during the analysis.

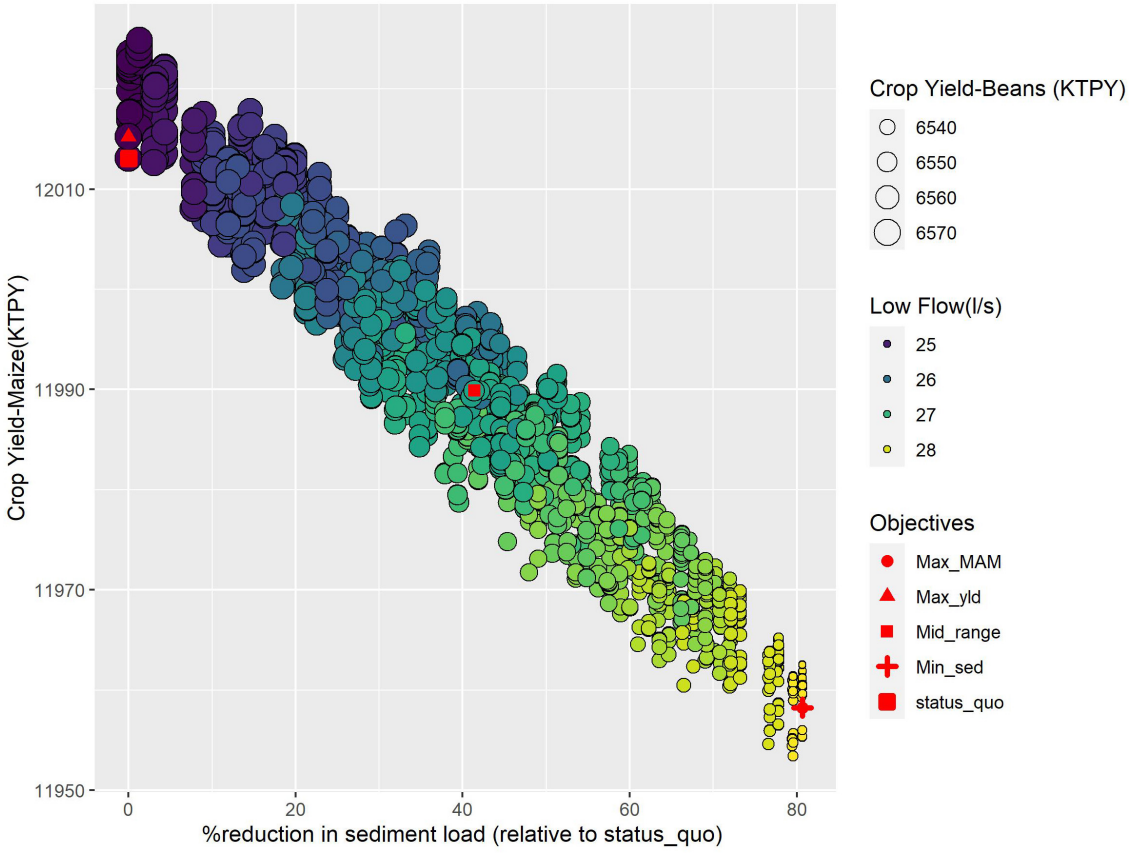

FIGURE 5
Performance of the pareto solutions of scenario 3 for MAM, sediment load and crop yield objective functions.

It should be noted that the complete set of Pareto-optimal solutions yields a set of different land-use configurations and it is up to the stakeholders to assess and select the solution most preferred. The use of land-use optimization tools such as CoMOLA allows for easy incorporation of stakeholders. This can be done before or after the optimization process. When done before, they are imperative not only in identifying the main problems in the catchment (e.g., defining the multiple objectives) but also in designing solutions that the communities would be willing to adopt. However, including the stakeholders before the optimization process may constrain the search space for feasible solutions. This is solved by involving them in the selection of the preferred solution once the Pareto optimal solutions are reached (Lee and Lautenbach, 2016; Kaim et al., 2020). The results indicate that the Nyangores catchment represents an upstream-downstream kind of trade-off. Although incentive based measures such as payment for ecosystem services (PES) schemes remain administratively and logistically challenging (Kindu et al., 2022), they can offer a way to effect the desired changes. Since upstream changes such as forest establishment, management and adoption of CA are oriented toward positive changes in the whole catchment, the upstream land-owners can be paid by the downstream stakeholders for forgoing their normal production.

TABLE 1 Summary of performance of all the scenarios under the various objectives.

Objective	Scenario 1 (%)	Scenario 2 (%)	Scenario 3 (%)
MAM	−5.2	+14	+5
Sed_yld	−66	−78	−41
Soy_yld	−11.4	−3.4	−2.9
Mai_yld	−12.8	−3.8	−3

A negative sign indicates a reduction/deterioration with reference to an objective while a positive sign indicates an increase/improvement.

Well-designed agroforestry and CMSs should meet both ecosystems and livelihood needs (Muthee et al., 2022). For example, for agroforestry systems, potential ecosystem benefits such as; (i) water quality regulation, (ii) soil enrichment, (iii) biodiversity conservation, and (iv) carbon sequestration (Jose, 2009) must be simultaneously assessed against livelihood securities. The methodology adopted can be used to present the various ecosystem trade-offs and synergies in quantitative

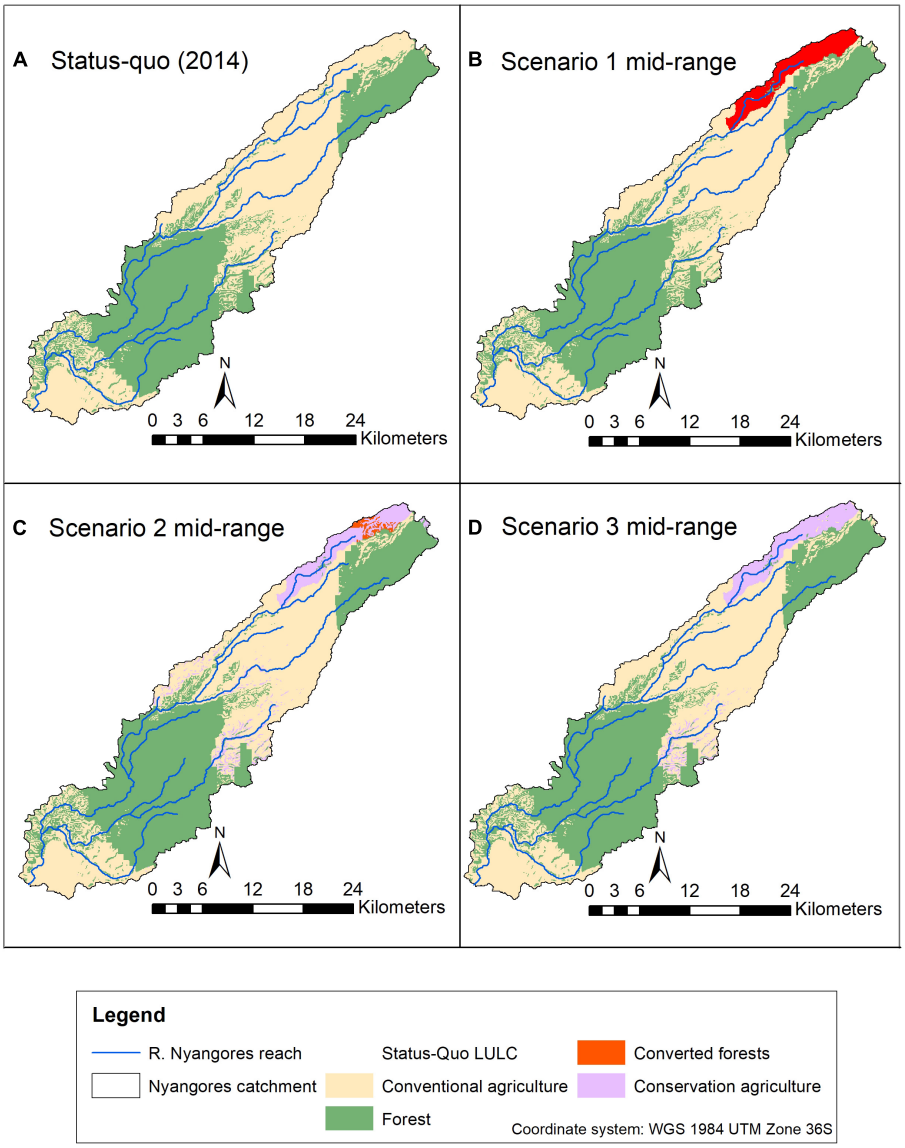

FIGURE 6
Spatial distribution of the different land-uses for the mid-range solution for Scenario 1 **(B)**, Scenario 2 **(C)**, and Scenario 3 **(D)**, relative to the base Scenario **(A)**.

measures which stakeholders can use to identify solutions according to their preferences and needs. With this scientific foundation, different land-use policies can be developed and contextualized for the sustainability of any catchment.

Conclusion

In this study, the SWAT model was coupled with CoMOLA to select land-use combinations providing the smallest trade-off amongst sediment load, MAM stream low flow indicator, and the crop yield of maize and soybean. The SWAT model was run for different HRU management and land cover configurations and the outputs were assessed. The obtained results are influenced by the model parameterization which heavily depends on the quality and availability of the required data. This is often a major challenge in data-scarce areas, such as the Nyangores catchment, which are mostly in need of scientific backed research to inform decisions related to catchment management. The major limitations faced in this study were the lack of water quality data, more recent discharge data and crop yield records. This was overcome by using older data and values from literature as well as information derived from interviewing selected farmers. The calibration outputs obtained from the simulation were regarded as satisfactory. The

introduced approach can be adopted for other catchments and different multi-objective problems.

The mid-range solutions of both Scenarios 1 and 2 exhibited land-use optimization preference for locating the trees in the upper part of the catchment. Scenario 2 was superior with regards to most of the ecosystem objectives as it resulted in the smallest trade-off. The Pareto-optimal solutions identified under this scenario provide different configuration options allowing for stakeholders to assess and select their most preferred solution which would achieve the highest sustainable output with the least degree of environmental degradation. Kaim et al. (2020) provided a promising example on how to involve stakeholders to select their preferred solutions from the full set of Pareto-optimal solutions. Although the reduction in crop yield could raise concerns for the communities, it must be viewed within the greater context of the nexus approach to water resource management. Water, soils and food production are interlinked and must be managed in an integrated manner. Also, in the long run, these conservation practices could elicit increased crop yield due to improved water and nutrient retention (Pooniya et al., 2021). With climate change inducing more frequent floods and droughts in the Nyangores catchment, protecting the remaining forests together with the adoption of agroforestry and other soil and conservation practices is critical not in just offsetting the excess water and sediments during floods but also ensuring water availability through groundwater recharge during the extended droughts.

Finally, this methodology can play an integral part in ensuring the sustainability of multifunctional landscapes. It provides a way to quantitatively assess multiple trade-offs of ecosystem services when adopting CMSs. It also promotes the inclusion of stakeholders which further increases the acceptance of these strategies.

Data availability statement

The original contributions presented in this study are included in the article/**Supplementary material**, further inquiries can be directed to the corresponding author.

Author contributions

AK, MS, HM, K-HF, JS, and SJ contributed to the conception, design, and analysis of the study. AK wrote the first draft of the manuscript. All authors contributed to manuscript revision, read, and approved the submitted version.

Funding

This work was funded by Graduate Academy, TU Dresden through the Travel Grants for Short-Term Research stays abroad and the Scholarship Program for the Promotion of Early-Career Female Scientists scholarship programs.

Conflict of interest

The authors declare that the research was conducted in the absence of any commercial or financial relationships that could be construed as a potential conflict of interest.

Publisher's note

Supplementary material

The Supplementary Material for this article can be found online at: https://www.frontiersin.org/articles/10.3389/ffgc.2022.1046371/full#supplementary-material

SUPPLEMENTARY FIGURE 1
Nyangores catchment sub-basin annual soil loss.

References

Adimassu, Z., Langan, S., Johnston, R., Mekuria, W., and Amede, T. (2017). Impacts of soil and water conservation practices on crop yield, run-off, soil loss and nutrient loss in ethiopia: review and synthesis. *Environ. Manag.* 59, 87–101. doi: 10.1007/s00267-016-0776-1

Arnold, J. G., Moriasi, D. N., Gassman, P. W., Abbaspour, K., White, M. J., Srinivasan, R., et al. (2012). SWAT: model use, calibration, and validation. *Trans. ASABE* 55, 1491–1508. doi: 10.13031/2013.42256

Asres, M. T., and Awulachew, S. B. (2010). SWAT based runoff and sediment yield modelling: a case study of the Gumera watershed in the Blue Nile basin. *Ecohydrol. Hydrobiol.* 10, 191–199. doi: 10.2478/v10104-011-0020-9

Atangana, A., Khasa, D., Chang, S., and Degrande, A. (2014). Tropical agroforestry. *Agroforest Syst.* 88, 385–385. doi: 10.1007/s10457-013-9668-z

Bajocco, S., De Angelis, A., Perini, L., Ferrara, A., and Salvati, L. (2012). The impact of land use/land cover changes on land degradation dynamics: a mediterranean case study. *Environ. Manag.* 49, 980–989. doi: 10.1007/s00267-012-9831-8

Bartkowski, B., Beckmann, M., Drechsler, M., Kaim, A., Liebelt, V., Müller, B., et al. (2020). Aligning Agent-Based Modeling With Multi-Objective Land-Use Allocation: Identification of Policy Gaps and Feasible Pathways to Biophysically Optimal Landscapes. *Front. Environ. Sci.* 8:13. doi: 10.3389/fenvs.2020.00103

Bartram, J., Ballance, R., Organization, W. H., and Programme, U. N. E. (1996). *Water Quality Monitoring?: A Practical Guide to the Design and Implementation of Freshwater Quality Studies and Monitoring Programs*. New York, NY: E & FN Spon. doi: 10.4324/9780203476796

Batjes, N. H. (2008). *ISRIC-WISE Harmonized Global Soil Profile Dataset (Ver. 3.1)*. Available online at: 10.13140/2.1.4306.7683 (accessed on August 21, 2020).

Boretti, A., and Rosa, L. (2019). Reassessing the projections of the World Water Development Report. *npj Clean Water* 2, 1–6. doi: 10.1038/s41545-019-0039-9

Borrelli, P., Robinson, D. A., Fleischer, L. R., Lugato, E., Ballabio, C., Alewell, C., et al. (2017). An assessment of the global impact of 21st century land use change on soil erosion. *Nat. Commun.* 8, 1–13. doi: 10.1038/s41467-017-02142-7

Cao, K., Batty, M., Huang, B., Liu, Y., Yu, L., and Chen, J. (2011). Spatial multi-objective land use optimization: extensions to the non-dominated sorting genetic algorithm-II. *Int. J. Geograph. Inform. Sci.* 25, 1949–1969. doi: 10.1080/13658816.2011.570269

Chapagain, A., Shimabuku, M., Morrison, J., Brill, G., Matthews, J. H., Davis, K., et al. (2021). *Water Resilience Assessment Framework. Alliance for Global Water Adaptation, CEO Water Mandate, International Water Management Institute, Pacific Institute, and World Resources Institute*. New York, NY: UN Global Compact.

Cohen, M. J., Brown, M. T., and Shepherd, K. D. (2006). Estimating the environmental costs of soil erosion at multiple scales in Kenya using emergy synthesis. *Agricult. Ecosyst. Environ.* 114, 249–269. doi: 10.1016/j.agee.2005.10.021

Deb, K., Pratap, A., Agarwal, S., and Meyarivan, T. (2002). A fast and elitist multiobjective genetic algorithm: NSGA-II. *IEEE Trans. Evol. Comput.* 6, 182–197. doi: 10.1109/4235.996017

EarthExplorer-USGS (2019). Available online at: https://earthexplorer.usgs.gov/ (accessed on March 10, 2020).

FAO (2011). Land & water | Food and agriculture organization of the United Nations. Available online at: https://www.fao.org/land-water/databases-and-software/crop-information/soybean/en/ (accessed November 21, 2022).

Femeena, P. V., Sudheer, K. P., Cibin, R., and Chaubey, I. (2018). Spatial optimization of cropping pattern for sustainable food and biofuel production with minimal downstream pollution. *J. Environ. Manag.* 212, 198–209. doi: 10.1016/j.jenvman.2018.01.060

Foley, J. A., Defries, R., Asner, G. P., Barford, C., Bonan, G., Carpenter, S. R., et al. (2005). Global consequences of land use. *Science* 309, 570–574. doi: 10.1126/science.1111772

Gathagu, J. N., Mourad, K. A., and Sang, J. (2018). Effectiveness of contour farming and filter strips on ecosystem services. *Water* 10:1312. doi: 10.3390/w10101312

Jat, R. K., Sapkota, T. B., Singh, R. G., Jat, M. L., Kumar, M., and Gupta, R. K. (2014). Seven years of conservation agriculture in a rice–wheat rotation of Eastern Gangetic Plains of South Asia: Yield trends and economic profitability. *Field Crops Res.* 164, 199–210. doi: 10.1016/j.fcr.2014.04.015

Jose, S. (2009). Agroforestry for ecosystem services and environmental benefits: an overview. *Agroforest Syst.* 76, 1–10. doi: 10.1007/s10457-009-9229-7

Kaim, A., Bartkowski, B., Lienhoop, N., Schröter-Schlaack, C., Volk, M., and Strauch, M. (2021). Combining biophysical optimization with economic preference analysis for agricultural land-use allocation. *Ecol. Soc.* 26:9. doi: 10.5751/ES-12116-260109

Kaim, A., Cord, A. F., and Volk, M. (2018). A review of multi-criteria optimization techniques for agricultural land use allocation. *Environ. Model. Softw.* 105, 79–93. doi: 10.1016/j.envsoft.2018.03.031

Kaim, A., Strauch, M., and Volk, M. (2020). Using stakeholder preferences to identify optimal land use configurations. *Front. Water* 2:579087. doi: 10.3389/frwa.2020.579087

Kamamia, A. W., Mwangi, H. M., Feger, K.-H., and Julich, S. (2019). Assessing the impact of a multimetric calibration procedure on modelling performance in a headwater catchment in Mau Forest, Kenya. *J. Hydrol. Region. Stud.* 21, 80–91. doi: 10.1016/j.ejrh.2018.12.005

Kamamia, A. W., Vogel, C., Mwangi, H. M., Feger, K. H., Sang, J., and Julich, S. (2021). Mapping soil aggregate stability using digital soil mapping: A case study of Ruiru reservoir catchment, *Kenya. Geoderma Reg.* 24:e00355. doi: 10.1016/j.geodrs.2020.e00355

Kamamia, A. W., Vogel, C., Mwangi, H. M., Feger, K., Sang, J., and Julich, S. (2022). Using soil erosion as an indicator for integrated water resources management: a case study of Ruiru drinking water reservoir, Kenya. *Environ. Earth Sci.* 81:502. doi: 10.1007/s12665-022-10617-0

Kennedy, C. M., Hawthorne, P. L., Miteva, D. A., Baumgarten, L., Sochi, K., Matsumoto, M., et al. (2016). Optimizing land use decision-making to sustain Brazilian agricultural profits, biodiversity and ecosystem services. *Biol. Conserv.* 204, 221–230. doi: 10.1016/j.biocon.2016.10.039

Khamsouk, B., De, G., and Benali, I. (2002). "New data concerning erosion processes and soil management on andosols from ecuador and martinique," in *Proceeding of the Sustainable Utilization of Global Soil and Water Resources: 2. Process of soil erosion and its environnment effect, International Soil Conservation Organisation Conference*. Pékin: Tsinghua University.

Kindu, M., Mai, T. L. N., Bingham, L. R., Borges, J. G., Abildtrup, J., and Knoke, T. (2022). Auctioning approaches for ecosystem services – Evidence and applications. *Sci. Total Environ.* 853:158534. doi: 10.1016/j.scitotenv.2022.158534

Kiragu, G. M. (2009). *Assessment of Suspended Sediment Loadings and Their Impact on the Environmental Flows of the Upper Transboundary Mara River, Kenya*. Kenya: JKUAT.

Kirschke, S., Zhang, L., and Meyer, K. (2018). Decoding the wickedness of resource nexus problems—examples from water-soil nexus problems in China. *Resources* 7:67. doi: 10.3390/resources7040067

Kogo, B. K., Kumar, L., and Koech, R. (2020). Impact of land use/cover changes on soil erosion in western Kenya. *Sustainability* 12:9740. doi: 10.3390/su12229740

Konrad, C. E. II (1996). Relationships between precipitation event types and topography in the southern blue ridge mountains of the southeastern USA. *Int. J. Climatol.* 16, 49–62. doi: 10.1002/(SICI)1097-0088(199601)16:1<49::AID-JOC993>3.0.CO;2-D

Lautenbach, S., Volk, M., Strauch, M., Whittaker, G., and Seppelt, R. (2013). Optimization-based trade-off analysis of biodiesel crop production for managing an agricultural catchment. *Environ. Model. Softw.* 48, 98–112. doi: 10.1016/j.envsoft.2013.06.006

Lee, H., and Lautenbach, S. (2016). A quantitative review of relationships between ecosystem services. *Ecol. Indic.* 66, 340–351. doi: 10.1016/j.ecolind.2016.02.004

Legesse, D., Vallet-Coulomb, C., and Gasse, F. (2003). Hydrological response of a catchment to climate and land use changes in Tropical Africa: case study South Central Ethiopia. *J. Hydrol.* 275, 67–85. doi: 10.1016/S0022-1694(03)00019-2

Liniger, H. P., Cahill, D., Critchley, W., van Lynden, G. W. J., and Schwilch, G. (2002). *Categorization of SWC Technologies and Approaches*. Beijing: YUMPU.

Mango, L. M., Melesse, A. M., McClain, M. E., Gann, D., and Setegn, S. G. (2011). Land use and climate change impacts on the hydrology of the upper Mara River Basin, Kenya. *Hydrol. Earth Syst. Sci.* 15, 2245–2258. doi: 10.5194/hess-15-2245-2011

Mati, B. M., Mutie, S., Gadain, H., Home, P., and Mtalo, F. (2008). Impacts of land-use/cover changes on the hydrology of the transboundary Mara River, Kenya/Tanzania. *Lakes Reserv. Sci. Policy Manag. Sustain. Use* 13, 169–177. doi: 10.1111/j.1440-1770.2008.00367.x

Memarian, H., Balasundram, S. K., Abbaspour, K. C., Talib, J. B., Boon Sung, C. T., and Sood, A. M. (2014). SWAT-based hydrological modelling of tropical land-use scenarios. *Hydrol. Sci. J.* 59, 1808–1829. doi: 10.1080/02626667.2014.892598

Mitchell, M. (1996). *An Introduction to Genetic Algorithms*. Cambridge, MA: A Bradford Book.

Moriasi, D. N., Arnold, J. G., Van Liew, M. W., Bingner, R. L., Harmel, R. D., and Veith, T. L. (2007). Model evaluation guidelines for systematic quantification of accuracy in watershed simulations. *Trans. ASABE* 50, 885–900. doi: 10.13031/2013.23153

Mulinge, W., Gicheru, P., Murithi, F., Maingi, P., Kihiu, E., Kirui, O. K., et al. (2016). "Economics of land degradation and improvement in Kenya," in *Economics of Land Degradation and Improvement – A Global Assessment for Sustainable Development*, eds E. Nkonya, A. Mirzabaev, and J. von Braun (Cham: Springer International Publishing), 471–498. doi: 10.1007/978-3-319-19168-3_16

Munialo, S., Dahlin, A. S., Maa, C. O., Oluoch-Kosura, W., Marstorp, H., and Öborn, I. (2020). Soil and management-related factors contributing to maize yield gaps in western Kenya. *Food Energy Secur.* 9:e189. doi: 10.1002/fes3.189

Muthee, K., Duguma, L., Majale, C., Mucheru-Muna, M., Wainaina, P., and Minang, P. (2022). A quantitative appraisal of selected agroforestry studies in the Sub-Saharan Africa. *Heliyon* 8, e10670. doi: 10.1016/j.heliyon.2022.e10670

Mwangi, H. M. (2011). *Evaluation of the Impacts of Soil and Water Conservation Practices on Ecosystem Services in Sasumua Watershed, Kenya, using SWAT Model*. JKUAT Abstracts of PostGraduate Thesis, Jomo Kenyatta University, Kenya.

Mwangi, H. M., Julich, S., Patil, S. D., McDonald, M. A., and Feger, K.-H. (2016a). Modelling the impact of agroforestry on hydrology of Mara River Basin in East Africa. *Hydrol. Proces.* 30, 3139–3155. doi: 10.1002/hyp.10852

Mwangi, H. M., Julich, S., Patil, S. D., McDonald, M. A., and Feger, K.-H. (2016b). Relative contribution of land use change and climate variability on discharge of upper Mara River, Kenya. *J. Hydrol. Region. Stud.* 5, 244–260. doi: 10.1016/j.ejrh.2015.12.059

Mwangi, J. K., Shisanya, C. A., Gathenya, J. M., Namirembe, S., and Moriasi, D. N. (2015). A modeling approach to evaluate the impact of conservation practices on water and sediment yield in Sasumua Watershed, Kenya. *J. Soil Water Conserv.* 70, 75–90. doi: 10.2489/jswc.70.2.75

Mwangi, K., Musili, A. M., Otieno, V. A., Endris, H. S., Sabiiti, G., Hassan, M. A., et al. (2020). Vulnerability of Kenya's water towers to future climate change: an assessment to inform decision making in watershed management. *Am. J. Clim. Change* 9, 317–353. doi: 10.4236/ajcc.2020.93020

Nair, P. K. R., Kumar, B. M., and Nair, V. D. (2021). "Classification of agroforestry systems," in *An Introduction to Agroforestry: Four Decades of Scientific Developments*, eds P. K. R. Nair, B. M. Kumar, and V. D. Nair (Cham: Springer International Publishing), 29–44. doi: 10.1007/978-3-030-75358-0_3

Neitsch, S. L., Arnold, J. G., Kiniry, J. R., and Williams, J. R. (2011). *Soil and Water Assessment Tool Theoretical Documentation Version 2009*. Texas: Texas Water Resources Institute.

Ngome, A., Becker, M., Mtei, K., and Mussgnug, F. (2013). Maize productivity and nutrient use efficiency in Western Kenya as affected by soil type and crop management. *Int. J. Plant Product.* 7, 517–536.

Omonge, P., Herrnegger, M., Gathuru, G., Fürst, J., and Olang, L. (2020). Impact of development and management options on water resources of the upper Mara River Basin of Kenya. *Water Environ. J.* 34, 644–655. doi: 10.1111/wej.12554

Panagopoulos, Y., Makropoulos, C., and Mimikou, M. (2012). Decision support for diffuse pollution management. *Environ. Model. Softw.* 30, 57–70. doi: 10.1016/j.envsoft.2011.11.006

Pooniya, V., Zhiipao, R. R., Biswakarma, N., Jat, S. L., Kumar, D., Parihar, C. M., et al. (2021). Long-term conservation agriculture and best nutrient management improves productivity and profitability coupled with soil properties of a maize–chickpea rotation. *Sci. Rep.* 11:10386. doi: 10.1038/s41598-021-89737-9

Reynolds, E. R. C., Thompson, F. B., and University, U. N. (1988). *Forests, Climate, and Hydrology*. Tokyo: United Nations University.

Rodriguez, H. G., Popp, J., Maringanti, C., and Chaubey, I. (2011). Selection and placement of best management practices used to reduce water quality degradation in Lincoln Lake watershed. *Water Resour. Res.* 47:141. doi: 10.1029/2009WR008549

Schmitz, T., and Kihara, F. (2021). "Investing in ecosystems for water security: the case of the Kenya water towers," in *The Palgrave Handbook of Climate Resilient Societies*, ed. R. C. Brears (Cham: Springer International Publishing), 117–135. doi: 10.1007/978-3-030-42462-6_23

Schwarz, N., Hoffmann, F., Knapp, S., and Strauch, M. (2020). Synergies or Trade-Offs? optimizing a virtual urban region to foster plant species richness, climate regulation, and compactness under varying landscape composition. *Front. Environ. Sci.* 8:16. doi: 10.3389/fenvs.2020.00016

Seppelt, R., Lautenbach, S., and Volk, M. (2013). Identifying trade-offs between ecosystem services, land use, and biodiversity: a plea for combining scenario analysis and optimization on different spatial scales. *Curr. Opin. Environ. Sustain.* 5, 458–463. doi: 10.1016/j.cosust.2013.05.002

Speranza, C. I. (2010). *Resilient Adaptation to Climate Change in African Agriculture*. Bonn: Deutsches Institut für Entwicklungspolitik.

Strauch, M., Cord, A. F., Pätzold, C., Lautenbach, S., Kaim, A., Schweitzer, C., et al. (2019). Constraints in multi-objective optimization of land use allocation – Repair or penalize? *Environ. Model. Softw.* 118, 241–251. doi: 10.1016/j.envsoft.2019.05.003

Strauch, M., and Volk, M. (2013). SWAT plant growth modification for improved modeling of perennial vegetation in the tropics. *Ecol. Model.* 269, 98–112. doi: 10.1016/j.ecolmodel.2013.08.013

Tanto, T., and Laekemariam, F. (2019). Impacts of soil and water conservation practices on soil property and wheat productivity in Southern Ethiopia. *Environ. Syst. Res.* 8:13. doi: 10.1186/s40068-019-0142-4

Verhagen, W., van der Zanden, E. H., Strauch, M., van Teeffelen, A. J. A., and Verburg, P. H. (2018). Optimizing the allocation of agri-environment measures to navigate the trade-offs between ecosystem services, biodiversity and agricultural production. *Environ. Sci. Policy* 84, 186–196. doi: 10.1016/j.envsci.2018.03.013

Wang, Q., Wang, L., Huang, W., Wang, Z., Liu, S., and Savić, D. A. (2019). Parameterization of NSGA-II for the optimal design of water distribution systems. *Water* 11:971. doi: 10.3390/w11050971

Wicki, S., Schwaab, J., Perhac, J., and Grêt-Regamey, A. (2021). Participatory multi-objective optimization for planning dense and green cities. *J. Environ. Plan. Manag.* 64, 1–22. doi: 10.1080/09640568.2021.1875999

Witing, F., Forio, M. A. E., Burdon, F. J., Mckie, B., Goethals, P., Strauch, M., et al. (2022). Riparian reforestation on the landscape scale: Navigating trade-offs among agricultural production, ecosystem functioning and biodiversity. *J. Appl. Ecol.* 59, 1456–1471. doi: 10.1111/1365-2664.14176

WOCAT (2007). *Where the Land is Greener: Case Studies and Analysis of Soil and Water Conservation Initiatives Worldwide (2007)*. Switzerland: WOCAT.

World Agroforestry (2021). *What is Agroforestry? World Agroforestry | Transforming Lives and Landscapes with Trees*. Available online at: https://www.worldagroforestry.org/about/agroforestry (accessed on September 22, 2021).

WRUA (2011). *Nyangores River Sub-Catchment Management Plan*. Available online at: http://dpanther.fiu.edu/sobek/FIMA000012/00001 (accessed on October 25, 2022).

PAPER III

Geoderma Regional 24 (2021) e00355

Contents lists available at ScienceDirect

Geoderma Regional

journal homepage: www.elsevier.com/locate/geodrs

Mapping soil aggregate stability using digital soil mapping: A case study of Ruiru reservoir catchment, Kenya

Ann W. Kamamia [a,*], Cordula Vogel [a], Hosea M. Mwangi [b], Karl-Heinz Feger [a], Joseph Sang [b], Stefan Julich [a]

[a] Institute of Soil Science and Site Ecology, Technische Universität Dresden, Pienner Str. 19, 01737 Tharandt, Germany
[b] Soil, Water and Environmental Engineering Department, Jomo Kenyatta University of Agriculture and Technology (JKUAT), Nairobi, Kenya

ARTICLE INFO

Article history:
Received 3 September 2020
Received in revised form 13 December 2020
Accepted 15 December 2020

Keywords:
Aggregate stability
Erosion
Digital soil mapping
Andosols
Nitisols
Catchment-based management
Land-use
Mean weight diameter
Conditioned latin hypercube sampling
Cubist model

ABSTRACT

Water erosion results in sedimentation, which reduces storage capacities in reservoirs and lowers their productive life. To effectively develop strategies for the mitigation of reservoir sedimentation, an assessment of the spatial variation of erosion is necessary. In data-scarce areas, soil erosion proxies such as aggregate stability can be used to map erosion hotspots. To assess the potential of using aggregate stability as a proxy for soil erosion, 90 sampling sites in the Ruiru catchment (Kenya) were selected using conditioned latin hypercube-based sampling. Aggregate stabilities were determined based on mean weight diameter (MWD). Thereafter, digital soil mapping (DSM) of MWD was applied to identify erosion-prone areas. Correlation analysis between MWD, soil properties and covariates revealed that organic carbon had the highest influence (27.9%) on MWD. When comparing the MWDs under different land-uses, areas under cropland and tea plantations had lower MWDs (2.54 ± 0.39 mm and 2.83 ± 0.36 mm, respectively) than forested areas (3.18 ± 0.09 mm) and were more susceptible to aggregate breakdown. A spatial map created using DSM revealed that earthen roadsides had the lowest MWD of 2.07 ± 0.27 mm; thus, highlighting their potential role in contributing to erosion. From our findings, the prediction of aggregate stability appears to be a valuable resource tool to identify erosion 'hotspots' and might be used for the development of catchment management plans aiming at mitigation of soil degradation.

1. Introduction

Globally, water erosion is the primary cause of soil degradation and is mainly induced by deforestation and unsustainable agricultural management (Wynants et al., 2019). East Africa has experienced drastic land-use changes through the extension and intensification of agriculture, at the expense of forests and other ecosystems (Dunne, 1979; Ovuka, 2000a, 2000b), resulting in increased soil erosion and associated land degradation (Borrelli et al., 2017; Pimentel et al., 1995; Vanmaercke et al., 2014). Water erosion has also led to increasing sediment loads in rivers (Dunne, 1979) as well as lakes and reservoirs (Hunink et al., 2013; Maloi et al., 2016; Stoof-Leichsenring et al., 2011; Vanmaercke et al., 2014; Vogl et al., 2017; Wooldridge, 1984), which has resulted in negative feedback on agricultural productivity in the catchment, water supply and hydropower energy generation, as sedimentation affects the trophic state of water bodies and reduces the storage capacity of reservoirs (Hunink et al., 2013). An example, therefore, is the Ruiru reservoir in Central Kenya, East Africa. The Ruiru dam supplies a third of the total water to the residents of Nairobi, a city with a population of over 4,500,000 (Macrotrends, 2010). Since the establishment of the dam in 1949, the land-use pattern has been changing drastically. Based on a bathymetric survey, Maloi et al. (2016) concluded that due to sediment deposition, the reservoir has lost about 11–14% of its storage capacity over 65 years. An annual sediment yield of 38.4 t/ha places this study area among the regions with the highest sediment yields worldwide (Maloi et al., 2016). Reduced storage capacity has contributed to frequent water rationing in Nairobi and its surroundings (The Nature Conservancy, 2015).

To mitigate these negative effects, erosion hotspots need to be identified to effectively develop soil conservation measures. Such hotspots can be identified through in-situ experiments, such as rainfall simulations on runoff plots (Duiker et al., 2001; Iserloh et al., 2013; Vaezi et al., 2016), with the spatial calculation of the Universal Soil Loss Equation (USLE) with the aid of Geo-Information-Systems (GIS) (Kouli et al., 2009) or with process-based models such as WEPP or SWAT (Flanagan et al., 2007; Hunink et al., 2013). However, in-situ runoff experiments are expensive, time consuming and limited in spatial coverage. Models are data driven and the amount, type and resolution of data required depend on the specific model. For Ruiru reservoir catchment, as it is the case with many watersheds in the world and particularly in Africa, the data may not be available or sufficient to run the models. (Kwakye and Bárdossy, 2020; Näschen et al., 2018; Tegegne et al., 2017).

* Corresponding author.
E-mail address: ann.kamamia@mailbox.tu-dresden.de (A.W. Kamamia).

https://doi.org/10.1016/j.geodrs.2020.e00355

To overcome these challenges, easy-to-estimate indicators, such as aggregate stability (Amézketa, 1999; Demenois et al., 2017), which are strongly related to soil erosion (Le Bissonnais, 1996), have been developed. For example, soil aggregate stability has been suggested as a proxy for erosion susceptibility (Le Bissonnais, 1996). It has an impact on soil structure, soil organic carbon storage, infiltration rate, aeration, water retention, soil compaction and hydraulic properties (Kalhoro et al., 2017) and, consequently, on the intensity of soil erosion. Although the breakdown of aggregates occurs naturally, through climatic factors such as precipitation and freeze-and-thaw cycles, in general, it is more often human-induced (Demenois et al., 2017). Factors such as tillage intensity, timing, seedbed preparation, cropping, addition of organic matter and the use of heavy machinery may affect soil aggregate breakdown (Kalhoro et al., 2017). Decreased soil disturbance, as in no-till or minimum tillage systems, enhances the formation of aggregates (Kalhoro et al., 2017). Chaplot et al. (2019) recorded a 40% increase in C_{org} in a no-till system (13.80 ± 0.14 g kg^{-1}) that had been under direct sowing for more than 23 years as compared to a till system (9.85 ± 0.71 g kg^{-1}) that had been cultivated yearly using a mouldboard. Aggregate stability can be expressed by different indices, which are categorised depending on the amount of force required to break the aggregate, and the aggregate amount remaining under the different fractions after a disruptive force has been exerted. The most common index is the mean weight diameter (MWD) (van Bavel, 1950), which indicates the soil's ability to withstand physical forces associated with splashing, which contributes to soil aggregate breakdown, dispersion and, subsequently, erosion. Higher MWD levels represent stable aggregates, whereas low MWD characterise weak aggregates that are susceptible to soil erosion.

Even for a single soil parameter/property and where the aim is to have a good spatial coverage of the landscape, soil surveys are expensive and time consuming. The scarcity of soil spatial data has therefore stimulated the development of Digital Soil Mapping (DSM) (Lagacherie, 2008; McBratney et al., 2003). DSM is defined as the creation and population of spatial soil information systems by numerical models inferring the spatial and temporal variations of soil types and properties from observations and knowledge of related environmental variables (Lagacherie, 2008). This approach has been applied to overcome the limitations of traditional soil surveys which employ polygon data that undergo considerable generalisation within spatial as well as parameter domains due to scalability (Zhang et al., 2017). Additionally, DSM methods have the advantages of: i.) providing quantitative predictions (with uncertainty) of soil attributes, ii.) producing conventional soil maps faster and more cost-efficiently iii.) easy automation and regular updating and iv.) allowing for ranking of the most important factors affecting the different soil properties (Arrouays et al., 2020). Using high-resolution data representing soil-forming covariates, point data and a suit of interpolation techniques, raster estimates of soil property maps can be derived. Thus, DSM has been successfully applied in data-scarce areas to yield satisfactory predictions of different soil properties. For example, Prado et al. (2008) mapped available potassium contents at a regional scale using limited soil profile data, considering different biomes in Brazil. Similarly, Lemercier et al. (2008) illustrated the variability of soil pH and its relationship to the evolution of soil phosphorus at a spatio-temporal scale in France. Furthermore, Giasson et al. (2008) used logistic regression to predict soil units based on several terrain parameters obtained from the Digital Elevation Model (DEM) in the south of Brazil. The most popularly used DSM methods allow the flexible modelling of non-linear and non-parametric data, making them more suitable for real-world processes. These include the cubist method (Quinlan, 1992) and random forest method (Breiman, 2001).

Numerous studies have shown the high correlation between aggregate stability and susceptibility to erosion (Annabi et al., 2017; Bieganowski et al., 2018; Demenois et al., 2017; Egashlra et al., 1983; Mainuri and Owino, 2013; Six et al., 2000; Souza et al., 2009; Zhou et al., 2020), whereas fewer studies have mapped aggregate stability as MWD using DSM. Annabi et al. (2017), for example, compared MWD predictions obtained using pedotransfer functions to regression kriging, using only geological ancillary data (covariates) in an 800-km^2 agricultural area in Tunisia with samples collected randomly. The two methods produced comparable results ($R^2 = 0.61$–0.74), but regression kriging was preferred as it was less laborious and time-consuming. Mainuri and Owino (2017) established that land-use and landscape interactions influence the spatial variability of MWD, using random sampling in predefined landscapes in the Njoro catchment, Kenya, with the application of Empirical Bayesian kriging (RMSE = 0.9). Ye et al. (2018) then applied ordinary kriging using both spectral and terrain ancillary data for a catchment under farmland, shrubland and woodland on the Loess Plateau, China, using soil samples collected via a random stratified approach. Although they obtained a lower MWD (R^2 of 0.4) as compared to Annabi et al. (2017), they identified factors influencing aggregate stability under various land-uses. Recently, Shi et al. (2020) explored the possibility of using hyperspectral remote sensing imaging to produce a 2 × 2-m high-resolution spatial MWD consisting of more than 700 bare soil fields (R^2 of 0.50), using an external validation dataset for a 230-km^2 mixed agriculture loam belt in Belgium. The timelines in the above studies indicate a trend in the use of DSM for aggregate stability prediction. First, there was a shift from simple to complex landscapes. Second, the predictors (ancillary data) describing complex landscapes increased, which resulted in more elaborate prediction models. Third, the sampling techniques shifted from random to more purposeful. Finally, there has been a recent trend to use machine-learning algorithms and higher-resolution satellite data and a shift to validate models using an external independent dataset for a completely unbiased assessment of model quality (Malone et al., 2017; Zhang et al., 2017).

Using proxies such as aggregate stability (mapped as MWD) combined with digital soil mapping is a potential method for easily and quickly mapping soil erosion 'hotspots' particularly for areas with data scarcity and where resources (time and money) are limiting.

Thus, the objective of this study was to assess the potential of Digital Soil Mapping (DMS) of soil aggregate stability (mapped as MWD) as a proxy for soil erosion mapping in data scarce tropical areas. We applied this approach to the catchment of the Ruiru reservoir in Central Kenya, East Africa under different land-covers/land-uses to investigate their influence aggregate stability. For our study, spatial interpolation was done using a machine learning algorithm and kriging technique on samples collected using conditioned latin hypercube procedure which has hardly been tested for similar studies in the region.

2. Material and methods

2.1. Ruiru reservoir catchment

The Ruiru reservoir catchment is located in Kiambu County, Central Kenya. It covers an area of 51 km^2, extending from Uplands near the Rift Valley escarpment to the Ruiru dam near Githunguri Town (Fig. 1). The Ruiru reservoir catchment is a major tea-dairy farming zone. Subsistence farming of crops such as maize, vegetable and fruits - characterised by low-input low-output production - is also commonly practiced (Jaetzold et al., 2006). The elevation ranges from 1940 to 2434 m asl (Fig. 2), with an average annual rainfall between 1300 and 1500 mm. Rainfall reliability during the first rainy season (March to May) and the second rainy season (October to December) ranges between 700 and 850 mm and between 250 and 470 mm, respectively (Jaetzold et al., 2006). Soil formation is affected by the underlying pyroclastic and intermediate igneous volcanic geology, formed from the cooling of magma from the Rift Valley fault. The two major soil types are Andosols and Nitisols (Fig. 1), which are deeply developed, well-drained and highly fertile, contributing to a considerably high agricultural productivity (Maloi et al., 2016).

The Ruiru reservoir catchment population translates to 1678 people per km^2 (Macrotrends LLC, 2010). Population expansion in the

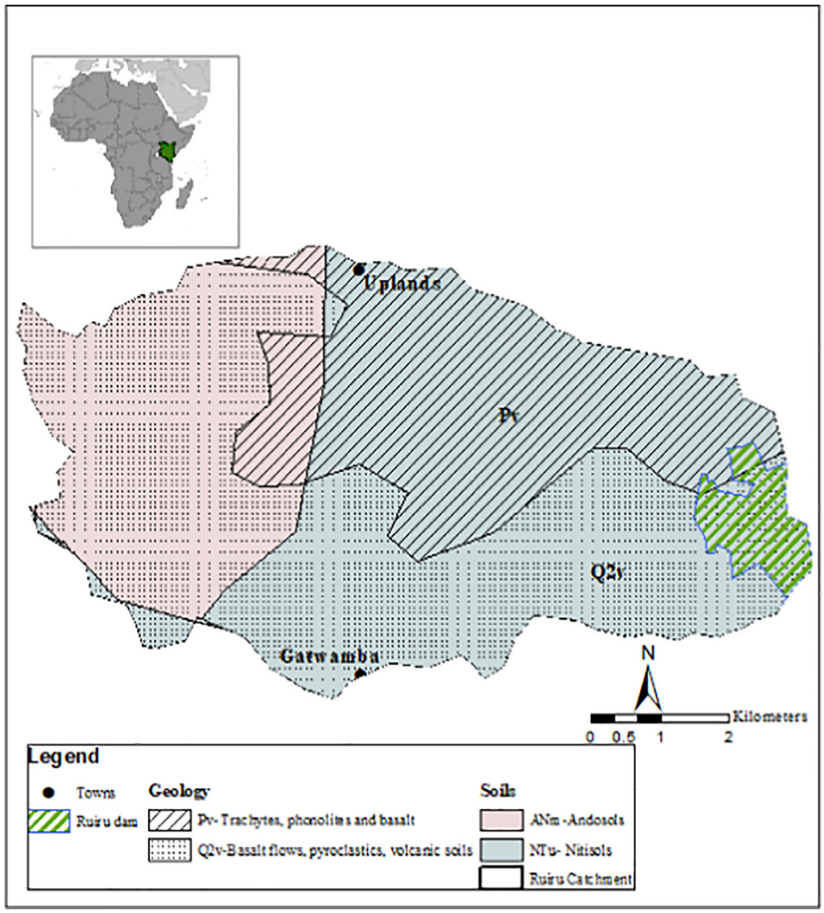

Fig. 1. Ruiru reservoir catchment: location, geology and soils (source: Jaetzold et al., 2006 and Survey of Kenya).

catchment between 1990 and 2010 resulted in an increased demand for land and water resources (Mwangi et al., 2017), which prompted an increase in clear cutting of forests for agriculture as well as settlements and an intensified cultivation on steep slopes and river banks (Maloi et al., 2016). As a consequence, land degradation from intense land-use increased soil erosion and related sedimentation in the Ruiru reservoir. The establishment of state corporations, such as the Water Resource- Authority (WRA) under the Kenya Water Act, 2016, has attempted to ensure sustainability in the management of water resources through efforts such as protecting riparian areas and regulating water abstraction. However, this has been inadequate for the Ruiru reservoir catchment with a rapid population growth of 4.6% per year (Macrotrends LLC, 2010).

2.2. Sample collection and analysis

2.2.1. Determination of sampling size and location

A 30-m Digital Elevation Model (DEM) and Landsat-8 Operational Land Imager (OLI) were downloaded from the Earth Explorer hosted by the United States Geological Survey (EarthExplorer - USGS, 2019). A soil map (scale 1: 250000) was obtained from the Soil and Terrain (SOTER) database of the International Soil Reference and Information Centre (ISCRIC) (Batjes, 2008). A coarse geology map was obtained from the Survey of Kenya (SOK). Using the System for Automated Geoscientific Analyses-SAGA-GIS (Conrad et al., 2015), a sink-filled DEM was used to calculate various DEM derivatives, including primary terrain attributes (slope, aspect, plan curvature, profile curvature, aspect, relief and elevation) and secondary terrain attributes (topographic wetness index (TWI) and hillshading). The plan curvature was taken into account as it illustrates the hydrological patterns and can display the flow acceleration and deceleration areas (Webster, 2007). The TWI was additionally selected as it provides information on flow patterns and the likelihood of accumulation by displaying flow patterns. In addition to the soil, geology and land-use maps, these DEM derivatives were stacked together and split into 30-m segments, using the fishnet tool in ArcGIS (ArcMap version 10.2). Therefore, each pixel was represented by a set of different covariates (Fig. 3).

Sampling distribution was determined using the conditioned Latin Hypercube sampling (cLHS) algorithm (Minasny and McBratney, 2006) present in the clhs package (Roudier et al., 2012) in the statistical software package R version 3.5.1. (R Core Team, 2019). The different sample sizes (60, 90, 120 and 200 samples, respectively) were initially selected as potential sampling sites. Thereafter, the sampling distributions of sample sizes were visually compared against each other using density plots (Fig. 4) to determine which sample size closely approximated the values of the covariate. The cLHS sampling is based on the concept of Latin hypercube sampling, where the sampling space is independently stratified into equal continuous intervals according to the cumulative density function (CDF). The samples are then randomly drawn from each interval. In cLHS, the sample space is first divided into as many dimensions as the number of covariates (strata) present, thus forming a 'hypercube'. Each dimension is further divided into as many

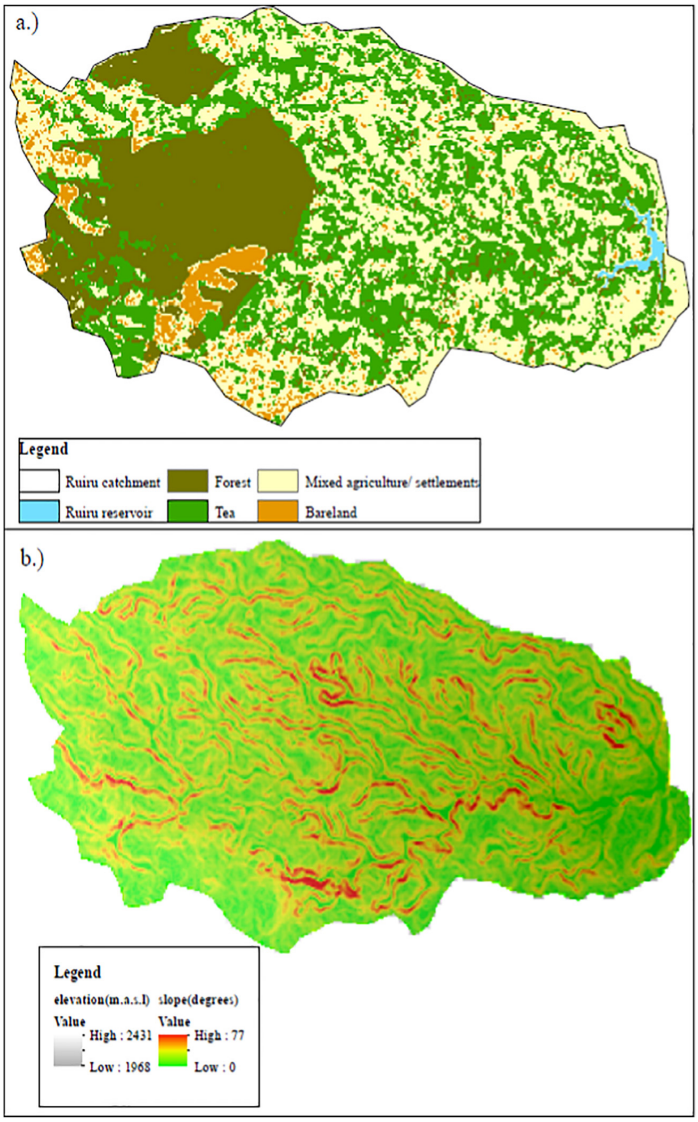

Fig. 2. Ruiru reservoir catchment. a) Land-use/land-cover map (source: Landsat Classification) and b) slope (represented by colours) and elevation (represented by shading) map (source: SAGA GIS version 2.3.2).

rows and columns (intervals) as the number of samples to be selected. One sample is then selected from each row and column throughout the whole hypercube of covariates. The cLHS adds the condition that each point must exist on the actual landscape. The soil surveyor then selects the most optimal distribution, which corresponds to a number of samples to be collected.

The sample size of 90, whose spatial distribution is presented in Fig. 5, was selected for further analysis as it closely represented the distribution for most of the covariates (Brungard and Boettinger, 2010). Using already geo-referenced potential sampling locations, similarity sites within a 500-m radius for each site were determined. These were set as alternative sites in case of inaccessibility to the originally selected sampling site, where, for example, there was no permission to access private land or where it was impossible to access sites in the thick indigenous forest.

2.2.2. Fieldwork

The sampling sites were located in the field by GPS. It was ensured that samples were collected from the exact coordinates obtained from the selection process (Section 2.2.1), which was imperative to capture the influences of slope, geology, vegetation and soil type, which are heterogeneous in nature. At each site, undisturbed samples were taken using metal core rings (100 cm^3) for the determination of bulk density (BD). To determine soil texture, organic carbon content (C_{org}) and aggregate stability, another set of samples was obtained from the top 0–20 cm at the same sites. This depth was selected as the topsoil accounts for most of the soil loss in the Ruiru catchment (Lewis, 1985). The samples were transported in boxes to diminish aggregate breakdown during transportation.

2.2.3. Laboratory analysis

2.2.3.1. Determination of basic soil parameters. Soil moisture content results, assessed gravimetrically from the core rings, were used to calculate BD. Soil texture was determined using a combined wet sieving and sedimentation procedure. The sand fraction was obtained using wet sieving, whereas the silt and clay fractions were quantified by employing sedimentation analysis based on Stoke's equation in the

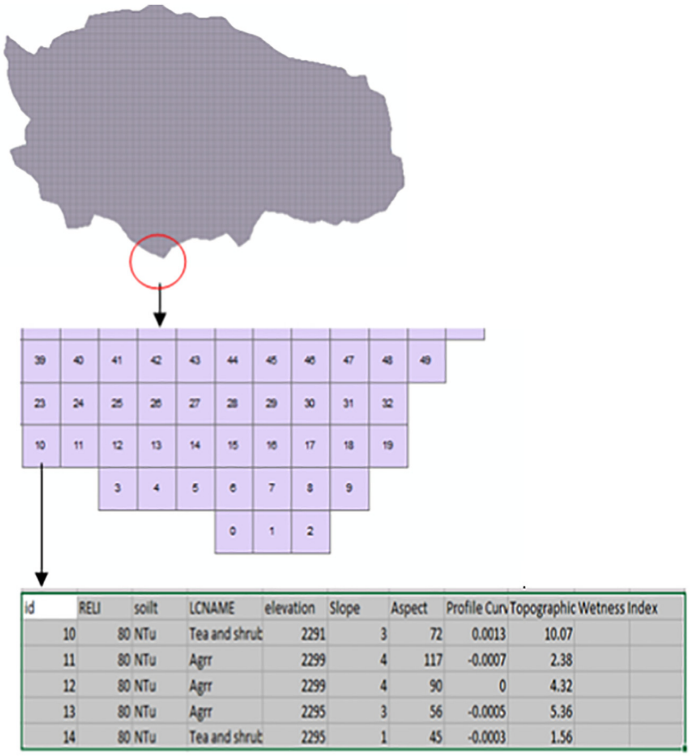

id	RELI	soilt	LCNAME	elevation	Slope	Aspect	Profile Curv	Topographic Wetness Index
10	80	NTu	Tea and shrub	2291	3	72	0.0013	10.07
11	80	NTu	Agrr	2299	4	117	-0.0007	2.38
12	80	NTu	Agrr	2299	4	90	0	4.32
13	80	NTu	Agrr	2295	3	56	-0.0005	5.36
14	80	NTu	Tea and shrub	2295	1	45	-0.0003	1.56

Fig. 3. Splitting catchment based on coarse land-use, soil map and DEM derivatives (elevation, slope, aspect, profile curvature, topographic wetness index).

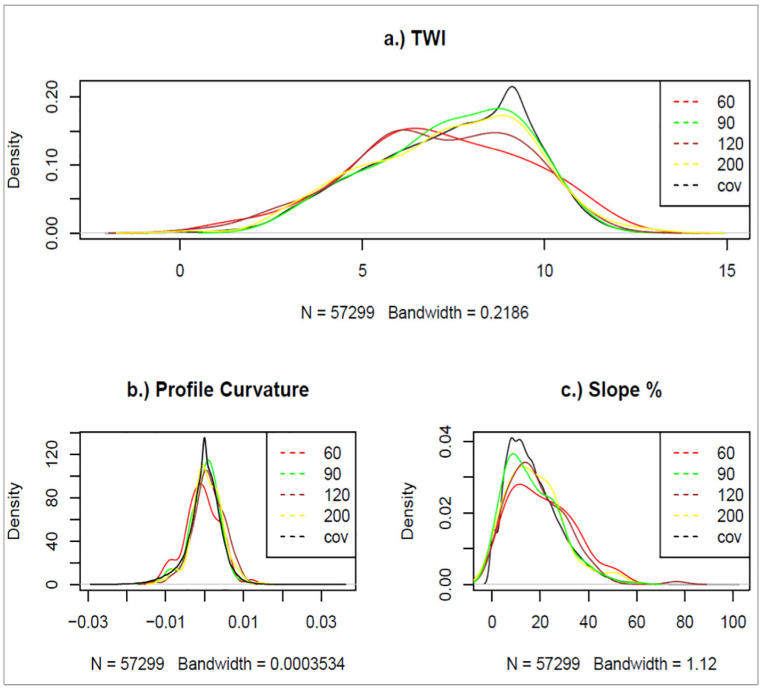

Fig. 4. Density plots of a) topographic wetness index (TWI), b) profile curvature, and c) slope (%) covariates and 60, 90, 120, 200 samples and covariate (cov), respectively.

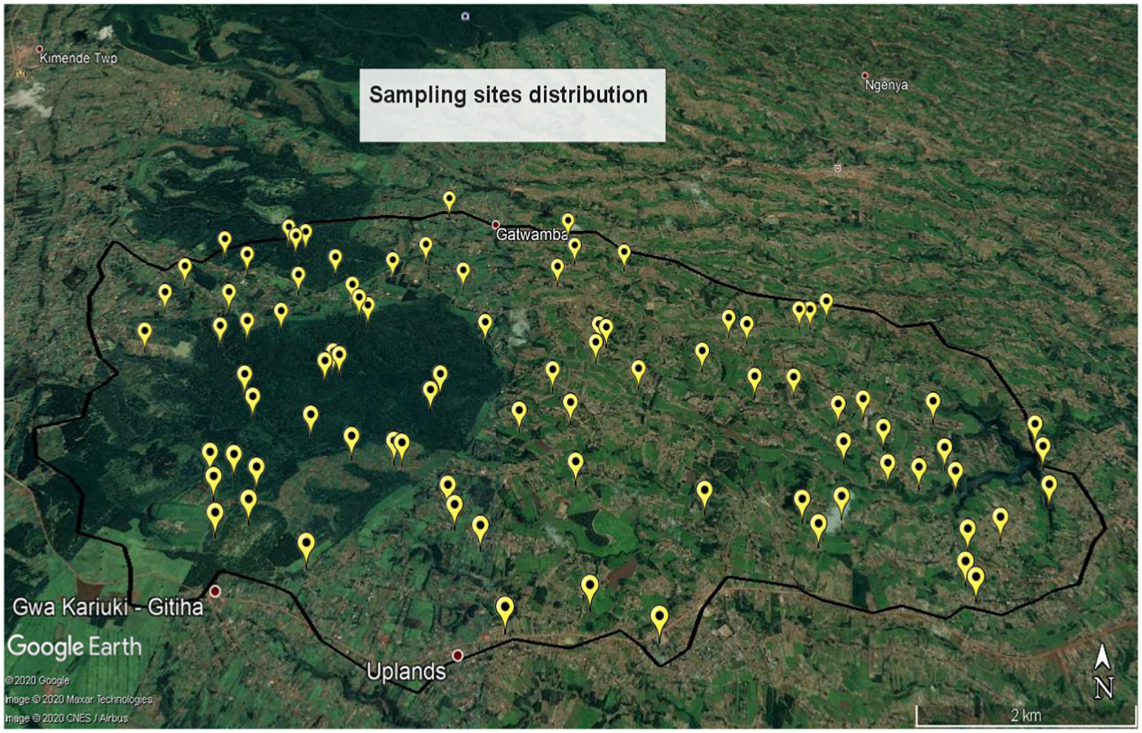

Fig. 5. Google Earth image of the distribution of the selected sampling points in the Ruiru reservoir catchment (source: Google Earth, earth.google.com/web/).

Sedimat 4–12 equipment (Umwelt-Geräte-Technik (UGT) GmbH, Müncheberg, Germany). The levels of C_{org} and total nitrogen were determined by dry combustion using the Vario TOC Cube Elementar equipment (Elementar Analysensysteme GmbH, Langenselbold, Germany).

2.2.3.2. Soil aggregation and the aggregate stability test by fast wetting. The fast wetting method following Le Bissonais (2016), which induces slaking action typical of rapid rainfall events, was applied to determine aggregate stability of the undisturbed soil samples. The soil fraction between 2 and 4.6 mm was selected for testing aggregate stability as this was the largest aggregate fraction and thus most prone to aggregate breakdown under raindrop impact. Before performing the tests, the samples were oven-dried at 40 °C for 24 h to ensure a constant matric potential (Le Bissonnais, 1996). About 2 g of the sample was weighed and placed in a 0.063-mm open sieve cup. The soil samples were then quickly immersed in beakers with about 50 mL of deionized water for 10 min. Thereafter, the samples were transferred to a wet-sieving apparatus (Eijkelkamp Soil & Water, Giesbeek, The Netherlands) containing ethanol, which minimises the destruction of aggregates during sieving and prevents them from bonding during drying (Rohošková and Valla, 2011). After 3 min, the samples were transferred into glass dishes and placed into the oven at 105 °C for about 24 h.

Finally, a set of five sieves between 0.063 and 2 mm was used to determine the aggregate size distribution after the disruptive forces. The lowest possible amplitude (0.5 mm) and the shortest time (1 min) were set on the sieving machine AS 200 control "g" (Retsch, Haan, Germany) to minimise aggregate breakdown. The mass of the different fractions 2–4 mm, 1–2 mm, 1–0.63 mm, 0.25–0.63 mm, 0.063–0.25 mm and < 0.063 mm was determined using a precision scale. The MWD was then calculated for each mass fraction by Eq.1

$$MWD = \sum_{i=1}^{i=n}(m_i \times d_i) \times 0.01 \quad (1)$$

with m_i as weighted percentages of the aggregates in the fraction i and d_i as mean diameter of the size fraction.

2.3. Data analysis

2.3.1. Datasets and software

Exploratory analysis was undertaken using the R statistical software version 3.5.1. (R Core Team, 2019). Geostatistical analyses and mapping were performed using the packages sp. (Pebesma and Bivand, 2005), raster (Hijmans et al., 2020), rgdal (Bivand et al., 2019), GSIF (Hengl et al., 2019), aqp (Beaudette et al., 2020), Cubist (Quinlan, 1992) and gstat (Pebesma and Wesseling, 1998), loaded in the R statistical software. To extract terrain attributes from the DEM, SAGA GIS version 2.3.2 (Conrad et al., 2015) was used. In addition to the terrain attributes obtained during the selection of the sampling points, Landsat-8 Operational Land Imager (OLI) images for both dry (February) and wet (October) months were obtained from the United States Geological Survey Earth Resources Observation and Science (USGS EROS) Centre archive (Landsat-8 image courtesy of the U.S. Geological Survey) to increase the robustness of the predictions. Based on the Landsat images parameters like the Normalized Difference Vegetation Index for the dry season (NDVID), the Normalized Difference Vegetation Index for the wet season (NDVIW) and the Green Vegetation Index (GVI) were calculated with the Raster calculator tool in QGIS (Version 3.8.3-Zanzibar).

2.3.2. Land-use/land-cover classification

The land-use/land-cover (LULC) classification presented in Table 1 was based on the major LULC in the catchment. This included indigenous forests (FORI), planted forests (FORP), grasslands/shrubland (GR/SH), Napier grass (NAP), roadsides (RD), riparian vegetation (RIP),

cropland (AG) and tea plantations (TEA). All these LULCs were under different management strategies.

2.3.3. Exploratory analysis

In this step, a suite of covariates representing 'scorpan' factors (which is a mnemonic for soil (s), climate (c), organisms (o), relief (r), parent material (p), age (a), spatial position (n) and ϵ represents the spatial dependent residuals- Eq. 2) was selected to represent the secondary data (McBratney et al., 2003).

$$S = \int (s, c, o, r, p, a, n) + \in \tag{2}$$

This secondary data included remote sensing images, DEM and their derivatives. A large number of potential covariates are available, and the selection of the covariates is based on expert judgement (Lagacherie, 2008). In this study, the selection of the covariates was based on previously published articles (Malone et al., 2017; Mora-Vallejo et al., 2008; Taghizadeh-Mehrjardi et al., 2019) and the availability of covariates. For the DSM exercise, a final dataset of 15 covariates, with similar grid size and geo-reference, was compiled (Table 2).

Subsequently, the relaimpo package in R was applied to determine the relative importance of the soil properties and covariates in predicting the aggregate stability distribution. This was done by weighing the proportionate contribution of a covariate in the prediction of a criterion to that when combined with all other covariates in the regression equation (Groemping, 2006). For statistical analysis, the different distributions were represented graphically using violin plots.

2.3.4. Assessing performance of model predictions

For assessing the performance of the predictions, R^2, RMSE and BIAS were selected; R^2 is referred to as coefficient of determination and is defined as the ratio between the observed MWD and their corresponding predicted MWD. It measures the precision of the relationship between observed and predicted values, using the following equation:

$$R^2 = \frac{\sum_{i=1}^{n}\left(obs_i - \overline{obs}\right)\left(pred_i - \overline{pred}\right)}{\sqrt{2}\sqrt{\sum_{i=1}^{n}\left(obs_i - \overline{obs}\right)^2}\sqrt{2}\sqrt{\sum_{i=1}^{n}\left(pred_i - \overline{pred}\right)^2}}, \tag{3}$$

where *obs* is the observed MWD, *pred* is the predicted MWD, n is the number of observations.

The RMSE measures how much the estimates deviate from the measured values on average. As this measure is sensitive to both random and systematic errors, it is ideal for determining the accuracy of predictions on a validation dataset. The equation is as follows:

$$RMSE = \sqrt{2}\sqrt{\frac{\sum_{i=1}^{n}(obs_i - pred_i)^2}{n}} \tag{4}$$

Bias is defined as

$$Bias = E(H) - \theta, \tag{5}$$

where H is the estimator and θ is the predictor.

Bias is an error index that measures the average tendency of the simulated constituent values to be larger or smaller than the measured data.

Table 1
Land-use/land-cover description.

Land-use	Description
Cropland (AG)	Area predominantly composed of agricultural food crops either used for commercial or subsistence purposes.
Indigenous forest (FORI)	Area predominantly composed of trees that have not been established by planting and/or deliberate seeding. This was identified with the assistance of a Kenyan Forest Service (KFS) officer.
Planted forest (FORP)	Area predominantly composed of trees that have been established by planting and/or deliberate seeding.
Grassland/shrubland (GR/SH)	Area characterised by vegetation devoid of trees and dominated by shrubs, often including herbs and grasses. Included both tall, low closed and open scrub.
Napier grass (NAP)	Area characterised by Napier grass forage crop serving as fodder for dairy animals.
Roadside (RD)	Area located between road and adjacent landscape.
Riparian vegetation (RIP)	Interface between land and river system. This is ideally 0–30 m from the river system (Water Resource Management Authority, WRMA 2002).
Tea (TEA)	Area characterised by the evergreen tree shrub *Camellia sinensis* at the different stages of growth.

Table 2
Description of covariates used in Digital Soil Mapping (DSM).

Covariate name	Description
1. Band4d (red band for dry season)	Landsat 8 OLI Band4 red (R) date: 01-Feb-2019 (dry season) path: 168 row: 61 cloud cover: 4%. Discriminates vegetation slopes
2. Band5d (near infrared band for dry season)	Landsat 8 OLI Band4 red (R) date: 01-Feb-2019 (dry season) path:168 row: 61 cloud cover: 4%. Emphasises biomass content/ecology
3. Band4w (red band for wet season)	Landsat 8 OLI Band4 red (R) date: 29-Sept-2019 (wet season) path: 168 row: 61 cloud cover:4%. Discriminates vegetation slopes
4. Band5w (near infrared band for wet season)	Landsat 8 OLI Band4 red (R) date: 29-Sept-2019 (wet season) path: 168 row: 61 cloud cover:4%. Emphasises biomass content
5. NDVID (normalized difference vegetation index–dry season)	(Band5d-Band4d)/(Band5d + Band4d) Range − 1 to 1 (Least vegetated to most vegetated). Represents the photoactivity of vegetation and is used to monitor growth
6. NDVIW (normalized diffference vegetation index-wet season)	(Band5w-Band4w)/(Band5w + Band4w) Range − 1 to 1 (Least vegetated to most vegetated). Represents the photoactivity of vegetation and is used to monitor growth
7. GVI (degree of green vegetation index)	0.2941*Band2-0.243*Band3 0.5424*Band4 + 0.7276*Band5 + 0.0713*Band6-0.1608*Band7. Ignores the interaction and effects of atmosphere, soil and vegetation and determines the correlation between vegetation covers (Xue and Su, 2017)
8. Aspect	Compass direction of steepest downhill slope and describes solar irradiance (Travis et al., 1975)
9. Elevation	Primary terrain attribute
10. Hill-shading (analytical hill-shading)	Determines the angle at which light from its source would strike the surface
11. Longitudinal_c (longitudinal curvature)	Local morphometric terrain attribute describing the curvature in the down/slope direction
12. Plan_c (plan curvature)	Local morphometric terrain attribute describing the rate of change of aspect and describes the converging and diverging flows and soil water properties
13. Profile_c (profile curvature)	Local morphometric terrain attribute describing the rate of change of slope as concave, convex or horizontal and describes erosion and depositional zones
14. Slope	Local morphometric terrain attribute that assesses the topographic erosion potential (Travis et al., 1975)
15. TWI (Topographic wetness index)	ln (a/tanβ), where a is the local upslope area draining through a certain point per unit contour length and tanβ is the local slope. Indicates the potential runoff generation

2.3.5. Continuous spatial mapping

The Cubist model with regression kriging is based on the "scorpan" approach (McBratney et al., 2003) introduced in section 2.3.3. The cubist model was applied as the deterministic component of the predictions. This is a rule-based model that hierarchically partitions the data into different partitions/subsets/clusters, which are similar with respect to environment variables (Malone et al., 2017). This means that each data point belongs to a specific subset and cannot be included in another subset. Each subset is defined by a rule represented using a conditional statement which may include one or more covariates. Consequently, each of the formed subset is then regressed according to the rule defining it, which results in the prediction of the soil property of interest. This indicates that the regression equations are local to the data partitions and hence have smaller errors in magnitude (Malone et al., 2017). Moreover, the cubist algorithm requires the establishment of three parameters: rules, committees and extrapolations. Data partitioning is based on the rules, and the extrapolations constrain the model. Committees define the number of boosting iterations. Since soils properties vary locally and their spatial pattern can be discerned (Goovaerts, 1998; Keskin and Grunwald, 2018), kriging interpolation was used to define the residual/stochastic part of the equation (Eq. 2) and to estimate the spatially dependent residuals (Keskin and Grunwald, 2018; Malone et al., 2017). Regression kriging is a spatial interpolation technique that combines the output of a regression model, such as the Cubist model, with interpolated regression residuals (difference between the predicted and observed values) (Ma et al., 2017). Therefore, a semivariogram quantifying the spatial structure of the residuals is developed and fitted into the model. Based on this structure, the prediction residuals are kriged and combined with the regression from a deterministic model, such as the cubist method.

Following Malone et al. (2017), the cubist method with regression kriging was executed as shown below:

i.)All covariates (Table 2) were transformed into 30 × 30-m grids, based on the resolution of the raster dataset, and were set to the same geographic co-ordinate system.

ii.) The covariates were overlaid with each other to form a raster stack. Using the georeferenced 90-point MWD values, the covariate values associated with each sample point were extracted. The resulting dataset was split into two segments representing the training and testing data (~80 and ~20%).

iii.) The cubist model was applied to the training data. In this study, the rules and extrapolations were both set to 5, and the committee parameter was set to 1.

iv.) The predictions within each subset were evaluated using leave- one-out cross validation (LOOCV) to overcome the bias estimates of the quantiles of the residual/model error (Solomatine and Shrestha, 2009).

v.) Once the model was trained, it was employed to determine the quantile distribution of the model error for the test set. Given the small test dataset (20% of data), a 10-fold jack-knifing technique was used to resample the data (Hengl and MacMillan, 2019).

vi.) Regression kriging, exemplifying the stochastic component, was then undertaken.

vii.) The uncertainty of the model was estimated using the prediction interval (PI) (Solomatine and Shrestha, 2009). This involved obtaining the 5th and 95th quantile percentiles of the residual distribution for each data partition, summing them up and ultimately adding this to the final prediction obtained from the cubist method with regression kriging. This step was used to determine the upper and lower prediction limits, using the model errors/residuals (Malone et al., 2017).

viii.)At the end, a spatial map was created from the augmentation of the cubist method and regression kriging.

3. Results and discussion

3.1. Soil parameter exploratory analysis

The soil texture triangle illustrates that the soils in the Ruiru reservoir catchment were mainly classified as loam, clay-loam and clay (Fig. 6). Nitisols, characterised by high clay contents (up to ~80%), present the dominating soil types. Andosols, characterised by high silt contents of up to ~70%, are located in the western part of the catchment. As the Andosols have lower clay contents, they are well-drained and easy to work with. However, these soils are mostly under FORI and FORP.

Analysis using the relative importance regression equations demonstrated that the soil properties had a higher influence on the MWD as compared to the spectral, vegetation and terrain covariates (Table 3). Specifically, C_{org} had the highest influence of 27.9% on aggregate stability. This can be underpinned by the findings of Chenu et al. (2000), who demonstrated that C_{org} was a good predictor ($R^2 = 0.72$) of aggregate stability. Also, Mainuri and Owino (2013) reported a positive correlation between C_{org} and MWD.

Aside from the soil properties (Table 3), spectral data (Bands 4 and 5) and vegetation indices (NDVI and GVI) generally acted as better predictors for MWD as compared to the terrain attributes. Jones et al. (2020) reported that NDVI was one of the most important predictors of aggregate stability, whereas attributes such as aspect and elevation performed poorly. Vegetation indices act as surrogates for vegetation cover and influence the landscape patterns. Spectral data provide information on the physical properties of land surfaces relevant to soils, such as soil texture, soil moisture and mineral composition (Browning and Duniway, 2011). Of the terrain attributes, elevation had the highest relative importance of 9.1%, whereas slope contributed only 0.22% to predicting the MWD. The Ruiru reservoir catchment is located in a high-elevation area with steep slopes, where intensive agricultural activities are performed. Jin et al. (2008) concluded that elevation is the most important terrain factor affecting the spatial distribution of vegetation. In turn, vegetation serves as a source of SOM, which contributes directly to the formation and stabilisation of aggregates (Celik, 2005). It can thus be concluded that aggregate stability is highly dependent on soil properties and vegetation. While soil properties cannot be adjusted to reduce the risk of erosion, human intervention using vegetation can be adopted.

The results of BD and C_{org} of the individual LULC are presented in Fig. 7a, b as violin plots. In addition to representing the interquartile ranges and the median, violin plots depict the entire distribution of data. The C_{org} values decreased in the following order:

FOR1-8.97 ± 1% > FORP-7.03 ± 1.63% > TEA- 6.39 ± 2.40% > RIP-6.21 ± 1.34% > GR/SH- 5.86 ± 1.57% > NAP-5.81 ± 1.57% > AG-

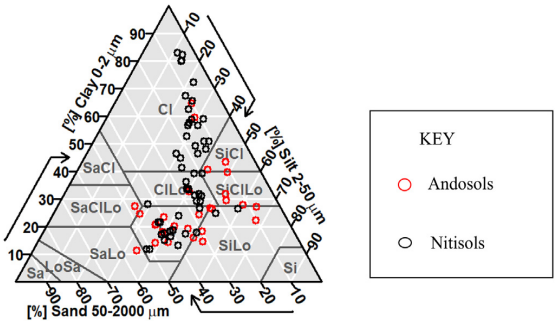

Fig. 6. Texture classification of soils in the Ruiru reservoir catchment based on the USDA soil texture triangle.

Table 3
Relative importance values of soil properties and covariates.

Variable	Rank	% Relative importance
Soil property: C_{org}, BD, K, clay, silt, sand, pH	1, 2, 7,9,10,12, 14	27.89, 18.27, 3.87, 2.42, 2.92, 1.81, 0.97
Spectral data: Band4d, Band5w, Band5d, Band4w	3, 6, 11,13	11.30, 4.29, 2.06, 1.53
Vegetation indices: NDVID, GVI, NDVIW	5, 8,16	7.71, 2.90, 0.92
Terrain data: Elevation, Hillshading Aspect, Longitudinal_c, Profile_c, Plan_c, slope, TWI	4, 15, 17, 18, 19, 20, 21,22	9.05, 0.94, 0.60, 0.30, 0.27, 0.25, 0.22,0.14

5.80 ± 1.97% > RD- 5.0 ± 0.72%. The BD values followed a decreasing order: AG-1.0 ± 0.13 g/cm^3 > RD-0.72 ± 0.16 g/cm^3 > TEA- 0.66 ± 0.14 g/cm^3 > GR/SH-0.67 ± 0.17 g/cm^3 > NAP 0.67 ± 0.08 g/cm^{3-} > FORP-0.64 ± 0.11 g/cm^3 > RIP-0.63 ± 0.05 g/cm^3 > FORI-0.60 ± 0.04 g/cm. Generally, BD showed a decreasing trend and C_{org} showed an increasing trend from AG to FORI. Similar differences between AG and FORI have been reported by Amanuel et al. (2018) and Takele et al. (2015), who attributed this to the low organic matter application to cultivated soils, complete biomass (SOM) removal and mechanical tilling, which stimulates decomposition by microorganisms. Six et al. (2000) found that disturbances by ploughing under continuous tillage accelerated the decomposition of SOM twice as fast as non-tillage systems. A depletion of SOM increases the mineral fraction, which is denser than SOM, resulting in a higher BD. In forest systems (FORI and FORP), aggregate breakdown is reduced due to the protection and stabilisation of SOM within these aggregates, leading to the accumulation of carbon in the top 0 to 10-cm layer, which has increased soil volume and less weight (Six et al., 2000). Therefore, management activities such as minimum-tillage, direct sowing or mulching could be alternative strategies to preserve C_{org} and BD in the Ruiru reservoir catchment.

The higher values of BD and C_{org} under TEA can be explained as follows: i) soil compaction from continuous trampling by tea workers during the various management practices (Abrishamkesh et al., 2010) and ii) external SOM input by residue from pruning, which is distributed as mulch. The BD observed under GR/SH was similar to that under NAP, although GR/SH showed higher C_{org} values. The NAP LULC is mostly a cut-and-carry system which leads to the removal of biomass. The low BD under RIP values can be explained by their continued protection and availability of water, which results in high SOM accumulation. It is also worth noting that the violin plots of the BD exhibited a variable distribution as compared to that of C_{org}. Rühlmann and Körschens (2009) reported that in addition to C_{org}, there are several other factors influencing the BD and causing soils with similar C_{org} values to exhibit extremely different BDs. For example, the clay content directly influences the BD of a soil (Céspedes-Payret et al., 2017; Rühlmann and Körschens, 2009).

3.2. Aggregate stability and relationship with LULC

The highest MWD of 3.18 ± 0.09 mm was found under FORI, whereas that of 2.07 ± 0.27 mm under RD was the lowest (Fig. 8). All roads leading to the smallholder farms and tea plantations within the Ruiru reservoir catchment are earthen and formed from cut-and-fill embankments, therefore lacking proper drainage and watercourse crossings. Moreover, these roads are continuously used by heavy vehicles that collect tea and milk from the small-scale farmers. The continuous impact by heavy load vehicles compresses the road, forcing the edges of the road to break away. Often overlooked in most parts of Africa in areas with earthen roads is the erosion that occurs on the roadside (Parsakhoo et al., 2014). This compares with the highest aggregate stabilities under FORI, which can be attributed to higher root densities of older trees and greater leaf biomass, which contribute to increased soil organic matter levels (Gupta et al., 2009; Iori et al., 2014) and hence higher percentages of larger sized and more stable aggregates. However, FORP showed higher MWD values of 2.87 ± 0.39 mm compared to GR/SH (2.80 ± 0.37 mm). Most of the individual tree stands are comprised of either native trees to restore forest ecosystems or short-rotation plantations of fast-growing *Eucalyptus* species mostly grown on previously over-cultivated soils or on degraded land. Various studies observed that afforestation substantially increased C_{org} stocks

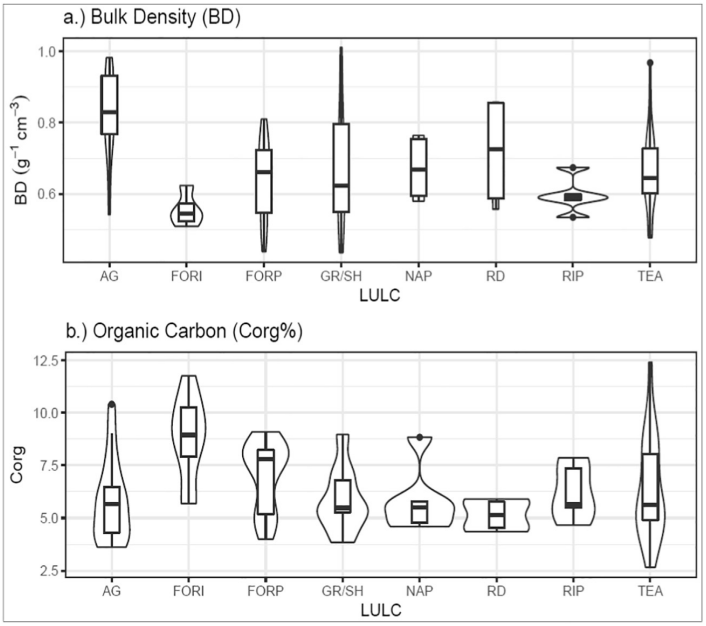

Fig. 7. a-b: Violin plots of a) BD, b) C_{org} content of the LULC in the Ruiru reservoir catchment. BD – bulk density, AG - cropland, FORI - indigenous forest, FORP - planted forest, GR/SH - grassland/shrubland, NAP - Napier grass, RD - roadside, RIP - riparian area, TEA - tea.

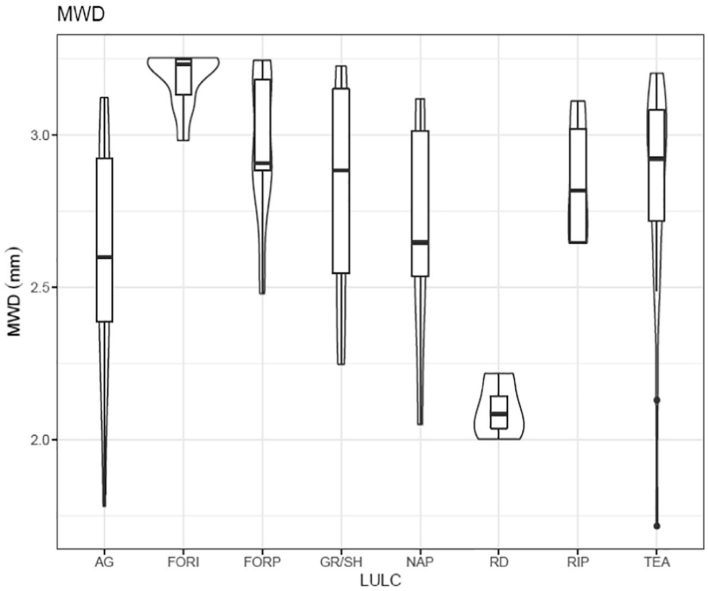

Fig. 8. Violin plots of MWD under different LULC systems. MWD – mean weight diameter, LULC – land-use/land-cover, AG - cropland, FORI - indigenous forest, FORP - planted forest, GR/SH - grassland/shrubland, NAP - Napier grass, RD - roadside, RIP - riparian area, TEA - tea.

when starting from crop or degraded land (Boulmane et al., 2017; Nogueira et al., 2006), which might increase aggregate stability. The NAP LULC also presented slightly higher MWD values of 2.68 ± 0.40 mm against those of AG (2.54 ± 0.39 mm). Mutegi et al. (2008) reported that adoption of Napier grass as vegetative hedges has a potential for improving soil productivity on steep arable land, in addition to serving as fodder for animals. When intercropped with leguminous crops, Napier hedges are effective in significantly reducing soil erosion and increasing soil organic matter. This means that this LULC could provide a solution to degraded croplands as it improves the soil MWD and has an added economic benefit. Furthermore, high MWDs of 2.89 ± 0.21 mm were observed under RIP, which indicates some gradual protection of these sensitive areas. The enactment of the Water Act 2016 acknowledged the importance of community participation in the management of water resources, resulting in the formation of Water Resource Users Associations (WRUAs). The WRUA-Ruiru has been actively enforcing the directive by the government prohibiting cultivation on riparian land by ensuring those flouting this directive face legal ramifications.

The large variation in MWDs (1.71–3.2 mm) exhibited under tea (TEA) can be explained by the different ages of the tea trees and the different land management practices taken up by the various farmers. Generally, higher MWDs were found in established tea plantations and low MWDs in young tea plantations undergoing pruning and other management practices. Tea is a major export cash crop for Kenya and is grown by both smallholders and on large-scale estates (Aragie, 2018). Most of the tea plantations in the Ruiru reservoir catchment are located along steep slopes. In the early years of tea planting, there is frequent pruning and deep weeding as the young tea plants need to be protected from weed overgrowth. This results in continuous soil disturbance, making the soil more vulnerable to erosion. As the forage is under-developed, rainfall will have more significant impact on the detachment and further transport of the soil aggregates. After the establishment of the tea plantations (2–3 years after planting), there is occasional pruning of the crop before full canopy formation (Allaway and Cox, 1989). Likewise, pruning in the tea estates is performed at different times, and this could very well vary even within one tea estate. During this time, soil loss may occur along footpaths within the tea rows. On the contrary, established and well-managed tea plantations produce slightly more erosion than forests (Allaway and Cox, 1989). The MWDs of FORI are comparable to those of established tea plantations, as represented by the upper quartile of the TEA violin plots in Fig. 8. At this stage, the thick forage offers protection to the soil against heavy rainfall, and the roots mechanically reinforce the soil aggregates (Kuriakose and van Beek, 2011).

3.3. Spatial mapping

Using 80% of the data for training and a raster stack of the covariates, the cubist method split the data into two parts with 47 and 25 samples, respectively. This partitioning relied heavily on the spectral data (Band4w, Band4d, Band5w) and vegetation indices (NDVID, GVI) rather than on terrain (hillshading and elevation) attributes. A similar trend was observed during the independent determination of the relative importance of the covariates to MWD, where, for example, these covariates accounted for three of the top five predictors. Howell et al. (2008) reported that predictive models tend to focus more on hyperspectral satellite data in areas where large variations in vegetation and precipitation occur. The reason is that spectral features related to characteristic absorption bands of SOM and soil moisture can be mapped with more detail and represent accurate predictors for the spatial and temporal variation of vegetation and precipitation (Howell et al., 2008). Fig. 9 depicts the map obtained after overlaying and summing up the results of the cubist method with regression kriging. The spatial map identified areas around and adjacent to the forested area on the upper/western part of the catchment as having lower MWDs as compared to that under FORI. These were previously under forest cover but have been converted into cropland (AG) and tea (TEA) production areas. Moreover, the Andosols in this part of the catchment have high silt contents (up to 70%), making them vulnerable to potential soil erosion by water and eventual deposition into the Ruiru reservoir. The lowest aggregate stability of 1.56 was found for the south eastern part of the catchment under RD. Most of the areas having low MWDs were under AG and TEA. It is important to note that most of areas with low aggregate stability were located close to the Ruiru reservoir, which is on the lowest/eastern extreme end of the catchment.

The performance results presented on Table 4 indicates that the model performed better during training ($R^2 = 0.53$) than testing.

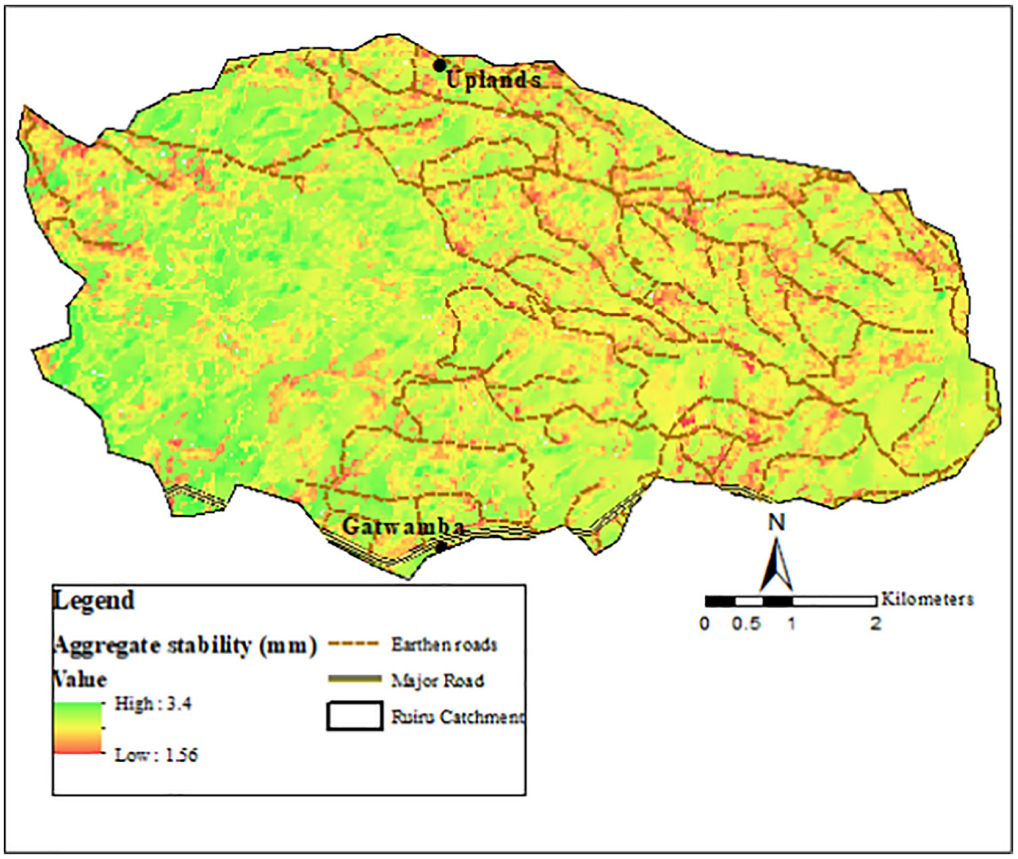

Fig. 9. Spatial distribution of aggregate stability represented as mean Weight Diameter- MWD (mm) derived from the cubist method with regression kriging.

Training validation involves the use of sets used when tuning parameters while testing validation involves the use of a test set that is not in any way used during the training of the model (Malone et al., 2017). From the literature review, no comprehensive model evaluation guideline was found and the model output was compared with other published works. Annabi et al. (2017) reported RMSE values from 0.37 to 0.55 when mapping aggregate stability using the MWD in Tunisia. Ye et al. (2018) reported a comparable R^2 value of 0.4 and a higher RMSE of 0.53 for MWD of a small catchment on the Loess plateau in China. Shi et al. (2020) reported an R^2 of 0.5 when mapping aggregate stability using high resolution Airborne Prism Experiment hyperspectral images in croplands. All authors attributed the models' performances to the selection of covariates that represented most (not all) of the spatial variation of aggregate stability in the various areas. Noteworthy are the lower RMSE values recorded in this study, which lead us to infer that the model more accurately predicted the MWD, although not all predictors could explain the variability in MWD.Fig. 10 illustrates boxplots of the upper and lower prediction limits against the observed MWD. The upper prediction range was 2.97–3.93 mm and the lower prediction range 1.02–2.70 mm. The observed range was 1.70–3.28 mm. Although all prediction values fell within the PIs, only 30% of the predicted data fell within the lower PI; the remaining ones were within the upper PI. The width of the PI obtained from the test set indicated a larger level of model uncertainty when compared to the observed value range. This method of error estimation takes into account all sources of errors without attempting to disaggregate their contribution given their individual sources, which might result in wider uncertainty ranges (Solomatine and Shrestha, 2009). Some studies that reported lower levels of uncertainty even when applying DSM for the prediction of other soil properties accredited this to the inclusion of categorical covariates, which better explained the heterogeneity of the target soil property, or the use of higher-quality covariates, such hyperspectral images, gamma radiometric data and higher-resolution satellite images (Jones et al., 2020; Rivero et al., 2007; Zhang et al., 2012). Hence, it would be necessary to test whether the MWD predictions can be improved with the inclusion of similar data where accessible.

Table 4
Coefficient of determination (R^2), Mean Square Error (MSE), Root Mean Square Error (RMSE) and Bias performance measures of the Cubist model for training and testing.

Model	R^2	MSE	RMSE	Bias
1. Cubist model - Training (80% data)	0.53	0.07	0.26	3.362985e-07
2. Cubist model – Testing (20% data)	0.39	0.13	0.37	0.05

Nevertheless, the results suggest that the different LULCs in the Ruiru reservoir catchment have the largest influence on aggregate stability and thus on potential soil erosion. Therefore, improved watershed management is essential for combating water-driven soil erosion. The aggregate stability prediction map for the study area was effective in identifying potentially degraded areas for which catchment-based management plans should be developed. With this study, we showed that
i) the existing forests should be protected and riparian protection efforts should be maintained, ii) roadsides should be stabilised, possibly by using vegetation, iii) options that increase SOM, such as afforestation, no-till systems, agroforestry and Napier grass as vegetation hedges, should be carefully integrated, focusing first on the most critical areas to ensure a maximum impact on the reduction of sedimentation – the critical problem for the Ruiru reservoir.

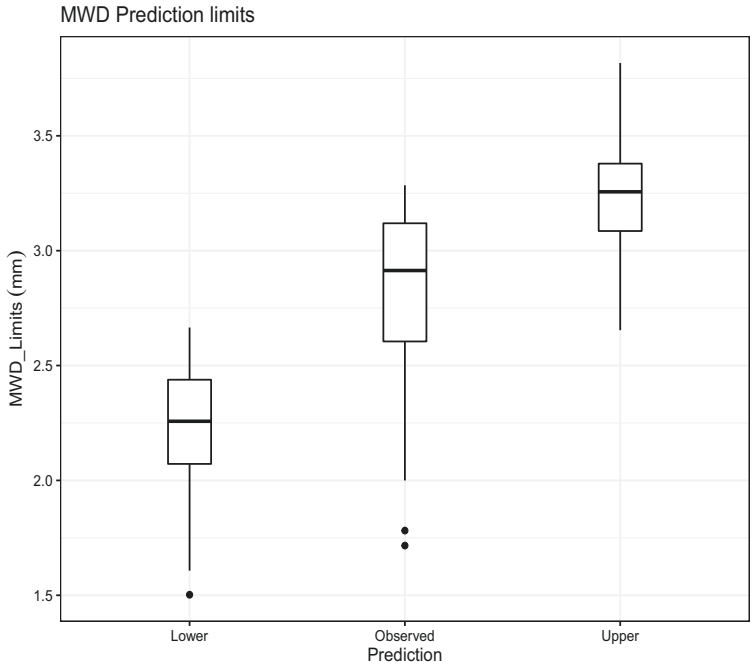

Fig. 10. Boxplot of observed MWD values against upper and lower MWD prediction limits. MWD-Mean Weight Diameter.

4. Conclusions

Using readily available data (DEM and derivatives from satellite images) as covariates and measured point data, a predictive spatial map for the aggregate stability was developed. The results revealed that the different LULCs had higher influences on aggregate stability as compared to the terrain attributes. Furthermore, the prediction map developed from DSM was used as a tool to identify different LULCs with high and low aggregate stability. Based on the aggregate stability maps, susceptibility to erosion by water exists under cropland, tea plantations and roadsides, which are located in the eastern part of the catchment, and deforested areas on the western side. Using this spatial variability of erosion-prone areas, a specific watershed management plan prioritising intervention in those areas could be established.

Declaration of Competing Interest

None.

Acknowledgements

We appreciate the assistance of Samuel Nderitu, Jackson Warui (Water Resource Users Association), Daniel Waweru (Kenya Forest Service) during fieldwork and Artur Säuberlich (TU Dresden) during laboratory work. This work was supported by the Graduate Academy of TU Dresden through the first author's Travel Grants for Short-Term Research stays abroad and the Scholarship Program for the Promotion of Early-Career Female Scientists scholarship programs.

References

EarthExplorer - USGS [WWW Document], 2019. URL https://earthexplorer.usgs.gov/ (accessed 3.10.20).

Jin, X.M., Zhang, Y.K., Schaepman, M.E., Clevers, J.G.P.W., Su, Z., Cheng, J., Jiang, J., van Genderen, J., 2008. Impact of elevation and aspect on the spatial distribution of vegetation in the Qilian mountain area with remote sensing data. In: Jin, X.M., Zhang, Y.K., Schaepman, Michael E., Clevers, J.G.P.W., Su, Z. (Eds.), Impact of Elevation and Aspect on the Spatial Distribution of Vegetation in the Qilian Mountain Area with Remote Sensing Data. In: XXIth ISPRS Congress, Beijing, 3 Juli 2008–11 Juli 2008, 1385–1390. Presented at the XXIth ISPRS Congress, International Society for Photogrammetry and Remote Sensing, Beijing, pp. 1385–1390. https://doi.org/10.5167/uzh-77426.

The Nature Conservancy, 2015. Upper Tana-Nairobi Water Fund: A Business Case.

Abrishamkesh, S., Gorji, M., Asadi, H., 2010. Long-term effects of land use on soil aggregate stability. Int. Agrophysics 25, 103–108.

Allaway, J., Cox, P.M.J., 1989. Forests and competing land uses in Kenya. Environ. Manag. 13, 171–187. https://doi.org/10.1007/BF01868364.

Amanuel, W., Yimer, F., Karltun, E., 2018. Soil organic carbon variation in relation to land use changes: the case of birr watershed, upper Blue Nile River basin. Ethiopia J. Ecol. Environ. 42, 16. https://doi.org/10.1186/s41610-018-0076-1.

Amézketa, E., 1999. Soil aggregate stability: a review. J. Sustain. Agric. 14, 83–151. https://doi.org/10.1300/J064v14n02_08.

Annabi, M., Gomez, C., Raclot, D., Bahri, H., Bailly, J.S., Bissonnais, Y.L., 2017. Spatial variability of soil aggregate stability at the scale of an agricultural region in Tunisia. Catena 153, 157–167.

Aragie, E., 2018. Identifying opportunities for value chain development in the Kenyan coffee sector: a modelling approach. Outlook Agric. 47, 150–159. https://doi.org/10.1177/0030727018766956.

Arrouays, D., McBratney, A., Bouma, J., Libohova, Z., Richer-de-Forges, A.C., Morgan, C.L.S., Roudier, P., Poggio, L., Mulder, V.L., 2020. Impressions of digital soil maps: the good, the not so good, and making them ever better. Geoderma Reg. 20. https://doi.org/10.1016/j.geodrs.2020.e00255.

Batjes, N.H., 2008. ISRIC-WISE Harmonized Global Soil Profile Dataset (Ver. 3.1) (No. ISRIC Report 2008/02).

van Bavel, C.H.M., 1950. Mean weight-diameter of soil aggregates as a statistical index of aggregation. Soil Sci. Soc. Am. J. 14, 20–23. https://doi.org/10.2136/sssaj1950.03615995001400C0005x.

Beaudette, D., Roudier, P., Brown, A., 2020. aqp: Algorithms for Quantitative Pedology.

Bieganowski, A., Zaleski, T., Kajdas, B., Sochan, A., Józefowska, A., Beczek, M., Lipiec, J., Turski, M., Ryżak, M., 2018. An improved method for determination of aggregate stability using laser diffraction. Land Degrad. Dev. 29, 1376–1384. https://doi.org/10.1002/ldr.2941.

Bivand, R., Keitt, T., Rowlingson, B., Pebesma, E., Sumner, M., Hijmans, R., Rouault, E., Warmerdam, F., Ooms, J., Rundel, C., 2019. rgdal: Bindings for the "Geospatial" Data Abstraction Library.

Borrelli, P., Robinson, D.A., Fleischer, L.R., Lugato, E., Ballabio, C., Alewell, C., Meusburger, K., Modugno, S., Schütt, B., Ferro, V., Bagarello, V., Oost, K.V., Montanarella, L., Panagos, P., 2017. An assessment of the global impact of 21st century land use change on soil erosion. Nat. Commun. 8, 2013. https://doi.org/10.1038/s41467-017-02142-7.

Boulmane, M., Oubrahim, H., Halim, M., Bakker, M.R., Augusto, L., 2017. The potential of Eucalyptus plantations to restore degraded soils in semi-arid Morocco (NW Africa). Ann. For. Sci. 74, 57. https://doi.org/10.1007/s13595-017-0652-z.

Breiman, L., 2001. Random forests. Mach. Learn. 45, 5–32. https://doi.org/10.1023/A:1010933404324.

Browning, D.M., Duniway, M.C., 2011. Digital soil mapping in the absence of field training data: a case study using terrain attributes and semiautomated soil signature derivation to distinguish ecological potential. Appl. Environ. Soil Sci. https://doi.org/10.1155/2011/421904.

Brungard, C.W., Boettinger, J.L., 2010. Conditioned Latin hypercube sampling: optimal sample size for digital soil mapping of arid rangelands in Utah, USA. In: Boettinger, Janis L., Howell, D.W., Moore, A.C., Hartemink, A.E., Kienast-Brown, S. (Eds.), Digital Soil Mapping: Bridging Research, Environmental Application, and Operation, Progress in Soil Science. Springer, Netherlands, Dordrecht, pp. 67–75. https://doi.org/10.1007/978-90-481-8863-5_6.

Celik, I., 2005. Land-use effects on organic matter and physical properties of soil in a southern Mediterranean highland of Turkey. Soil Tillage Res. 83, 270–277. https://doi.org/10.1016/j.still.2004.08.001.

Céspedes-Payret, C., Bazzoni, B., Gutiérrez, O., Panario, D., 2017. Soil organic carbon vs. Bulk Density Following Temperate Grassland Afforestation Environ Process 4, 75–92. https://doi.org/10.1007/s40710-016-0197-4.

Chaplot, V., Darboux, F., Alexis, M., Cottenot, L., Gaillard, H., Quenea, K., Mutema, M., 2019. Soil tillage impact on the relative contribution of dissolved, particulate and gaseous (CO2) carbon losses during rainstorms. Soil Tillage Res. 187, 31–40. https://doi.org/10.1016/j.still.2018.11.010.

Chenu, C., Bissonnais, Y.L., Arrouays, D., 2000. Organic matter influence on clay wettability and soil aggregate stability. Soil Sci. Soc. Am. J. 64, 1479–1486. https://doi.org/10.2136/sssaj2000.6441479x.

Conrad, O., Bechtel, B., Bock, M., Dietrich, H., Fischer, E., Gerlitz, L., Wehberg, J., Wichmann, V., Böhner, J., 2015. System for automated geoscientific analyses (SAGA) v. 2.1.4. Geosci. Model Dev. 8, 1991–2007. https://doi.org/10.5194/gmd-8-1991-2015.

Core Team, R., 2019. R: A Language and Environment for Statistical Computing [WWW Document]. URL. https://www.r-project.org/.

Demenois, J., Carriconde, F., Rey, F., Stokes, A., 2017. Tropical plant communities modify soil aggregate stability along a successional vegetation gradient on a Ferralsol. Ecol. Eng., Soil Bio- and Eco-Engineering: The Use of Vegetation to Improve Slope Stability - Proceedings of the Fourth International Conference 109, pp. 161–168. https://doi.org/10.1016/j.ecoleng.2017.07.027.

Duiker, S.W., Flanagan, D.C., Lal, R., 2001. Erodibility and infiltration characteristics of five major soils of Southwest Spain. Catena 45, 103–121. https://doi.org/10.1016/S0341-8162(01)00145-X.

Dunne, T., 1979. Sediment yield and land use in tropical catchments. J. Hydrol. 42, 281–300. https://doi.org/10.1016/0022-1694(79)90052-0.

Egashlra, K., Kaetsu, Y., Takuma, K., 1983. Aggregate stability as an index of erodibility of ando soils. Soil Sci. Plant Nutr. 29, 473–481. https://doi.org/10.1080/00380768.1983.10434650.

Flanagan, D.C., Gilley, J.E., Franti, T.G., 2007. Water Erosion Prediction Project (WEPP): Development History, Model Capabilities, and Future Enhancements. Presented at the Transactions of the ASABE.

Giasson, E., Figueiredo, S.R., Tornquist, C.G., Clarke, R.T., 2008. Digital soil mapping using logistic regression on terrain parameters for several ecological regions in southern Brazil. In: Hartemink, A.E., McBratney, A., Mendonça-Santos, M. (Eds.), Digital Soil Mapping with Limited Data. Springer, Netherlands, Dordrecht, pp. 225–232. https://doi.org/10.1007/978-1-4020-8592-5_19.

Goovaerts, P., 1998. Geostatistical tools for characterizing the spatial variability of microbiological and physico-chemical soil properties. Biol. Fertil. Soils 27, 315–334. https://doi.org/10.1007/s003740050439.

Groemping, U., 2006. Relative importance for linear regression in R: the package relaimpo. J. Stat. Softw. 17, 1–27. https://doi.org/10.18637/jss.v017.i01.

Gupta, N., Kukal, S., Bawa, S., Dhaliwal, G., 2009. Soil organic carbon and aggregation under poplar based agroforestry system in relation to tree age and soil type. Agrofor. Syst. 76, 27–35. https://doi.org/10.1007/s10457-009-9219-9.

Hengl, T., MacMillan, B., 2019. Predictive Soil Mapping with R. OpenGeoHub Foundation, Wageningen, The Netherlands.

Hengl, T., Kempen, B., Heuvelink, G., Malone, B., 2019. GSIF: Global Soil Information Facilities.

Hijmans, R.J., van Etten, J., Sumner, M., Cheng, J., Bevan, A., Bivand, R., Busetto, L., Canty, M., Forrest, D., Ghosh, A., Golicher, D., Gray, J., Greenberg, J.A., Hiemstra, P., Hingee, K., Geosciences, I.M.A., Karney, C., Mattiuzzi, M., Mosher, S., Nowosad, J., Pebesma, E., Lamigueiro, O.P., Racine, E.B., Rowlingson, B., Shortridge, A., Venables, B., Wueest, R., 2020. 2020. raster: Geographic Data Analysis and Modeling. R package version 3-0-7. https://CRAN.R-project-org/package=raster.

Howell, D., Kim, Y.G., Haydu-Houdeshell, C.A., 2008. Development and application of digital soil mapping within traditional soil survey: what will it grow into? In: Hartemink, A.E., McBratney, A., Mendonça-Santos, M. (Eds.), Digital Soil Mapping with Limited Data. Springer, Netherlands, Dordrecht, pp. 43–51. https://doi.org/10.1007/978-1-4020-8592-5_4

Hunink, J.E., Niadas, I.A., Antonaropoulos, P., Droogers, P., de Vente, J., 2013. Targeting of intervention areas to reduce reservoir sedimentation in the Tana catchment (Kenya) using SWAT. Hydrol. Sci. J. 58, 600–614. https://doi.org/10.1080/02626667.2013.774090.

Iori, P., Dias Junior, M., Ajayi, A.E., Guimarães, P.T.G., Abreu Júnior, Á.A., 2014. Influence of field slope and coffee plantation age on the physical properties of a red-yellow latosol. Rev Bras Ciênc Solo 38, 107–117. https://doi.org/10.1590/S0100-06832014000100010.

Iserloh, T., Ries, J.B., Arnáez, J., Boix-Fayos, C., Butzen, V., Cerdà, A., Echeverría, M.T., Fernández-Gálvez, J., Fister, W., Geißler, C., Gómez, J.A., Gómez-Macpherson, H., Kuhn, N.J., Lázaro, R., León, F.J., Martínez-Mena, M., Martínez-Murillo, J.F., Marzen, M., Mingorance, M.D., Ortigosa, L., Peters, P., Regüés, D., Ruiz-Sinoga, J.D., Scholten, T., Seeger, M., Solé-Benet, A., Wengel, R., Wirtz, S., 2013. European small portable rainfall simulators: a comparison of rainfall characteristics. Catena 110, 100–112. https://doi.org/10.1016/j.catena.2013.05.013.

Jaetzold, R., Schmidt, H., Hornetz, B., Shisanya, C., 2006. Farm Management Handbook of Kenya Volume II: Natural Conditions and Farm Management Information. Part C: East Kenya. Subpart C1: Eastern Province. GTZ, Nairobi, Kenya.

Jones, E.J., Filippi, P., Wittig, R., Fajardo, M., Pino, V., McBratney, A.B., 2020. Mapping soil slaking index and assessing the impact of management in a mixed agricultural landscape. SOIL Discuss., pp. 1–22. https://doi.org/10.5194/soil-2020-29

Kalhoro, S.A., Xu, X., Chen, W., Hua, R., Raza, S., Ding, K., 2017. Effects of different land-use systems on soil aggregates: a case study of the loess plateau (northern China). Sustainability 9, 1349. https://doi.org/10.3390/su9081349.

Keskin, H., Grunwald, S., 2018. Regression kriging as a workhorse in the digital soil mapper's toolbox. Geoderma 326, 22–41. https://doi.org/10.1016/j.geoderma.2018.04.004.

Kouli, M., Soupios, P., Vallianatos, F., 2009. Soil erosion prediction using the revised universal soil loss equation (RUSLE) in a GIS framework, Chania, northwestern Crete. Greece Environ. Geol. 57, 483–497. https://doi.org/10.1007/s00254-008-1318-9.

Kuriakose, S.L., van Beek, L.P.H., 2011. Plant root strength and slope stability. In: Gliński, J., Horabik, J., Lipiec, J. (Eds.), Encyclopedia of Agrophysics. Springer Netherlands, Dordrecht, pp. 622–627. https://doi.org/10.1007/978-90-481-3585-1_222.

Kwakye, S.O., Bárdossy, A., 2020. Hydrological modelling in data-scarce catchments: black Volta basin in West Africa. SN Appl. Sci. 2, 628. https://doi.org/10.1007/s42452-020-2454-4.

Lagacherie, P., 2008. Digital soil mapping: a state of the art. In: Hartemink, A.E., McBratney, A., Mendonça-Santos, M. (Eds.), Digital Soil Mapping with Limited Data. Springer, Netherlands, Dordrecht, pp. 3–14. https://doi.org/10.1007/978-1-4020-8592-5_1.

Le Bissonnais, Y., 1996. Aggregate stability and assessment of soil crustability and erodibility: I. Theory and methodology. Eur. J. Soil Sci. 47, 425–437. https://doi.org/10.1111/j.1365-2389.1996.tb01843.x.

Lemercier, B., Arrouays, D., Follain, S., Saby, N.P.A., Schvartz, C., Walter, C., 2008. Broad-scale soil monitoring through a Nationwide soil-testing database. In: Hartemink, A.E., McBratney, A., Mendonça-Santos, M. (Eds.), Digital Soil Mapping with Limited Data. Springer, Netherlands, Dordrecht, pp. 273–281. https://doi.org/10.1007/978-1-4020-8592-5_23.

Lewis, L.A., 1985. Assessing soil loss in Kiambu and Murang'a districts. Kenya Geogr. Ann. Ser. Phys. Geogr. 67, 273–284. https://doi.org/10.2307/521104.

Ma, Y., Minasny, B., Wu, C., 2017. Mapping key soil properties to support agricultural production in eastern China. Geoderma Reg. 10, 144–153. https://doi.org/10.1016/j.geodrs.2017.06.002.

Macrotrends, L.L.C., 2010. Ruiru, Kenya population 1950-2020. WWW Document. www.macrotrends.net (accessed 4.6.20).

Mainuri, Z.G., Owino, J.O., 2013. Effects of land use and management on aggregate stability and hydraulic conductivity of soils within river Njoro watershed in Kenya. Int. Soil Water Conserv. Res. 1, 80–87. https://doi.org/10.1016/S2095-6339(15)30042-3.

Mainuri, Z.G., Owino, J.O., 2017. Spatial variability of soil aggregate stability in a disturbed river watershed. Eur. J. Econ. Bus. Stud. Artic 3.

Maloi, S.K., Sang, J.K., Raude, J.M., Mutwiwa, U.N., Mati, B.M., Maina, C.W., 2016. Assessment of sedimentation status of Ruiru reservoir, Central Kenya. Am. J. Water Resour. 4, 77–82. https://doi.org/10.12691/ajwr-4-4-1.

Malone, B.P., Minasny, B., McBratney, A.B., 2017. Using R for Digital Soil Mapping, Progress in Soil Science. Springer International Publishing, Cham https://doi.org/10.1007/978-3-319-44327-0.

McBratney, A.B., Mendonça Santos, M.L., Minasny, B., 2003. On digital soil mapping. Geoderma 117, 3–52. https://doi.org/10.1016/S0016-7061(03)00223-4.

Minasny, B., McBratney, A.B., 2006. A conditioned Latin hypercube method for sampling in the presence of ancillary information. Comput. Geosci. 32, 1378–1388. https://doi.org/10.1016/j.cageo.2005.12.009.

Mora-Vallejo, A., Claessens, L., Stoorvogel, J., Heuvelink, G.B.M., 2008. Small scale digital soil mapping in southeastern Kenya. Catena 76, 44–53. https://doi.org/10.1016/j.catena.2008.09.008.

Mutegi, J.K., Mugendi, D.N., Verchot, L.V., Kung'u, J.B., 2008. Combining napier grass with leguminous shrubs in contour hedgerows controls soil erosion without competing with crops. Agrofor. Syst. 74, 37–49. https://doi.org/10.1007/s10457-008-9152-3.

Mwangi, W., Isaiah, N., Shadrack, K., 2017. Spatio-temporal dynamics of land use practices on rivers in tropical regions: a case study of Ruiru and Ndarugu basins, Kiambu County. Kenya Afr. J. Environ. Sci. Technol. 11, 426–437. https://doi.org/10.5897/AJEST2017.2325.

Näschen, K., Diekkrüger, B., Leemhuis, C., Steinbach, S., Seregina, L.S., Thonfeld, F., van der Linden, R., 2018. Hydrological modeling in data-scarce catchments: the Kilombero floodplain in Tanzania. Water 10, 599. https://doi.org/10.3390/w10050599.

Nogueira, M.A., Albino, U.B., Brandão-Junior, O., Braun, G., Cruz, M.F., Dias, B.A., Duarte, R.T.D., Gioppo, N.M.R., Menna, P., Orlandi, J.M., Raimam, M.P., Rampazo, L.G.L., Santos, M.A., Silva, M.E.Z., Vieira, F.P., Torezan, J.M.D., Hungria, M., Andrade, G., 2006. Promising indicators for assessment of agroecosystems alteration among natural, reforested and agricultural land use in southern Brazil. Agric. Ecosyst. Environ. 115, 237–247. https://doi.org/10.1016/j.agee.2006.01.008.

Ovuka, M., 2000a. More people, more erosion? Land use, soil erosion and soil productivity in Murang'a district. Kenya Land Degrad. Dev. 11, 111–124. https://doi.org/10.1002/(SICI)1099-145X(200003/04)11:2<111::AID-LDR371>3.0.CO;2-I.

Ovuka, M., 2000b. Land use changes in Central Kenya from the 1950s — a possibility to generalise? GeoJournal 51, 203–209. https://doi.org/10.1023/A:1017597411522.

Parsakhoo, A., Lotfalian, M., Kavian, A., Hosseini, S.A., 2014. Assessment of soil erodibility and aggregate stability for different parts of a forest road. J. For. Res. 25, 193–200. https://doi.org/10.1007/s11676-014-0445-2.

Pebesma, E., Bivand, R.S., 2005. Classes and Methods for Spatial Data: The Sp Package.

Pebesma, E.J., Wesseling, C.G., 1998. Gstat: a program for geostatistical modelling, prediction and simulation. Comput. Geosci. 24, 17–31. https://doi.org/10.1016/S0098-3004(97)00082-4.

Pimentel, D., Harvey, C., Resosudarmo, P., Sinclair, K., Kurz, D., McNair, M., Crist, S., Shpritz, L., Fitton, L., Saffouri, R., Blair, R., 1995. Environmental and economic costs of soil erosion and conservation benefits. Science 267, 1117–1123. https://doi.org/10.1126/science.267.5201.1117.

Prado, R.B., Benites, V.M., Machado, P.L.O.A., Polidoro, J.C., Dart, R.O., Naumov, A., 2008. Mapping potassium availability from limited soil profile data in Brazil. In: Hartemink, A.E., McBratney, A., Mendonça-Santos, M. (Eds.), Digital Soil Mapping with Limited Data. Springer, Netherlands, Dordrecht, pp. 91–101. https://doi.org/10.1007/978-1-4020-8592-5_8.

Quinlan, J.R., 1992. Learning with continuous classes. World Scientific 343–348.

Rivero, R.G., Grunwald, S., Bruland, G.L., 2007. Incorporation of spectral data into multivariate geostatistical models to map soil phosphorus variability in a Florida wetland. Geoderma 140, 428–443. https://doi.org/10.1016/j.geoderma.2007.04.026.

Rohošková, M., Valla, M., 2011. Comparison of two methods for aggregate stability measurement – a review. Plant Soil Environ. 50, 379–382. https://doi.org/10.17221/4047-PSE.

Roudier, P., Beaudette, A.E., Hewitt, A.E., 2012. A conditioned Latin hypercube sampling algorithm incorporating operational constraints. In: Minasny, B., Malone, B.P., McBratney, A.B. (Eds.), Digital Soil Assessments and beyond, Proceedings of the 5th Global Workshop on Digital Soil Mapping 2012. Sydney, Australia, pp. 227–232. https://doi.org/10.1201/b12728-46.

Rühlmann, J., Körschens, M., 2009. Calculating the effect of soil organic matter concentration on soil bulk density. Soil Sci. Soc. Am. J. 73, 876–885. https://doi.org/10.2136/sssaj2007.0149.

Shi, P., Castaldi, F., van Wesemael, B., van Oost, K., 2020. Large-scale, high-resolution mapping of soil aggregate stability in croplands using APEX hyperspectral imagery. Remote Sens. 12, 666. https://doi.org/10.3390/rs12040666.

Six, J., Elliott, E.T., Paustian, K., 2000. Soil macroaggregate turnover and microaggregate formation: a mechanism for C sequestration under no-tillage agriculture. Soil Biol. Biochem. 32, 2099–2103. https://doi.org/10.1016/S0038-0717(00)00179-6.

Solomatine, D.P., Shrestha, D.L., 2009. A Novel Method to Estimate Model Uncertainty Using Machine Learning Techniques. https://doi.org/10.1029/2008WR006839.

Stoof-Leichsenring, K.R., Junginger, A., Olaka, L.A., Tiedemann, R., Trauth, M.H., 2011. Environmental variability in Lake Naivasha, Kenya, over the last two centuries. J. Paleolimnol. 45, 353–367. https://doi.org/10.1007/s10933-011-9502-4.

Taghizadeh-Mehrjardi, R., Bawa, A., Kumar, S., Zeraatpisheh, M., Amirian-Chakan, A., Akbarzadeh, A., 2019. Soil erosion spatial prediction using digital soil mapping and RUSLE methods for Big Sioux River watershed. Soil Syst. 3, 43. https://doi.org/10.3390/soilsystems3030043.

Takele, L., Chimdi, A., Abebaw, A., 2015. Impacts of land use on selected physicochemical properties of soils of Gindeberet area, Western Oromia. Ethiopia Sci. Technol. Arts. Res. J. 3, 36–41. https://doi.org/10.4314/star.v3i4.5.

Tegegne, G., Park, D.K., Kim, Y.-O., 2017. Comparison of hydrological models for the assessment of water resources in a data-scarce region, the Upper Blue Nile River Basin. J. Hydrol. Reg. Stud. 14, 49–66. https://doi.org/10.1016/j.ejrh.2017.10.002.

Travis, M.R., Elsner, G.H., Iverson, W.D., Johnson, C.G., 1975. VIEWIT: computation of seen areas, slope, and aspect for land-use planning. p. 11.

Vaezi, A.R., Hasanzadeh, H., Cerdà, A., 2016. Developing an erodibility triangle for soil textures in semi-arid regions, NW Iran. Catena 142, 221–232. https://doi.org/10.1016/j.catena.2016.03.015.

Vanmaercke, M., Poesen, J., Broeckx, J., Nyssen, J., 2014. Sediment yield in Africa. Earth Sci. Rev. 136, 350–368. https://doi.org/10.1016/j.earscirev.2014.06.004.

Vogl, A.L., Bryant, B.P., Hunink, J.E., Wolny, S., Apse, C., Droogers, P., 2017. Valuing investments in sustainable land management in the upper Tana River basin. Kenya J. Environ. Manage 195, 78–91. https://doi.org/10.1016/j.jenvman.2016.10.013.

Webster, R., 2007. Digital soil mapping: an introductory perspective. Eur. J. Soil Sci. 58, 1217–1218. https://doi.org/10.1111/j.1365-2389.2007.00943_6.x.

Wooldridge, R., 1984. Sedimentation in reservoirs: Tana River basin, Kenya. III - Analysis of hydrographic surveys of three reservoirs in June/July 1983. HR Wallingford: Hydraulics Research, Report no. 61.

Wynants, M., Kelly, C., Mtei, K., Munishi, L., Patrick, A., Rabinovich, A., Nasseri, M., Gilvear, D., Roberts, N., Boeckx, P., Wilson, G., Blake, W.H., Ndakidemi, P., 2019. Drivers of increased soil erosion in East Africa's agro-pastoral systems: changing interactions between the social, economic and natural domains. Reg. Environ. Chang. 19, 1909–1921. https://doi.org/10.1007/s10113-019-01520-9.

Xue, J., Su, B., 2017. Significant remote sensing vegetation indices: a review of developments and applications. J. Sens. 2017, 1–17. https://doi.org/10.1155/2017/1353691.

Ye, L., Tan, W., Fang, L., Ji, L., Deng, H., 2018. Spatial analysis of soil aggregate stability in a small catchment of the loess plateau, China: I Spatial variability. Soil Tillage Res. 179, 71–81. https://doi.org/10.1016/j.still.2018.01.012.

Zhang, S., Huang, Y., Shen, C., Ye, H., Du, Y., 2012. Spatial prediction of soil organic matter using terrain indices and categorical variables as auxiliary information. Geoderma 171–172, 35–43. https://doi.org/10.1016/j.geoderma.2011.07.012.

Zhang, G., Liu, F., Song, X., 2017. Recent progress and future prospect of digital soil mapping: a review. J. Integr. Agric. 16, 2871–2885. https://doi.org/10.1016/S2095-3119(17)61762-3.

Zhou, M., Liu, C., Wang, J., Meng, Q., Yuan, Y., Ma, X., Liu, X., Zhu, Y., Ding, G., Zhang, J., Zeng, X., Du, W., 2020. Soil aggregates stability and storage of soil organic carbon respond to cropping systems on Black Soils of Northeast China. Sci. Rep. 10, 265. https://doi.org/10.1038/s41598-019-57193-1.

PAPER IV

Environmental Earth Sciences (2022) 81:502
https://doi.org/10.1007/s12665-022-10617-0

THEMATIC ISSUE

Using soil erosion as an indicator for integrated water resources management: a case study of Ruiru drinking water reservoir, Kenya

Ann W. Kamamia[1] · Cordula Vogel[1] · Hosea M. Mwangi[2] · Karl-heinz Feger[1] · Joseph Sang[2] · Stefan Julich[1]

Received: 29 July 2021 / Accepted: 24 September 2022

Abstract

Functions and services provided by soils play an important role for numerous sustainable development goals involving mainly food supply and environmental health. In many regions of the Earth, water erosion is a major threat to soil functions and is mostly related to land-use change or poor agricultural management. Selecting proper soil management practices requires site-specific indicators such as water erosion, which follow a spatio-temporal variation. The aim of this study was to develop monthly soil erosion risk maps for the data-scarce catchment of Ruiru drinking water reservoir located in Kenya. Therefore, the Revised Universal Soil Loss Equation complemented with the cubist–kriging interpolation method was applied. The erodibility map created with digital soil mapping methods ($R^2 = 0.63$) revealed that 46% of the soils in the catchment have medium to high erodibility. The monthly erosion rates showed two distinct potential peaks of soil loss over the course of the year, which are consistent with the bimodal rainy season experienced in central Kenya. A higher soil loss of 2.24 t/ha was estimated for long rains (March–May) as compared to 1.68 t/ha for short rains (October–December). Bare land and cropland are the major contributors to soil loss. Furthermore, spatial maps reveal that areas around the indigenous forest on the western and southern parts of the catchment have the highest erosion risk. These detected erosion risks give the potential to develop efficient and timely soil management strategies, thus allowing continued multi-functional use of land within the soil–food–water nexus.

Keywords Erosion · Soil–water nexus · Digital soil mapping · Spatio-temporal dynamics · RUSLE · Erodibility

This article is part of a Topical Collection in Environmental Earth Sciences on "The Soil–Water–Atmosphere Nexus", guest edited by Daniel Karthe, Lulu Zhang, Sabrina Kirschke, Nora Adam, Serena Caucci, and Edeltraud Günther.

✉ Ann W. Kamamia
ann.kamamia@mailbox.tu-dresden.de

Cordula Vogel
covogel@msx.tu-dresden.de

Hosea M. Mwangi
hmwangi@jkuat.ac.ke

Karl-heinz Feger
karl-heinz.feger@tu-dresden.de

Joseph Sang
j.sang@jkuat.ac.ke

Stefan Julich
stefan.julich@tu-dresden.de

[1] Institute of Soil Science and Site Ecology, Technical University Dresden, Dresden, Germany [2] School of Biosystems and Environmental Engineering, Jomo Kenyatta University of Agriculture and Technology, Juja, Kenya

Introduction

Soils form a critical component influencing the hydrological cycle and are crucial in supporting and protecting food and energy production. Several sustainable development goals (SDGs) defined by the United Nations (Goals 1–3, 6–7, 11 and 13) are linked to soil health (United Nations 2015). Soil health must therefore be maintained as they are critical elements of the water–energy–food nexus (Lal et al. 2017). However, the ability of soils to provide their functions is under threat due to degradation mainly through accelerated water erosion. Most soils today can be regarded as being in a state of fair, poor or very poor condition (FAO ITPS 2015). This is the result of human activities such as deforestation, overgrazing, intensive tillage on steep terrain, over-cropping and poor soil management practices (Borrelli et al. 2017; Ebabu et al. 2019). While onsite effects of erosion include land degradation and the loss of soil fertility (Kidane et al. 2019; Lambin et al. 2003), off-site effects include siltation, sedimentation, eutrophication of surface

Published online: 18 October 2022

water bodies and even induced flooding (Borrelli et al. 2017; Ozsoy et al. 2012). Borrelli et al. (2017) rated African countries around the equator as erosion hotspots. Due to high population growth compounded by an agriculture-based economy, existing forests are subjected to increasing pressure. This has resulted in deforestation to pave way for other competing land uses such as settlement and agriculture (Carr 2004; Mulinge et al. 2016). Deforestation coupled with high rainfall and fragile terrains with exposed soils has led to severe soil erosion. Maloi et al. (2016) showed that a shift in land use, primarily from forests to cultivation, has increased siltation in the Ruiru Reservoir (Kenya), thereby decreasing its storage capacity by 11–14% in 65 years. There is an urgent need to identify areas with high susceptibility to erosion to implement strategies to mitigate erosion to maintain soil health and prevent impairment of water quality of surface water bodies such as rivers, lakes, and reservoirs. Patil (2018) suggested that the assessment of the soil erosion risks can assist in watershed assessment in areas where erosion is a major threat. Moreover, the processes involved in soil loss by water underlie a high spatio-temporal variability which should be taken into account in integrated water resource management (IWRM). IWRM refers to "a process which promotes the coordinated development and management of water, land and land related resources, in order to maximise the resultant economic and social welfare in an equitable manner" (GWP 2000). This denotes that water and land/soil are interrelated (Calder 2006). Problems concerning water quality and quantity cannot be treated in isolation and a "system thinking approach" between the water–soil nexus needs to be adopted. Using average erosion soil rates can camouflage erosion occurring at smaller scales (Hatfield et al. 2017). Furthermore, extreme events in precipitation as a result of climate change have increased the potential for soil erosion in ways that are not well understood and assessed. Hence, proper spatio-temporal analysis could provide a better understanding of the climate variability and soil ecosystem services intersection. Based on such information, decision-makers and land resource managers can develop more timely and targeted cost-effective measures in the frame of IWRM (Mwangi et al. 2016a, b).

Different studies have been undertaken to quantify soil erosion. The most accurate and ideal methods involve conducting field experiments using erosion plots. Here, erosion measurements are carried out under natural conditions (Ampofo et al. 2002; Boardman and Evans 2019). Alternatively, the rain events can be simulated, where parameters such as rainfall intensity, drop size and spatial variability can be adjusted (Duiker et al. 2001; Stroosnijder 2005; Ries et al. 2013; Iserloh et al. 2013). Other methods include the use of radionuclide tracers (Maina et al. 2018). Nevertheless, direct erosion measurements are expensive, unstandardised, time-consuming and limited in terms of spatial and temporal variation (Lal 2001; Stroosnijder 2005; Ries et al. 2013). The setbacks faced by direct measurements have resulted in the use of models to predict soil erosion. These models are primarily classified into three (physical, conceptual and empirical) depending on model input and the extent of the underlying theoretical principles (Igwe et al. 2017; Patil 2018). Physical models take the individual components affecting soil erosion into account, e.g., spatial and temporal variability. Such models include the European Soil Erosion Model (EUROSEM) (Morgan et al. 1998). Conceptual models like the Soil and Water Integrated Model (SWIM) (Krysanova et al. 1998) represent processes in terms of fluxes at different spatial and temporal resolutions. Empirical models are the least data intense and focus primarily on observed data and their responses. These include the Universal Soil Loss Equation (USLE) (Wischmeier and Smith 1978) and its revised version, the Revised Universal Soil Loss Equation (RUSLE) (Renard et al. 2017), which are conventionally applied to quantify long-term average soil loss (Alewell et al. 2019). They are used to calculate the annual erosion rate using factors which include rainfall erosivity (R-factor), soil erodibility (K-factor), slope steepness and length (LS-factor), cover management (C-factor) and support practices (P-factor). The R-factor highly correlates with rainfall amount and intensity (Schmidt et al. 2016). Hence, it is expected that there will be an inter-annual and seasonal variation of this factor wherefrom dynamic soil erosion risks can be identified. Recent studies on the temporal variability of the R-factor revealed a distinct seasonality influenced by intense rainfall events in Switzerland (Schmidt et al. 2016). The K-factor, defined as soil loss rate per erosion index, expresses the susceptibility of a soil to be detached and transported by rainfall and runoff (Renard et al. 2017). Direct measurements of this factor require long-term soil erosion studies or the use of soil property data (Wischmeier and Smith 1958). Although there exists a dataset on soil erodibility at higher resolution (up to 500 m) for some developed regions such as Europe (Panagos et al. 2014), only coarse estimates are available for Africa (Borrelli et al. 2017). Since the K-factor is a significant parameter in the soil erosion process, its spatial variability across different landscapes should be considered (Zhu et al. 2010). The spatial variability of the K-factor has been mapped through interpolation methods (Addis and Klik 2015; Avalos et al. 2018) and machine learning algorithms such as the cubist method (Panagos et al. 2014). The LS-factor accounts for the effects of slope steepness and length on erosion (Alexandridis et al. 2015). The C-factor represents the effect of plants as well as soil cover, biomass and disturbing activities on erosion. Schmidt et al. (2018) identified crop cover as one of the main triggers of soil erosion as it is highly dependent on their seasonal dynamics and growth curve. The P-factor includes erosion control measures such as contour cropping, terracing, grass strips and all other

enhancements that reduce slope length, thereby reducing the amount and rate at which the soil is lost (Renard et al. 2017).

The RUSLE has been reported to generate quantitative estimates of soil loss in ungauged catchments that have been applied in designing sound conservation measures (Asis and Omasa 2007). Moreover, recent applications of soil loss models such as RUSLE have been complemented by the application of GIS and remote sensing technologies. Such technologies include the use of satellite images and geospatial algorithms such as interpolation distance weighing (IDW) (Angulo-Martínez et al. 2009; Gaubi et al. 2017), kriging (Wang et al. 2002; Kouli et al. 2009), regression equations (Panagos et al. 2014) and machine learning available through digital soil mapping (DSM) (Avalos et al. 2018; Taghizadeh-Mehrjardi et al. 2019). Jenny (1941) established that soil physical and chemical properties are influenced by five soil-forming factors, namely, climate, organisms, topography, parent material and time. This can be exploited with DSM which assumes that a relationship exists between environmental conditions and soil properties (McBratney et al. 2003). By using prediction algorithms, a suite of environmental covariates and measured soil properties, this relationship can be obtained and extended to areas without observations. This means that soil properties such as soil erodibility can be mapped at much lower costs and effort. With access to both geospatial algorithms and higher quality input data, models such as RUSLE can be applied at higher temporal and spatial scales (Uddin et al. 2016; Schmidt et al. 2019; Wang et al. 2019). Schmidt et al. (2016) demonstrated that it is possible to predict soil loss dynamics by modelling the intra-annual variability of the R-factor and C-factor within the RUSLE. By applying the RUSLE equation on Swiss grassland with a sub-annual resolution at a national scale, the authors showed that the mean monthly soil loss by water was 48 times higher in summer as compared to winter. However, the effectiveness of the application of RUSLE depends on the availability of datasets. For developing countries, global datasets are sometimes the only data available. Although providing valuable data, this may still be considered too coarse for effective application. But by undertaking purposive soil sampling and applying digital soil mapping, time and spatial variability of soil properties and vulnerabilities can effectively be determined in data-scarce areas such as Africa (Kamamia et al. 2021). In the presented study, we applied a combination of DSM with the RUSLE to estimate erosion loss on monthly time steps for a data-scarce watershed in Kenya, East Africa. We additionally compared the predicted monthly soil loss with estimates from a global soil loss dataset for this region. With the application of the temporally and spatially variable RUSLE prediction, we wanted to address the following questions. (1) What is the impact of rainy periods on erosion and soil loss in the study area? (2) What is the contribution of the different land-use classes (LULC) to sediment yields in the catchment? (3) Can the assessment of spatio-dynamic erosion inform the planning of soil conservation measures to mitigate soil erosion?

This paper is organised into five sections. "Ruiru Reservoir catchment" (following the introduction) describes the study area. "Methodology" summarises the site selection procedure, data collection phase and laboratory analysis. It further presents a step-by-step methodological approach adopted including the plausibility check. "Results and discussion" discusses the spatio-temporal analysis and links this to the major land uses. Final section concludes the impact of the major findings on the soil–water nexus.

Ruiru Reservoir catchment

The Ruiru Reservoir catchment (Fig. 1a) is located in Kiambu County, Kenya. The catchment covers 51 km^2 from the uplands close to the Rift Valley escarpments to the Ruiru Reservoir at the catchment's outlet. A humid highland subtropical climate with wet and dry seasons characterises the local climate. An average annual rainfall of 1300–1500 mm is received in the catchment. Long rains are experienced between March and May, while short rains are experienced between October and December. Daily temperatures range between 13.0 and 24.9 °C. Temperatures are highest from January to March and lowest in July–August (Nyakundi et al. 2017). Nitisols are the dominating soils in the catchment, whereas a small portion of Andosols can be found in the upper part of the catchment (Fig. 1a). These soils are influenced by pyroclastic and igneous volcanic parent material. The region belongs to the tea–dairy zone and subsistence farming is characterised by low-input low-output production (Kamamia et al. 2021). The Ruiru Reservoir in which the Ruiru River drains, located in the lowest part of the catchment, was designed to supply 23,000 m^3/day of water to the residents of Nairobi, the capital city of Kenya. Maloi et al. (2016) reported that land-use change, majorly from forest to agriculture, has increased sediments in runoff into the reservoir especially during the rainy seasons, thus increasing the treatment costs. Hence, land-use management must address the water insecurities in the catchment to ensure sustainable supply of good quality water (Calder 2006).

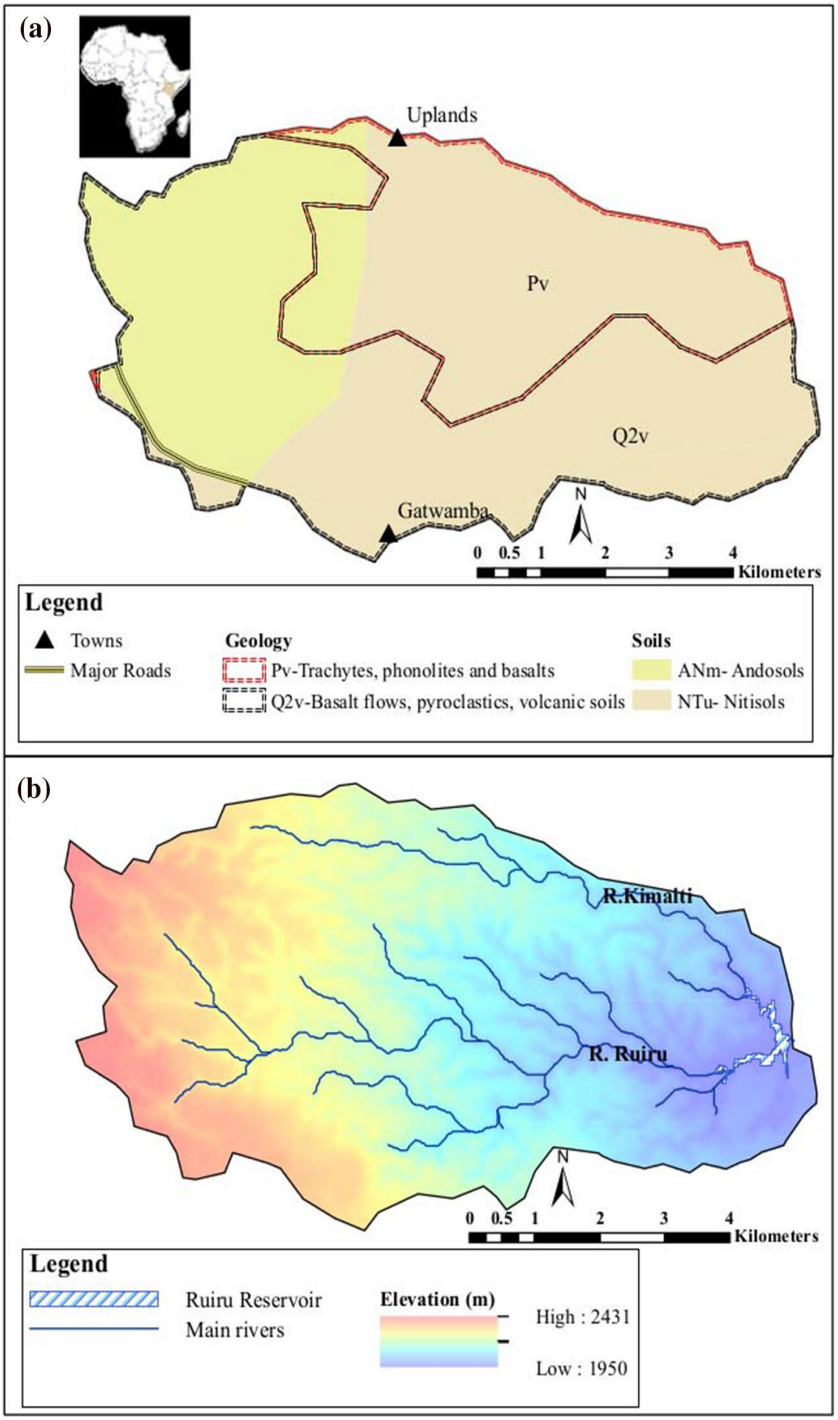

Fig. 1 The Ruiru Reservoir catchment: **a** location, soils, geology and location, **b** elevation, main rivers and location of the Ruiru Reservoir

Methodology

Figure 2 presents a flowchart of the approach followed in the spatio-temporal analysis. The first step involved the collection and synthesis of raw data. In the second step, the individual RUSLE factors were determined. These factors were then integrated and compared to the Global Soil Erosion Model (GloSEM) in the third step.

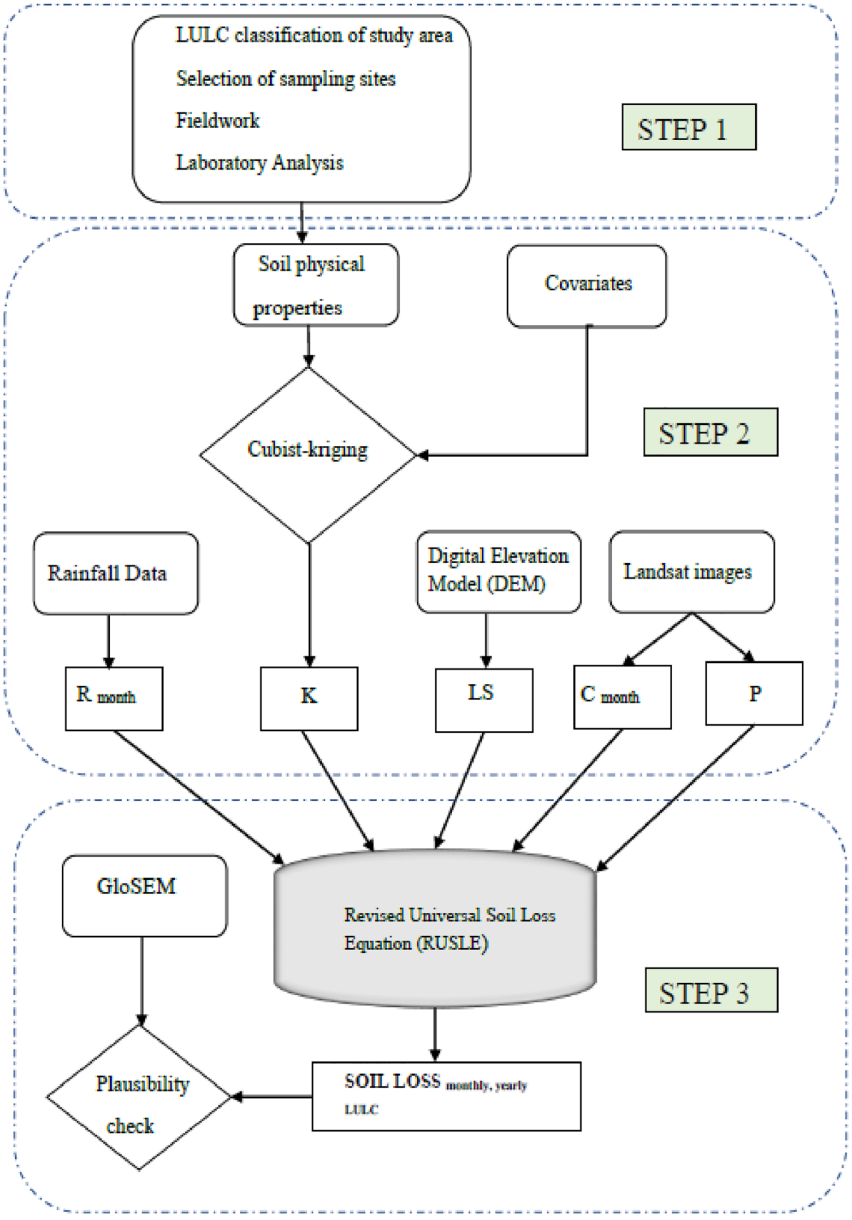

Fig. 2 Flowchart of the application of RUSLE equation and plausibility check; digital elevation model (DEM), rainfall erosivity (R-factor), soil erodibility (K-factor), slope steepness and length factor (LS-factor), cover management factor (C-factor), support practices factor (P-factor) and Global Soil Erosion Model (GloSEM) (Borrelli et al. 2017)

Step 1: creation of land-use land cover map, data collection and synthesis

Supervised classification of the major land uses in the Ruiru catchment

A Landsat 8 image Operational Land Imager (OLI) for August was downloaded from the Earth explorer (EarthExplorer, USGS 2019) and was used in combination with the semi-automatic classification plugin in QGIS 3.4 (QGIS.org 2019). All the bands were then clipped to the study area size and converted to reflectance (Young et al. 2017). A band set with Band5, Band4 and Band3 (Bands 5–4–3), which represents a temporary virtual raster that allows for the display of composite colours, was created (NASA 2013). Next, the training sites were defined by creating regions of interest (ROI). In addition to georeferenced points obtained during the field campaign, Google Earth was used to increase the number of ROIs. The main defined land-use classes were water (WTR), bare land (BARE), cropland (AG), tea (TEA), grassland and shrubland (GR/SH), built-up (BLD) and forests (FOR). The classification was carried out by using the maximum likelihood algorithm (MLA) (Benediktsson et al. 1990). The MLA is a rule-based algorithm that is based on

Table 1 Landsat 8 band description and combination

Band number	Description
Band 1	Coastal
Band 2–4	Visible blue, green, red
Band 5–7	Infrared (near, shortwave (1.56–1.66 µm), shortwave (2.10–2.30 µm)
Band 8	Panchromatic
Band 9	Cirrus
Band 10–11	Infrared (longwave (10–11.3 µm), longwave (11.5–12.5 µm)

Source: https://landsat.gsfc.nasa.gov/landsat-8/landsat-8-bands/

the probability that a given pixel belongs to a particular class. MLA was applied iteratively and with the Band 5–4–3 (see description in Table 1) band combination.

Each time the classification was done, the spectral signatures (reflectance as a function of the shortwave and different objects have unique signatures which can be used for classification) (NASA 1999) were assessed. However, during classification similar spectral signatures may be recorded for different materials which could lead to misclassification. To overcome this, more training sites were delineated to allow MLA to discriminate between the various vegetation cover and between bare land and built-up areas. The post-processing step included the removal of raster polygons smaller than the minimum mapping unit (MMU), which was set at 25. As the GR/SH vegetation was limited, a new class "Natural Vegetation (NV)" was created by aggregating the grasslands, shrublands and forests. A final land-use map with an accuracy of 71% obtained from the confusion matrix was created (Fig. 3). The distribution of the main LULC for determining soil loss was BARE (4.8%), AG (38.3%), TEA (34.8%), NV (16.6%). The remaining distribution represented built-up areas and the Ruiru Reservoir.

Selection of sampling sites

A 30 m sink-filled digital elevation model (DEM) (Earth Explorer, USGS 2019) was used to extract derivatives using the System for Automated Geoscientific Analyses (SAGA-GIS) (Conrad et al. 2015). From the DEM, slope, aspect, plan curvature, profile curvature, relief, elevation,

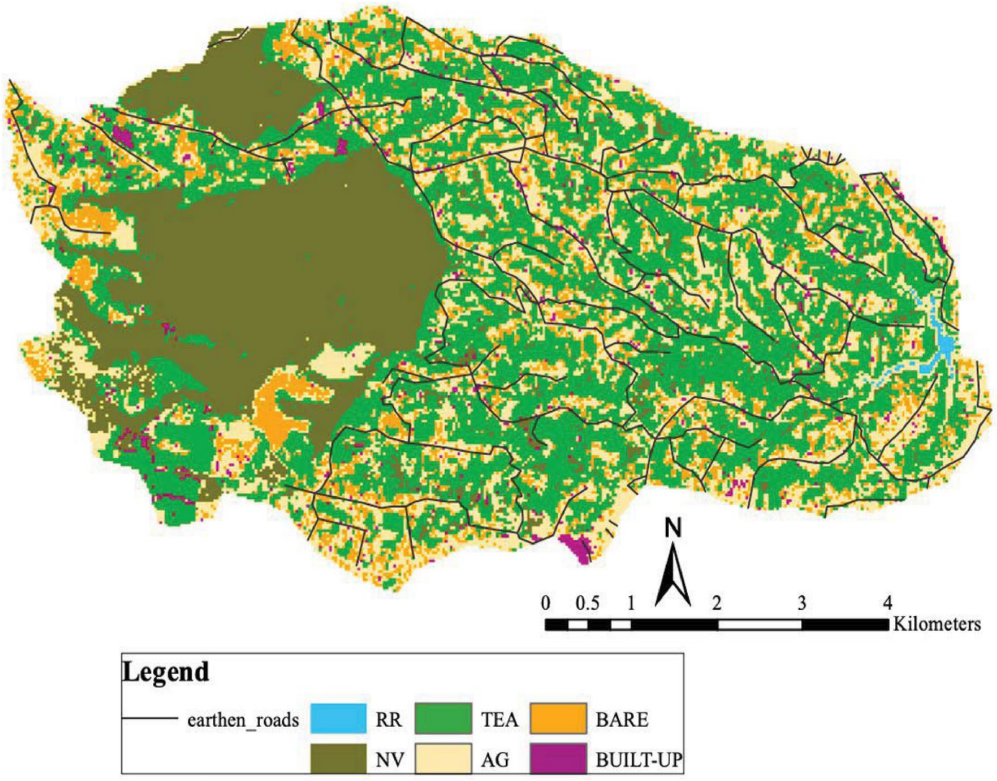

Fig. 3 Land-use land cover of Ruiru catchment obtained from supervised classification using Landsat 8 image Operational Land Imager (OLI) downloaded from the Earth explorer (EarthExplorer—USGS 2019)

Topographic Wetness Index (TWI) and hill shading derivatives were extracted. Additional data acquired include a Soil map at a scale 1:250,000 from the Soil and Terrain (SOTER) database of the International Soil Reference and Information Centre (ISCRIC) (Batjes 2008) and a geology map from the Survey of Kenya (SOK).

All DEM derivatives and additional data were stacked together and split into 30-m segments in ArcGIS (ArcMap version 10.2). This means that each segment was represented by a series of a different set of covariates which included the DEM derivatives, geology, soil, and land-use values. The sampling distribution was determined by using the conditioned Latin hypercube sampling algorithm (cLHS) (Minasny and McBratney 2006) included in the *cLHS* package (Roudier et al. 2012) of the R statistical software, version 3.5.1 (R Core Team 2019). 90 soil sampling sites whose distribution is presented in the supplementary information (Online Resource 1) were selected for this study. Similarity sites within a 500-m radius for each site were determined. These were set as alternative sampling sites to the originally selected sampling sites. For example, the sites would act as substitute sites where permission to access private land was not granted or where accessibility was constrained due to geographical barriers or safety reasons.

Fieldwork and laboratory analysis

The soil sampling sites were located in the field with the aid of a GPS. Caution was exercised to ensure that samples were collected from the exact coordinates obtained from the selection process. At each site, undisturbed soil samples from the top 0–30 cm were collected by using soil cores for the determination of bulk density, texture and organic carbon content (Kamamia et al. 2021).

For soil texture analysis, the combined wet sieving and sedimentation method was applied. The sand fraction was determined using wet sieving, while the silt and clay fractions were analysed using sedimentation analysis using the Sedimat 4–12 equipment (Umwelt-Geräte-Technik—UGT GmbH, Müncheberg, Germany). The organic carbon content (C_{org}) was determined by dry combustion using the Vario TOC Cube (Elementar Analysensysteme GmbH, Langenselbold, Germany). A summary of this data is presented as supplementary information (Online Resource 2).

STEP 2: calculating the individual RUSLE factors

Soil loss was calculated with RUSLE (Renard et al. 2017) by multiplying all factors represented below:

$$A = R * K * L * S * C * P \quad (1)$$

where A is the annual soil loss in t $ha^{-1} yr^{-1}$

R is the rainfall erosivity $\left(\text{MJ mm ha}^{-1}\text{h year}\right)$

K is the soil erodibility factor $\left(\text{t ha}^{-1}\text{R unit}^{-1}\right)$

LS is the topographic factor (dimensionless)

C is the cropping management factor (dimensionless)

P is the practice support factor (dimensionless)

This equation was modified to calculate the monthly soil loss based on Schmidt et al. (2019) (Eq. 1).

$$A_{\text{monthly}} = \text{R}_{\text{month}} * K * L * S * C_{\text{month}} * P, \quad (2)$$

where A_{month} is the monthly soil loss in t $ha^{-1} month^{-1}$

The data sources and derivation of the RUSLE factors are given in Table 2.

R-factor

The required daily rainfall data for the determination of R_{month} for the years between 2011 and 2017 was obtained from the Kenya Forest Service (KFS) for the Upland Station located in the western part of the Ruiru Reservoir catchment. This is the only existing station in the catchment. These data were complemented with gridded daily rainfall of the Climate Hazard Group Infrared Precipitation (CHIRPS) (Climate Hazards Center—UC Santa Barbara 2020) (Funk et al. 2015). This freely available high-resolution data combines 0.05° resolution satellite imagery with in situ station data to create gridded time series data starting 1981 to near-present. CHIRPS daily precipitation data for the period corresponding to that of the observed daily rainfall was extracted and used to fill any gaps present in the observed data. The extracted Modified Fournier Index (MFI) (Arnoldus 1977) and consequently the R_{month} factor were determined using Eq. 3 (Table 2). For each month, R_{month} was assumed to be spatially static. It was deemed adequate, as the area of the river catchment is 51 km^2 and does not experience a large monthly rainfall variation.

K-factor

Soil texture, permeability and organic matter content of the topsoil were used to determine the K-factor for the 90 sampled points using the Schwertmann et al. (1987) approach (Eq. 4). The cubist method (Quinlan 1992) combined with

Table 2 Overview of the individual risk factors, datasets and formulae used as input to RUSLE

Erosion factor	Data source	Calculation
Rainfall erosivity (monthly), R_{month} factor	Rainfall station data	$MFI = \frac{Pi^2}{P}$ $R = 1.735 * 10^{(1.5*Log\text{MFI}-0.8188)}$ (Tiwari et al. 2016), (3) MFI represents the Modified Fournier Index (Arnoldus 1977) pi is the monthly rainfall P is the annual rainfall
Soil erodibility, K-factor	Measured soil texture, soil organic matter, soil permeability	$K = 2.77 * 10^{-6} * M^{1.14} * (12 - OM) + 0.043 * (A - 2) + 0.033 * (4 - D)$ (4) with: $M = (\%\text{silt} + \%\text{fine sand}) * (\%\text{silt} + \%\text{sand(fine sand excluded)})$ $OM = \%\text{Organic matter}$ $A =$ aggregate stability class $D =$ permeability class
Cover and management (monthly), C_{month} factor	Landsat 8 + (monthly)	$NDVI = \frac{NIR-IR}{NIR+IR}$ (5) where NIR is the near infrared IR is the reflection in the visible spectrum $C = 0.1\left(\frac{-NDVI+1}{2}\right)$ (6)
Slope length and slope steepness, LS-factor	Digital elevation model	$LS = \left(\frac{X}{22.13}\right)^n (0.0065 + 0.045s + 0.0065s^2)$ (7) where X is slope length in meters s is the slope gradient% n is the exponent according to the angle of slope

Table 3 Overview of the terrain and spectral covariate data used for cubist–kriging DSM

Covariate type	Description
Terrain data	Slope, aspect, elevation, topographic wetness index (TWI), profile curvature, plan curvature, longitudinal curvature, hill shading, catchment area, flow accumulation, multiresolution ridge top flatness (MrRTF), multiresolution valley bottom flatness (MrVBF), upslope length factor, Software: SAGA GIS (version 2.3.2) Requires: Sink-filled DEM (https://earthexplorer.usgs.gov/)
Spectral data	Blue, green, red, near-infrared, Normalised Difference Vegetation Index (NDVI) wet (ndvid) and dry season (ndviw), Green Vegetation Index (GVI) Software: ArcMap version 10.2

regression kriging (Malone et al. 2017) and selected covariates (Table 3) was applied as DSM to create a continuous map of soil erodibility.

The cubist model divides data into partitions based on rules associated with covariates and fits a regression equation to each subset. Predictions are then determined based on the relative importance of the covariates. Moreover, three parameters must be established: rules—maximum number of partitions allowed, committees—maximum number of boosting iterations, and extrapolation—model constraints (Malone et al. 2017). On the other hand, regression kriging is a spatial interpolation technique that uses a semi-variogram to quantify the spatial structure of residuals (difference between the predicted and observed values) (Ma et al. 2017). In this study, soil erodibility data from the 90 sampling sites were split into two segments representing the training and testing data (~ 70% and ~ 30%, respectively). First, the Cubist model was applied where the data was partitioned based on the most relevant covariates present. This represented the deterministic component of the predictions. Regression kriging, representing the stochastic component, was then undertaken. Finally, these two components were added together to arrive at the final prediction. A leave-one-out cross-validation scheme was applied to assess the accuracy of the predictions, which were represented using the coefficient of determination R^2. A detailed description can be found in Malone et al. (2017).

C-factor

The monthly C-factors were adjusted based on the normalised difference vegetation index (NDVI) (Jong 1994), which was calculated from Landsat 8 images for the year 2017. The NDVI values range between −1, for almost bare surfaces and water bodies, to 1 for densely vegetated surfaces. The values for NDVIs were afterward converted to the C-factor using Eq. 6 (Almagro et al. 2019), by applying the Raster Calculator tool in ArcGIS (ArcMap version 10.2).

In the months where cloud cover was ≥ 10% (April, May, November), the C-factor values were obtained from spline interpolation. The spline interpolation method is a minimum curvature function that passes through the data with the accuracy of their mean errors. In this method, all the data points influence the value of the interpolated point, with those closest to the main station having the greatest impact on the value of the interpolated point (Niedzielski 2015). Using the polynomials, the first and second derivatives can easily be derived, making them applicable in biological modelling such as developing plant growth curves (Quero et al. 2015).

LS-factor and P-factor

Using the DEM as an input, the LS-factor was determined by using Eq. 7 in Table 2 in ArcGIS (ArcMap version 10.2). Only sporadic conservation practices were observed in the Ruiru Reservoir catchment. This included 'fanya juu' terraces (Mati 2005) on steep agricultural lands and grass strips along the riparian region. To account for this traditional land management practice, a threshold of 25% slope was set for agricultural lands. This means that this conservation measure would be implemented in areas with a slope above 25%. As not all farmers have adopted this conservation measure, 10% of all the possible pixels were randomly selected. Using the *dply* package in R statistical software version 3.5.1 (R core Team 2019), all pixels were loaded and the first filter according to the slope was implemented. The 10% of remaining pixels were selected using random sampling and a value of 0.7 was assigned according to Angima et al. (2003). Furthermore, the P-factor value for all pixels within 30 m of the Ruiru River was adjusted to 0.9 following Mwangi et al. (2015) to account for grass strips. These have been developed along the Ruiru River as part of an integrated water resource protection initiative by Water Rural User Association (WRUA) (Kamamia et al. 2021). For all other LULC, the P-Factor was set to 1.

STEP 3: plausibility check with GloSEM data

As a plausibility check, the monthly soil loss values (REG_SL) were compared with annual soil loss estimates from GloSEM (Borrelli et al. 2017). As presented in the flowchart (Fig. 2), the individual RUSLE factors were overlaid and multiplied with each other using the Raster Calculator tool in ArcGIS (ArcMap version 10.2). The K-factor, LS-factor and P-factors remained static, while the R-factor and C-factor were substituted for each month.

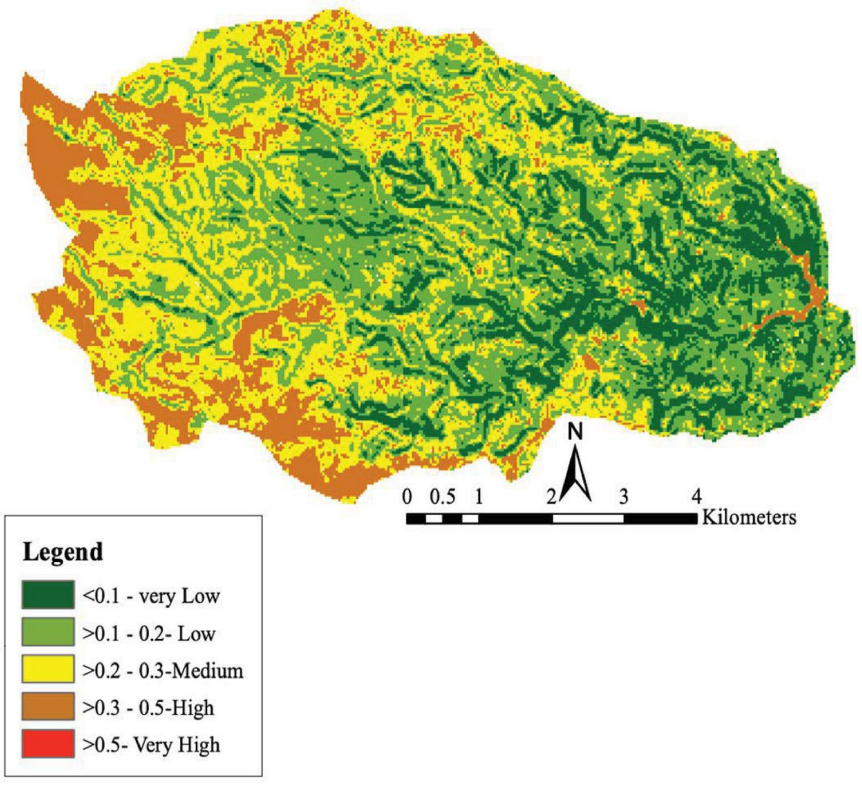

Fig. 4 Map of soil erodibility of the Ruiru Reservoir catchment

Monthly soil loss was then compared for the different LULC by using the land-use map created from Landsat 8 + data.

Results and discussion

Map of soil erodibility

A spatial soil erodibility map with an R^2 of 0.63 for the validation dataset was obtained from the DSM analysis (Fig. 4). The most important predictors were slope, elevation, MrRTF, Band5d, ndvid and GVI. Given that no comprehensive model evaluation guideline was found on the model output, these results were compared with other published works. Avalos et al. (2018) reported R^2 values of 0.31 for DSM by using only terrain attributes and obtained a significant linear relationship between slope and erodibility. Taghizadeh-Mehrjardi et al. (2019) reported R^2 values of 0.71. Panagos et al. (2014) reported an R^2 of 0.74 on cross-validation when applying the cubist method with the multi-level B splines interpolation technique with both spectral and terrain attributes. Although the combined use of these covariates improved the predictions, latitude and elevation covariates were ranked as the most important predictors.

The importance of terrain factors may be attributed to the information they contain on landscape positioning. These covariates can discriminate between hillslopes which are dominated by erosion and transport processes and consequently high erodibility (Gallant and Dowling 2003; Jones et al. 2020). Noteworthy is the preference for MrRTF over MrVTF as a predictor. In general, the RUSLE equation does not account for depositional areas such as valley bottoms represented using the MrVFT (Alewell et al. 2019). The importance of spectral data may be attributed to the information they contain on vegetation development, which is an input source of soil organic matter. Taghizadeh-Mehrjardi et al. (2019) found a strong negative correlation between the K-factor and soil organic matter. Zhao et al. (2018) and Addis and Klik (2015) reported that soil erodibility has an indirect relationship with vegetation type, which influences the soil organic matter and soil particle distribution. This means that soil erodibility is a dynamic property that can be highly influenced by anthropogenic activities such as changes in land-use or land management (Lal 2001).

According to Schwertmann et al. (1987), erodibility can be classified as follows: $K < 0.1$—'very low', $0.1 < K < 0.2$—'low', $0.2 < K < 0.3$—'medium', $0.3 < K < 0.5$—'high' and $K > 0.5$—'very high'. Hence, 46% of the catchment can be ranked as either having medium or high erodibility (Fig. 4). The highest erodibility is observed in areas surrounding the indigenous forest on the western part of the catchment and in the northern and southern extremes (see Fig. 3). Moreover, steeper slopes are classified as having higher erodibility as compared to lower slopes. For the different LULCs (Fig. 5), the highest K-factors were recorded under cropland and bare land. The lowest K-factors were predicted under some tea plantations and not under the indigenous forest as expected. The K-factor is affected by the complex interaction between the different environmental factors, which vary within the different LULC. For the silt-dominated soils of the Loess Plateau of China, Zhao et al. (2018) reported that for the native vegetation, soil properties and topography were the dominant factors which influence soil erodibility. For managed and restored vegetation, soil organic matter highly influenced erodibility (Zhao et al. 2018). Terrain factors such as slope and elevation influence the physical

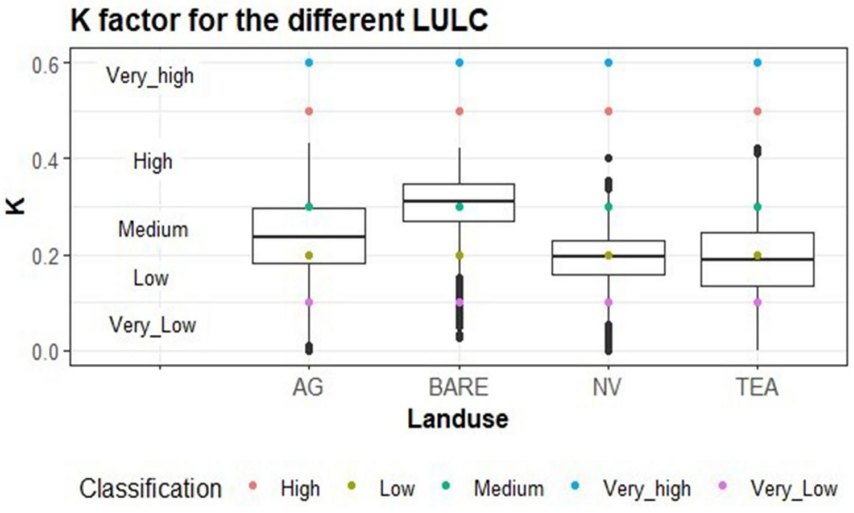

Fig. 5 K-factor for the different land-use and land cover classes (LULC) in the Ruiru Reservoir catchment cropland (AG), bare land (BARE), natural vegetation (NV) and tea plantation (TEA)

and chemical properties of soils leading to changes in soil particle composition and soil erodibility. Higher elevations were associated with higher erosion of silt material, which is then deposited in the lower elevation (Zhao et al. 2018). Against this background, the presence of andosol (high content of silt and organic matter) in the high elevation could have recorded lower K-factor values due to the effect of long-term erosion. Conversely, the use of high organic amendments such as mulch from pruned residues could explain the low erodibility observed under some tea plantations. The use of mulch protects the soil against

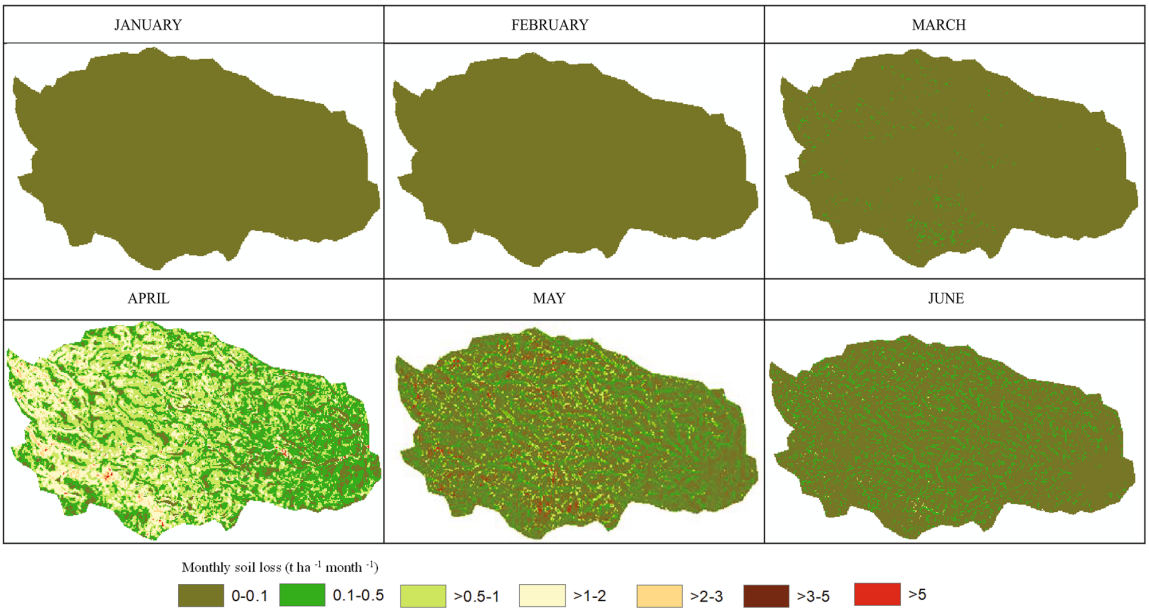

(a)

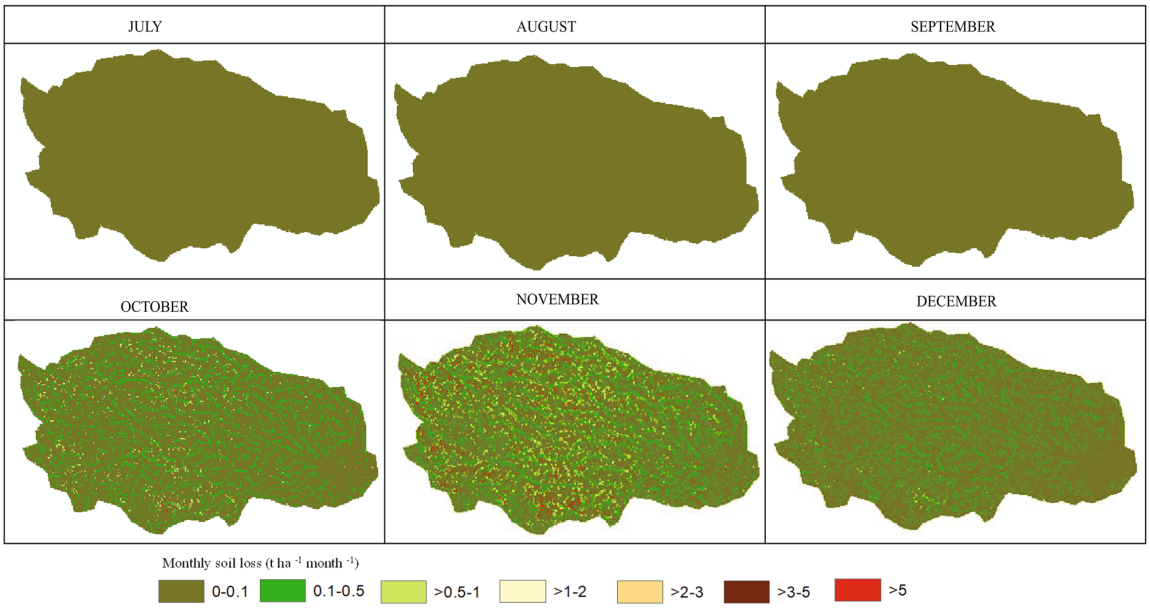

(b)

Fig. 6 **a** Water erosion risk maps for the Ruiru Reservoir catchment for January–June. **b** Water erosion risk maps for the Ruiru Reservoir catchment for July–December

the impact of raindrops and increases soil organic matter, which stabilises the soil aggregates and making them less prone to erosion (Ni et al. 2016; Xianchen et al. 2020).

Temporal and spatial soil erosion dynamics

An overview of the spatial monthly soil erosion (Fig. 6a and b) shows that most of the soil loss occurs within two distinct periods. The first is between March and June and the second is between October and December. Furthermore, they reveal that the areas in the vicinity of the indigenous forest on the western and southern parts of the catchment have at the highest erosion risk. These are mostly deforested areas that are now either bare land or have sparse shrub cover. Consequently, increased rainfall further increases the risk of erosion along the slopes in the Ruiru catchment. These results can be corroborated by Kamamia et al. (2021) who found that these areas are characterised by low aggregate stability and are therefore highly susceptible to erosion.

From Fig. 7 a cumulative monthly soil loss of 2.23 t/ha and 1.68 t/ha was estimated from the long rainy season (March 0.11 t/ha/month, April 1.70 t/ha/month, May 0.43 t/ha/month) and short rainy season (October 0.56 t/ha/month, November 0.89 t/ha/month, December 0.22 t/ha/month). The highest soil loss was observed in April, while the lowest soil loss of 0.003 t/ha/month was observed in July. Ongoma (2019) reported that precipitation in Kenya reaches its peak in April and is lowest in July. A comparison with the monthly average of 0.27 t/ha/month estimated from GloSEM shows that the average soil loss in April predicted by REG_SL is 6.3 times higher than the average cumulative yearly soil loss from GloSEM. This illustrates that the use of such averages for the design of erosion control measures could lead to the under-designing and construction of ineffective control measures. This situation could further be exacerbated where such measures fail, resulting in damage to crops and even loss of lives.

Soil loss can be described with two main mechanisms: erosion by raindrop impact and erosion by surface runoff. In reality, both mechanisms occur simultaneously. Thus, soil erosion mechanisms should be classified based on the degree of susceptibility of one mechanism relative to another (Kinnell 2005). There are two cropping seasons in the Ruiru Reservoir catchment that take advantage of the bimodal rainfall in the catchment. Before the onset of the rainy seasons, the soils are dry and possess high infiltration rates. Despite this, the soils are loose and bare due to tilling. At the start of the rains, the soils are more susceptible to erosion by raindrop impact. Over time, the soil pores gradually get saturated with water and therefore increased precipitation causes more raindrops to penetrate through the flow detaching soil particles which are then lifted and transported (Kinnell 2005). Higher soil loss recorded during the long rains is due to increased precipitation events. Wei et al. (2009) concluded that rainfall events with long durations but relatively low intensities play important roles in inducing severe erosion. Therefore, it is imperative to note that measures protecting the soil against rainfall drops (such as increased plant cover) would markedly reduce soil losses in the Ruiru catchment at the onset of rainfall.

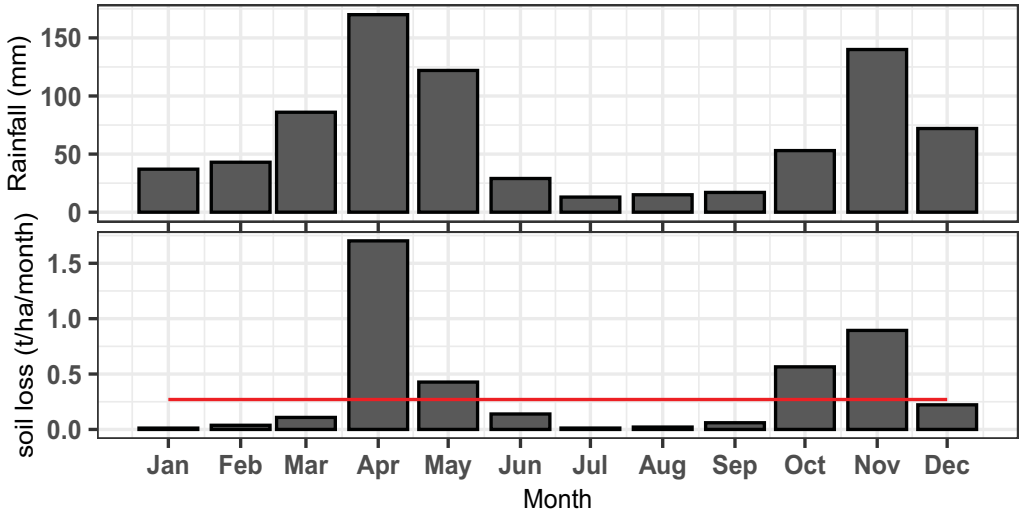

Fig. 7 Graph showing on the top: line graph of monthly rainfall distribution. Bottom: dynamic (REG_SL- bar plot) and static (GloSEM- line graph) monthly water erosion risk

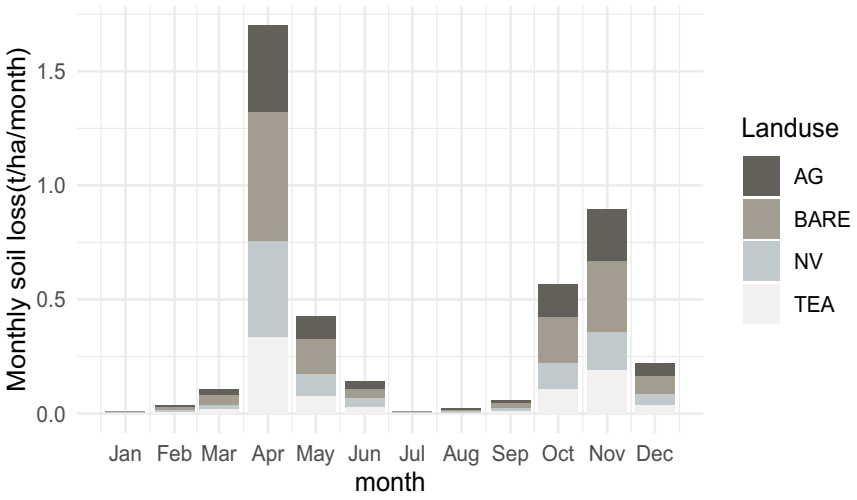

Fig. 8 Soil erosion dynamics under different land use and land cover (LULC). Cropland (AG), bare land (BARE), natural vegetation (NV) and tea plantation (TEA)

Soil loss dynamics under different LULC

The monthly soil loss trend observed in Fig. 8 for all months was BARE > AG > TEA > NV. Despite occupying the smallest area (4.8%), BARE contributes largest to soil erosion. Online Resource 2 indicates that these areas have the lowest clay percentages making them highly prone to erosion and probably the largest contributor to siltation in the Ruiru Reservoir catchment. This LULC includes some deforested areas and areas around homesteads and roadsides. These roads recorded high soil losses as observed from the maps (Fig. 6a and b). Most of the feeder roads within the Ruiru catchment occur on steep slopes and are made of earthen material. They are constantly used by heavy vehicles that carry milk and tea from the smallholder farmers to the various processing units. This impact compresses the roads, forcing the edges to break away leaving the bare soils susceptible to water erosion. Cerdan et al. (2010) found a positive relationship between erosion rates and slope length on bare soils. As this LULC records the highest soil loss, vegetative or structural stabilisation of roadsides for example, by use of gabions (Laflen et al. 1985) could offer an all-year solution to mitigate erosion in these areas. The establishment of grasses/turfs around homesteads and reforestation of areas surrounding the forests (see Fig. 3) also recording the high soil loss in March and November could protect the bare soils against erosion.

Cropland with an aerial coverage of 38.3% is the dominating land-use in the Ruiru catchment and recorded the second-highest soil loss throughout the year. Most of the farmers in the Ruiru catchment practice rain-fed mixed annual agriculture. At the onset of the long rains in March and short rains in November, the soils are usually tilled and sowed. Tilling activities destroy soil aggregates and lack of vegetation exposes the soil to the direct impact of raindrops. Exposure of the already loose soil to rain leads to severe denudation of the topsoil (Feng et al. 2016; Muoni et al. 2020). This variation also changes with the rainfall intensity with higher erosion rates being experienced during higher precipitation (Fig. 8). Adoption of more appropriate crop and tillage activities such as conservation tillage and strip cropping could be used as a strategy to reduce the soil loss recorded at the onset of both the long and short rainfall. Mulching activities can further protect the soil surface from the erosive forces of raindrop impact and overland flow especially during times where crops are less developed. Finally, the adoption of agroforestry can serve as a more permanent solution to reducing erosion by water.

Tea plantations in the Ruiru catchment, covering an area of 34.8%, occur mostly along steep slopes. High soil loss may occur due to the general topography and poor management strategies (Krishnarajah 1985; Mupenzi et al. 2011). In consequence, soil erosion on top of slopes could lead to loss of productivity, which may be irreversible as the rate of soil loss greatly supersedes its formation rate. Soil loss occurs during (1) establishment of new tea plantations, which are undertaken without any conservation measures and (2) management activities such as pruning and weeding often lead to trampling, which loosens the soil, making it more susceptible to erosion. Soil loss in the tea plantations is particularly high within the first two months of the long (April and May) and short (October and November) rains. Before these months, productivity is usually low, there is largescale pruning and weeding in the catchment, as a result, the soil is loosened and exposed. This soil is then lost during the next rainy season. Contrary to this, some studies have concluded that well-managed tea bushes or developed tea bushes have erosion rates comparable to natural forests (Krishnarajah 1985; Allaway and Cox 1989). For Sri Lanka, Krishnarajah (1985) reported that conservation measures

such as mulching with pruning residues and grass cuttings as well as the use of terraces resulted in almost complete elimination of soil erosion in tea plantations along steep slopes. The author further observed that mulching during replanting reduced soil erosion. Reduction of water erosion risk for this LULC can be attained by applying mulch during the establishment of new tea plantations. Moreover, mulching before pruning and weeding activities could protect the soil against trampling which induces erosion.

The NV LULC with a share of 16.6%, recorded the lowest soil loss throughout the year. NV included indigenous forest located on the western part of the catchment, afforested land as well as grasslands and shrublands. Afforested lands are part of an initiative by the Kenya Forestry Service (KFS) to restore degraded or deforested areas using mixed species of indigenous trees. Some of the afforested areas contain young tree stands. In addition to possessing underdeveloped tree canopies, the spacing between planted trees is usually wider during the establishment phase (Oliveira et al. 2013). This leaves a lot of open spaces where the impact of raindrops is much higher due to the lack of canopy, litter and underdeveloped tree roots (Drzewiecki et al. 2014). Over time, the trees' canopies develop, and the leaf area index (LAI) increases. The increased litter forms a mulch layer protecting the soil surface (Oliveira et al. 2013). Only then, trees are efficiently capable of controlling soil erosion while increasing soil biomass as in the case of indigenous ones. Nevertheless, the major advantages associated with trees, especially indigenous, should be exploited through the adoption of agroforestry systems. During the formative years, the crops can provide ground cover for the young trees. The trees would then later on control soil erosion and increase base flow through increased infiltration (Nair 2008). This was also observed by Ligonja and Shrestha (2015), who concluded that on-farm tree planting contributed significantly to a 7% reduction of areas under very high erosion between 1986 and 2008 in addition to increasing flow during the dry periods in Kondoa area, Tanzania. Likewise, Nambajimana et al. (2020) recommended a reforestation scheme of rapidly growing tree species as an important feature for erosion control in eroded areas of Rwanda. Waithaka et al. (2020) reported that most grasslands and shrublands (now occupying ~ 6% of the catchment) have been converted into settlement areas in the Ruiru catchment. The remaining scattered portions serve as alternate pasture for the dairy cattle in the catchment. Grass and shrublands have shown the potential to reduce soil erosion.

Thus, it is clear that vegetation coverage is an important factor for soil erosion, as it reduces the direct impact of rain drops and alleviates runoff through increased infiltration which finally affects the quality of surface and river runoff (Cerdan et al. 2010; Feng et al. 2016). It should be however noted that extreme rainfall, such as that received in April, may at times increase the uncertainty of the effectiveness of vegetation in reducing erosion (Wei et al. 2009). Finally, the spatial distribution of vegetation on the slopes is a key factor for the Ruiru Reservoir catchment. This affects the source-sink spatial landscape patterns which influence the runoff generation and sediment transport (Liu et al. 2018). For instance, if done properly, adjusting vegetation patterns along slopes could greatly reduce soil losses into streams and the Ruiru Reservoir and therefore improve water quality and preserve the water quantity.

Annual regional soil loss vs GloSEM

An average cumulative yearly soil loss of 3.24 t/ha/yr (range: 2.33–17.52 t/ha/yr) was obtained for the study area while using the GloSEM (Online Resource 3a). Although the REG_SL (Online Resource 3b) recorded a much lower average cumulative soil loss of 1.72 t/ha/yr, the soil loss range was much wider (0.0003–38.29 t/ha/yr). Online Resource 3a–b show that there is a spatial agreement between the two estimates of high erosion risk on the farthest western part of the catchment. However, the differential map further shows that the GloSEM overpredicted soil loss for most of the catchment and underpredicted for the areas where REG_SL recorded high erosion rates. The cumulative REG_SL unlike the GloSEM displayed the small-scale spatial heterogeneity, which exposed the various erosion hotspots. Borrelli et al. (2020) argued that although the GloSEM model provides pioneering assessment to determine potential erosion at global scales, it is heavily data dependent and is not able to capture all the varying conditions to which it is applied given its global scale. Therefore, the coarse nature of the GloSEM grids could have resulted in spatial aggregation /generalisation and the loss of small soil loss inclusions.

Conclusion

Sustainable soil management, in the context of integrated water resource management, improves soil functions which impact positively on the SDGs. Suitable indicators such as risk of soil erosion is needed to transfer the complexity of the soil–water nexus into a format that can be assessed and measured. More often these indicators have not been well explored and little or no data is available in developing countries. Here, we established that through the combination of efficient soil sampling, analysis of remote sensing data and DSM useful information such as maps of monthly soil loss can be developed in data-scarce areas to aid in developing IWRM measures. Moreover, we demonstrated

that the static annual erosion could misrepresent the true dimensions of soil loss with averages disguising areas of low and high erosion potential. The monthly erosion risk maps reveal that a monthly average obtained from average cumulative yearly soil loss from the GloSEM average soil loss is 6.3 times higher than the average soil loss obtained from April. Furthermore, the bare land LULC (occupying the smallest areal coverage) was the largest contributor to erosion indicating that at times a small portion of the catchment is responsible for a large proportion of the total erosion.

As the RUSLE does not account for all complex soil erosion exchanges, the results obtained should be taken as estimates and not absolute values (Benavidez et al. 2018). But as highlighted in this study, it is ideal for determining soil loss at landscape areas especially in data-scarce areas. Varying both the R-factor and C-factor greatly impacted the dynamics of soil loss in the Ruiru catchment. While the spatio-temporal distribution of rainfall is largely uncontrollable, the crop management factor is greatly influenced by the type and intensity of human intervention. Thus, it is only natural that erosion control focuses on improving catchment management practices "where" and "when" erosion is highest. This means that the spatio-temporal maps can be used by different stakeholders during the development of watershed management plans (Mwangi et al. 2016b, c). Within these plans, landscape-scale measures including timely allocation of scarce erosion mitigation and protection measures, proper crop selection that reduces erosion, as well as time-dependent planting and harvesting techniques for agriculture, can be purposefullly incorporated. For Ruiru drinking water reservoir catchment, a successful watershed management plan will require joint effort from the different stakeholders: small-scale farmers/communities, large-scale tea estate farmers, The Nairobi Water and Sewerage Company and the Kenya Forest Service. Only then will the sustainable use of soil and water resources and related ecosystem services in the catchment be achieved.

Supplementary Information The online version contains supplementary material available at https://doi.org/10.1007/s12665-022-10617-0.

Acknowledgements We would like to acknowledge Kenya Forest Service (KFS) for availing rainfall data used in the study. We appreciate the assistance of Samuel Nderitu, Jackson Warui (Water Resource Users Association) and Daniel Waweru (Kenya Forest Service) during fieldwork. The work was funded by the Graduate Academy, TU Dresden through the Travel Grants for short-term research stays abroad and the Scholarship Program for the Promotion of Early-Career Female Scientists scholarship programmes and DFG proj no. 471154408.

Funding Open Access funding enabled and organized by Projekt DEAL. Graduate Academy, TU Dresden through the Travel Grants for Short-Term Research stays abroad and the Scholarship Program for the Promotion of Early-Career Female Scientists scholarship programmes and DFG proj no. 471154408.

Availability of data and material N/A.

Code availability Software application.

Declarations

Conflict of interest N/A.

References

Addis HK, Klik A (2015) Predicting the spatial distribution of soil erodibility factor using USLE nomograph in an agricultural watershed, Ethiopia. Int Soil Water Conserv Res 3:282–290. https://doi.org/10.1016/j.iswcr.2015.11.002

Alewell C, Borrelli P, Meusburger K, Panagos P (2019) Using the USLE: chances, challenges and limitations of soil erosion modelling. Int Soil Water Conserv Res 7:203–225. https://doi.org/10.1016/j.iswcr.2019.05.004

Alexandridis TK, Sotiropoulou AM, Bilas G et al (2015) The effects of seasonality in estimating the C-factor of soil erosion studies. Land Degrad Dev 26:596–603. https://doi.org/10.1002/ldr.2223

Allaway J, Cox PMJ (1989) Forests and competing land uses in Kenya. Environ Manag 13:171–187. https://doi.org/10.1007/BF01868364

Almagro A, Thomé TC, Colman CB et al (2019) Improving cover and management factor (C-factor) estimation using remote sensing approaches for tropical regions. Int Soil Water Conserv Res 7:325–334. https://doi.org/10.1016/j.iswcr.2019.08.005

Ampofo EA, Muni RK, Bonsu M (2002) Estimation of soil losses within plots as affected by different agricultural land management. Hydrol Sci J 47:957–967. https://doi.org/10.1080/02626660209493003

Angima SD, Stott DE, O'Neill MK et al (2003) Soil erosion prediction using RUSLE for central Kenyan highland conditions. Agric Ecosyst Environ 97:295–308. https://doi.org/10.1016/S0167-8809(03)00011-2

Angulo-Martínez M, López-Vicente M, Vicente-Serrano SM, Beguería S (2009) Mapping rainfall erosivity at a regional scale: a comparison of interpolation methods in the Ebro Basin (NE Spain). Hydrol Earth Syst Sci 13:1907–1920. https://doi.org/10.5194/hess-13-1907-2009

Arnoldus HMJ (1977) Methodology used to determine the maximum potential average annual soil loss due to sheet and rill erosion in Morocco. In: FAO Soils Bulletins (FAO). pp 39–48

Asis A, Omasa K (2007) Estimation of vegetation parameter for modeling soil erosion using linear spectral mixture analysis of Landsat

ETM data. ISPRS J Photogramm Remote Sens. https://doi.org/10.1016/J.ISPRSJPRS.2007.05.013
Avalos FAP, Silva MLN, Batista PVG et al (2018) Digital soil erodibility mapping by soilscape trending and kriging. Land Degrad Dev 29:3021–3028. https://doi.org/10.1002/ldr.3057
Batjes NH (2008) ISRIC-WISE Harmonized Global Soil Profile Dataset (Ver. 3.1)
Benavidez R, Jackson B, Maxwell D, Norton K (2018) A review of the (Revised) Universal Soil Loss Equation ((R)USLE): with a view to increasing its global applicability and improving soil loss estimates. Hydrol Earth Syst Sci 22:6059–6086. https://doi.org/10.5194/hess-22-6059-2018
Benediktsson JA, Swain PH, Ersoy OK (1990) Neural network approaches versus statistical methods in classification of multisource remote sensing data. IEEE Trans Geosci Remote Sens 28:540–552. https://doi.org/10.1109/TGRS.1990.572944
Boardman J, Evans R (2019) The measurement, estimation and monitoring of soil erosion by runoff at the field scale: challenges and possibilities with particular reference to Britain. Prog Phys Geogr Earth Environ. https://doi.org/10.1177/0309133319861833
Borrelli P, Robinson DA, Fleischer LR et al (2017) An assessment of the global impact of 21st century land use change on soil erosion. Nat Commun 8:2013. https://doi.org/10.1038/s41467-017-02142-7
Borrelli P, Robinson DA, Panagos P et al (2020) Land use and climate change impacts on global soil erosion by water (2015–2070). Proc Natl Acad Sci 117:23205–23207. https://doi.org/10.1073/pnas.2017314117
Calder I (2006) Blue revolution: Integrated land and water resource management, second edition. Blue revolution: Integrated land and water resource management. Wiley. https://doi.org/10.1002/0470848944.hsa192
Carr DL (2004) Proximate population factors and deforestation in tropical agricultural frontiers. Popul Environ 25:585–612. https://doi.org/10.1023/B:POEN.0000039066.05666.8d
Cerdan O, Govers G, Le Bissonnais Y et al (2010) Rates and spatial variations of soil erosion in Europe: a study based on erosion plot data. Geomorphology 122:167–177. https://doi.org/10.1016/j.geomorph.2010.06.011
Climate Hazards Center—UC Santa Barbara (2020) CHIRPS: Rainfall Estimates from Rain Gauge and Satellite Observations. https://www.chc.ucsb.edu/data/chirps. Accessed 7 Nov 2020
Conrad O, Bechtel B, Bock M et al (2015) System for automated geoscientific analyses (SAGA) v. 2.1.4. Geosci Model Dev 8:1991–2007. https://doi.org/10.5194/gmd-8-1991-2015
de la Mupenzi JP, Li L, Ge J et al (2011) Assessment of soil degradation and chemical compositions in Rwandan tea-growing areas. Geosci Front 2:599–607. https://doi.org/10.1016/j.gsf.2011.05.003
de Nambajimana JD, He X, Zhou J et al (2020) Land use change impacts on water erosion in Rwanda. Sustainability 12:50. https://doi.org/10.3390/su12010050
Drzewiecki W, Wężyk P, Pierzchalski M, Szafrańska B (2014) Quantitative and qualitative assessment of soil erosion risk in Małopolska (Poland), supported by an object-based analysis of high-resolution satellite images. Pure Appl Geophys 171:867–895. https://doi.org/10.1007/s00024-013-0669-7
Duiker SW, Flanagan DC, Lal R (2001) Erodibility and infiltration characteristics of five major soils of southwest Spain. CATENA 45:103–121. https://doi.org/10.1016/S0341-8162(01)00145-X
EarthExplorer (2019) USGS. https://earthexplorer.usgs.gov/. Accessed 10 Mar 2020
Ebabu K, Tsunekawa A, Haregeweyn N et al (2019) Effects of land use and sustainable land management practices on runoff and soil loss in the Upper Blue Nile basin, Ethiopia. Sci Total Environ 648:1462–1475. https://doi.org/10.1016/j.scitotenv.2018.08.273
FAO-ITPS (2015) Status of the World's Soil Resources (SWSR)—Main Report. Food and Agriculture Organization of the United Nations and Intergovernmental Technical Panel on Soils, Rome, Italy
Feng Q, Zhao W, Wang J et al (2016) Effects of different land-use types on soil erosion under natural rainfall in the Loess Plateau, China. Pedosphere 26:243–256. https://doi.org/10.1016/S1002-0160(15)60039-X
Funk C, Peterson P, Landsfeld M, et al (2015) The climate hazards infrared precipitation with stations—a new environmental record for monitoring extremes. Sci Data 2:150066. https://doi.org/10.1038/sdata.2015.66
Gallant JC, Dowling TI (2003) A multiresolution index of valley bottom flatness for mapping depositional areas. Water Resour Res. https://doi.org/10.1029/2002WR001426
Gaubi I, Chaabani A, Ben Mammou A, Hamza MH (2017) A GIS-based soil erosion prediction using the Revised Universal Soil Loss Equation (RUSLE) (Lebna watershed, Cap Bon, Tunisia). Nat Hazards 86:219–239. https://doi.org/10.1007/s11069-016-2684-3
GWP (2000) Integrated water resources management. Global Water Partnership (GWP) Technical Advisory Committee, Background Paper No.4
Hatfield JL, Sauer TJ, Cruse RM (2017) Chapter one—Soil: the forgotten piece of the water, food, energy nexus. In: Sparks DL (ed) Advances in Agronomy. Academic Press, pp 1–46
Igwe PU, Onuigbo AA, Chinedu OC et al (2017) Soil erosion: a review of models and applications. Int J Adv Eng Res Sci 4:237–341. https://doi.org/10.22161/ijaers.4.12.22
Iserloh T, Ries JB, Arnáez J et al (2013) European small portable rainfall simulators: a comparison of rainfall characteristics. CATENA 110:100–112. https://doi.org/10.1016/j.catena.2013.05.013
Jenny H (1941) Factors of soil formation, a system of quantitative pedology. McGraw-Hill, New York
Jones EJ, Filippi P, Wittig R et al (2020) Mapping soil slaking index and assessing the impact of management in a mixed agricultural landscape. Soil Discuss. https://doi.org/10.5194/soil-2020-29
Jong SM (1994) Applications of reflective remote sensing for land degradation studies in a Mediterranean environment. Koninklijk Nederlands Aardrijkskundig Genootschap
Kamamia AW, Vogel C, Mwangi HM et al (2021) Mapping soil aggregate stability using digital soil mapping: a case study of Ruiru reservoir catchment Kenya. Geoderma Reg 24:e00355. https://doi.org/10.1016/j.geodrs.2020.e00355
Kidane M, Bezie A, Kesete N, Tolessa T (2019) The impact of land use and land cover (LULC) dynamics on soil erosion and sediment yield in Ethiopia. Heliyon 5:e02981. https://doi.org/10.1016/j.heliyon.2019.e02981
Kinnell PIA (2005) Raindrop-impact-induced erosion processes and prediction: a review. Hydrol Process 19:2815–2844. https://doi.org/10.1002/hyp.5788
Kouli M, Soupios P, Vallianatos F (2009) Soil erosion prediction using the Revised Universal Soil Loss Equation (RUSLE) in a GIS framework, Chania, Northwestern Crete, Greece. Environ Geol 57:483–497. https://doi.org/10.1007/s00254-008-1318-9
Krishnarajah P (1985) Soil erosion control measures for tea land in Sri Lanka. Sri Lanka J Tea Sci 54:91–100
Krysanova V, Müller-Wohlfeil D-I, Becker A (1998) Development and test of a spatially distributed hydrological/water quality model for mesoscale watersheds. Ecol Model 106:261–289. https://doi.org/10.1016/S0304-3800(97)00204-4

Laflen JM, Highfill RE, Amemiya M, Mutchler CK (1985) Structures and methods for controlling water erosion. Soil erosion and crop productivity. Wiley, pp 431–442

Lal R (2001) Soil degradation by erosion. Land Degrad Dev 12:519–539. https://doi.org/10.1002/ldr.472

Lal R, Mohtar RH, Assi AT et al (2017) Soil as a basic nexus tool: soils at the center of the food–energy–water nexus. Curr Sustain Energy Rep 4:117–129. https://doi.org/10.1007/s40518-017-0082-4

Lambin EF, Geist HJ, Lepers E (2003) Dynamics of land-use and land-cover change in tropical regions. Annu Rev Environ Resour 28:205–241. https://doi.org/10.1146/annurev.energy.28.050302.105459

Ligonja PJ, Shrestha RP (2015) Soil erosion assessment in Kondoa eroded area in Tanzania using Universal Soil Loss Equation, geographic information systems and socioeconomic approach. Land Degrad Dev 26:367–379. https://doi.org/10.1002/ldr.2215

Liu J, Gao G, Wang S et al (2018) The effects of vegetation on runoff and soil loss: multidimensional structure analysis and scale characteristics. J Geogr Sci 28:59–78. https://doi.org/10.1007/s11442-018-1459-z

Ma Y, Minasny B, Wu C (2017) Mapping key soil properties to support agricultural production in Eastern China. Geoderma Reg 10:144–153. https://doi.org/10.1016/j.geodrs.2017.06.002

Maina CW, Sang JK, Mutua BM, Raude JM (2018) A review of radiometric analysis on soil erosion and deposition studies in Africa. Geochronometria 45:10–19. https://doi.org/10.1515/geochr-2015-0085

Maloi SK, Sang JK, Raude JM et al (2016) Assessment of sedimentation status of Ruiru reservoir, Central Kenya. Am J Water Resour 4:77–82. https://doi.org/10.12691/ajwr-4-4-1

Malone BP, Minasny B, McBratney AB (2017) Using R for digital soil mapping. Springer International Publishing, New York

Mati BM (2005) Overview of water and soil nutrient management under smallholder rainfed agriculture in East Africa. Working Paper 105. Colombo, Sri Lanka: International Water Management Institute (IWMI)

McBratney AB, Mendonça Santos ML, Minasny B (2003) On digital soil mapping. Geoderma 117:3–52. https://doi.org/10.1016/S0016-7061(03)00223-4

Minasny B, McBratney AB (2006) A conditioned Latin hypercube method for sampling in the presence of ancillary information. Comput Geosci 32:1378–1388. https://doi.org/10.1016/j.cageo.2005.12.009

Morgan RPC, Quinton JN, Smith RE et al (1998) The European Soil Erosion Model (EUROSEM): a dynamic approach for predicting sediment transport from fields and small catchments. Earth Surf Process Landf 23:527–544. https://doi.org/10.1002/(SICI)1096-9837

Mulinge W, Gicheru P, Murithi F et al (2016) Economics of land degradation and improvement in Kenya. In: Nkonya E, Mirzabaev A, von Braun J (eds) Economics of land degradation and improvement—a global assessment for sustainable development. Springer International Publishing, Cham, pp 471–498

Muoni T, Koomson E, Öborn I et al (2020) Reducing soil erosion in smallholder farming systems in east Africa through the introduction of different crop types. Exp Agric 56:183–195. https://doi.org/10.1017/S0014479719000280

Mwangi JK, Shisanya CA, Gathenya JM et al (2015) A modeling approach to evaluate the impact of conservation practices on water and sediment yield in Sasumua Watershed, Kenya. J Soil Water Conserv 70:75–90. https://doi.org/10.2489/jswc.70.2.75

Mwangi HM, Julich S, Feger KH (2016a) Introduction to watershed management. In: Pancel L, Köhl M (eds) Tropical forestry handbook, 2nd edn. Springer-Verlag, Berlin, Heidelberg, pp 1869–1896

Mwangi HM, Julich S, Feger KH (2016b) Watershed management practices in the tropics. In: Pancel L, Köhl M (eds) Tropical forestry handbook, 2nd edn. Springer-Verlag, Berlin, Heidelberg, pp 1897–1915

Mwangi HM, Julich S, Patil SD et al (2016c) Modelling the impact of agroforestry on hydrology of Mara River Basin in East Africa. Hydrol Process 30:3139–3155. https://doi.org/10.1002/hyp.10852

Nair PKR (2008) Agroecosystem management in the 21st century: it is time for a paradigm shift. J Trop Agric 46:1–12

NASA (1999) Remote Sensing. https://earthobservatory.nasa.gov/features/RemoteSensing/remote_05.php. Accessed 5 Nov 2020

NASA (2013) Landsat 8 Bands | Landsat Science. https://landsat.gsfc.nasa.gov/landsat-8/landsat-8-bands/. Accessed 5 Nov 2020

Ni X, Song W, Zhang H et al (2016) Effects of mulching on soil properties and growth of tea olive (*Osmanthus fragrans*). PLoS ONE 11:e0158228. https://doi.org/10.1371/journal.pone.0158228

Niedzielski T (ed) (2015) Satellite technologies in geoinformation science. Birkhäuser Basel

Nyakundi R, Mwangi J, Makokha M, Obiero C (2017) Analysis of rainfall trends and periodicity in Ruiru location, Kenya. Int J Sci Res Publ 7:28–39

Oliveira PT, Wendland E, Nearing MA (2013) Rainfall erosivity in Brazil: a review. CATENA 100:139–147. https://doi.org/10.1016/j.catena.2012.08.006

Ongoma V (2019) Why Kenya's seasonal rains keep failing and what needs to be done. In: ReliefWeb. https://reliefweb.int/report/kenya/why-kenya-s-seasonal-rains-keep-failing-and-what-needs-be-done. Accessed 4 Feb 2020

Ozsoy G, Aksoy E, Dirim MS, Tumsavas Z (2012) Determination of soil erosion risk in the Mustafakemalpasa River Basin, Turkey, using the revised universal soil loss equation, geographic information system, and remote sensing. Environ Manag 50:679–694. https://doi.org/10.1007/s00267-012-9904-8

Panagos P, Meusburger K, Ballabio C et al (2014) Soil erodibility in Europe: a high-resolution dataset based on LUCAS. Sci Total Environ 479–480:189–200. https://doi.org/10.1016/j.scitotenv.2014.02.010

Patil RJ (2018) Spatial techniques for soil erosion estimation. In: Patil RJ (ed) Spatial techniques for soil erosion estimation: remote sensing and GIS approach. Springer International Publishing, Cham, pp 35–49

QGIS.org (2019) QGIS Geographic Information System. Version 3.4. Open-Source Geospatial Foundation Project. URL https://qgis.org/de/site/

Quero G, Simondi S, Borsani O (2015) Segmental interpolation surface: a tool to dissect environmental effects on plant water-use efficiency in drought prone scenarios. bioRxiv. https://doi.org/10.1101/033308

Quinlan JR (1992) Learning with continuous classes. World Scientific, pp 343–348

R Core Team (2019) R: A language and environment for statistical computing. https://www.r-project.org/. Accessed 10 Mar 2020

Renard KG, Laflen JM, Foster GR et al (2017) The revised universal soil loss equation. In: Soil eros. res. Methods. https://www.taylorfrancis.com/. Accessed 15 Jul 2020

Ries J, Iserloh T, Seeger M, Gabriels D (2013) Rainfall simulations—constraints, needs and challenges for a future use in soil erosion research. Z Geomorphol Suppl Issues 57:1–10. https://doi.org/10.1127/0372-8854/2013/S-00130

Roudier P, Beaudette D, Hewitt AE (2012) A conditioned Latin hypercube sampling algorithm incorporating operational constraints. Digital soil assessments and beyond. CRC Press, pp 1–6

Schmidt S, Alewell C, Panagos P, Meusburger K (2016) Seasonal dynamics of rainfall erosivity in Switzerland. Ecohydrology/modelling approaches

Schmidt S, Alewell C, Meusburger K (2018) Mapping spatio-temporal dynamics of the cover and management factor (C-factor) for grasslands in Switzerland. Remote Sens Environ 211:89–104. https://doi.org/10.1016/j.rse.2018.04.008

Schmidt S, Alewell C, Meusburger K (2019) Monthly RUSLE soil erosion risk of Swiss grasslands. J Maps 15:247–256. https://doi.org/10.1080/17445647.2019.1585980

Schwertmann U, Vogl W, Kainz M (1987) Bodenerosion durch Wasser: Vorhersage des Abtrags und Bewertung von Gegenmaßnahmen. Ulmer, Stuttgart

Stroosnijder L (2005) Measurement of erosion: is it possible? CATENA 64:162–173. https://doi.org/10.1016/j.catena.2005.08.004

Taghizadeh-Mehrjardi R, Bawa A, Kumar S et al (2019) Soil erosion spatial prediction using digital soil mapping and RUSLE methods for Big Sioux River Watershed. Soil Syst 3:43. https://doi.org/10.3390/soilsystems3030043

Tiwari H, Rai SP, Kumar D, Sharma N (2016) Rainfall erosivity factor for India using modified Fourier index. J Appl Water Eng Res 4:83–91. https://doi.org/10.1080/23249676.2015.1064038

Uddin K, Murthy MSR, Wahid SM, Matin MA (2016) Estimation of soil erosion dynamics in the Koshi basin using GIS and remote sensing to assess priority areas for conservation. PLoS ONE 11:e0150494. https://doi.org/10.1371/journal.pone.0150494

United Nations (2015) Transforming our world: the 2030 Agenda for Sustainable Development |Department of Economic and Social Affairs

Waithaka A, Murimi S, Obiero K (2020) Assessing the effects of land use/land cover change on discharge using SWAT Model in River Ruiru Watershed, Kiambu County, Kenya. Appl Ecol Environ Sci 8:303–314. https://doi.org/10.12691/aees-8-5-18

Wang G, Gertner G, Singh V et al (2002) Spatial and temporal prediction and uncertainty of soil loss using the revised universal soil loss equation: a case study of the rainfall–runoff erosivity R factor. Ecol Model 153:143–155. https://doi.org/10.1016/S0304-3800(01)00507-5

Wang J, He Q, Zhou P, Gong Q (2019) Test of the RUSLE and key influencing factors using GIS and probability methods: a case study in Nanling National Nature Reserve, South China. Adv Civ Eng 7129639. https://www.hindawi.com/journals/ace/2019/7129639

Wei W, Chen L, Fu B et al (2009) Responses of water erosion to rainfall extremes and vegetation types in a loess semiarid hilly area, NW China. Hydrol Process 23:1780–1791. https://doi.org/10.1002/hyp.7294

Wischmeier WH, Smith DD (1958) Rainfall energy and its relationship to soil loss. Eos Trans Am Geophys Union 39:285–291. https://doi.org/10.1029/TR039i002p00285

Wischmeier WH, Smith DD (1978) Predicting rainfall erosion losses: a guide to conservation planning. Department of Agriculture, Science and Education Administration

Xianchen Z, Huiguang J, Xiaochun W, Yeyun L (2020) The effects of different types of mulch on soil properties and tea production and quality. J Sci Food Agric 100:5292–5300. https://doi.org/10.1002/jsfa.10580

Young NE, Anderson RS, Chignell SM et al (2017) A survival guide to Landsat preprocessing. Ecology 98:920–932. https://doi.org/10.1002/ecy.1730

Zhao W, Wei H, Jia L et al (2018) Soil erodibility and its influencing factors on the Loess Plateau of China: a case study in the Ansai watershed. Solid Earth 9:1507–1516. https://doi.org/10.5194/se-9-1507-2018

Zhu B, Li Z, Li P et al (2010) Soil erodibility, microbial biomass, and physical–chemical property changes during long-term natural vegetation restoration: a case study in the Loess Plateau, China. Ecol Res 25:531–541. https://doi.org/10.1007/s11284-009-0683-5

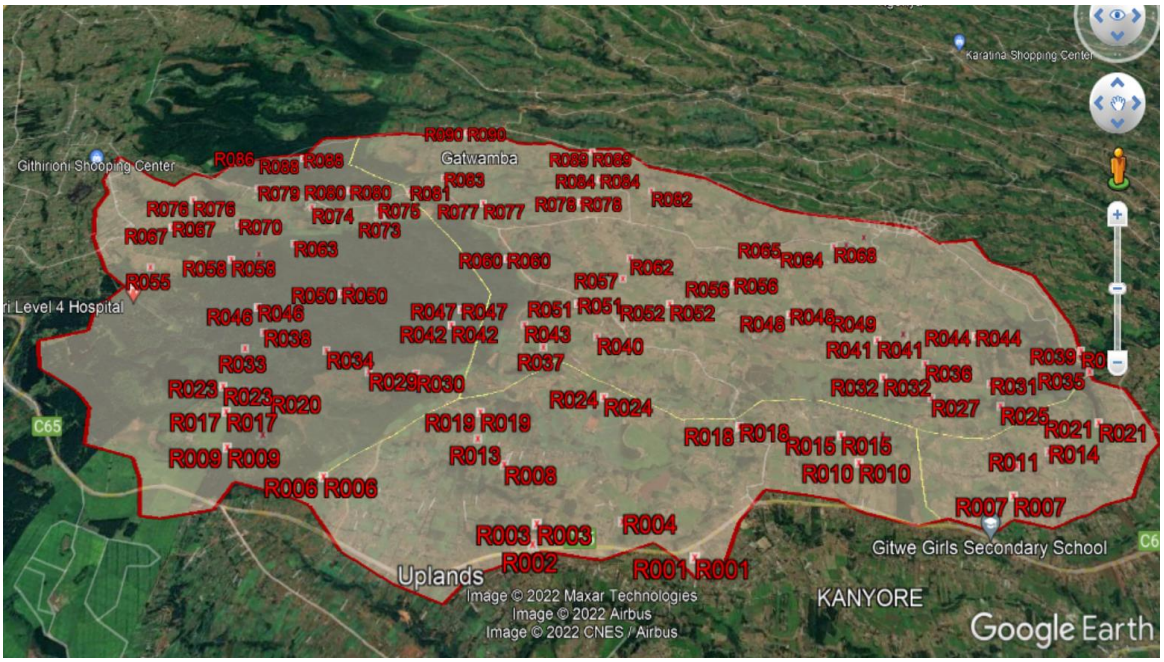

Online Resource 1: Summary of physical soil properties from laboratory analysis

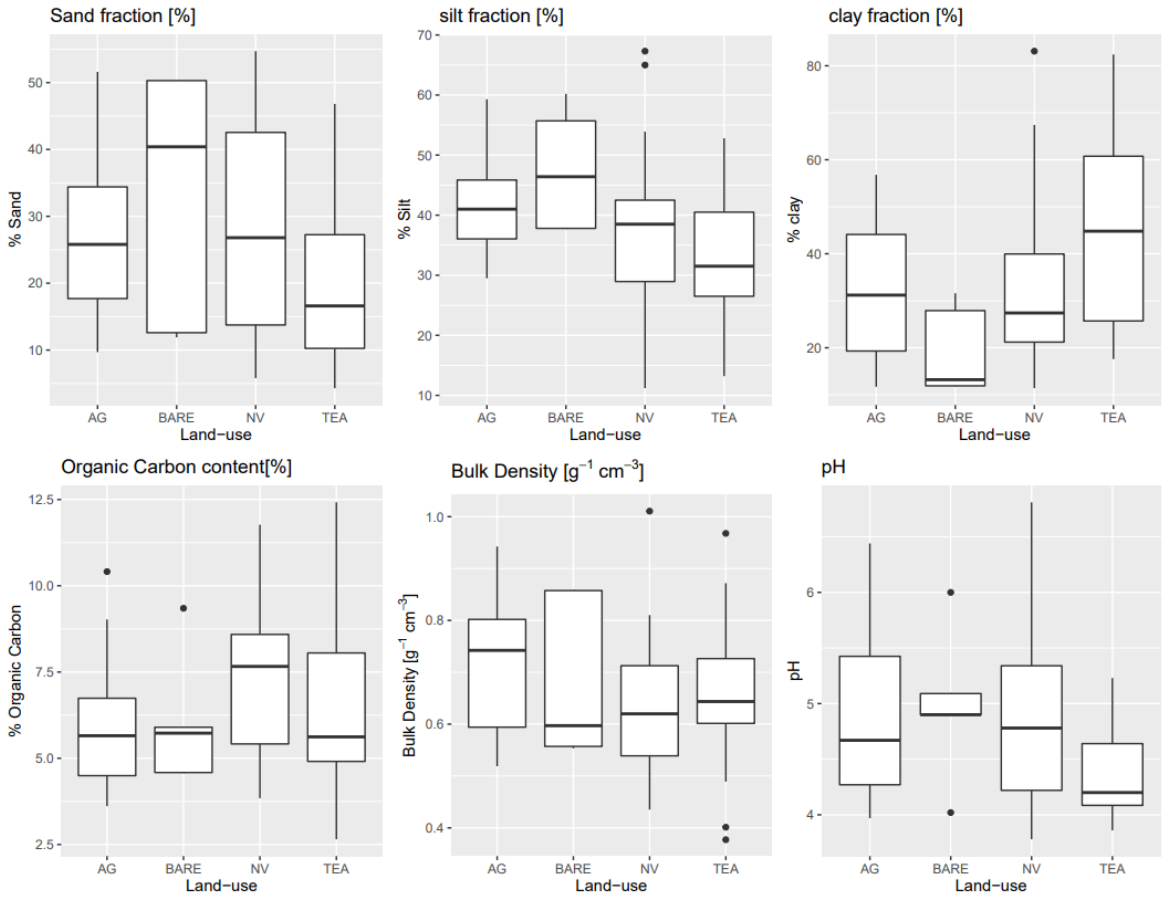

Online Resource 2: Summary of physical soil properties from laboratory analysis

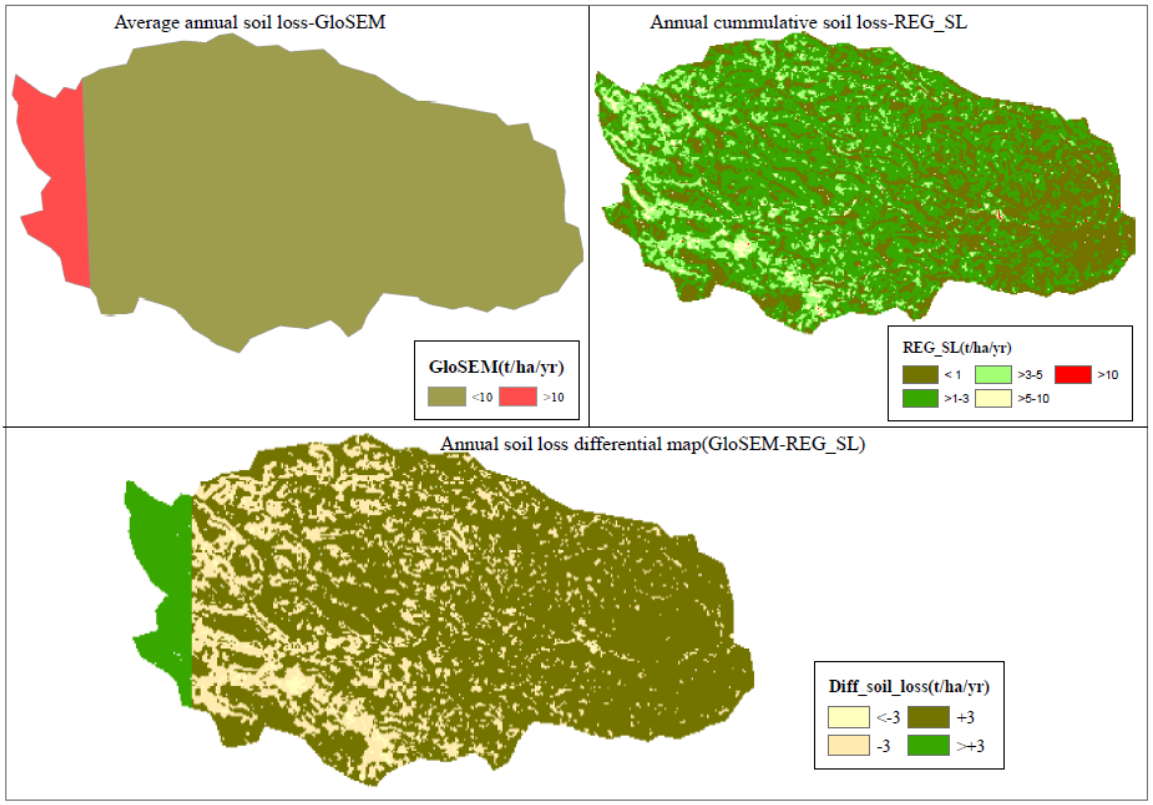

Online Resource 3: Average annual soil loss differential map for Ruiru catchment with a.) representing the annual soil loss obtained from the GloSEM (Borrelli et al. 2017) and b.) Annual REG_SL c.) Annual differential soil loss map